STUDIES IN PHOSPHORUS-SELENIUM CHEMISTRY

Jacqueline Garland

A Thesis Submitted for the Degree of PhD
at the
University of St Andrews

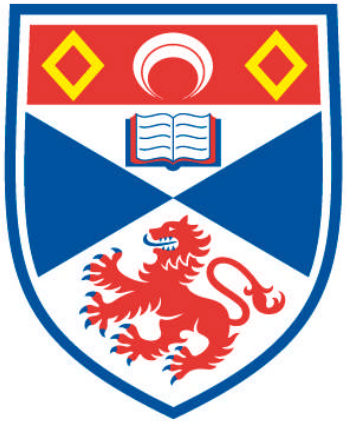

2013

Studies in Phosphorus-Selenium Chemistry

Jacqueline Garland

This thesis is submitted in partial fulfilment for the degree of

Doctor of Philosophy (PhD.)
at the
University of St Andrews

and

Doctor rerum naturalium (Dr. rer. nat.)
at the
Universität Leipzig

21st February 2013

Supervisors: Prof. J. D. Woollins
Prof. E Hey-Hawkins

Declarations

I, Jacqueline Garland, hereby certify that this thesis, which is approximately 53000 words in length, has been written by me, that it is the record of work carried out by me and that it has not been submitted in any previous application for a higher degree.

I was admitted as a research student in September, 2008 and as a candidate for the degree of July 2009; in the higher study for which this is a record was carried out in the University of St Andrews and the Universität Leipzig between 2008 and 2013.

Date: 21st February 2013 Signature of candidate:

I hereby certify that the candidate has fulfilled the conditions of the Resolution and Regulations appropriate for the degree of PhD. in the University of St Andrews and that the candidate is qualified to submit this thesis in application for that degree.

Date: 21st February 2013 Signature of supervisor:

I hereby certify that the candidate has fulfilled the conditions of the Resolution and Regulations appropriate for the degree of Dr. rer. nat. in the Universität Leipzig and that the candidate is qualified to submit this thesis in application for that degree.

Date: 21st February 2013 Signature of supervisor:

In submitting this thesis to the University of St Andrews and the Universität Leipzig I understand that I am giving permission for it to be made available for use in accordance with the regulations of the University Library for the time being in force, subject to any copyright vested in the work not being affected thereby. I also understand that the title and the abstract will be published, and that a copy of the work may be made and supplied to any bona fide library or research worker, that my thesis will be electronically accessible for personal or research use unless exempt by award of an embargo as requested below, and that the library has the right to migrate my thesis into new electronic forms as required to ensure continued access to the thesis. I have obtained any third-party copyright permissions that may be required in order to allow such access and migration, or have requested the appropriate embargo below.

The following is an agreed request by candidate and supervisor regarding the electronic publication of this thesis:

(i) Access to printed copy and electronic publication of thesis through the University of St Andrews and the Universität Leipzig.

Date: 21st February 2013 Signature of candidate:

Date: 21st February 2013 Signature of supervisor:

Date: 21st February 2013 Signature of supervisor:

Acknowledgements

First and foremost, I would like thank Derek, without whom I would be half the chemist I am today. Thank you for believing in me, supporting me and giving me the odd nudge when I needed it. Thanks also must go to Alex, who has offered endless support and natters, just as I thought I was going mad. Many thanks go to Prof. Hey-Hawkins, for her help and guidance on the project and for giving me the opportunity to work in her laboratories.

Without the help of the technicians and other academic staff in analysis, none of this work would have been characterised. Many thanks therefore are needed to go to Tomas and Melanja in NMR (extra thanks to Tomas for putting up with my less than intelligent questions), Caroline Horsburgh in MS, Stephen Boyer at London Met for the experimental analyses and a massive thanks to Alex and Team Crystallography, for all their work on solving my 'I made something' efforts. Here I must also mention Bobby Cathcart for his unending banter and all those in the workshops, stores and offices.

I must also thank the conglomerate for an enjoyable experience both in the lab and in the pub. I am indebted to Dr. Ken Armstrong and Matt Ray for teaching me the rules of football, Dr. Brian Morton for teaching me the rules of fashion and Dr. Paul Waddell for filling in the vast gaps between. Special thanks go to Fergus and Lynzi for reading and correcting my book and their diplomacy for never once saying it was dull. Becca, Lucy and Marie, my Mafia, I thank for their support and love, as well as destroying my house and my sleep patterns and of course Fergus for employing us all. I thank Conor for the countless cups of tea, Kasun, Joy and Paula for being the shiny, happy and smily people that they are and Surge for the banter. A big shout out must go to the UEA gang, without whom I would have gone mental in the final six months. Dr. Mould: We did it.

To my girlies: Alex, Dani, Ini, Lynzi, Sarah and Zoe thank you for putting up with my moaning, stress and tears, but also giving me the love and support that I need. Thanks for reminding me that I am both not as clever as I make out to be and yet also smarter than I think I am. I feel I must also give a special mention to gin here, and his girlfriend tonic, without whom I would be more well off, but a lot more stressed.

Ich möchte mich bei Dr. Sebastian Bauer, Dr. Carolin Limburg, Dr. Steffen Tschirschwitz und Dr. Matthias Scholz bedanken für ihre Hilfe, Unterstützung und all ihre Ratschläge im Labor. Ich habe eine wunderschöne Zeit in den Leipziger Laboren gehabt und ihre Weisheit war nicht zu toppen! Zunächst möchte ich mich bei all denjenigen im AK H^2 bedanken, insbesondere Ivana, Julian, Tobi, Paul und Susi die mich während der Promotion unterstützt haben. Ein besonderen dank gilt an Tobi und Sebastian für das Korrekturlesen.

Mein Dank gilt auch an Dr. Peter Lönnecke für die Messung und Lösung der Kristallstrukturen, Frau Zäbe für die zahlreiche NMR-Messungen, Frau Scholz für die Aufnahme der IR-Spektren, sowie Fr. Oehme für die Aufnahme der Massenspektren und den Herren Eckert und Fatum für die Anfertigung und Reparatur von Glasgeräten.

An Frau Aust: Danke danke danke, für all die Unterstützung, Liebe und Hilfe die du mir immer gegeben hast als ich sie brauchte. An mein kleines Brüderchen: *That face*. An Jule, Steffen, Anna, Basti und Nicole, Team Arschtritt: ich hätte es nie geschafft ohne eure Unterstützung. Tausend mal dank! An die Herren Groß, Eschberger, Hirschfeld und Geigenmüller, Team Gin: stellt mal den Hendrick's kalt und bereitet schonmal das Boot vor, ich bin gleich wieder da.

An den Chemie-, Ba-Hu- und mittlerweile auch Medielferrat, sowie alle Leiziger Studentenclubs: Ihr seid die Besten. Vielen lieben dank für die Erinnerungen, den Spass sowie den Schwachsinn, der dazu gehört hat, Mitglied im Elferrat zu sein. Es war mir eine Ehre, bleibt so wie ihr seid und behaltet eure Narrheit.

To Mum, Dad, my Maffew and the rest of the supporting cast I call my family:

Thanks to all of you for being there and doing what you do best: Picking me up when I'm down and helping me see the lighter side of life. Without you guys I would be lost!! Oh and thanks to Skimble for 'writing' the whole thing for me/with me.

One final question though… Chemiker, wo seid ihr?

Abstract

Phosphorus-Selenium chemistry has seen a surge in development over the last five to ten years thanks to the optimisation of the synthesis of 2,4-diphenyl-1,3,2,4-diselenadiphosphetane-2,4-diselenide, Woollins' Reagent. This selenium analogue of the well known Lawesson's Reagent has proved itself to be a valuable asset to modern inorganic chemistry, providing a route to novel heterocycles, as well as acting as a selenation reagent with a wide range of functional groups.

A series of new ammonium phenylphosphonamidodiselenoate ligands were synthesised *via* the reaction of Woollins' Reagent with a range of amines. The products were obtained in high yields and could be used as ligands for the synthesis of novel metal complexes. The reaction of diisopropylamine *N*-isopropyl-*P*-phenylphosphonamidodiselenoate with nickel(II) acetate produces a dimeric structure, whilst the reaction with copper(II) acetate yields a beautiful cluster of the form $Cu_6Se_3L_6$.

The phenylphosphonamidodiselenoate ligands were further reacted with a range of *cis*-$Pt(PR_3)_2Cl_2$ complexes to form a library of 20 novel compounds, which were studied by $^{31}P\{^1H\}$, $^{77}Se\{^1H\}$ and $^{195}Pt\{^1H\}$ NMR spectroscopy. The X-ray crystal structure of one of these compounds was obtained, which confirmed the atom connectivity and spatial arrangement of the complexes and the geometry around the platinum centre.

During investigations into the above-mentioned platinum complexes, it was postulated that an increase in steric bulk of the phosphine ligands would aid crystallisation of the products. As such, trimesityl-, dimesitylphenyl- and mesityldiphenyl phosphine were synthesised and reacted with elemental sulfur and selenium and hydrogen peroxide, as well as $Pt(cod)Cl_2$ and $K_2[PtCl_4]$, yielding nine new structures, all of which were characterised by X-ray crystallography, $^{31}P\{^1H\}$, $^{13}C\{^1H\}$ and ^1H NMR spectroscopy.

Finally Woollins' Reagent was reacted directly with a selection of metal complexes, yielding some new insights into its reactivity with inorganic moieties, which has been relatively sparsely reported until now.

Referat

In den letzten fünf bis zehn Jahren hat die Phosphor-Selen Chemie einen Anstieg der Entwicklung gesehen, dank der Optimierung der Synthese von 2,4-Diphenyl-1,3,2,4-diselenadiphosphetane-2,4-Diselenid, Woollins' Reagenz. Dieses Selenanalogon des bekannten Lawesson's Reagenz hat sich als eine wertvolle Bereicherung für moderne anorganische Chemie bewiesen, das eine neue Route zu neuartigen Heterocyclen beschaffen hat. Man kann Woollins' Reagenz auch als ein Selenierung Reagenz für eine Vielzahl von funktionellen Gruppen einsetzen.

Eine Reihe neuer Ammoniumphenylphosphonamidodiselenoat Liganden wurde durch die Reaktion von Woollins' Reagenz mit einer Reihe von Aminen synthetisiert. Die Produkte wurden in hohen Ausbeuten erhalten und konnten als Liganden für die Synthese von ungewöhnlichen Metallkomplexen verwendet werden. Die Umsetzung von Diisopropylamin N-Isopropyl-P-phenylphosphonamidodiselenoat mit Nickel(II) acetat ergibt eine dimere Struktur, während die Umsetzung mit Kupfer(II) acetat einen Cluster der Form $Cu_6Se_3L_6$ produziert.

Die phenylphosphonamidodiselenoat Liganden wurden mit einer Reihe von *cis*-$[PtCl_2(PR_3)_2]$ Komplexen umgesetzt, um eine Bibliothek von 20 neuen Verbindungen herzustellen. Die neue Verbindung wurden durch $^{31}P\{^1H\}$-, $^{77}Se\{^1H\}$- und $^{195}Pt\{^1H\}$-NMR Spektroskopie charakterisiert. Die Kristallstruktur von einer dieser Verbindungen wurde durch Einkristallröntgenstrukturanalyse erhalten. Dies bestätigt die Atomkonnektivität und räumliche Anordnung der Komplexe und die Geometrie um das Platinzentrum.

Während die oben genannten Untersuchungen an den Platinkomplexen durchgeführt wurden, wurde postuliert, dass eine Erhöhung der sterischen Hinderung der Phosphanliganden die Kristallisation der Produkte erleichtern könnte. Somit wurde Trimesityl-, Dimesitylphenyl-und Mesityldiphenylphosphan synthetisiert und mit elementarem Schwefel, Selen und Wasserstoffperoxid, sowie $[PtCl_2(cod)]$ und $K_2[PtCl_4]$ umgesetzt. Dadurch konnten neun Strukturen erhalten werden, die alle durch Kristallographie, $^{31}P\{^1H\}$-, $^{13}C\{^1H\}$- und ^1H-NMR-Spektroskopie charakterisiert wurden.

Zuletzt wurde Woollins’ Reagenz direkt mit eine Auswahl von Metallkomplexen umgesetzt um Einblick in seiner Reaktivität mit anorganische Substanzen zu erhalten, da diese bis jetzt relativ wenig erforscht wurden.

Contents

List of Abbreviations

Aq	Aqueous
BenzA	benzyl amine
BenzAWR	The *N*-benzyl-*P*-phenylphosphonamidodiselenoate ligand
BuLi	butyllithium
Chiraphos	bis(diphenylphosphino)butane
cod	cyclooctadiene
Cp	cyclopentadiene
DCM	dichloromethane
diPr	diisopropylamine
DMAD	dimethyl acetylenedicarboxylate
dppe	1,2-bis(diphenylphosphino)ethane
Et	ethyl
Fc	ferrocene
^{i}Pr	isopropyl
^{i}PrA	isopropylamine
^{i}PrAWR	The *N*-isopropyl-*P*-phenylphosphonamidodiselenoate ligand
IR	infrared
LR	Lawesson's Reagent
Me	methyl
Mes	mesityl
^{n}Bu	*n*-butyl
^{n}BuA	*n*-butylamine
^{n}BuAWR	The *N*-butyl-*P*-phenylphosphonamidodiselenoate ligand
nbd	norbornadiene
NMR	Nuclear Magnetic Resonance
Ph	phenyl
Phox	phosphinooxazoline
^{s}Bu	*sec*-butyl
^{s}BuA	*sec*-butyl amine

^{s}BuAWR	The *N*-*sec*-butyl-*P*-phenylphosphonamidodiselenoate ligand
^{t}Bu	*tert*-butyl
^{t}BuA	*tert*-butyl amine
^{t}BuAWR	The *N*-*tert*-butyl-*P*-phenylphosphonamidodiselenoate ligand
THF	tetrahydrofuran
TMEDA	tetramethylethylene diamine
WR	Woollins' Reagent

NMR Spectroscopy Abbreviations

Ar	aryl
bs	broad singlet
Cq	quaternary carbon
d	doublet
dd	doublet of doublets
Hz	Hertz
m	multiplet
ppm	parts per million
pt	pseudo triplet
q	quartet
s	singlet
sep	septet
t	triplet

IR Spectroscopy Abbreviations

m	medium
s	strong
w	weak
vs	very strong

List of Tables

Chapter 2

Chapter 3

Chapter 4

Chapter 5

Chapter 6

List of Figures

Chapter 1

Chapter 2

Chapter 3

Chapter 4

Chapter 5

Chapter 6

1. Introduction

1.1 Phosphorus-Chalcogen Chemistry

Phosphorus-chalcogen chemistry has been established and researched for over a hundred years. It is of great interest as it is so wide-reaching and varied, encompassing a large array of small molecules right up to large polymeric substances. The smallest scale molecules contain solely phosphorus and chalcogen atoms, in the form P_xE_y (where E = O, S or Se), whilst small heterocycles containing three to four atoms are also well reported.[1] At the other end of the spectrum, large biological macromolecules and metal-based clusters are also of prominence.[2]

Whilst phosphorus-oxygen and phosphorus-sulfur compounds and cages have been extensively explored, investigated and synthesised, much less is known of their heavier cousins containing selenium. It was noted by Sowerby[3] in 1987 that, although such compounds theoretically exist, their chemistry is (probably) more limited and had been much less researched. This is still mostly true today, though selenium chemistry has seen greater interest since the discovery of the 21st amino acid, selenocysteine. Indeed there are almost 25 times more structures containing a phosphorus-sulfur bond than there are containing a phosphorus-selenium bond, at the time of writing, reported in literature on the Scifinder database.[4] These types of compounds have a great many uses in established industries as well as modern chemistry, from flame retardant additives,[5] extreme pressure additives in gear oil,[6] 'strike anywhere' matches, drying agents, flotation agents for zinc and lead sulfur ores and pesticides,[7] to useful reagents for thionation and selenation in synthesis.

1.2 Phosphorus-Chalcogen Binary Structures

1.2.1 **Phosphorus-Oxygen Compounds**

Phosphorus-oxygen cages are amongst the most important compounds of phosphorus.[8] The most basic phosphorus oxide is P_4O_6 (Figure 1.1), which can be produced in the oxidation of P_4 in a 75% oxygen to 25% nitrogen atmosphere, or by reaction with N_2O.[9]

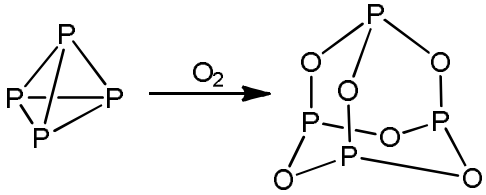

Figure 1.1: P_4O_6, produced by the oxidation of the P_4 cage

The oxygen inserts into each of the P-P bonds, giving the P_4O_6 structure with tetrahedral symmetry. The structure is made up of four 6-membered P_3O_3 rings, has a remarkably low melting point and is soluble in non-polar solvents.[10] Upon heating P_4O_6, similar structures, with varying numbers of external oxygen atoms and P(V) centres, can be obtained (Figure 1.2).

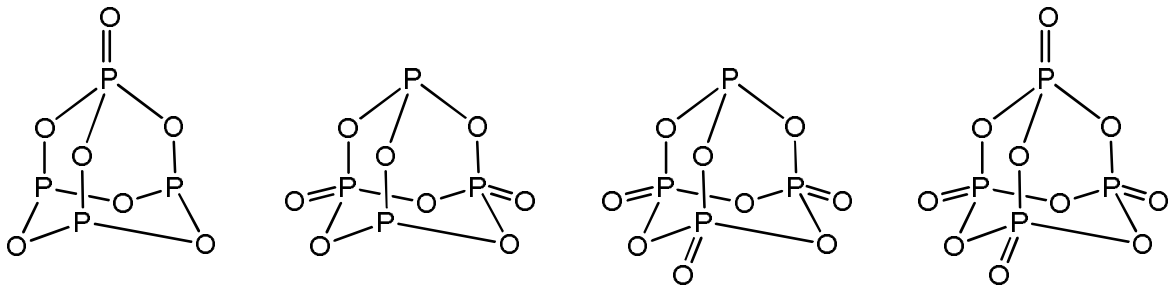

P_4O_7 **P_4O_8** **P_4O_9** **P_4O_{10}**

Figure 1.2: Further oxidised P_4O_6 clusters

Phosphorus pentoxide (P_4O_{10}) is the most important and common oxide of these structures and is produced by the complete combustion of P_4 or by further oxidation of P_4O_6. Additionally, P_4O_{10} can be hydrolysed to give H_3PO_4, whilst the hydrolysis of P_4O_6 yields H_3PO_3.[11]

1.2.2 **Phosphorus-Sulfur Compounds**

Of the chalcogenides, sulfur has the most binary compounds, with nine well-defined examples of the formula P_4S_n. The first examples of these compounds were synthesised by heating sulfur with red phosphorus in an inert atmosphere in the corresponding stoichiometries, or by reacting sulfur and white phosphorus under reflux at high temperatures.1 Other phosphorus sulfides have been afforded by novel syntheses and further examples have been isolated as side products thereof. All of these compounds are based on the P_4 unit, with structures similar to the oxide analogues. However, only P_4S_9 and P_4S_{10} are actually analogous to the lighter congeners (Figure 1.3).

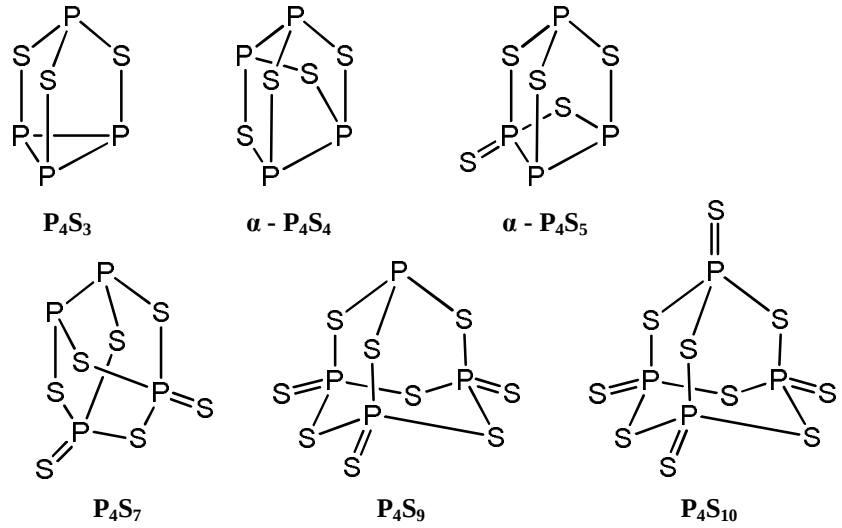

Figure 1.3: Examples of phosphorus sulfides

Of the sulfides shown above, P_4S_3, whose conformation is of an interest as it retains the P_3 ring, is the most stable. It is also of importance as it is widely used in 'strike anywhere' matches, a use discovered by Cahen and Sévène in 1898. P_4S_3 reacts with $KClO_3$ on contact with a rough surface, igniting the match head.[6] P_4S_{10} is, however, by far the most produced of these compounds and is used in organic synthesis as a thionation agent or as a precursor to organothiophosphorus compounds.[12] Industrially, P_4S_{10} is also used in the preparation of lubricant additives and pesticides.

1.2.3 **Phosphorus-Selenium Compounds**

There are fewer well-characterised phosphorus selenides. These are generally much more reactive and less stable than their oxide and sulfide counterparts, owing to the weaker bonds therein. The smallest of these compounds is P_2Se_5, which is not at all analogous to any of the phosphorus oxide or sulfide compounds, but instead takes the form of norbornane,[13, 14] wherein two phosphorus atoms are formally in oxidation state three, bonded to three selenium atoms. P_4Se_4 can also take this form, however, each 'norbornane' consists of a P_4Se_3 unit, with the 4th selenium atom bridging to the next molecule (Figure 1.4).[15]

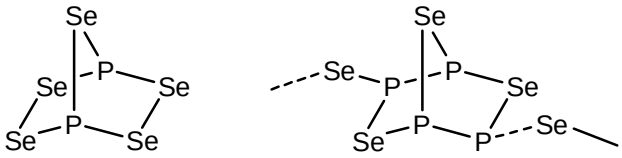

P_2Se_5 **P_4Se_4**

Figure 1.4: Structures of P_2Se_5 and P_4Se_4

This lesser known motif for P_2Se_5 can either be produced by tempering P_2Se_5 glass above its glass transition temperature, followed by a long extraction with CS_2 or alternatively be achieved by using $P_4Se_3I_2$ as the starting material and systematically replacing two of the PI groups with a selenium atom. P_2Se_5 is then obtained as the decomposition product of the monoiodide.[13] Lathrop and Eckert[16] suggested that the P_4Se_4 structure in Figure 1.4 exists as a dimer. However, Blachnik *et al.*[15] counter this view by stating that P_4Se_4 does not crystallise well even after longer tempering times, which in turn does not allow for good crystal data. This property, considered with the fact that the product is insoluble in all organic solvents, suggests a polymeric structure instead of single molecules.

There are two further forms of P_4Se_4 which adopt conformations analogous to that of α-P_4S_4 and β-P_4S_4 (Figure 1.5), which can be handled in air. An allotropic transition between the two can be observed upon heating to 300 °C.

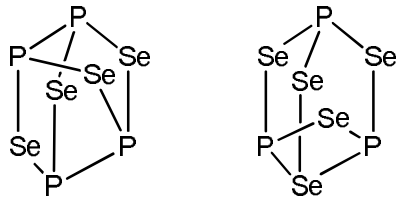

Figure 1.5: α-P_4S_4 (L) and β-P_4S_4 (R)

P_4Se_3, P_4Se_5, P_4Se_7 and P_4Se_{10} all adopt the same conformation as their equivalent sulfides (see Figure 1.6). It is interesting to note that phosphorus pentaselenide has two distinct structures, P_2Se_5 and P_4Se_{10}, unlike phosphorus pentasulfide, P_2S_5 and P_4S_{10} or phosphorus pentaoxide, P_4O_{10}.

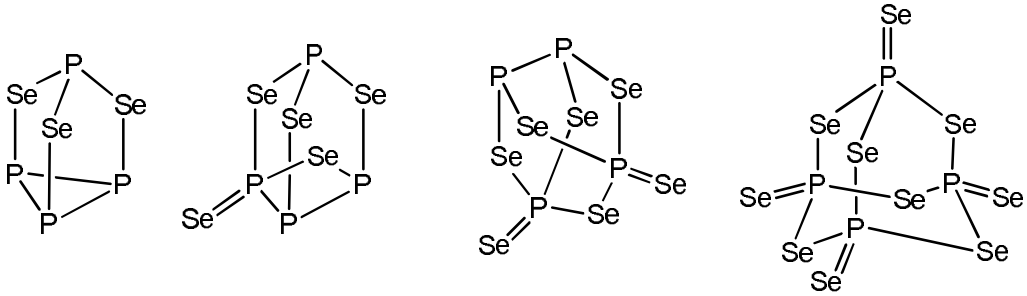

Figure 1.6: (L-R) The structures of P_4Se_3, P_4Se_5, P_4Se_7 and P_4Se_{10}

Penney and Sheldrick[17] reported that when P_4Se_3 is reacted with bromine in CS_2, then the mixture is set aside for three days in diffuse light, P_4Se_5 crystals can be obtained in an analogous reaction to that of P_4S_3. P_4Se_7 on the other hand, could only be synthesised as a Lewis base adduct in the reaction of – for example – pyridine and P_2Se_5, which were refluxed together for 48 hours, then washed with dry benzene.[18] In 1974, Monteil and Vincent[19] heated a mixture of selenium and red phosphorus to yield P_4Se_{10} and the then unknown P_4Se_4 and charted the transitions from P_4Se_{10} to P_4Se_4 *via* a P_4Se_3 intermediate, see Figure 1.7.

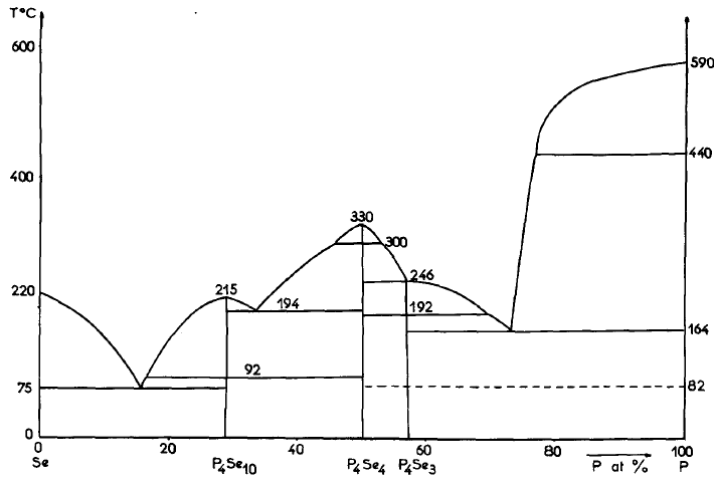

Figure 1.7: Monteil and Vincent's phase diagram of the reaction of red phosphorus with selenium[19]

Further applications and reactions of the phosphorus selenides are very scarcely reported. Early work from Behrens and Haschka[20] and Zingaro *et al.* reported on reactions of phosphorus pentaselenide with ammonia and alcohols[21] and amines[22] respectively. The reaction of P_2Se_5 with a range of alcohols yield O,O'-dialkyldiselenophosphates, which can only be isolated by further reaction with KOH to form their potassium salts. The products, formed *via* the equation shown below (Equation 1.1), can then be reacted with chromium(III) chloride to produce the tris(O,O'-dialkyldiselenophosphato) chromium(III) product shown in Equation 1.2.

$$4\ ROH + P_2Se_5 \xrightarrow{\text{Heptane}} 2(RO)_2P(Se)SeH + H_2Se \qquad \textbf{Eqn. 1.1}$$

$$2(RO)_2P(Se)SeH + CrCl_3.6H_2O \xrightarrow{\text{EtOH}} Cr[Se_2P(OR)_2]_3 + 3HCl + 6H_2O \qquad \textbf{Eqn. 1.2}$$

More recent research by Chondroudis and Kanatzidis[23] has looked at reactions with metals and the formation of one-dimensional selenodiphosphates of the form $A_2MP_2Se_6$, where A is an alkali metal, (either K, Rb or Cs) and *M* is a late transition metal, such as Pd, Zn, Cd or Hg. Limited selenation reactions and reactions with phosphorus selenide glasses have also been reported by Tejchman *et al.*[24] and Sokolov and co-workers.[25]

1.3 Phosphorus-Chalcogen Containing Compounds

1.3.1 **Phosphorus-Chalcogen Containing Heterocycles**

A great number of phosphorus-chalcogen containing heterocycles are known to exist, of which a large proportion contain exclusively phosphorus and at least one chalcogen atom, the simplest form being P_2E, where E can be S, Se or Te, see Equations 1.3 and 1.4.

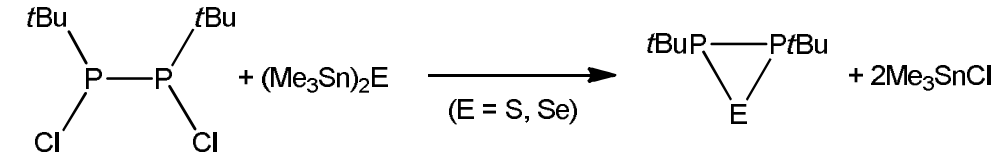

Eqn 1.3[26]

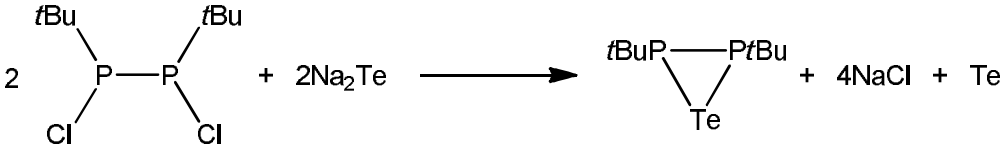

Eqn 1.4[27]

Of these heterocyclic compounds, dithiadiphosphetane disulfides (P_2S_2 species) and their selenium analogues (P_2Se_2 species) have become of interest, owing to their ability to perform thionation and selenation reactions. These substances, in particular the sulfur analogues, are the most studied, due to their hydrolytic and thermal stability. Heterocycles containing selenium are also of interest as they are potentially biologically active, with possible antitumor and antiviral activity.[28]

1.3.2 **Phosphorus-Sulfur Heterocycles**

As early as 1943 US patents were reporting the reaction of alcohols, alkenes and cycloalkenes with phosphorus pentasulfide.[29] The products of these reactions have interesting properties as oil additives. Following this, Fay and Lankelma[30] investigated similar reactions of cyclohexene and Lecher *et al.*[31] turned their interests to aromatic compounds including benzene, *o*-xylene and anisole to name but a few. Each of these products exhibited the dithiadiphosphetane structure, a four membered ring with alternating phosphorus and sulfur atoms. It was noted that the reaction with anisole could be performed easily and a high yield was obtainable. Starting in the late 70s, Lawesson and co-workers performed intense research into the properties and reactions of the product, 2,4-bis(*p*-methoxyphenyl)-1,3-dithiadiphosphetane-2,4-disulfide,[37] making it a well known reagent for thionation and thus dubbing it Lawesson's Reagent,[32] *LR*, which is discussed in further depth in Section 1.3.3.

1.3.3 **Lawesson's Reagent**

The reaction of P_4S_{10} with differing aryl substrates yields a wealth of dithiadiphosphetane disulfides, *via* a convenient and relatively simple synthesis.[37] These reactions are also high yielding and the products can be used for a range of thionation reactions. The most prolific member of this class of compounds is $[(p\text{-}MeOC_6H_4)P(S)(\mu\text{-}S)]_2$, which has been known for many years as Lawesson's Reagent (*LR*), shown in Figure 1.8.

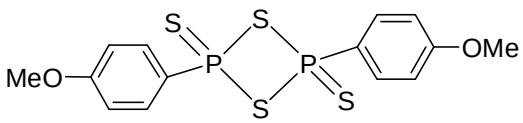

Figure 1.8: Lawesson's Reagent

During the past 50 years Lawesson's Reagent has become one of the thionating reagents of choice as it gives high yields, is easy to handle, simple to synthesise and only decomposes in solution at temperatures in excess of 110 °C.[33] Other more

'classical' reagents, such as P_4S_{10} require large excesses and often require longer reaction times and provide much lower yields. Another option is to use hydrogen sulfide, however this reaction requires an acid catalyst and is also not overly successful: the products of such reactions are often the cyclic trimers of the desired thiocarbonyl.[34] Lawesson's Reagent, however, has a much higher success rate, is commercially available and can be reacted with a wide array of substrates from small molecules such as methyl benzoate to large steroid structures[35] and cyclic peptides.[36] Furthermore, reactions with Lawesson's Reagent are carried out in almost equimolar ratios (unless at temperatures above 110 °C, where a slight excess of *LR* is needed to allow for decomposition products) and most products are easily purified.

Lawesson proved that this reagent is very versatile: he and his co-workers reported the smooth conversions of aromatic and aliphatic ketones to thioketones, esters to thionoesters,[37] pyranones to pyranthiones[38] and amides to thiocarboxamides,[39] amongst many other reactions, a selection of which are summarised in Figure 1.9.

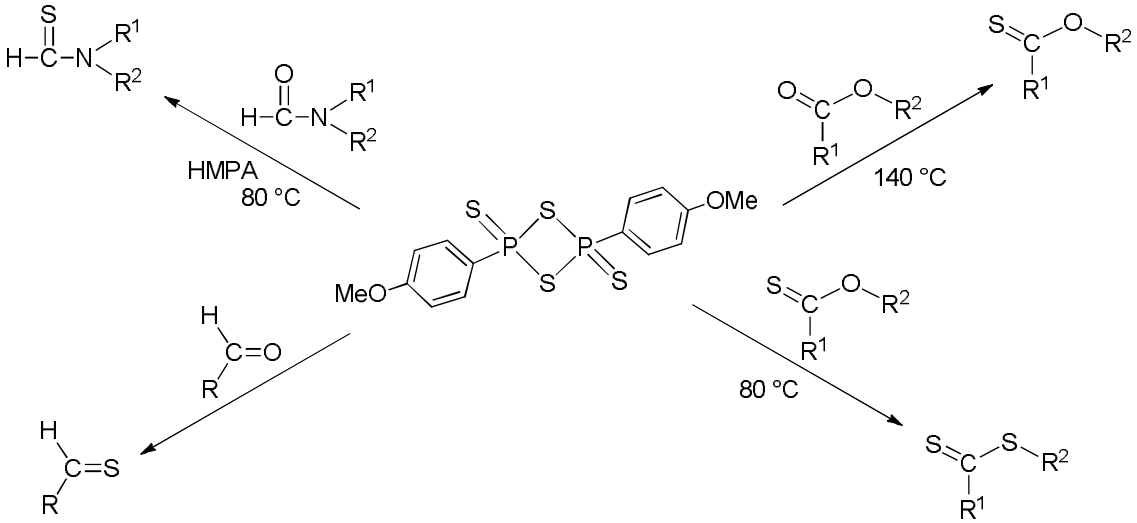

Figure 1.9: A selection of reactions of Lawesson's Reagent

More recently, increasingly complex molecules have been reacted with *LR*, yielding diazaphospholines and azaoxaphospholines as well as a host of other four to seven-membered ring systems.[33] Reactions with transition metal complexes, transformations of alcohols to thiols and the synthesis of thiacage compounds confirm that *LR* is an all-purpose reagent for novel sulfur-containing compounds.

1.3.4 **Phosphorus-Selenium Heterocycles**

The reaction between selenium and the $(PhP)_5$ pentamer yields a great number of phosphorus-selenium heterocycles with varying phosphorus:selenium stoichiometries (Figure 1.10). Reacting the $(PhP)_5$[44] with 1.25 equivalents of selenium affords a P_4Se ring structure, whilst a 1:3.33 ratio yields a P_3Se_2 pentamer. Further increasing the ratios to 1:5 and 1:10 results in oxidation of the phosphorus centre, to give compounds with exocyclic selenium atoms double bonded to a five- and four-membered ring, respectively. Product **4**, shown below, has become known as Woollins' Reagent, *WR*, and is discussed in greater detail in Section 1.3.5.

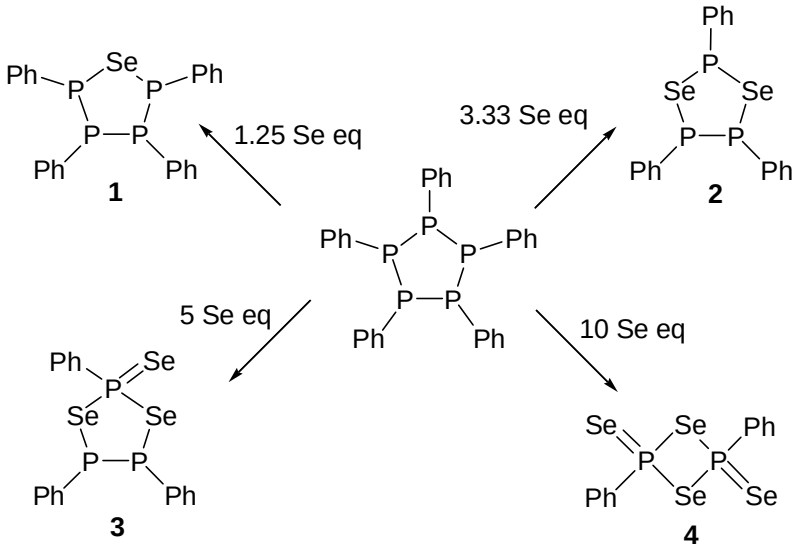

Figure 1.10: Reactions of $(PhP)_5$ with different amounts of selenium

The reduction of the $(PhP)_5$ pentamer with elemental potassium opens the ring, forming a four-membered phosphorus chain intermediate, which can then be further reacted with elemental selenium, as shown in Figure 1.11. The products on the left hand side of the diagram are obtained when R = H and the P_4C pentamer is reacted with nine equivalents of selenium. Similarly, the products on the right are yielded when R = Me and the central pentamer is also reacted with nine equivalents of selenium.[40]

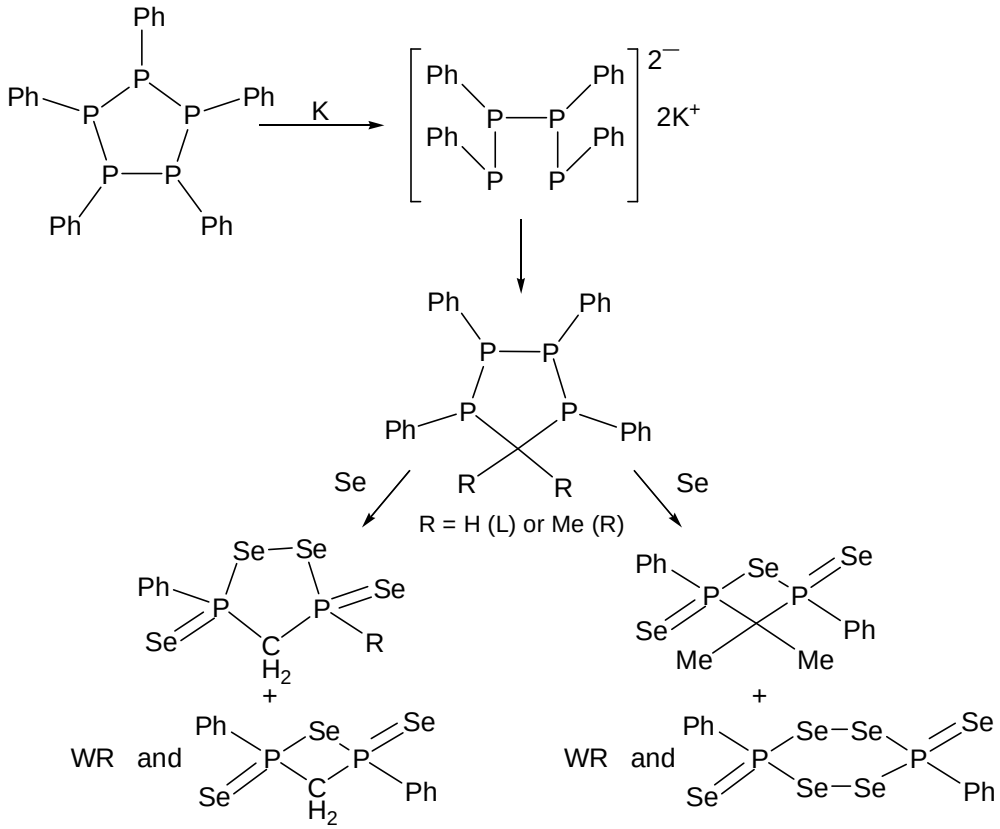

Figure 1.11: Further PSe heterocycles

Other phosphorus selenium heterocycles include the eight-membered P_3Se_5 ring, which is produced by the reaction of a phosphine with elemental selenium.[41] Further heterocycles containing phosphorus and selenium are discussed later in Section 1.3.5.1.

1.3.5 **Woollins' Reagent**

Whilst phosphorus-sulfur P_2S_2 heterocyclic compounds can be relatively easily synthesised by simple processes,[42] there is no simple standardised method for obtaining a wide range of P_2Se_2 rings. The first example of these compounds, 2,4-bis(*tert*-butyl)-1,3,2,4-diselenadiphosphetane-2,4-diselenide, was published by Shore *et al.* in 1988[43] and is formed *via* the reaction of dichloro-*tert*-butylphosphine and Li_2Se_2 in benzene. In the last 20 years considerable research into this field has been carried out with methyl, ethyl, butyl, phenyl and its derivatives and ferrocenyl substituents being used as R groups on the phosphorus, shown in Figure 1.12.

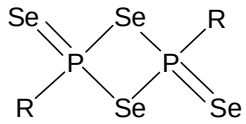

Figure 1.12: General diselenadiphosphetane diselenide structure

In the same year, 2,4-bis(phenyl)-1,3,2,4-diselenadiphosphetane-2,4-diselenide was synthesised by the reaction of cyclic $(PPh)_5$ with metallic selenium, in toluene under reflux, in a one to ten ratio.[44] Varying the pentamer to selenium ratio yields a range of heterocycles, although the most versatile of these has proven to be $(PhPSe_2)_2$, Woollins' Reagent. Although Woollins' Reagent can be successfully synthesised in this way, the method has its drawbacks, e.g., the synthesis of the starting pentamer is not convenient in larger amounts as scaling up affords poorer yields. To this end, a novel synthesis was sought and developed, which allows *WR* to be synthesised on a much larger (150 g) scale *via* the reaction of sodium selenide with dichlorophenyl phosphine in refluxing toluene. The product can be simply filtered off and *WR* is now available commercially from Sigma Aldrich. Extensive research using Woollins' Reagent over the last 15 years has shown that it is a useful, though sparingly soluble reagent: most syntheses must be carried out in refluxing toluene and yields can be low due to a range of products being afforded. It is also due to this limited solubility that the crystal structure of Woollins' Reagent was gained much later in 2001.[45]

1.3.5.1 Reactions with Organic Substrates

It has been shown over recent years that Woollins' Reagent is a highly reactive species. Bhattacharyya *et al.*[46] describe the use of Woollins' Reagent as a selenation agent, in which it exchanges a carbonyl oxygen atom for a selenium atom, producing selenocarbonyl structures, such as the series of selenoamides and selenoaldehydes seen in Figure 1.13.

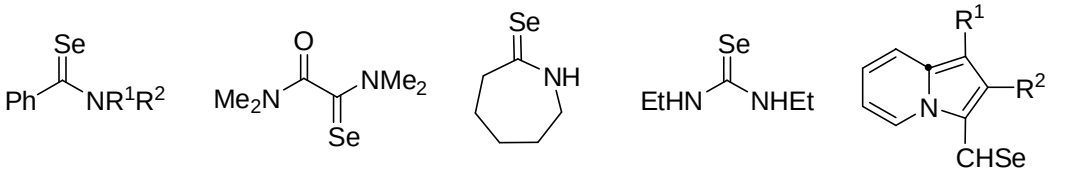

R^1 = Me, R^2 = Me
R^1 = H, R^2 = Me
R^1 = H, R^2 = ^{t}Bu
R^1 = R^2 = H

R^1 = H, R^2 = Me
R^1 = H, R^2 = ^{t}Bu
R^1 = Me, R^2 = ^{t}Bu

Figure 1.13: Selenocarbonyl products formed using Woollins' Reagent

It was shown that *WR* readily converts secondary amides to selenoamides compared to $PhP(Se)Cl_2$ and this publication concluded, that the stability, handling and preparation of the relatively air stable Woollins' Reagent is as good as, if not better than other selenation reagents, such as NaHSe, H_2Se, $(^iBu_2Al)_2Se$, $(Me_3Si)_2Se$ and bis(1,5-cyclooctanediylboryl)selenide.[13]

Primary selenoamides provide a viable route to C-Se-N heterocycles,[47] however a viable route to these reagents was previously unknown. Syntheses using, for example, Se/CO or P_2Se_5/H_2O may require long reaction times, be difficult to handle or have poor reactivity, thus making them undesirable.[48] By reacting selenium metal with $^iBu_2AlH$ to give a mixture of $(^iBu_2AlSe)_2$ and $(^iBuAlSe)_n$, a selenation reagent is produced, which, when reacted further with amides, produces a selenoamide product. The aluminium containing products are, however, unstable, toxic and have an unpleasant odour, leading to them neither being purified nor fully characterised and being used in the second step *in situ*. By contrast, it has been shown, that Woollins' Reagent can be used for the hydroselenation of aryl cyanides, which proceeds *via* the reaction shown in Scheme 1.1.

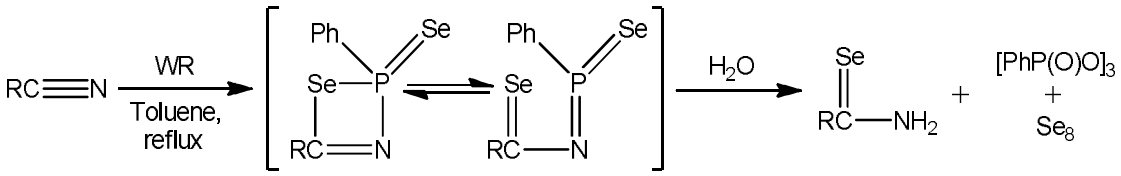

R = C_6H_6, 3-MeC_6H_4, 4-MeC_6H_4, 2,6-$Cl_2C_6H_4$, 4-$(CN)C_6H_4$, 3-$(CN)C_6H_4$, 4-$(O_2N)C_6H_4$, 3,4-$(H_3CO)_2C_6H_3$, 2,4-$(H_3CO)_2C_6H_3$,2,3-$(H_3CO)_2C_6H_3$, 4-$(H_3CO)C_6H_4$, 3-$(H_3CO)C_6H_4$, 2-$(H_3CO)C_6H_4$, 4-ClC_6H_4, 3-ClC_6H_4, 2-ClC_6H_4, 4-FC_6H_4 and 4-BrC_6H_4.

Scheme 1.1: Synthesis of arylselenoamides from aryl cyanides using *WR* and water

A wide range of arylselenoamides can be produced in this way, where the driving force for the second step - the hydrolysis reaction - is the formation of the six-membered ring, with alternating phosphorus and oxygen atoms. The reaction proceeds by refluxing the aryl cyanide with *WR* for 4 hours in toluene until a clear red-brown solution is obtained, before cooling to room temperature, adding water and continuing refluxing for a further hour.

Woollins' Reagent has also shown itself to form interesting heterocycles on reaction with unsaturated carbon-carbon bonds, such as reactive acetylenes and selected cyclic alkenes. On reaction with Woollins' Reagent in refluxing toluene, dimethyl acetylenedicarboxylate (DMAD) produces the three different heterocycles shown in Figure 1.14 in varying yields. Only one of the products (**5**) was expected, as it is analogous to the product of the reaction of phenylacetylene and *WR* also in refluxing toluene (Figure 1.14).[49] It has also been reported that Woollins' Reagent reacts with methyl phenylpropiolate in much the same way as DMAD also affording three products.[50] One of these products (**9**) is the expected transformation and also analogous to the dimethyl acetyledicarboxylate product. The second product (**10**) is an isomer of (**9**), where the carboxylate is closer to the phosphorus atom in the heterocycle, whilst the third product retains the selenium-selenium bond in the ring but has the phosphorus-containing moiety in an exocyclic position on the other side of the ring.

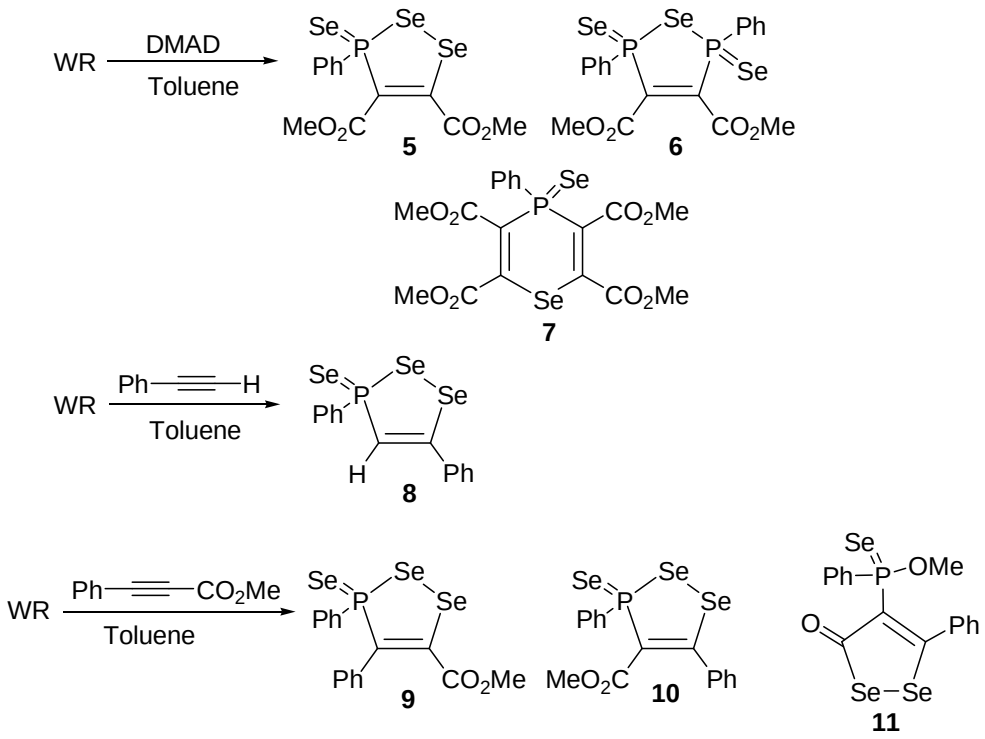

Figure 1.14: Heterocycle formation from alkynes

Similar and related products have also been obtained with diynes[51] and azobenzene, where four- and five-membered heterocyclic rings can be obtained in the first instance and a four-membered P-Se-P-N ring was formed in the latter.[45] Other applications of Woollins' Reagent include use as a deoxygenating/coupling reagent via a reductive dimerisation of a range of aldehydes and ketones. The products of such reactions are symmetrical and unsymmetrical *E*-alkenes, as well as less expected heterocyclic systems.[52]

1.3.5.2 Reactions with Metal-containing Compounds

Parkin *et al.*[53] described the first synthesis of $PPtSe_2$ rings *via* the direct reaction of Woollins' Reagent with a range of platinum chlorides in the form *cis*-$PtCl_2(PR_3)_2$, where PR_3 = ½ dppe, PEt_3, PPh_2Me and PMe_2Ph. The products were obtained in good yields (~70%), with the reaction carried out in either liquid ammonia at -78 °C or THF at room temperature.

Baxter *et al.*[54] describe the use of Woollins' Reagent to selenate a metal complex containing a C=O bond on tungsten and molybdenum metal centres to form

selenoketenyl complexes. The metal complexes used in the reactions were of the form [ML(η^2-OCCR)(CO)(Tp)], where Tp = hydrotris(pyrazol-1-yl)borate), R = $PhOMe_3$ and the phosphorus ligands (L) were PPh_3, PMe_2Ph, $P(OMe)_3$.

Rothenberger's group in Germany have also reported that Woollins' Reagent can be reacted with copper(I)thiolates to give copper complexes. Such reactions yielded unexpected P/Se anions such as $[PhSe_2PPSePh]^{2-}$ or $[PhP(Se)S^tBu]^-$.[55] In other work, they recorded reactions between Woollins' Reagent and KO^tBu, KOAc, CuOAc, $NaOAc{\cdot}3H_2O$ and $NaSe^tBu$, which yielded polymeric organometallic structures, containing, for example $[PhP(O^tBu)Se_2]^{2-}$ anion units bound by two K^+ ions.[56] Such compounds offer new routes to synthesising materials suitable for chalcogen transfer reactions or organometallic coordination polymers.

Looking to larger clusters containing dialkyl diselenophosphate ligands, Fenske and Krautscheid[57] reported the synthesis of $Cu_{20}(\mu_8\text{-}Se)Se_{12}(PEt_3)_{12}$, an exceedingly large, selenide centred Cu_8 cubic cluster. Liu *et al.*[58] reported the synthesis of the first selenide-centred discrete Cu_8 cubane, $\{Cu_8(\mu_8\text{-}Se)[Se_2P(OPr^i)_2]_6\}$, wherein the diselenophosphate ligands bridge each side of the cube. Thereafter they reported several similar novel clusters, including a rare co-crystallising $Ag_8(\mu_8\text{-}Se)[Se_2P(OPr^i)_2]_6$ - $Ag_6[Se_2P(OPr^i)_2]_6$ structure, in which the two structures share a common $Ag_6[Se_2P(OPr^i)_2]_6$ unit, which are discussed in Chapter 2.

Whilst there has been an increasing interest shown in P-Se structures and the use of ligands containing the PSe_2 moiety, it is clear that there are still gaps in the research into these compounds compared to their sulfur containing analogues. Often such species require difficult syntheses and produce low yields. Woollins' Reagent has helped drastically by often providing easier, higher yielding synthetic routes to ligands and novel complexes. Woollins' Reagent has become a well-established selenation reagent, as well as being a useful tool for synthesising heterocycles containing phosphorus-selenium moieties.

The work presented herein intends to expand on existing research in this field, by studying the reactions of Woollins' Reagent and the wide variety of organic substrates with which it has already been reacted, and developing analogous reactions with inorganic substrates. It has already been shown that versatile ligands are produced from

the reaction of *WR* with sodium alkoxides in MeOH or EtOH,[65] and most recently we have detailed the reaction of Woollins' Reagent with some primary amines to produce ammonium phenylphosphonamidodiselenoate ligands.[69] The next stage, therefore, in this research is to take the aforementioned ligands and explore their chemistry with a range of metal centres. With this in mind, seven ligands were synthesised, for use as ligands for platinum phosphine complexes in order to study their properties and NMR spectra.

The properties of eight mesitylphosphine chalcogenide complexes were studied by X-ray crystallography and multinuclear NMR spectroscopy, enabling a more in depth investigation of the effects steric bulk on the geometry of these compounds. *trans*-$Pt(PMesPh_2)_2Cl_2$ was also synthesised, becoming one of the bulkiest platinum phosphine complexes known. The crystallographic Tolman's cone angle of these species is also investigated.

Furthermore, some direct reactions of Woollins' Reagent with inorganic moieties were studied to ascertain if they behave in the same way as their related organic compounds. With this in mind, reactions of *WR* with a range of metal carbonyl complexes were carried out, and the results studied with a variety of analytical methods. The reactions of acetyl ferrocene and derivatives with *WR* were also performed, resulting in a novel heterocycle being synthesised. Lastly, the reaction of Woollins' Reagent with 1,1'-dilithioferrocene or 1,2-dilithio-*closo*-dicarbadodecaborane resulted in the synthesis of an interesting species containing a P-P bond, whose chemistry, whilst beyond the scope of this research, would be an interesting species for further investigation.

2. Ammonium Phenylphosphonamidodiselenoates

2.1 Introduction

The mixed chalcogen sodium diethylselenothiophosphinate[59] and indeed sodium diethyldiselenophosphonate[60] have been known since the sixties, when Kuchen and Knop synthesised the former by the reaction of sodium selenide with the 1,1,2,2-tetraethyldiphosphine 1,2-disulfide dimer, shown in Scheme 2.1.

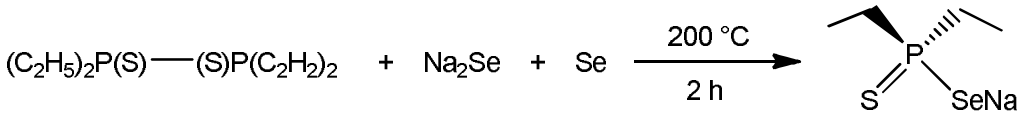

Scheme 2.1: Synthesis of the mixed chalcogenide sodium diethylselenothiophosphinate

Kuchen and Knop's route to the diselenophosphonate is slightly more tricky than that to the mixed chalcogen compound, also proceeding from the 1,1,2,2-tetraethyldiphosphine 1,2-disulfide dimer. Nevertheless, the products of each reaction were subsequently reacted with transition metals (zinc, cadmium, nickel) and metal salts (amongst others $ZnCl_2$, $CdCl_2$ and $PbCl_2$) to form complexes of the type shown in Figure 2.1. There is, however, no NMR data to support these synthetic procedures.

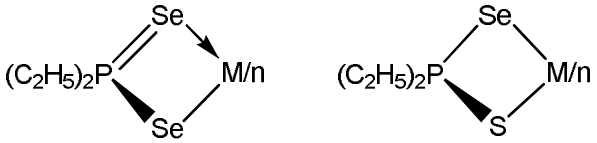

Figure 2.1: Kuchen and Knop's dichalcogenophosphonate complexes

Kuchen and Hertel[61] also studied the metal complexes of thiophosphinic and selenophosphinic acids including the chelating abilities of these ligand systems in discrete monomers and dimers, as well as some coordination polymers of zinc(II) and cadmium(II). Their results are based on IR studies performed by Coates and

Mulcherjee,[62] which confirms the presence of the P-Se bonds by showing peaks between 400 and 500 cm^{-1}. These mirror the values observed in the compounds reported herein.

In the late 1990's and early 2000's research on selenophosphorus ligands was conducted by Davies *et al.*,[63] with a view to investigating semiconducting metal selenides, and the coordination chemistry of diselenophosphonate complexes, such as the tris-(diselenophosphinato)indium complex shown in Figure 2.2.[64] The product was obtained in a 46% yield complexed with THF and the P-Se bonds are of bond order 1½.

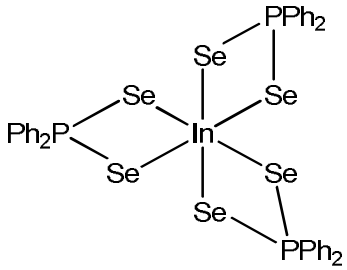

Figure 2.2: tris-(Diselenophosphinato)indium presented by Davies *et al.*

As with all the selenium chemistry reported herein, reactions with metal containing compounds and complexes are much less reported than those of their sulfur analogues. One similar reaction of Woollins' and Lawesson's Reagent is the reaction with sodium alkoxides in the corresponding alcohol. This forms a sodium diselenophosphonate[65] or sodium dithiophosphonate,[66] respectively (Figure 2.3).

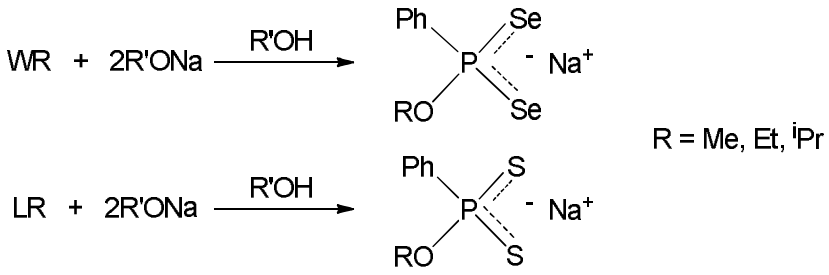

Figure 2.3: Reactions of *WR* and *LR* with sodium alkoxides

The diselenophosphate $[Ph(OR)PSe_2]^-$ anions are unstable in air and to moisture, however soluble in polar solvents. No crystal structure of these diselenophosphonates

has been obtained, however an interesting degradation product of the ligand was obtained, with the cubane-like structure shown in Figure 2.4.

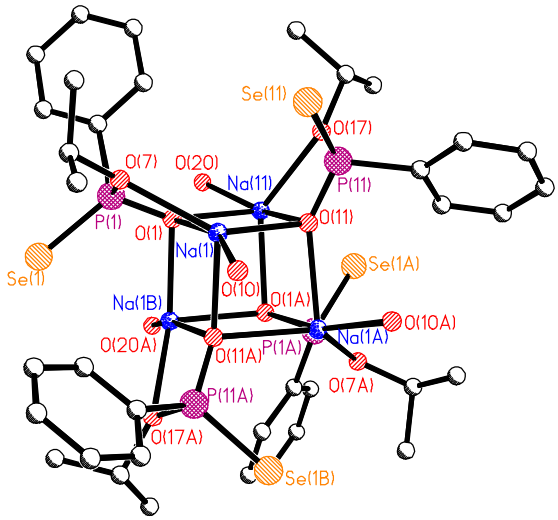

Figure 2.4: Degradation product of $[Ph(O^{i}Pr)PSe_2]^-$ [65]

On dissolving diselenophosphates in the respective alcohol to the R group of the ligand (MeOH, EtOH or ^{i}PrOH), many reactions with transition metal salts can be performed, which allows complexation to a wide variety of metal centres including Ni, Cd, Hg, Pb, Pd, Pt, Sn and Zn. The reaction with nickel(II) chloride gives a square planar complex with two of the diselenophosphate ligands (**Figure 2.5**), whilst utilising the same reaction conditions with a cadmium centre forms a dimeric $[M_2L_4]$ system, see Figure 2.6.

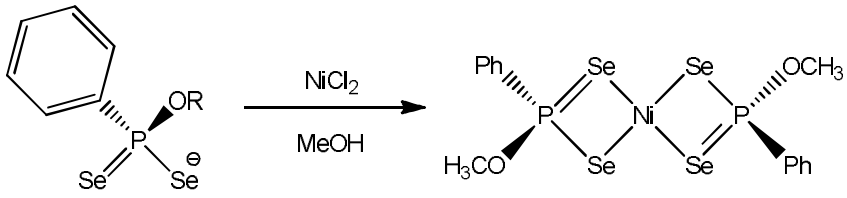

Figure 2.5: Reaction of the (methoxy)phenylphosphonodiselenoate sodium salt with $NiCl_2$ [65]

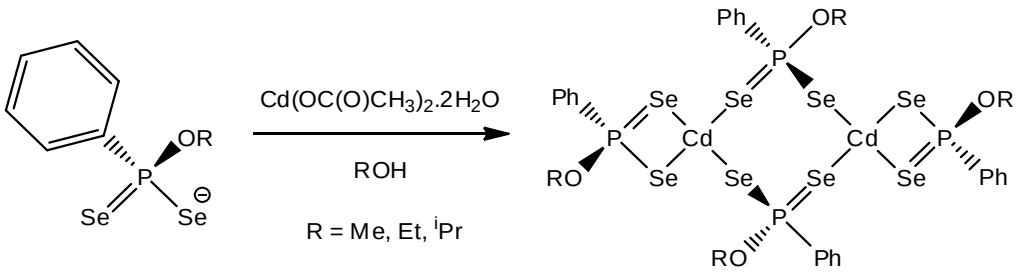

Figure 2.6: Reactions of phenylphosphonodiselenoate sodium salt with cadmium acetate[65]

Whilst monomeric and dimeric species are the most common products of this type of reaction, several 'mega' clusters which contain diselenophosphate ligands have been synthesised over the last decade. In 1998 Liu and co-workers[67] reported the first selenide-centred Cu^{I}_{8} cubic cluster incorporating dialkyl diselenophosphate ligands. The compound in question is $\{Cu_8(\mu_8\text{-}Se)[Se_2P(O^iPr)_2]_6\}$, shown in Figure 2.7, which is synthesised *via* the reaction of $NH_4Se_2P(O^iPr)_2$ with $[Cu(MeCN)_4][PF_6]$ at 0 °C in diethyl ether and was characterised by X-ray diffraction, ^1H and $^{31}P\{^1H\}$ NMR, as well as MS.

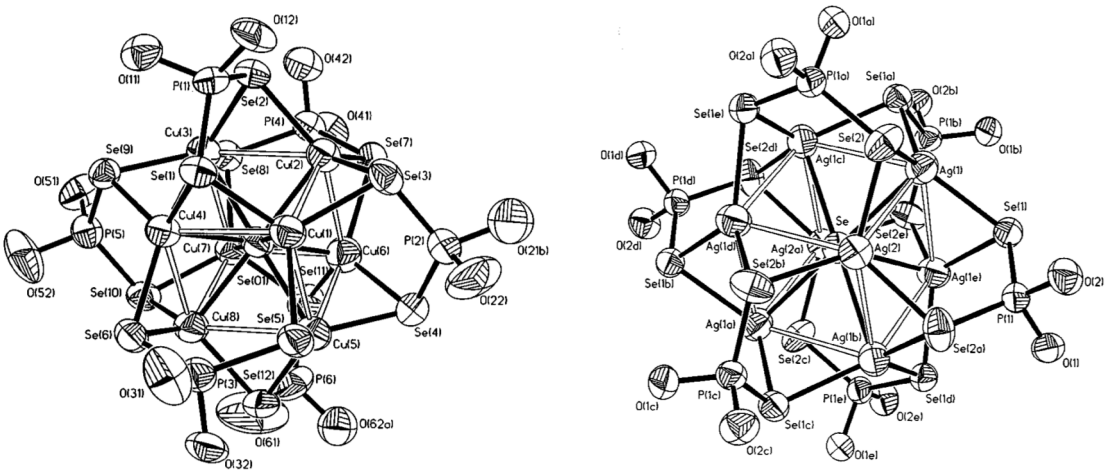

(a) **(b)**

Figure 2.7: **(a)** $\{Cu_8(\mu_8\text{-}Se)[Se_2P(O^iPr)_2]_6\}$[67] and its silver analogue **(b)** $Ag_8(Se)[Se_2P(O^iPr)_2]_6$[68] synthesised by Liu *et al.* Both have isopropyl groups omitted for clarity.

Following the success of the above synthesis, $Ag_8(\mu_8\text{-}Se)[Se_2P(O^iPr)_2]_6$ (Figure 2.7 **(b)**) and $Ag_6[Se_2P(O^iPr)_2]_6$ were synthesised. The interstitial selenium atom has a body centred cubic array with the twelve silver atoms surrounding it. The compound is

analogous with the copper cluster shown in Figure 2.7 **(a)** and is synthesised *via* the reaction of $[NH_4][Se_2P(O^iPr)_2]$ with $[Ag(MeCN)_4][PF_6]$.

Recent research carried out by our group has shown the first ever reported synthesis of ammonium phenylphosphonamidodiselenoates and the first metal complex thereof.[69] Preliminary reactions were performed between Woollins' Reagent and some low boiling amines, whose products are analogous to those presented by Gray *et al.* in 2005. The work reported within this chapter focuses on the synthesis of a selection of $[Ph(NHR)PSe_2]^-$ ligands and further reactions thereof.

2.2 Discussion

2.2.1 **Preparation of Ligands**

The direct reaction of Woollins' Reagent with various amines, without solvent, produces ammonium phenylphosphonamidodiselenates. These compounds are analogous to the previously reported anionic phosphonodiselenoato structures as mentioned above. During the reaction the four membered P_2Se_2 ring of Woollins' Reagent is cleaved to give different products of the type shown in **Figure 2.8** in high yields. These compounds are air and light sensitive, changing colour from colourless or pale yellow to dark oranges and reds on exposure. The $^{31}P\{^1H\}$ NMR spectra of these compounds show singlets in the region of δ_P = 42.0 - 55.8 ppm surrounded by selenium satellites, with coupling constants in the range of $^1J_{P\text{-}Se}$ = 613-634 Hz. The $^{77}Se\{^1H\}$ NMR spectra exhibit doublets with corresponding coupling constants, which confirm the P-Se bonds. These findings will be henceforth discussed in further detail.

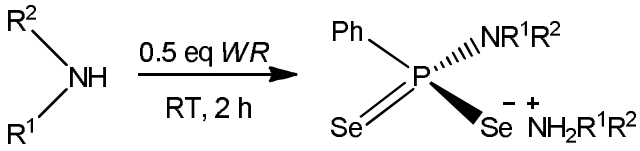

Figure 2.8: General reaction of *WR* with amines

Woollins' Reagent was reacted with an excess of isopropylamine at room temperature using only the amine as a solvent (Equation 2.1). The mixture was left to stir for an hour, in which time the clear solution turned a green-grey colour. On filtration, the solution was found to be bright yellow in colour. The solution was evaporated to dryness, yielding a yellow powder, which could be recrystallised by dissolving in DCM and layering with hexane. The product was characterised by $^{31}P\{^1H\}$, $^{77}Se\{^1H\}$, $^{13}C\{^1H\}$ and ^1H NMR spectroscopy, single crystal X-ray crystallography, mass spectrometry and IR spectroscopy. Both the crude and purified products are light and air sensitive, discolouring to a deep orange colour within 24 hours on exposure. It is thought that this is caused by the expulsion of selenium from the product, although this could not be confirmed by NMR spectroscopy.

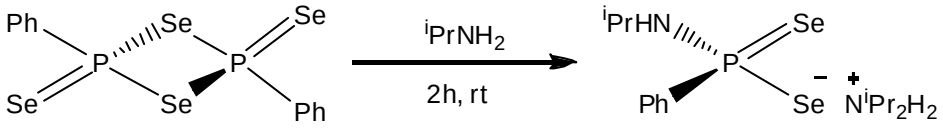

Eqn 2.1

The product of this reaction is slightly unexpected as, although isopropylamine is used in the synthesis, the counter ion of the product is seen to be a diisopropyl species. This is most likely formed from an impurity in the starting material, which was verified by running the ^{1}H NMR spectrum of the isopropylamine starting material. The diisopropylamine impurity is generated during the purification process using CaH_2.[69]

The $^{31}P\{^{1}H\}$ NMR spectrum of diisopropylammonium *N*-isopropyl-*P*-phenylphosphonamidodiselenoate (^{i}PrAWR, **2.1**) showed a single resonance at δ_P = 42.2 ppm, flanked by a set of selenium satellites with a coupling constant of $^{1}J_{P\text{-}Se}$ = 610 Hz and a set of carbon satellites with a coupling constant of $^{1}J_{P\text{-}C}$ = 79.8 Hz. All of these values are expected and correspond to those observed for similar compounds.[65] The presence of only one set of selenium satellites demonstrates that the two selenium atoms are equivalent, and the magnitude of the $^{1}J_{P\text{-}Se}$ suggests a P-Se bond order of 1½.

The $^{77}Se\{^{1}H\}$ NMR spectrum of compound (**2.1**) exhibits a doublet at δ_{Se} = 69.4 ppm with a coupling constant of $^{1}J_{Se\text{-}P}$ = 610 Hz. The peak lies at a chemical shift analogous to those expected of similar compounds.[70]

The $^{13}C\{^{1}H\}$ and ^{1}H NMR spectra of (**2.1**) are indicative of this species. The signals for the carbon atoms within the phenyl ring are all observed as doublets due to coupling to the P atom, with the *ipso*-C having the largest *J* value and the *para*-C having the smallest. The counter ion carbon peaks can be differentiated from the bonded carbon atom peaks as they appear as singlets, not doublets. In the ^{1}H NMR all amine H atoms can be accounted for and the diisopropylamine peaks lie downfield of the isopropylamine peaks.

In the IR spectrum, the νN-H peaks can be seen at 3282 cm^{-1} and 3086 cm^{-1}, the νC-H stretches are observed at 2961 cm^{-1} and 2942 cm^{-1}, a peak of medium intensity at 1470 cm^{-1} indicates the νP-Ph bond stretch and a strong peak at 541 cm^{-1} corresponds to νP=Se. A peak at *m/z* = 325.85 with an intensity of 100% in the mass spectrum corresponds to compound (**2.1**) without its counter ion.

Crystals suitable for X-ray structural analysis were grown and data was obtained on a Rigaku Mercury70 diffractometer with Mo-Kα radiation. The P-Se bond lengths present in (**2.1**) are 2.1562(19) Å and 2.1608(19) Å. The average bond length for a P-Se is 2.222 Å and the average bond length for P=Se is 2.111 Å, according to the CCDC database, indicating the P-Se bonds of (**2.1**) to be of bond order 1.5. The three N-C bonds are all equivalent, as are the N-H bonds, with no lengthening of the N-H bond being observed caused by the H-bonding to the Se atom. **Figure 2.9** depicts the structure of ^{i}PrAWR, whilst the main bond lengths and angles are given in Table 2.1. Further crystallographic data can be found in Appendix 1.

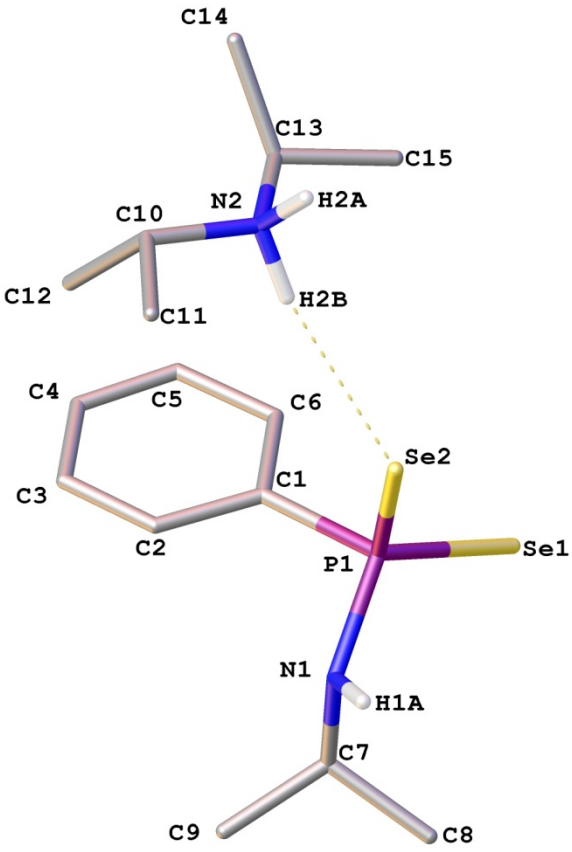

Figure 2.9: X-ray crystal structure of ^{i}PrAWR, (**2.1**).
C-H hydrogen atoms omitted for clarity.

Table 2.1: Selected crystal data for compound (**2.1**).

Bond	Length (Å)	Atoms	Angle (°)
P1-Se1	2.1562(19)	N1-P1-C1	102.7(3)
P1-Se2	2.1608(19)	N1-P1-Se1	115.1(2)
P1-N1	1.669(5)	C1-P1-Se1	104.7(2)
P1-C1	1.825(7)	N1-P1-Se2	105.8(2)
N1-C7	1.470(8)	C1-P1-Se2	109.0(2)
C1-C2	1.412(11)	Se1-P1-Se2	118.33(8)
C1-C6	1.396(10)	C7-N1-P1	121.3(4)
N2-C10	1.492(9)	C6-C1-C2	117.2(7)
N2-C13	1.508(8)	C6-C1-P1	122.4(6)
N2-H2B···Se2	2.52(3)	C2-C1-P1	120.4(5)

2.2.2 **Reaction with *n*-Butylamine**

Woollins' Reagent was reacted with an excess of *n*-butylamine at room temperature using the amine itself as a solvent (Equation 2.2). The mixture was left to stir for 30 minutes, in which time the suspension turned a green-grey colour. As before, on filtration, the solution was found to be a light yellow colour. The solution was evaporated to dryness, yielding a pale yellow powder, which could be recrystallised by dissolving in DCM and layering with hexane. The product, (**2.2**), was characterised by $^{31}P\{^{1}H\}$, $^{77}Se\{^{1}H\}$, $^{13}C\{^{1}H\}$ and ^{1}H NMR spectroscopy, single crystal X-ray crystallography, mass spectrometry and IR spectroscopy. Both the crude and purified products are again air and light sensitive, discolouring to a red colour within 24 hours on exposure, again releasing elemental selenium.

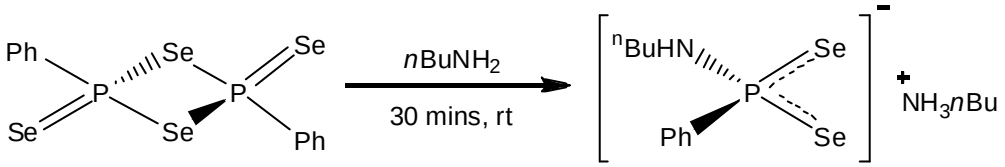

Eqn 2.2

A peak at δ_P = 44.3 ppm with coupling constants of $^{1}J_{P\text{-}Se}$ = 599 Hz and $^{1}J_{P\text{-}C}$ = 75.1 Hz can be found in the $^{31}P\{^{1}H\}$ NMR spectrum of (**2.2**). The corresponding couplings are seen in the $^{77}Se\{^{1}H\}$ and the $^{13}C\{^{1}H\}$ NMR spectra at $^{1}J_{Se\text{-}P}$ = 601 Hz and $^{1}J_{C\text{-}P}$ = 75.8 Hz, respectively. In the $^{77}Se\{^{1}H\}$ NMR spectrum, the peak is observed at δ_{Se} = 63.0 ppm, consistent with the peak observed for ^{i}PrAWR.

The $^{13}C\{^{1}H\}$ and ^{1}H NMR spectra of (**2.2**) are as expected, with splitting of the peaks for all carbon atoms within 4 bonds of the central P atom.

The IR spectrum is very similar to that of (**2.1**), as the species have the same functionalities. Peaks are observed at 3258 cm^{-1} (νN-H), 2959 cm^{-1} (νC-H), 2927 cm^{-1} (νC-H), 1434 cm^{-1} (νP-Ph) and 557 cm^{-1} for νP-Se. The mass spectrum shows a peak of 100% intensity at m/z = 339.79, which corresponds to (**2.2**) minus the counter ion.

Crystals were grown of (**2.2**) (Figure 2.10) and the X-ray structure obtained on a Rigaku Mercury70 diffractometer with Mo-Kα radiation. The P-Se bonds are 2.1393(13) Å for Se1-P1 and 2.1613(9) Å for Se2-P1 and as such the bonds are inequivalent, however have the same bond order at 1½.

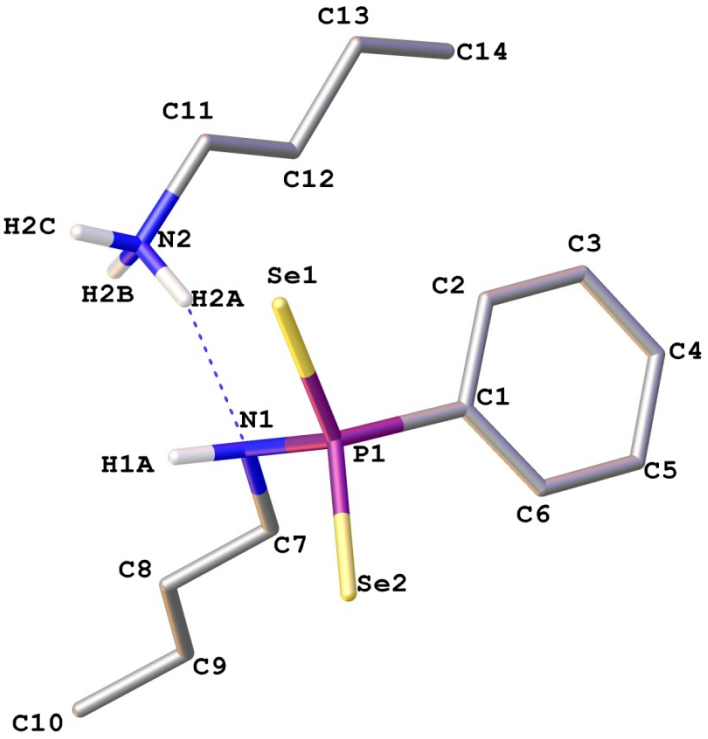

Figure 2.10: X-ray crystal structure of ^{n}BuAWR, (**2.2**).
C-H hydrogen atoms omitted for clarity.

It is interesting to note that in compound (**2.1**) – and indeed (**2.3**) presented later – the hydrogen bond between the counter ion and the ligand forms between a hydrogen atom of the ammonium and one of the selenium atoms of the ligand. In (**2.2**) this is not the case, and the hydrogen bond forms between H2A and N1. The average length of a P-N bond is 1.657 Å, according to the CCDC, and as such the P1-N1 bond in (**2.2**) is slightly longer than this value. The N-H and N-C bonds are seen to be of average length, including that of N2-H2A, despite the H-bonding observed between H2A and N1. The smallest angle seen around the P centre is that of N1-P1-C1 and the N1-P1-Se1 angle is significantly different to that of N1-P1-Se2, although this discrepancy is smaller than that seen for (**2.1**). The C6-C1-P1 and C2-C1-P1 angles are also inequivalent, suggesting some distortion of the phenyl ring. A selection of key bond lengths and angles are presented in Table 2.2, whilst complete crystallographic data for compound (**2.2**) can be found in Appendix 2.

Table 2.2: Selected crystal data for compound (**2.2**).

Bond	Length (Å)	Atoms	Angle (°)
P1-Se1	2.1393(13)	N1-P1-C1	101.94(12)
P1-Se2	2.1613(9)	N1-P1-Se1	106.41(9)
P1-N1	1.695(2)	C1-P1-Se1	110.88(11)
P1-C1	1.824(3)	N1-P1-Se2	111.73(9)
N1-C7	1.486(4)	C1-P1-Se2	109.99(10)
C1-C2	1.406(4)	Se1-P1-Se2	115.06(3)
C1-C6	1.392(4)	C7-N1-P1	119.02(19)
N2-C10	1.500(4)	C6-C1-C2	119.0(2)
N2-H2A···N1	2.05(2)	C6-C1-P1	122.1(2)
		C2-C1-P1	118.9(2)

2.2.3 **Reactions with 2-Aminobutane and 2-Aminopentane**

The reactions of Woollins' Reagent with either an excess of 2-aminobutane at room temperature, or a stoichiometric amount of 2-aminopentane in THF, yield the expected phenylphosphonamidodiselenoates ^{s}BuAWR (**2.3**) and ^{s}PentAWR (**2.6**). Both reactions proceed in a matter of minutes, with the deep red suspensions turning to grey-green solutions, which on filtration and removal of the precipitated metallic selenium are revealed to be yellow, consistent with the other reactions in this series.

^{s}BuAWR can be recrystallised in much the same way as (**2.1**) and (**2.2**), by removing the solvent, redissolving the crude product in DCM and layering with hexane. In this way, crystals suitable for X-ray diffraction were obtained. Crystals of ^{s}PentAWR could not be obtained, despite numerous attempts and solvent systems, however a purer powder form of the product was obtained in this manner. Once more, both products are air and light sensitive discolouring to dark orange powders if left even for 24 hours. The products of these experiments were further characterised by $^{31}P\{^{1}H\}$, $^{77}Se\{^{1}H\}$, $^{13}C\{^{1}H\}$ and ^{1}H NMR spectroscopy, mass spectrometry and IR spectroscopy.

The $^{31}P\{^{1}H\}$ NMR spectra of ^{s}BuAWR and ^{s}PentAWR are similar to all other ligands in this series exhibiting singlets at δ_P = 41.3 ppm and 41.6 ppm flanked by selenium satellites, with coupling constants of $^{1}J_{P\text{-}Se}$ = 599 Hz and 601 Hz, respectively. In the $^{77}Se\{^{1}H\}$ NMR spectra, however, two doublets at δ_{Se} = 73.3 ppm and 69.2 ppm, and 72.4 ppm and 67.4 ppm respectively are observed, see **Figure 2.11**.

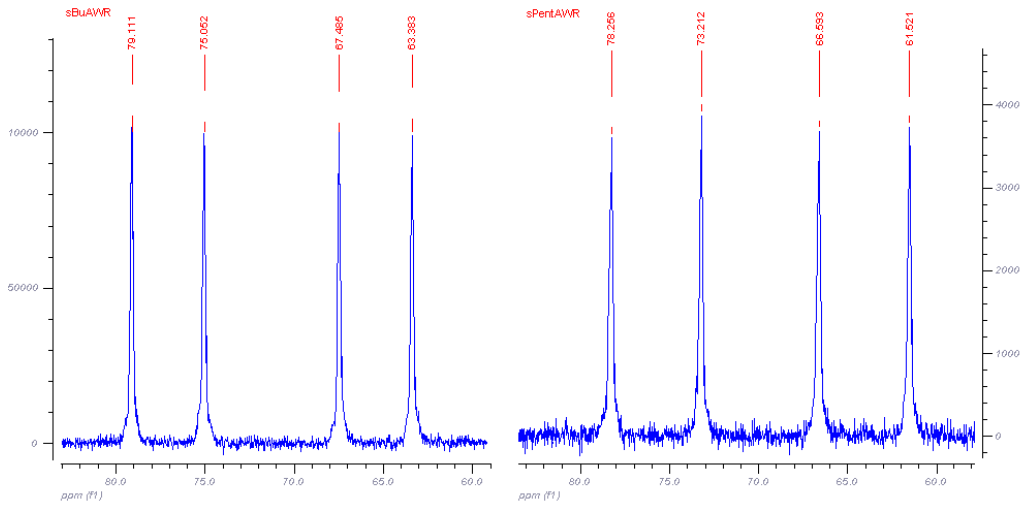

Figure 2.11: $^{77}Se\{^{1}H\}$ NMR spectrum of ^{s}BuAWR (L) and ^{s}PentAWR (R).

The coupling constants for these doublets are $^{1}J_{Se\text{-}P}$ = 598 Hz and 601 Hz in the ^{s}BuAWR spectrum and $^{1}J_{Se\text{-}P}$ = 601 Hz and 603 Hz in the ^{s}PentAWR spectrum, and are summarised in **Table 2.3**. The consistency in this data indicates the similarity of the compounds. We speculate that the observed doublets in the spectra arise from the formation of a weak hydrogen bond between one of the Se atoms and the H atom on the amine, making the Se atoms very slightly inequivalent (**Figure 2.12**). This can happen as a result of the bulkiness of the R group on the amine. These groups are more bulky than all other amines used previously and as such their limited rotation allows this weak interaction.

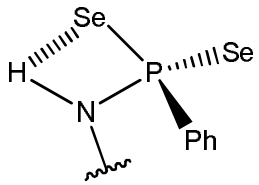

Figure 2.12: Weak hydrogen bonding in ^{s}BuAWR and ^{s}PentAWR

Table 2.3: Summary of ^{77}Se{^{1}H} NMR data for compounds (**2.3**) and (**2.6**).

^{s}BuAWR		^{s}PentAWR	
δ_{Se} (ppm)	Coupling (Hz)	δ_{Se} (ppm)	Coupling (Hz)
73.3	598	72.4	601
69.2	601	67.4	603

The ^{13}C{^{1}H} and ^{1}H NMR spectra of compounds (**2.3**) and (**2.6**) are as expected, with $^{1\text{-}4}J_{C\text{-}P}$ couplings being observed for all peaks in the ^{13}C{^{1}H} spectra, as are the IR spectra, wherein all functional groups are able to be identified. The mass spectrum of (**2.3**) shows *m/z* to be 339.78, corresponding to the ligand without its counter ion; however, mass data could not be obtained for ^{s}PentAWR.

^{s}BuAWR (Figure 2.13) crystallises in the P-1 space group with 2 crystallographic independent molecules present in the unit cell. The P-Se bonds, at

2.152(2) Å and 2.1670(18) Å are inequivalent to each other; however, both lie in the range between the average P-Se and P=Se bond lengths and so are of bond order 1½. The bond that is longer in length, P1-Se2, is hydrogen bonded to H2A of the counter ion, which could be the reason for this bond lengthening, although the N2-H2A bond is not correspondingly lengthened. The hydrogen bond between the counter ion and the ligand is 2.52(2) Å in length which is the same as that observed for the hydrogen bond in compound (**2.1**). The intramolecular hydrogen bond between Se1 and H1 is, at 2.813(18) Å, slightly longer than the intermolecular hydrogen bond and as such is slightly weaker.

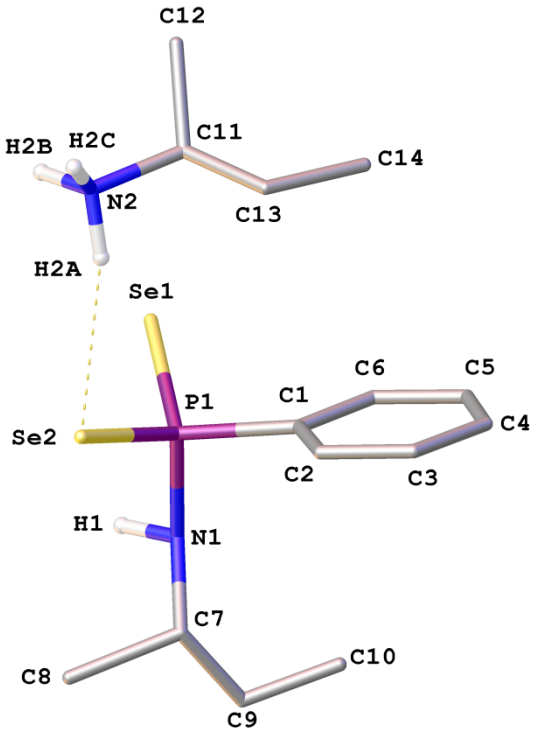

Figure 2.13: X-ray crystal structure of ^{s}BuAWR, (**2.3**).
C-H hydrogen atoms omitted for clarity.

The Se1-P1-Se2 angle in compound (**2.3**) was found to be the largest between any two substituents on P(1), at 116.00(8)°. This is larger than that observed for (**2.2**), but smaller than that recorded for (**2.1**). The angles around the phosphorus atom range from 103.1(3)° to 116.00(8)°, which is in accordance with the other compounds reported in this chapter. Selected bond lengths and angles discussed herein are presented in Table 2.4, whilst full crystallographic data for compound (**2.3**) can be found in Appendix 3.

Table 2.4: Selected crystal data for Compound (**2.3**).

Bond	Length (Å)	Atoms	Angle (°)
P1-Se1	2.152(2)	N1-P1-C1	103.1(3)
P1-Se2	2.1670(18)	N1-P1-Se1	105.6(2)
P1-N1	1.683(6)	C1-P1-Se1	110.8(2)
P1-C1	1.821(7)	N1-P1-Se2	113.5(2)
N1-C7	1.504(9)	C1-P1-Se2	107.1(2)
C1-C2	1.397(10)	Se1-P1-Se2	116.00(8)
C1-C6	1.403(10)	C7-N1-P1	120.4(5)
N2-C10	1.515(9)	C6-C1-C2	118.9(7)
N1-H1¨Se1	2.813(18)	C6-C1-P1	119.5(5)
N2-H2A¨Se2	2.52(2)	C2-C1-P1	118.9(7)

2.2.4 **Reaction with *tert*-Butylamine**

The solventless reaction (Equation 2.3) of *t*-butyl amine with Woollins' Reagent at room temperature yielded compound (**2.4**), 2-methylpropan-2-ammonium *N*-*tert*-butyl-*P*-phenylphosphonamidodiselenoate, ^{t}BuAWR.

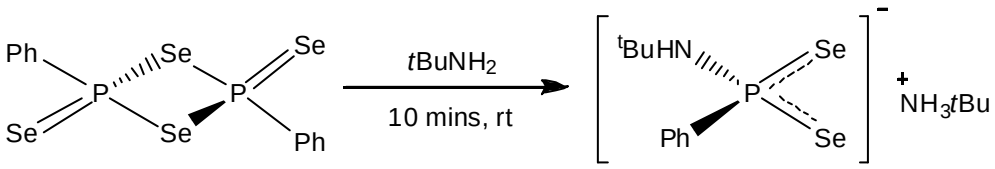

Eqn 2.3

The $^{31}P\{^{1}H\}$ NMR spectrum of ^{t}BuAWR exhibits a singlet at δ_P = 29.8 ppm surrounded by its selenium and carbon satellites ($^{1}J_{P\text{-}Se}$ = 594 Hz and $^{1}J_{P\text{-}C}$ = 79.4 Hz). The shift is much further upfield than all other shifts seen for this series of compounds, which could tentatively be assigned to two factors: the *t*-butyl group is more electron donating than the other organic groups under observation, thus the species is more electron rich, hence the lower shift. The *t*-butyl group is also much bulkier, which also, as a general rule, shifts the P NMR resonance further upfield. That said, a much wider range of compounds would have to be studied to confirm this statement.

The $^{77}Se\{^{1}H\}$ NMR spectrum exhibits the corresponding doublet at δ_{Se} = 142.1, with coupling constant $^{1}J_{Se\text{-}P}$ = 594 Hz. This is the highest ^{77}Se chemical shift seen for these compounds by almost 70 ppm, which is most likely caused by the steric bulk of the *t*-butyl group. The $^{13}C\{^{1}H\}$ and ^{1}H NMR spectra of compound (**2.4**) are in accord with the others in this chapter. The IR spectrum exhibits peaks characteristic of this species and is especially similar to those of *n*-butyl and *s*-butyl amine; amongst others, the N-H (3299 cm^{-1}), C-H stretches (2968 and 2867 cm^{-1}), P-Ph bend (1434 cm^{-1}) and the characteristic strong peak at 548 cm^{-1} of νP=Se. The mass spectrum shows *m/z* to be 339.78, M minus the counter ion, $H_2NC_4H_9^+$.

A further two ligands were synthesised in this series, those of benzylamine *N*-benzyl-*P*-phenylphosphonamidodiselenoate, (BenzAWR, **2.5**) and PropargylAWR (**2.7**). The latter was to observe if Woollins' Reagent preferentially reacts with the amine functional group of a species, as opposed to forming a heterocycle or

selenocarbonyl through reaction with the C≡N bond.[51] At room temperature it can be confirmed that the phenylphosphonamidodiselenoate is preferentially formed, however no variation in reaction conditions was carried out to ascertain if this is also the case at elevated temperatures. No further reactions were performed with this ligand species.

Benzylamine behaves in the same manner as all other compounds investigated in this chapter and reacts within minutes with Woollins' Reagent at room temperature. Stoichiometric amounts of benzylamine are used in this case, as the boiling point of benzylamine is high enough to prevent adequate removal under reduced pressure when used as the solvent and therefore the reaction was performed in dry THF, with a yield of 97% being obtained.

The $^{31}P\{^{1}H\}$ NMR spectrum of (**2.5**) reveals a singlet at δ_P = 45.8 with coupling constants of $^{1}J_{P\text{-}Se}$ = 626 Hz and $^{1}J_{P\text{-}C}$ = 77.3 Hz, which are also observed in the $^{77}Se\{^{1}H\}$ (δ_{Se} = 45.0, $^{1}J_{Se\text{-}P}$ = 629 Hz) and $^{13}C\{^{1}H\}$ (δ_C = 141.5, $^{1}J_{C\text{-}P}$ = 75.8 Hz) NMR spectra. The $^{13}C\{^{1}H\}$ and ^{1}H NMR spectra of BenzAWR confirm the presence of the 3 inequivalent rings and two CH_2 groups.

Crystals could not be grown of BenzAWR: different solvent systems were tried, as well as altering the temperature of the system, however most often the product precipitated too quickly out of solution. The resulting powder was used for IR spectroscopy and mass spectrometry, revealing the expected peaks and an *m/z* of 373.75 – the ligand without its counter ion.

Of the ligands synthesised in this chapter, five were taken on to use in follow up chemistry. The first investigations were performed using ^{i}PrAWR, compound (**2.1**), which was successfully reacted with a number of M(II)acetates (M = Cd, Ni, Cu) yielding a range of metal complexes (see Section 2.2.5).

Following the succesful results obtained therein, the ligands ^{i}PrAWR, ^{n}BuAWR, ^{s}BuAWR, ^{t}BuAWR and BenzAWR were reacted with a range of *cis*-dichloro(diphosphine)platinum(II) complexes, which are discussed in Chapter 3. The data obtained for the five ligands listed above has been summarised in Table 2.1, which will be referred back to in Chapter 3.

Table 2.5: Summary of data obtained for compounds (**2.1**) - (**2.5**).

	^{i}PrAWR	^{n}BuAWR	^{s}BuAWR	^{t}BuAWR	BenzAWR
δ_P (ppm)	42.2	44.3	41.3	29.8	45.8
$^1J_{P\text{-}Se}$ (Hz)	610	599	599	594	626
δ_{Se} (ppm)	69.4	63.0	73.3, 69.2	142.1	45.0
$^1J_{Se\text{-}P}$ (Hz)	610	601	598, 601	594	629
$\nu_{P\text{-}Se}$ (cm^{-1})	541	557	549	548	550
P-Se bond lengths (Å)	2.1562(19) 2.1608(19)	2.1393(13) 2.1613(9)	2.152(2) 2.1670(18)	- -	- -

2.2.5 **Reactions of ^{i}PrAWR**

^{i}PrAWR, (**2.1**), was reacted with nickel acetate and copper acetate following its successful reaction with cadmium acetate, Scheme 2.2.[69] The cadmium complex differs from the nickel complex in that it is a dimeric structure containing four ligand moieties. The nickel complex (**2.8**), by contrast, contains a single metal centre bound to two ligands. This reflects previous work into phosphonodiselenoato ligands performed by Gray *et al.*[65] The product of the reaction with copper acetate reveals a much more complex structure discussed later in this section.

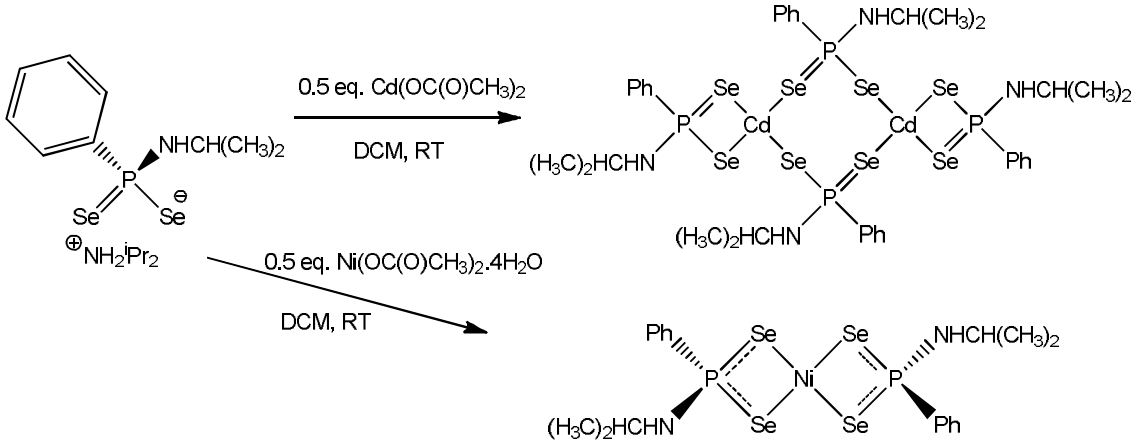

Scheme 2.2: Synthesis of cadmium and nickel complexes of ^{i}PrAWR from their corresponding acetates

The $^{31}P\{^{1}H\}$ NMR spectrum of (**2.8**) exhibits a singlet at δ_P = 21.8 ppm flanked by a single set of selenium satellites, showing that the Se atoms are all equivalent. The coupling constant is observed to be $^{1}J_{P\text{-}Se}$ = 485 Hz, which is much smaller than the unbound ligand (610 Hz). This shows that not only does the chemical shift change on complexation, most likely due to the change in electronic properties of the P atom, but also the decrease in coupling constant indicates a change in the nature of the P-Se bond: in the unbound ligand the bond order is 1½, whereas in nickel complex (**2.8**) the bond order is seen to have moved towards a formal single bond. In the $^{77}Se\{^{1}H\}$ NMR spectrum a corresponding doublet is seen at -17.0 ppm, which has a coupling constant of $^{1}J_{Se\text{-}P}$ = 488 Hz. The carbon and hydrogen NMR spectra are similar to the unbound ligand, indicating the presence of the phenyl and isopropyl moieties. The IR spectrum of (**2.8**) is very similar to that of the unbound ligand, whilst the *m/z* was found to be 730.38 $(MNa)^{+}$ by mass spectrometry.

Crystals suitable for X-ray diffraction were grown *via* layering the reaction mixture with hexane and placing in the refrigerator. Compound (**2.8**) crystallises in the $P\overline{1}$ space group and has two independent molecules in the unit cell, with the Ni atom being the inversion centre of the molecule shown in Figure 2.14.

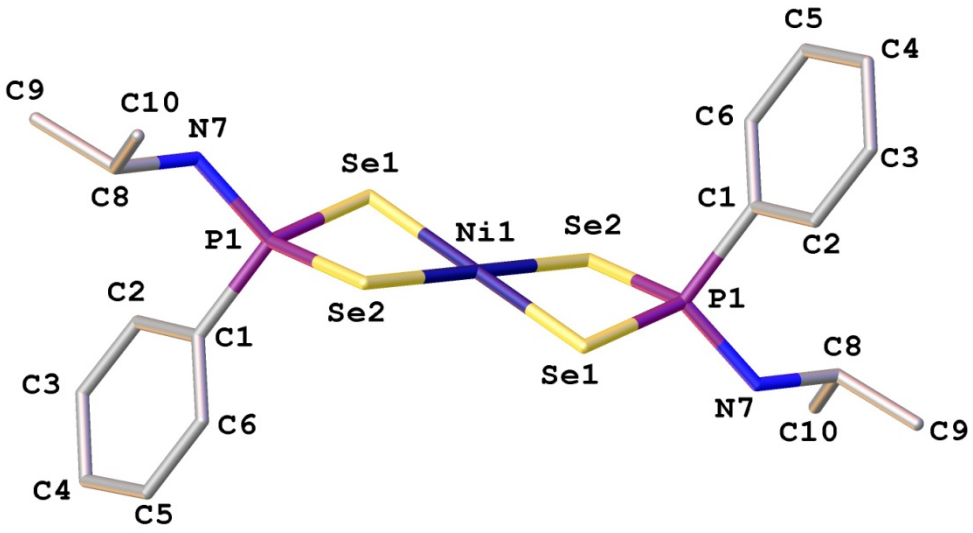

Figure 2.14: X-ray crystal structure of nickel complex (**2.8**).
Hydrogen atoms omitted for clarity.

The P-Se bonds in compound (**2.8**) lie in the range of 2.162(5) Å to 2.191(4) Å in length and as such are slightly longer than the values observed for the free ligand. This is consistent with the decrease in $J_{P\text{-}Se}$ coupling constant observed from the free to the bound ligand in the NMR spectra. It was mentioned before that the bond order of the P-Se bonds is 1.5 in the unbound ligand, however, in the metal complex one of these bonds is stretched by a larger degree, almost becoming the same length as the average single bond. The other remains very similar to that observed in the free ligand, which suggests it may form a dative bond with the nickel centre, however this theory is not confirmed by the selenium NMR data. The Ni-Se bonds are all between 2.345(2) Å and 2.3622(19) Å in length, which are comparable to the average reported in the CCDC database, at 2.348 Å. The four angles around the nickel centre lie in the range of 89.41(6)° to 90.59(6)°, showing it to have square planar geometry. The angles around the P atoms lie in the range 99.86(17)° to 118.9(6)°, the smallest of which being the Se(1)-P(1)-Se(1) angle, the largest being the N(1)-P(1)-Se(1) angle. This shows that the

overall geometry of the molecule is dominated by the nickel centre. The phenyl rings are *trans* to each other, with one being located above the plane of the $NiSe_4$ centre and the other lying below the plane of the centre. This has been seen in previous studies with both phosphonodiselenoato and phosphonodithioate complexes.[71] Bond lengths and angles of interest for fragment one are presented in Table 2.6 and full crystal data is given in Appendix 4.

Table 2.6: Selected crystal data for one fragment of compound (**2.8**).

Bond	Length (Å)	Atoms	Angle (°)
Ni(1)-Se(1)	2.3624(19)	Se(1)-Ni(1)-Se(1)	180.00(8)
Ni(1)-Se(2)	2.345(2)	Se(1)-Ni(1)-Se(2)	90.10(7)
Se(1)-P(1)	2.162(5)	Se(1)-Ni(1)-Se(2)	89.90(7)
Se(2)-P(1)	2.192(5)	Se(2)-Ni(1)-Se(2)	180.00(9)
P(1)-C(1)	1.807(17)	P(1)-Se(1)-Ni(1)	83.79(13)
P(1)-N(7)	1.632(15)	P(1)-Se(2)-Ni(1)	83.57(12)
N(7)-C(8)	1.46(3)	N(7)-P(1)-C(1)	103.3(8)
		N(7)-P(1)-Se(1)	109.8(6)
		C(1)-P(1)-(Se2)	110.9(6)
		C(1)-P(1)-Se(1)	114.8(5)
		N(7)-P(1)-Se(2)	118.7(6)
		Se(1)-P(1)-Se(2)	99.85(18)

The reaction of copper acetate with ^{i}PrAWR, (**2.1**), proceeded at elevated temperature, yielding an orange solution, which was filtered, layered with hexane and placed in the fridge for crystallisation. Two main peaks of interest were found in the ^{31}P NMR of the reaction mixture, a broad peak at 39.3 ppm and the other at 10.0 ppm. After some weeks, crystals were found of an unusual structure unlike any seen for the other compounds and complexes reported herein, as shown in Figure 2.15. The compound was obtained in a tiny yield and as such no further characterisation could be performed and subsequent attempts to obtain as targeted synthesis of compound (**2.9**) were not successful.

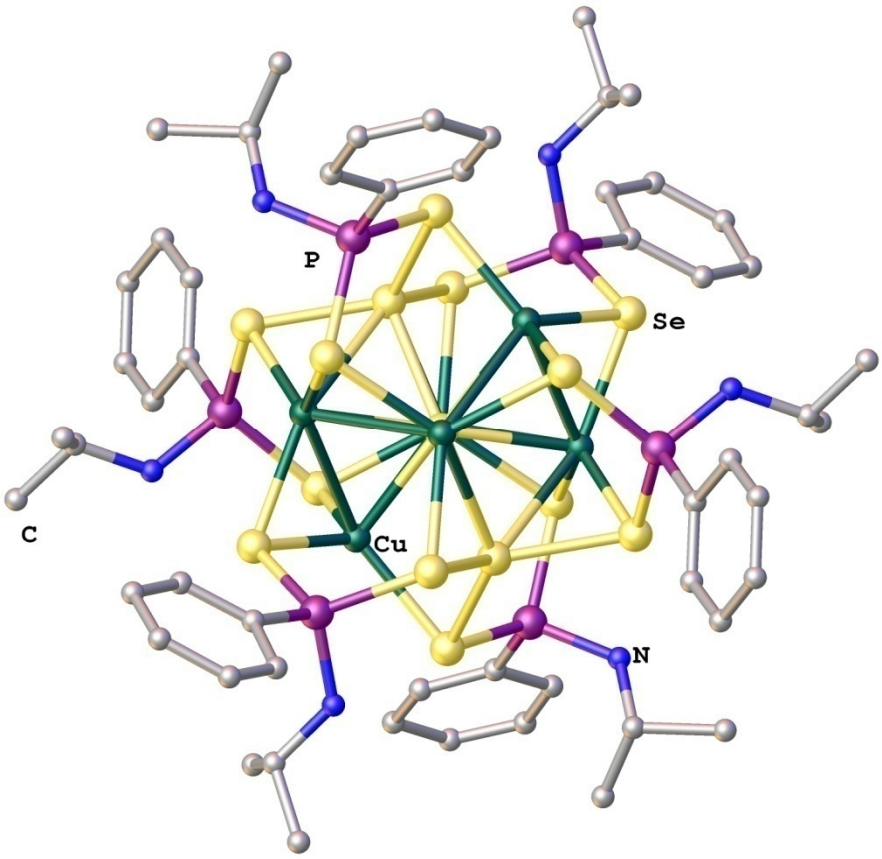

Figure 2.15: X-ray crystal structure of copper complex (**2.9**).
Hydrogen atoms omitted for clarity.

The obtained structure of (**2.9**) is of the form $(L_6)Cu_6Se_3$, where L is the ^{i}PrAWR ligand moiety. Overall the structure appears to be isostructural with the $\{Cu_8(\mu_8\text{-}Se)[Se_2P(OPr^{i})_2]_6\}$ copper cluster reported by Liu *et al.*, although in our structure, two of the copper atoms have been replace by two non-ligand Se atoms. The central selenium atom of the cluster is eight coordinate with cubic geometry (Figure 2.16 **(a)**),

as it is bonded to all six copper atoms and the other two 'non-ligand' selenium atoms, which make up a linear Se_3 chain running through the centre of the compound. The terminal Se atoms of the Se_3 chain are the central atoms of two selenium tetrahedra, which give an overall Se_4-Se-Se_4 backbone, as seen in Figure 2.16 **(b)**. This is the only compound in the CCDC database which contains a Se_5 chain.

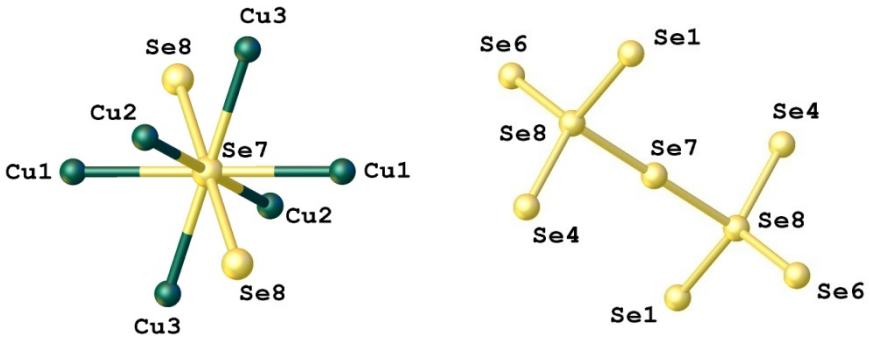

Figure 2.16: **(a)** 8 coordinate central Se atom and **(b)** central Se chain

Each of the terminal Se atoms of the chain has distorted trigonal prismatic geometry, being bonded to three ligand selenium atoms, the central selenium atom and two copper centres. One Se atom of each ligand bridges two Cu atoms, whilst the other bridges a Cu atom to one of the terminal Se atoms.

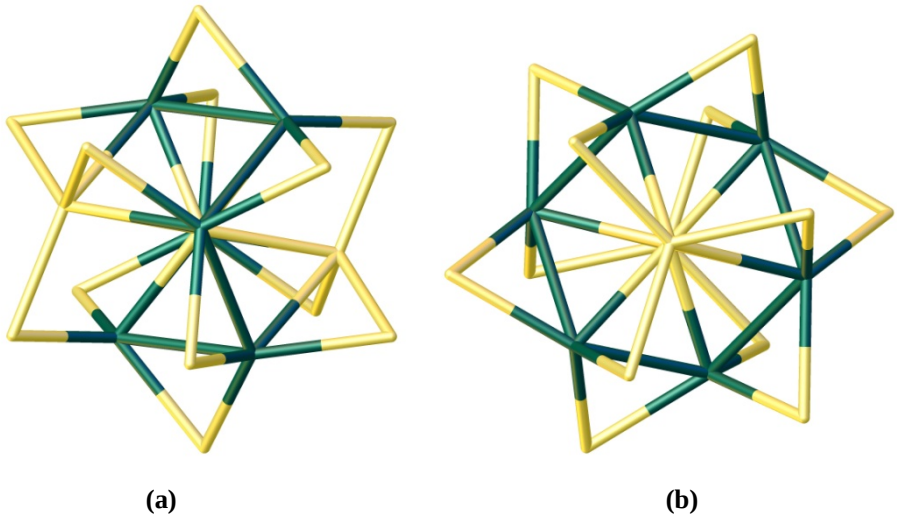

Figure 2.17: Central cluster viewed along **(a)** the Cu-Se-Cu axis and **(b)** the central Se_3 chain.

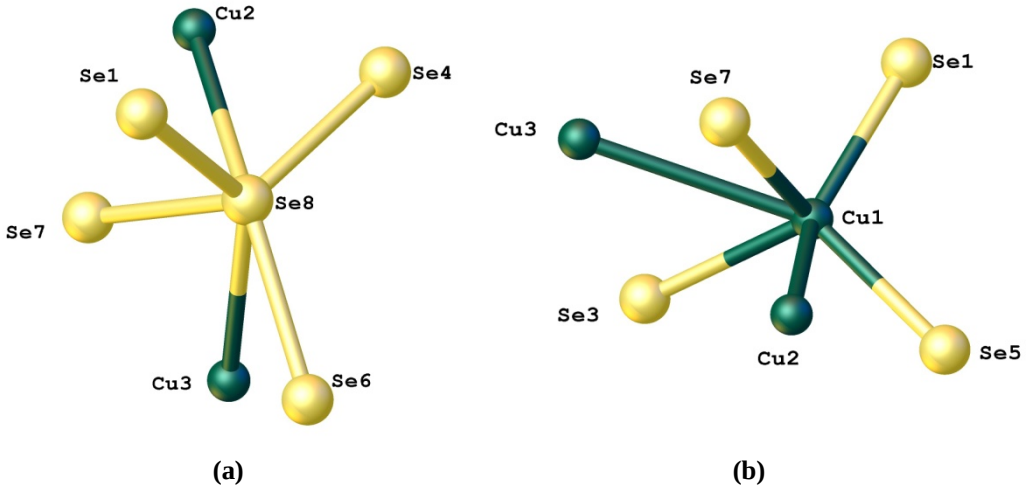

(a) **(b)**

Figure 2.18: Geometry around **(a)** terminal selenium atoms and **(b)** Cu1 atom

As previously mentioned, the two terminal selenium atoms lie in pseudo trigonal prismatic geometries, as does the Cu1, see **Figure 2.18**. The angles around each terminal selenium atom (Se8) lie in the range of 53.19(10)°-141.0(2)°. Within this range, the smallest angle is that of Se4-Se8-Cu2 and the largest is that of Se1-Se8-Cu3. The Cu1 atom is bonded to two copper atoms, the central selenium atom and three ligand selenium atoms. The angles around the Cu1 atom lie in the range of 53.42(10)°-141.39(13)°, wherein the smallest angle is that of $Se3^{1}$-Cu1-$Cu3^{1}$ and the largest is Se5-Cu1-$Cu3^{1}$. Cu2 and Cu3 are bonded to seven other atoms within the structure (Figure 2.19): two Cu atoms, the central and a terminal Se atom and three ligand Se atoms.

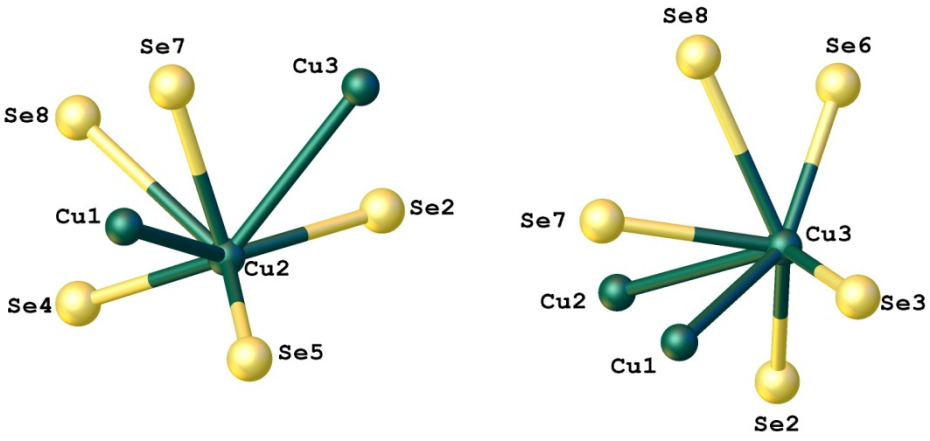

(a) **(b)**

Figure 2.19: Geometry around **(a)** Cu2 **(b)** Cu3

The angles around Cu2 lie in the range of 52.95(11)° to 141.78(14)°, where the smallest angle belongs to Se4-Cu2-Se8 and the largest to Se4-Cu2-Cu3[1]. The angles around Cu3 lie in the range of 53.55(16)° to 143.80(13)° with Se2[1]-Cu3-Cu2[1] representing the smallest angle and Se6-Cu3-Cu1[1] representing the largest. As such none of the three copper environments are equivalent. The Cu-Se bonds can be separated into three types: those between copper and a ligand selenium atom (Se_L), a terminal selenium atom (Se_T) and the central selenium atom (Se_C), which increase in length in that order. The Cu-Se_L bonds are in the range of 2.436(5) Å - 2.462(5) Å, Cu-Se_T are in the range 2.502(5) Å - 2.532(4) Å and Cu-Se_C are in the range 2.852(9) Å - 2.962(5) Å. The average according to the database is 2.468 Å.

The P-Se bond lengths in (**2.9**), at 2.182(6) Å - 2.210(7) Å, are all equivalent and are slightly longer than those for the free ligand (2.1562(19) Å and 2.1608(19) Å), but shorter than the average P-Se single bond, which is 2.222 Å according to the CCDC. They are also longer than those observed in the Liu $\{Cu_8(\mu_8\text{-}Se)[Se_2P(OPr^i)_2]_6\}$ cluster.[67]

Of the four Se-Se bonds, the bonds to between Se_L and Se_T are all equivalent to each other, but shorter than the bonds between Se_T and Se_C (2.448(5) Å - 2.451(6) Å *versus* 2.539(3) Å). All, however, are longer than the average in the database, of 2.364 Å. The selected bond length data is summarised in Table 2.7, whilst a full summary can be found in Appendix 5.

Table 2.7: Bond lengths in (**2.9**) compared to the averages in the CCDC.

	Bond lengths in (**2.9**) (Å)	Average in CCDC (Å)
P-Se	2.182(6) - 2.210(7)	2.222
Se-Se	2.448(5) - 2.539(3)	2.364
Cu-Se_L	2.436(5) - 2.462(5)	2.468
Cu-Se_T	2.502(5) - 2.532(4)	2.468
Cu-Se_C	2.852(9) - 2.962(5)	2.468
Cu-Cu	2.901(4) – 2.930(9)	2.735

2.3 Conclusion

This chapter has presented seven ligand systems prepared *via* the reaction of a variety of amines with Woollins' Reagent. Most were synthesised in high to quantitative yields, *via* the direct reaction using the amine in most cases as the solvent. The X-ray crystal structures of three of these ligands were obtained, showing no obvious correlation between the length of the P-Se bond and the coupling constant or chemical shift of the P/Se peak in the NMR spectrum. One can tentatively say that a trend appears in the butyl substrates, in that the δ_P decreases with steric bulk (^{n}Bu > ^{s}Bu > ^{t}Bu), whilst δ_{Se} increases with steric bulk (^{t}Bu> ^{s}Bu > ^{n}Bu), however more similar compounds would have to be investigated to confirm this trend.

Once the ligand systems were synthesised, trial reactions were performed with ^{i}PrAWR and some metal acetate compounds. Nickel complex (**2.8**) and the unusual copper cluster (**2.9**) were synthesised and characterised by single crystal X-ray diffraction. The nickel complex is a monomeric structure, which appears at 21.77 ppm in the $^{31}P\{^1H\}$ NMR spectrum and -16.96 ppm in the ^{77}Se NMR spectrum. The bond lengths of the P-Se bonds observed therein are longer than those observed in the free ligand, and become more inequivalent on complexation. Whilst one remains with a bond order of 1½, the other lengthens to almost have a bond order of 1.

The reaction of copper acetate with (**2.1**) yields an unusual cluster complex of the form $(L_6)Cu_6Se_3$, similar to those synthesised by Liu *et al.* in Taiwan.[68] Its unique structure exhibits a Se_5 chain, which forms a larger Se_4-Se-Se_4 network. The central Se atom has cubic geometry, whilst four of the six copper atoms in the structure have seven-coordinate geometry. The P-Se bonds in the structure are all equivalent, and, as in (**2.8**) are longer than those observed in the free ligand.

Further reactions were performed with ligands (**2.1**)-(**2.5**), which are discussed in Chapter 3.

2.4 Experimental

All experiments were carried out using standard Schlenk line techniques under an inert and dry nitrogen atmosphere, unless otherwise stated. Subsequent work up, such as chromatography, was performed in air unless otherwise indicated. Toluene, THF, hexane, dichloromethane, and diethyl ether were dried, degassed and purified using an MBraun Solvent Drying System. All other solvents used were distilled using standard techniques. All glassware was oven dried before use. All chemicals were obtained from Acros, Sigma Aldrich and Alfa Aesar and used as received.

NMR experiments were performed on a Jeol GSX 270 MHz spectrometer with δ(H) and δ(C) referenced to tetramethylsilane, δ(P) referenced to 85% H_3PO_4 and δ(Se) referenced to dimethyl selenide as external standards at 270, 68, 109 and 52 MHz respectively, unless otherwise indicated. All experiments were performed at room temperature, unless otherwise stated. Some NMR experiments were carried out on a Bruker Avance 300 MHz spectrometer and a Bruker Avance II 400 MHz spectrometer, which is highlighted in individual syntheses.

Infra-red spectra were recorded as KBr discs, unless otherwise stated, in the range 4000-400 cm^{-1} on a Perkin-Elmer System 2000 Fourier transform spectrometer.

2.4.1 **Preparation of Woollins' Reagent**[50]

Sodium metal (25.01 g, 1.09 mol) was cut into small pieces and added to stirring liquid ammonia (1.5 L) at -78 °C. The mixture was stirred for 15 min to ensure all sodium had dissolved. Selenium metal (42.92 g, 0.54 mol) was added in small portions to the solution, resulting in a dark blue solution. The mixture was allowed to reflux for 4 h at -33 °C. The ammonia was then allowed to evaporate, leaving sodium selenide as a white solid. Dry, degassed toluene (1.5 L) was added, followed by a slight excess of dry dichlorophenylphosphine (79.0 mL, 0.58 mol) and the resulting mixture was stirred under reflux for 24 h at 130 °C. The reaction was filtered to remove the resulting NaCl precipitate and selenium (69.97 g, 0.88 mol) was added. The reaction was refluxed for a further 24 h, forming a red suspension. A second amount of dichlorophenylphosphine (35 mL, 0.20 mol) was added to the reaction mixture and refluxed for a further 12 h period, removing the excess selenium present. The reaction mixture was cooled to room temperature, filtered and washed with toluene (4 x 30 mL). The product was finally dried *in vacuo* yielding Woollins' Reagent, a red solid, which was stored under nitrogen.

IR υ max (KBr disc)/cm^{-1}: 3431 (m, br), 3052 (Ar-CH stretch), 1631 (w), 1578 (w), 1474 (w), 1433 (P-Ph stretch), 1379 (w), 1302 (w), 1181 (w), 1145 (w), 1079 (m), 1022 (w), 997 (w), 939 (w), 926 (w), 839 (w), 801 (w), 737 (m), 696 (w), 679 (m), 614 (w), 509 (s), 487 (s) and 430(m).

2.5 Syntheses of Ligands

2.5.1 Synthesis of Diisopropylamine *N*-isopropyl-*P*-phenylphosphonamidodiselenoate (^{i}PrAWR) (2.1)

Woollins' Reagent (2.01 g, 3.75 mmol) was added to dry isopropylamine (20 cm^3). The suspension was stirred for 2 hours at room temperature until the solution turned a green-grey colour. The solution was then filtered and evaporated to dryness, yielding a light yellow precipitate, which was recrystallised from DCM and hexane.
Yield: 3.02 g, 95%.

^{1}H NMR: (270 MHz, $CDCl_3$, TMS) (ppm) δ_H = 8.52 (broad s, 2H, NH), 8.19-8.08 (m, 2H, Ar-H), 7.31-7.20 (m, 3H, Ar-H), 3.35 (sep, $^{3}J_{H-H}$ = 6.81 Hz, 3H, ^{i}Pr-CH), 2.45 (broad s, 1H, NH), 1.36 (d, $^{3}J_{H-H}$ = 6.62 Hz, 12H, CH_3) and 0.95 (d, $^{3}J_{H-H}$ = 6.32 Hz, 6H, CH_3).

^{13}C{^{1}H} NMR: (67.9 MHz, $CDCl_3$, TMS) (ppm) δ_C = 144.00 (d, $^{1}J_{C-P}$ = 79.9 Hz, C_q-P), 130.65 (d, $^{2}J_{C-P}$ = 12.5 Hz, *o*-C), 129.62 (d, $^{4}J_{C-P}$ = 3.11 Hz, *p*-C), 127.30 (d, $^{3}J_{C-P}$ = 13.5 Hz, *m*-C), 48.14 (s, $^{i}Pr_2$-CH), 46.15 (d, J_{C-P} = 4.16 Hz, ^{i}Pr-CH), 25.12 (d, J_{C-P} = 5.19 Hz, ^{i}Pr-CH_3) and 20.61 (s, $^{i}Pr_2$-CH_3).

^{31}P{^{1}H} NMR: (109.4 MHz, $CDCl_3$, H_3PO_4) (ppm) δ_P = 42.20 (s, $^{1}J_{P-Se}$ = 610 Hz, $^{1}J_{P-C}$ = 79.8 Hz).

^{77}Se{^{1}H} NMR: (51.5 MHz, $CDCl_3$) (ppm) δ_{Se} = 69.38 (d, $^{1}J_{Se-P}$ = 610 Hz).

Mass TOF MS ES$^-$: *m/z* = 325.85 (M – $H_2NC_6H_{14}$).

IR (KBr, cm^{-1}): 3282 (s, N-H), 3086 (m, N-H), 2961 (m, C-H), 2942 (m, C-H), 1571 (w), 1470 (m, P-Ph), 1391 (m), 1380 (m), 1155 (m), 1133 (m), 1121 (m), 1096 (m), 1016 (s), 876 (m), 748 (m), 694 (m), 541 (vs, P=Se) and 503 (s).

2.5.2 Synthesis of Butan-1-amine *N*-butyl-*P*-phenylphosphonamidodiselenoate (^{n}ButAWR) (2.2)

Woollins' Reagent (2.03 g, 3.79 mmol) was added to dry butan-1-amine (20 cm^3). The suspension was stirred for 30 minutes at room temperature until the solution had turned a green-grey colour. The solution was then filtered and evaporated to dryness, yielding a yellow oil, which was redissolved in DCM and recrystallised by layering with hexane.
Yield: 2.97 g, 96%.

^{1}H NMR: (270 MHz, $CDCl_3$, TMS) (ppm) δ_H = 8.18-8.08 (m, 2H, Ar-CH), 7.42 (bs, 3H, NH_3), 7.41-7.30 (m, 3H, Ar-CH), 2.87 (t, $^3J_{H-H}$ = 7.27 Hz, 2H, CH_2), 2.66 (t, $^3J_{H-H}$ = 8.03 Hz, 2H, CH_2), 1.63-1.52 (m, 2H, CH_2), 1.40-1.17, (m, 6H, CH_2) and 0.80 (q, $^3J_{H-H}$ = 8.32 Hz, 6H, CH_3).

^{13}C{^{1}H} NMR: (67.9 MHz, $CDCl_3$, TMS) (ppm) δ_C = 142.13 (d, $^1J_{C-P}$ = 75.8 Hz, C_q-P), 130.53 (d, $^2J_{C-P}$ = 11.4 Hz, *o*-C), 130.05 (d, $^4J_{C-P}$ = 3.11 Hz, *p*-C), 127.62 (d, $^3J_{C-P}$ = 12.5 Hz, *m*-C), 43.43 (d, $^4J_{C-P}$ = 4.15 Hz, CH_2), 41.71 (s, CH_2), 40.26 (s, CH_2), 33.12 (d, $^3J_{C-P}$ = 10.4 Hz, CH_2), 32.11 (s, CH_2), 20.05 (d, $^2J_{C-P}$ = 11.4 Hz, CH_2), 13.85 (s, CH_3) and 13.71 (s, CH_3).

^{31}P{^{1}H} NMR: (109.4 MHz, $CDCl_3$, H_3PO_4) (ppm) δ_p = 44.28 (s, $^1J_{P-Se}$ = 599 Hz, $^1J_{P-C}$ = 75.1 Hz).

^{77}Se{^{1}H} NMR: (51.5 MHz, $CDCl_3$) (ppm) δ_{Se} = 62.95 (d, $^1J_{Se-P}$ = 601 Hz).

Mass TOF MS ES$^-$: *m/z* = 339.79 (M – $H_2NC_4H_9$).

IR (KBr, cm^{-1}): 3258 (m, N-H), 2959 (s, C-H), 2927 (s, C-H), 2862 (s, C-H), 1581 (m), 1477 (m), 1434 (m, P-Ph), 1390 (m), 1115 (m), 1094 (m), 1068 (m), 1006 (m), 908 (m), 739 (m), 690 (s), 557 (vs, P=Se) and 495 (vs).

2.5.3 Synthesis of 2-Aminobutane *N-sec*-butyl-*P*-phenylphosphonamidodiselenoate (^{s}ButAWR) (2.3)

Woollins' Reagent (2.00 g, 3.73 mmol) was added to dry butan-1-amine (20 cm^3) under vigorous stirring. The suspension was stirred for 30 minutes at room temperature until the solution had turned a green-grey colour. The solution was then filtered and evaporated to dryness, yielding a yellow powder, which was redissolved in DCM and recrystallised by layering with hexane.
Yield: 2.94 g, 95%.

^{1}H NMR: (270 MHz, $CDCl_3$, TMS) (ppm) δ_H = 8.24-8.15 (m, 2H, Ar-CH), 7.58 (bs, 3H NH_3), 7.36-7.10 (m, 3H, Ar-CH), 3.22-2.95 (m, 2H, CH), 2.46 (bs, 1H, NH_3), 1.65-1.49 (m, 2H, CH_2), 1.42-1.21 (m, 2H, CH_2), 1.09 (d, $^{3}J_{H-H}$ = 6.52 Hz, 3H, CH_3), 0.82 (d, $^{3}J_{H-H}$ = 6.41 Hz, 3H, CH_3), 0.72 (t, $^{3}J_{H-H}$ = 7.45 Hz, 3H, CH_3) and 0.58 (t, $^{3}J_{H-H}$ = 7.45 Hz, 3H, CH_3).

^{13}C{^{1}H} NMR: (67.9 MHz, $CDCl_3$, TMS) (ppm) δ_C = 143.10 (d, $^{1}J_{C-P}$ = 76.9 Hz, C_q-P), 130.85 (d, $^{2}J_{C-P}$ = 12.5 Hz, *o*-C), 130.02 (d, $^{4}J_{C-P}$ = 3.12 Hz, *p*-C), 127.44 (d, $^{3}J_{C-P}$ = 13.5 Hz, *m*-C), 51.16 (d, $^{2}J_{C-P}$ = 5.19 Hz, CH), 50.13 (s, CH), 31.30 (d, $^{3}J_{C-P}$ = 6.23 Hz, CH_2), 28.14 (s, CH_2), 21.83 (d, $^{3}J_{C-P}$ = 4.15 Hz, CH_3), 18.59 (s, CH_3), 10.08 (s, CH_3) and 10.03(s, CH_3).

^{31}P{^{1}H} NMR: (109.4 MHz, $CDCl_3$, H_3PO_4) (ppm) δ_P = 41.34 (s, $^{1}J_{P-Se}$ = 599 Hz, $^{1}J_{P-C}$ = 77.2 Hz).

^{77}Se{^{1}H} NMR: (51.5 MHz, $CDCl_3$) (ppm) δ_{Se} = 73.30 (d, $^{1}J_{Se-P}$ = 598 Hz) and 69.20 (d, $^{1}J_{Se-P}$ = 601 Hz).

Mass TOF MS ES$^-$: *m/z* = 339.78 (M – $H_2NC_4H_9$).

IR (KBr, cm^{-1}): 3260 (w, N-H), 2970 (m, C-H), 2869 (m, C-H), 1580 (m), 1487 (m), 1458 (m, P-Ph), 1391 (m), 1131 (m), 1092 (m), 1032 (m), 1007 (m), 943 (m), 848 (m), 751 (m), 693 (s), 549 (s, P=Se) and 520 (m).

2.5.4 Synthesis of 2-Methylpropan-2-amine *N*-*tert*-butyl-*P*-phenylphosphonamidodiselenoate (^{t}ButAWR) (2.4)

Woollins' Reagent (2.00 g, 3.73 mmol) was added to dry *tert*-butylamine (20 cm^3) under vigorous stirring. The suspension was stirred for 30 minutes at room temperature until the solution had turned a green-grey colour. The solution was then filtered and evaporated to dryness, yielding a yellow powder, which was redissolved in DCM and recrystallised by layering with hexane.
Yield: 2.87 g, 93%.

^{1}H NMR: (270 MHz, $CDCl_3$, TMS) (ppm) δ_H = 8.17-8.09 (m, 2H, Ar-CH), 7.23-7.14 (m, 3H, Ar-CH), 6.55 (bs, 3H, NH_3), 3.50 (bs, 1H, NH_3) and 1.16 (s, 18H, CH_3).

^{13}C{^{1}H} NMR: (67.9 MHz, $CDCl_3$, TMS) (ppm) δ_C = 145.27 (d, $^{1}J_{C\text{-}P}$ = 79.9 Hz, C_q-P), 130.80 (d, $^{2}J_{C\text{-}P}$ = 12.5 Hz, *o*-C), 129.54 (d, $^{4}J_{C\text{-}P}$ = 2.08 Hz, *p*-C), 127.22 (d, $^{3}J_{C\text{-}P}$ = 13.5 Hz, *m*-C), 55.13 (d, $^{2}J_{C\text{-}P}$ = 7.26 Hz, C_q), 51.96 (s, C_q), 31.40 (d, $^{3}J_{C\text{-}P}$ = 5.19 Hz, CH_3) and 29.56 (s, CH_3).

^{31}P{^{1}H} NMR: (109.4 MHz, $CDCl_3$, H_3PO_4) (ppm) δ_P = 29.80 (s, $^{1}J_{P\text{-}Se}$ = 593.9 Hz, $^{1}J_{P\text{-}C}$ = 79.4 Hz).

^{77}Se{^{1}H} NMR: (51.5 MHz, $CDCl_3$) (ppm) δ_{Se} = 142.06 (d, $^{1}J_{Se\text{-}P}$ = 593.7 Hz).

Mass TOF MS ES$^-$: *m/z* = 339.78 (M – $H_2NC_4H_9$).

IR (KBr, cm^{-1}): 3299 (w, N-H), 2968 (m, C-H), 2867 (m, C-H), 1583 (m), 1485 (m), 1434 (m, P-Ph), 1402 (m), 1374 (m), 1286 (m), 1223 (m), 1091 (m), 1002 (m), 835 (m), 747 (m), 692 (s), 548 (s, P=Se) and 508 (m).

2.5.5 Synthesis of Benzylamine *N*-benzyl-*P*-phenylphosphonamidodiselenoate (BenzAWR) (2.5)

Woollins' Reagent (2.01 g, 3.75 mmol) was added to 4 eq of dry benzylamine (1.61 g, 15.0 mmol) in dry THF (20 cm^3). The suspension was stirred for 30 minutes at room temperature until the solution had turned a green-grey colour. The solution was then filtered and evaporated to dryness, yielding an off-white solid, which was redissolved in DCM and recrystallised by layering with hexane.
Yield: 1.75 g, 97%.

^{1}H NMR: (270 MHz, $CDCl_3$, TMS) (ppm) δ_H = 8.22 (bs, 3H, NH_3), 8.17-8.12 (m, 2H, Ar-H), 7.34-7.05 (m, 13H, Ar), 4.13 (s, 2H, CH_2), 3.61 (s, 2H, CH_2) and 3.13 (bs, 3H, NH).

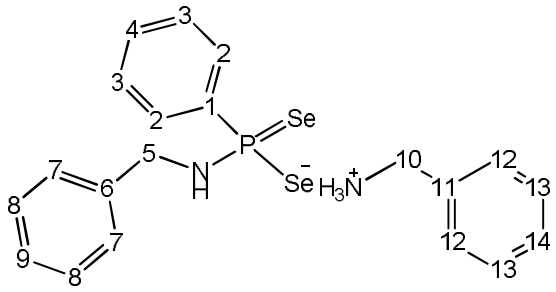

^{13}C{^{1}H} NMR: (67.9 MHz, $CDCl_3$, TMS) (ppm) δ_C = 141.54 (d, $^1J_{C\text{-}P}$ = 75.8 Hz, C1), 139.63 (d, $^3J_{C\text{-}P}$ = 11.4 Hz, C6), 132.44 (s, C11), 130.68 (d, $^2J_{C\text{-}P}$ = 12.6 Hz, C2), 130.36 (d, $^4J_{C\text{-}P}$ = 2.36 Hz, C4), 129.55 (s, Ar-H), 129.03 (s, Ar-H), 128.48 (s, Ar-H), 128.18 (s, Ar-H), 127.99 (s, Ar-H), 127.81 (s, Ar-H), 127.74 (d, $^3J_{C\text{-}P}$ = 13.8 Hz, C3), 47.76 (s, C10) and 43.41 (d, $^2J_{C\text{-}P}$ = 9.34 Hz, C5).

^{31}P{^{1}H} NMR: (109.4 MHz, $CDCl_3$, H_3PO_4) (ppm) δ_P = 45.81 (s, $^1J_{P\text{-}Se}$ = 626 Hz, $^1J_{P\text{-}C}$ = 77.3 Hz).

^{77}Se{^{1}H} NMR: (51.5 MHz, $CDCl_3$) (ppm) δ_{Se} = 44.95 (d, $^1J_{Se\text{-}P}$ = 629 Hz).

Mass TOF MS ES$^-$: *m/z* = 373.75 (M – $H_2NCH_2C_6H_5$).

IR (KBr, cm^{-1}): 3264 (m, N-H), 2925 (m, C-H), 2854 (m, C-H), 1571 (m), 1469 (m), 1436 (m, P-Ph), 1261 (m), 1098 (m), 1063 (m), 805 (m), 747 (m), 697 (s), 550 (s, P=Se) and 485 (s).

2.5.6 2-Aminopentane *N-sec*-pentyl-*P*-phenylphosphonamidodiselenoate (^{s}PentAWR) (2.6)

Woollins' Reagent (0.51 g, 0.95 mmol) was added to four equivalents 2-aminopentane (0.33 g, 3.81 mmol) in dry THF (20 cm^3). The suspension was stirred for 30 minutes at room temperature until the solution had turned a green-grey colour. The solution was then filtered and evaporated to dryness, yielding an off-white solid, which was redissolved in DCM and recrystallised by layering with hexane.
Yield: 0.40 g, 96%.

^{1}H NMR: (270 MHz, $CDCl_3$, TMS) (ppm) δ_H = 8.24-8.15 (m, 2H, Ar-H), 7.38 (bs, 3H, NH_3), 7.34-7.24 (m, 3H, Ar), 3.31-3.24 (m, 1H, CH), 3.20-3.16 (m, 1H, CH), 1.63-1.55 (m, 2H, CH_2), 1.46-1.31 (m, 2H, CH_2), 1.30-1.08 (m, 4H, CH_2), 1.21 (d, $^{3}J_{H-H}$ = 6.61 Hz, 3H, CH_3), 0.91 (d, $^{3}J_{H-H}$ = 6.3 Hz, 3H, CH_3), 0.77 (t, $^{3}J_{H-H}$ = 7.16 Hz, 3H, CH_3) and 0.68 (t, $^{3}J_{H-H}$ = 6.89 Hz, 3H, CH_3).

^{13}C{^{1}H} NMR: (67.9 MHz, $CDCl_3$, TMS) (ppm) δ_C = 143.04 (d, $^{1}J_{C-P}$ = 76.8 Hz, C_q-P), 130.96 (d, $^{2}J_{C-P}$ = 12.5 Hz, *o*-C), 130.64 (d, $^{4}J_{C-P}$ = 3.11 Hz, *p*-C), 127.41 (d, $^{3}J_{C-P}$ = 13.5 Hz, *m*-C), 49.61 (d, $^{2}J_{C-P}$ = 5.19 Hz, CH), 48.45 (s, CH), 31.11 (d, $^{3}J_{C-P}$ = 6.23 Hz, CH_2), 37.25 (s, CH_2), 23.71 (s, CH_3), 22.51 (d, $^{3}J_{C-P}$ = 3.11 Hz, CH_3), 19.00 (s, CH_2), 18.93 (s, CH_2) and 13.76 (s, CH_3).

^{31}P{^{1}H} NMR: (109.4 MHz, $CDCl_3$, H_3PO_4) (ppm) δ_P = 41.60 (s, $^{1}J_{P-Se}$ = 601 Hz, $^{1}J_{P-C}$ = 75.1 Hz).

^{77}Se{^{1}H} NMR: (51.5 MHz, $CDCl_3$) (ppm) δ_{Se} = 72.44 (d, $^{1}J_{Se-P}$ = 601 Hz) and 67.37 (d, J_{Se-P} = 603 Hz).

IR (KBr, cm^{-1}): 3250 (m, N-H), 2956 (m, C-H), 2929 (m, C-H), 2869 (m, C-H), 1590 (m, C=C), 1477 (m), 1435 (m, P-Ph), 1391 (m), 1093 (m), 1028 (m), 970 (m), 744 (s), 690 (s), 559 (s, P=Se) and 514 (m).

2.5.7 **(PropargylAWR) (2.7)**

Woollins' Reagent (0.25 g, 0.47 mmol) was added to four equivalents propargyl amine (0.10 g, 1.8 mmol) in dry THF (20 cm^3). The suspension was stirred for 30 minutes at room temperature until the solution had turned a green-grey colour. The solution was then filtered and evaporated to dryness, yielding an off-white solid, which was redissolved in DCM and recrystallised by layering hexane.
Yield: g, 87 %.

^{1}H NMR: (270 MHz, $CDCl_3$, TMS) (ppm) δ_H = 8.1-8.15 (m, 2H, Ar-H), 7.32-7.28 (m, 3H, Ar), 3.55 (d, $^4J_{H-H}$ = 2.76 Hz, 2H, CH_2), 3.51 (d, $^4J_{H-H}$ = 2.76 Hz, 2H, CH_2), 2.25 (t, $^4J_{H-H}$ = 2.22 Hz, 1H, CH) and 2.11 (t, $^4J_{H-H}$ = 2.49 Hz, 1H, CH).

^{13}C{^{1}H} NMR: (67.9 MHz, $CDCl_3$, TMS) (ppm) δ_C = 141.99 (d, $^1J_{C-P}$ = 74.7 Hz, *i*-C), 130.38 (d, $^2J_{C-P}$ = 12.5 Hz, *o*-C), 130.07 (d, $^4J_{C-P}$ = 2.07 Hz, *p*-C), 127.66 (d, $^3J_{C-P}$ = 12.5 Hz, *m*-C), 82.40 (s, C≡CH), 81.80 (d, $^3J_{C-P}$ = 14.5 Hz, C≡CH), 72.16 (s, C≡CH), 71.46 (s, C≡CH), 33.07 (s, CH_2) and 30.63 (s, CH_2),

^{31}P{^{1}H} NMR: (109.4 MHz, $CDCl_3$, H_3PO_4) (ppm) δ_P = 46.41 (s, $^1J_{P-Se}$ = 627 Hz).

^{77}Se{^{1}H} NMR: (51.5 MHz, $CDCl_3$) (ppm) δ_{Se} = 46.13 (d, $^1J_{Se-P}$ = 627 Hz).

2.5.8 **Synthesis of Complex (2.8)**

^{i}PrAWR (0.10 g, 0.024 mmol) was dissolved in DCM (15 mL) and stirred at room temperature. To this, nickel(II)acetate (0.03 g, 0.012 mmol) was added. The reaction was left to stir for 8 h in which time the solution changed from colourless to brown. The reaction mixture was filtered and the filtrate layered with hexane and placed in the refrigerator. Red crystals of the product were obtained.
Yield: 0.13 g, 77%.

^{1}H NMR: (270 MHz, $CDCl_3$, TMS) (ppm) δ_H = 8.01-7.93 (m, 4H, Ar-H), 7.50-7.48 (m, 6H, Ar-H), 3.41-3.31 (m, 2H, CH) and 1.46 (d, $^{3}J_{C\text{-}P}$ = 6.62 Hz, 12H, CH_3).

^{13}C{^{1}H} NMR: (67.9 MHz, $CDCl_3$, TMS) (ppm) δ_C = 144.78 (d, $^{1}J_{C\text{-}P}$ = 73.4 Hz, *i*-C-P), 131.64 (d, $^{2}J_{C\text{-}P}$ = 10.3 Hz, *o*-C), 130.87 (d, $^{4}J_{C\text{-}P}$ = 2.83 Hz, *p*-C), 128.35 (d, $^{3}J_{C\text{-}P}$ = 12.5 Hz, *m*-C), 43.84 (d, $J_{C\text{-}P}$ = 3.89 Hz, ^{i}Pr-CH) and 23.73 (d, $J_{C\text{-}P}$ = 4.62 Hz, ^{i}Pr-CH_3).

^{31}P{^{1}H} NMR: (109.4 MHz, $CDCl_3$, H_3PO_4) (ppm) δ_P = 21.77 (s, $^{1}J_{P\text{-}Se}$ = 490 Hz, $^{1}J_{P\text{-}C}$ = 72.8 Hz).

^{77}Se{^{1}H} NMR: (51.5 MHz, $CDCl_3$) (ppm) δ_{Se} = -16.96 (d, $^{1}J_{Se\text{-}P}$ = 496 Hz).

Mass TOF MS ES^{+}: *m/z* = 730.38 (MNa^{+}).

IR (KBr, cm^{-1}): 3304 (s, N-H), 2959 (m, C-H), 2922 (m, C-H), 1562 (m, C=C), 1460 (m), 1433 (m, P-Ph), 1396 (m), 1369, (m), 1297 (m), 1116 (s), 1098 (s), 1005 (s), 886 (m), 804 (m), 745 (m), 703 (m), 688 (m), 548 (s, P=Se), 505 (m), 524 (m) and 453 (m).

2.5.9 **Synthesis of Complex (2.9)**

^{i}PrAWR (0.10 g, 0.23 mmol) was dissolved in DCM (10 mL) and stirred at room temperature. To this, copper(II)acetate (0.19 g, 0.94 mmol) was added and the reaction was left to stir overnight in which time the solution changed from colourless to orange/brown. The reaction mixture was filtered and the filtrate layered with hexane and placed in the refrigerator. After 6 weeks, four orange crystals of the product were obtained. From the reaction mixture two main peaks can be observed, listed below. A conclusive assignment cannot be made as to which of these peaks belongs to the product, if either.

^{31}P{^{1}H} NMR: (109.4 MHz, $CDCl_3$, H_3PO_4) (ppm) δ_P = 39.3 (bs) and 10.0 (s).

3. Platinum Complex Chemistry

3.1 Introduction

This chapter discusses the complexation of ligands (**2.1**) - (**2.5**), which were described in the previous chapter, with a platinum centre. A brief introduction to platinum chemistry and Nuclear Magnetic Resonance spectroscopy of ^{31}P, ^{195}Pt and ^{77}Se are given. The reaction of each of the ligands with a selection of platinum precursors is then described in detail. Thereafter the general trends of these systems are shown and examples of the NMR are given.

3.1.1 **Platinum Phosphine Chemistry**

Platinum phosphine complexes have been known for over 150 years,[72] although intense research into their chemistry first started in the late 1950's and early 1960's. This resulted in a library of platinum complexes with almost every permutation of ligand being synthesised.[73] The simplest and most prolific type of platinum phosphine compound has the form $Pt(PR_3)_2Cl_2$. The addition of a phosphine ligand to a platinum salt increases the solubility in organic solvents tremendously, which thus paved the way for platinum group compounds to become some of the most widely used catalysts on the market. Phosphine ligands play a pivotal role in this chemistry as their electronic and steric properties can be tailored to fit the requirements of the system in question.[74]

Bis(phosphine)platinum(II) dihalides are well known for their ease of synthesis and variability of substituents. The most simple synthesis of this type of compound is the direct reaction of $Pt(cod)Cl_2$ with two equivalents of the phosphine in question, see Equation 3.1.

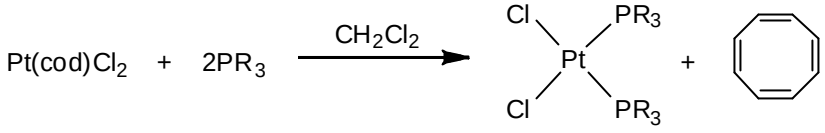

Eqn. 3.1

Complexes of the form $Pt(PR_3)_2Cl_2$ are of particular interest in terms of their NMR properties, owing to the strong coupling observed between the phosphorus atoms and the platinum centre. The chemical shifts and coupling constants allow insight into the bonding modes present in the species, which is discussed in some depth in this chapter.

3.1.2 **Nuclear Magnetic Resonance Spectroscopy**

In nuclear magnetic resonance spectroscopy the magic number is ½. A nuclear spin of ½ gives sharp peaks, which are easy to observe and is observed in nuclides with either an odd number of protons or an odd number of neutrons in its nucleus. The phosphorus 31 nucleus with its natural abundance of 100% and its nuclear spin of ½ is almost as important to some inorganic chemists as hydrogen NMR spectroscopy is to organic chemists, as it has been comprehensively studied for over 40 years. The majority of ^{31}P NMR resonances are most often observed between +250 and -350 ppm, however ^{31}P NMR chemical shifts can cover up to a range of 2000 ppm. $[\{Cr(CO)_5\}_2(\mu\text{–}PBu^t)]$, for example, has a chemical shift of δ_P = 1362 ppm. Electron rich substrates, such as P_4 are seen in the negative chemical shift regions, in this example δ_P = -488 ppm, whilst electron poor compounds are observed as low field resonances.

The presence of more than one NMR active element in a compound allows coupling between them and helps to solve the structure of an unknown substance *via* the relationship and multiplicity of the peaks observed. The chemical shift can be used to help determine the nature of the bonds around the atom and the environment in which the atoms sits.

In the complexes reported herein, five nuclei with spin ½ are present: ^{1}H, ^{13}C, ^{31}P, ^{77}Se and ^{195}Pt, which results in complicated spin systems and somewhat complicated spectra. For instance, the heteroatom NMR spectra must be run with ^{1}H decoupling, as the expected doublets/triplets become complicated multiplets due to ^{1}H coupling. This chapter focuses on three nuclei in particular: the ^{31}P, ^{77}Se and ^{195}Pt nuclei, as the ^{1}H and ^{13}C nuclei are not directly involved in the bonding modes and the spectra are not especially informative.

The 195 isotope of platinum has a natural abundance of 33.8% and a nuclear spin of ½, making NMR a favourable analytical technique for compounds with a Pt centre. The range for δPt is one of the largest known for all NMR active elements, spanning 13000 ppm; even a slight change in ligand substituent can lead to a 100 ppm change in chemical shift.[75] Owing to the sheer wealth of platinum phosphine complexes known, a fair amount has been documented about the trends in coupling constants and shifts of these species. The $^{1}J_{\text{Pt-P}}$ coupling constants for *cis*-$Pt(PR_3)_2Cl_2$ complexes typically lie in the range of 3400-3700 Hz, rising to up to 5800 Hz for platinum phosphine oxides.[76] Platinum oxidation states can be readily assigned from their ^{195}Pt NMR chemical shifts and when ^{2}J coupling between phosphine centres can be observed and *cis* and *trans* isomers are also straightforward to identify, since the $^{1}J_{\text{Pt-P}}$ coupling constants can have a difference in magnitude of up to 1000 Hz.

Of the seven isotopes of selenium, only selenium-77 is NMR active, with a nuclear spin of ½ and a natural abundance of 7.6%. Compared to ^{31}P and ^{195}Pt, ^{77}Se NMR is less well studied and the presence of selenium in compounds is often only observed as satellites, with fewer reports on direct observation of ^{77}Se. ^{77}Se NMR spans a range of roughly 3000 ppm, from -1000 to 2000 ppm, although the compounds in this chapter lie in the narrow window between 0 and 170 ppm. As with all NMR studies, the coupling constants between two atoms enables structure determination and provides insight into the type and strength of the bonds present. In this study, Se is bonded to both ^{31}P and ^{195}Pt atoms, for which the ^{31}P coupling is much more apparent; Selenium satellites are not seen in the ^{195}Pt NMR spectra we measured.

3.2 Discussion

Potassium tetrachloroplatinate, $K_2[PtCl_4]$, is one of the most versatile starting materials for the synthesis of platinum(II) phosphine complexes. Not only can it be directly reacted with bulky groups such as triphenyl phosphine, it is also the starting material for $Pt(cod)Cl_2$ and related compounds, which can be used for the synthesis of other bis(phosphine)platinum dichloride complexes. In this chapter, a series of four platinum phosphine starting materials are prepared: *cis*-$Pt(PMe_3)_2Cl_2$, *cis*-$Pt(PMe_2Ph)_2Cl_2$, *cis*-$Pt(PMePh_2)_2Cl_2$ and *cis*-$Pt(PPh_3)_2Cl_2$, and reacted with five of the ligands prepared in Chapter 2: ^{i}PrAWR (**2.1**), ^{n}BuAWR (**2.2**), ^{s}BuAWR (**2.3**), ^{t}BuAWR (**2.4**) and BenzAWR (**2.5**), synthesising twenty compounds (**3.1**) - (**3.20**). **Figure 3.1** depicts a schematic diagram of compounds (**3.1**) - (**3.20**), whilst Table 3.1 below shows the naming of these compounds.

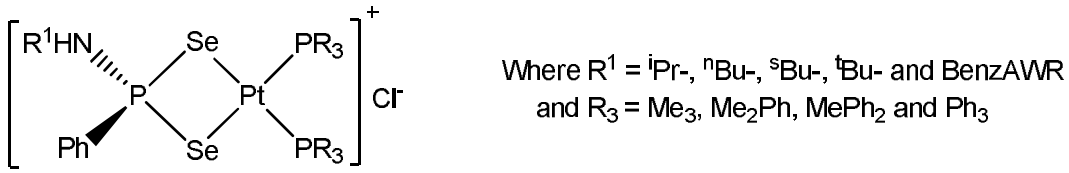

Figure 3.1: Generic diagram of compounds (**3.1**) - (**3.20**)

Table 3.1: Compound numbering in Chapter 3.

	^{i}PrAWR	^{n}BuAWR	^{s}BuAWR	^{t}BuAWR	BenzAWR
PMe_3	(**3.1**)	(**3.5**)	(**3.9**)	(**3.13**)	(**3.17**)
PMe_2Ph	(**3.2**)	(**3.6**)	(**3.10**)	(**3.14**)	(**3.18**)
$PMePh_2$	(**3.3**)	(**3.7**)	(**3.11**)	(**3.15**)	(**3.19**)
PPh_3	(**3.4**)	(**3.8**)	(**3.12**)	(**3.16**)	(**3.20**)

In Sections 3.2.2 – 3.2.6 the new complexes are discussed and compared with respect to the phenylphosphonamidodiselenoate ligand. In Sections 3.2.7 – 3.2.10 the compounds are compared with respect to their phosphine ligands, ie. all PMe_3/PMe_2Ph/$PMePh_2$/PPh_3 compounds.

3.2.1 **General Trends Observed in Compounds (3.1) – (3.20)**

The general case is outlined in this section, whilst the following sections are used to outline trends and observations which can be drawn from the data obtained. Regardless of the size of the ligands, only one phenylphosphonamidodiselenoate ligand binds to the platinum centre in each case, coordinating in a bidentate manner, with an ammonium chloride salt being formed as a byproduct. No dimeric species or doubly substituted species are observed. The generic product is an ionic species with the second chloride ion remaining to act as a counter ion, see Equation 3.2.

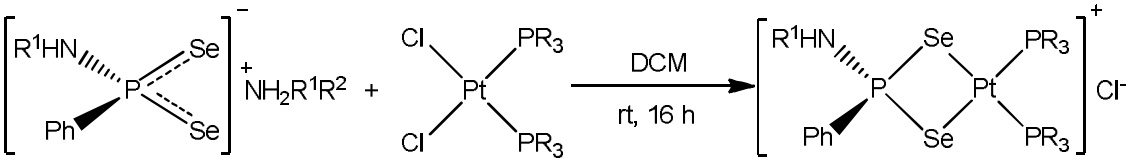

$+ NH_2R^1R^2Cl$ **Eqn 3.2**

The standard reaction between a platinum phosphine, *cis*-$Pt(PR_3)_2Cl_2$, and an ammonium phenylphosphonamidodiselenoate, $[Se_2PPh(NHR)][NH_2R^1R^2]$, is performed at room temperature in DCM and left to stir overnight. The mixture is then filtered, washed with distilled water to remove the salt byproduct, and purified by column chromatography with an eluent mixture of toluene or DCM and ethyl acetate in a varying ratio. The product is then purged from the column with methanol, and the solvent removed *in vacuo*. The products are stable in air and to oxidation, although decompose if left in chlorinated solvents.

The $^{31}P\{^1H\}$, $^{77}Se\{^1H\}$ and $^{195}Pt\{^1H\}$ NMR spectra of each compound were run in $CDCl_3$; examples of each are presented in Figure 3.2 – Figure **3.5**.

Figure 3.2 depicts an example of a typical $^{31}P\{^1H\}$ NMR spectrum of compound (**3.4**), synthesised *via* the reaction of ^{i}PrAWR and *cis*-$Pt(PPh_3)_2Cl_2$. All of the analogous

complexes showed similar P NMR spectra. There are two observed resonances: one at ~31 ppm and the other at ~17 ppm. The latter peak represents the two phosphine centres and is seen as a doublet due to the $^{3}J_{P\text{-}P}$ splitting. For most compounds this splitting is observed to be ~ 7 Hz. The doublets observed at ~3 ppm and ~33 ppm are the Pt satellites, with a $^{1}J_{P\text{-}Pt}$ coupling constant of just over 3000 Hz.

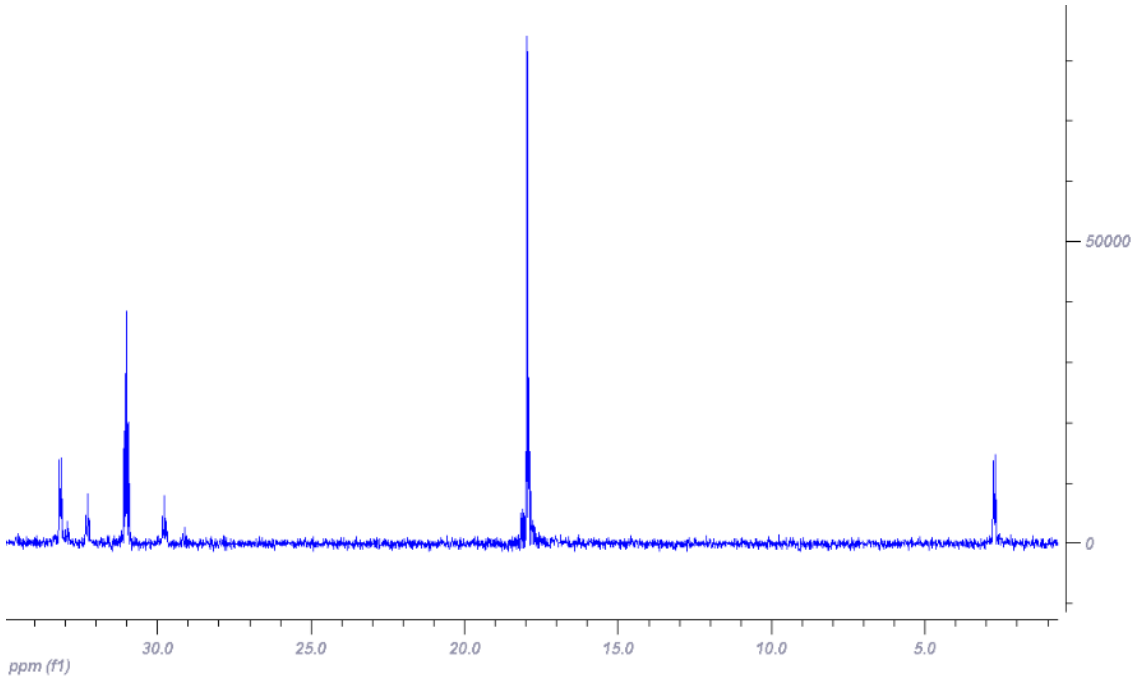

Figure 3.2: Example $^{31}P\{^{1}H\}$ NMR spectrum of a *cis*-$[(PR_3)_2PtSe_2PPh(NHR)]Cl$ complex

The downfield peak of these species, is always that of the phenylphosphonamidodiselenoate moiety and is most often observed as a series of triplets, see **Figure 3.3**, an expanded view of the spectrum taken from the reaction between ^{s}BuAWR and *cis*-$Pt(PMePh_2)_2Cl_2$. The triplets arise from the single phenylphosphonamidodiselenoate phosphorus atom coupling to the two equivalent phosphine P atoms and also have a corresponding $^{3}J_{P\text{-}P}$ splitting of ~ 7 Hz. The first set of satellites, the inner pair, represents the $^{2}J_{P\text{-}Pt}$ coupling, whose magnitude generally lies between 260 and 280 Hz. The second set of satellites, the smaller, outer satellites, are due to the $^{1}J_{P\text{-}Se}$ coupling and is usually around 420 – 430 Hz in magnitude, characteristic of a P-Se bond order of 1. Finally, depending on the strength of the sample, it is sometimes possible to see the Pt satellites of the selenium satellites, which in the example shown in Figure 3.3, have a coupling of $^{1}J_{Pt\text{-}Se}$ = 275 Hz.

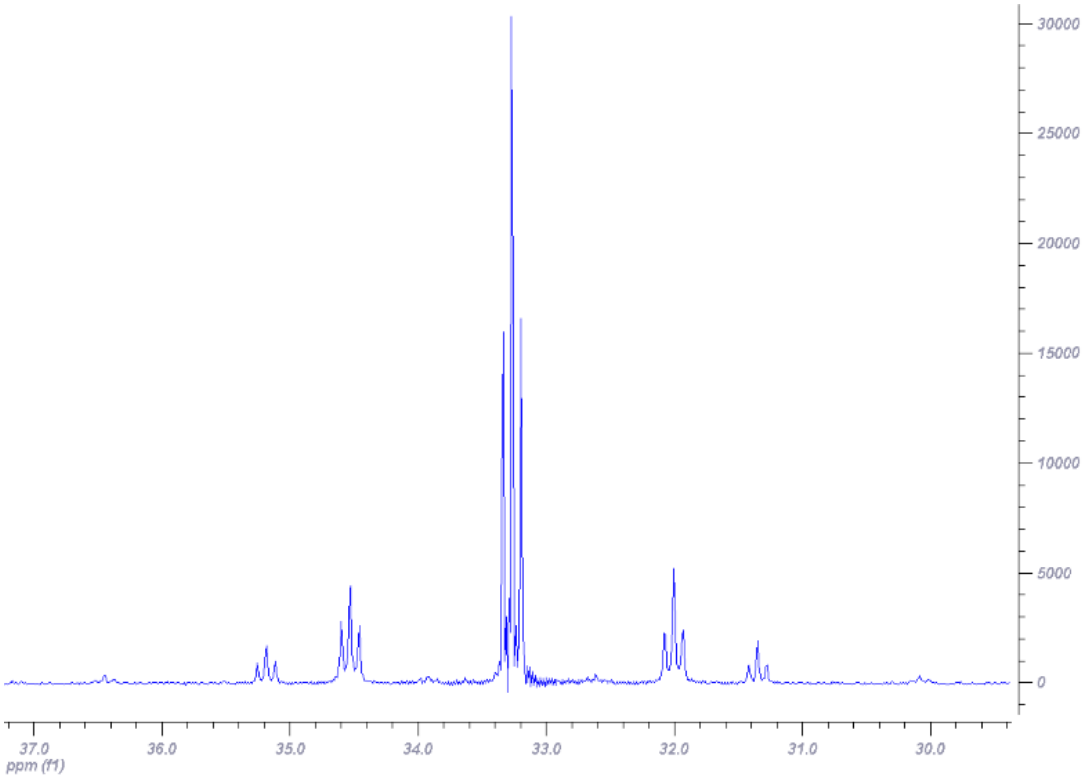

Figure 3.3: Example $^{31}P\{^{1}H\}$ NMR spectrum of a $[(PR_3)_2PtSe_2PPh(NHR)]Cl$ complex

Depending on the strength of the sample, and the frequency the spectrum is run at, $^{1}J_{P\text{-}C}$ coupling can also sometimes be observed for both peaks, as well as the $^{2}J_{P\text{-}Se}$ satellites for the phosphine P atom, however these are generally lost in the noise of the spectrum. As this is the case, such values are treated as extra data and not standard values for investigation.

The ^{195}Pt NMR must also be run with ^{1}H decoupling. As mentioned before, with five different spin ½ elements in these species, the spectra get very complicated when such measures are not taken, as shown in **Figure 3.4**. The top spectrum exhibits the expected splitting pattern of peaks: a doublet of triplets, wherein the large $^{1}J_{Pt\text{-}P}$ value is caused by coupling to the two phosphine ligands, with the smaller $^{2}J_{Pt\text{-}P}$ coupling to the phenylphosphonamidodiselenoate phosphorus atom. No selenium-platinum coupling is seen in the ^{195}Pt NMR spectra, however this to be expected as the satellites are very weak and thus lost in the noise of the spectrum.

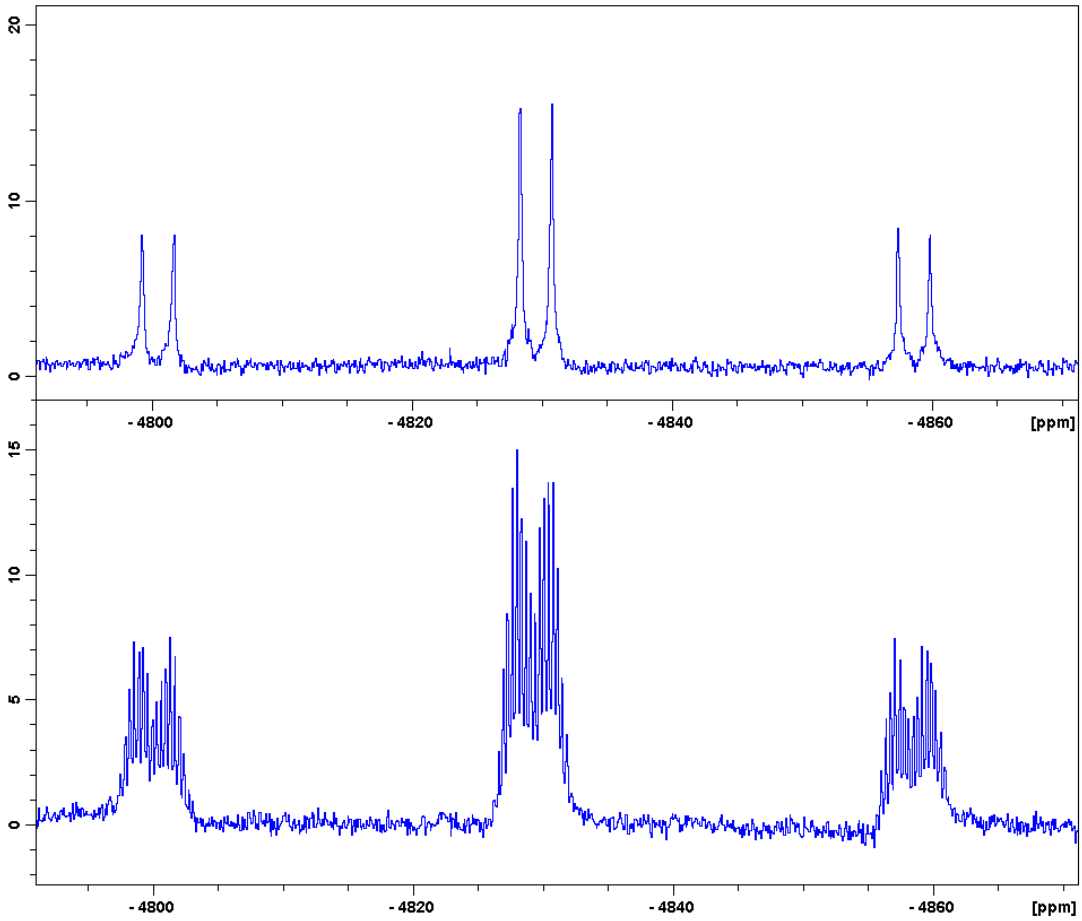

Figure 3.4: Comparison of the ^{195}Pt NMR spectrum (below) with the ^{195}Pt{^{1}H} NMR spectrum (above) for compound (**3.9**).

The most difficult to interpret of all the spectra is that of the ^{77}Se{^{1}H} NMR. Not only does selenium have the lowest natural abundance of the NMR active elements discussed herein, it also appears that both selenium atoms and the two phosphine phosphorus atoms are magnetically inequivalent in some complexes when rotation within the molecule is restricted. As such, between two and four resonances appear in the ^{77}Se{^{1}H} NMR spectra, often overlaying each other, giving complicated splitting patterns, and making the assignment of peaks and coupling constants very difficult. This is highlighted in **Figure 3.5**, which shows a selection of ^{77}Se{^{1}H} NMR spectra.

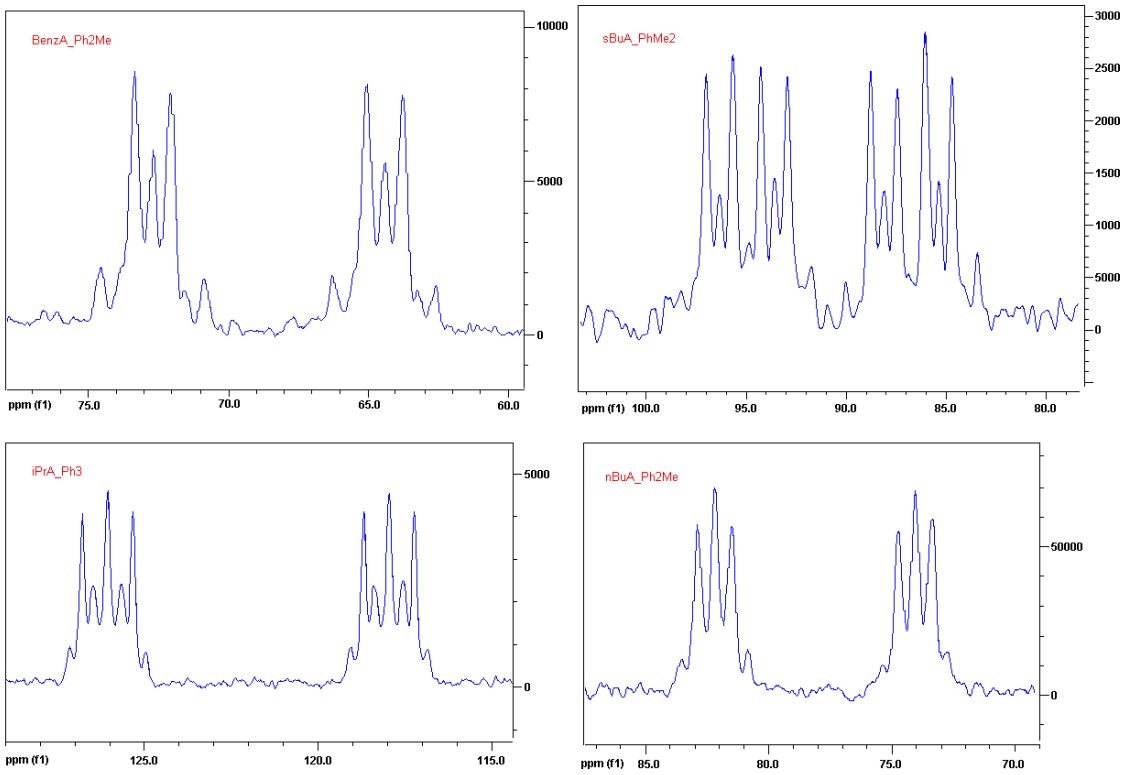

Figure 3.5: Selection of $^{77}Se\{^{1}H\}$ NMR spectra of compounds (**3.19**), (**3.10**), (**3.4**) and (**3.7**)

Using the data provided by the three multinuclear NMR spectra, trends in chemical shifts, coupling and thus bonding can be investigated to examine if there is any correlation between these properties, which will be presented over the next few Sections.

3.2.2 ^{i}PrAWR Compounds

Compound (**2.1**) (^{i}PrAWR) was reacted with the four *cis*-$Pt(PR_3)_2Cl_2$ complexes in DCM at room temperature. In each case, the reaction mixture was left to stir overnight after monitoring the reaction progression by $^{31}P\{^{1}H\}$ NMR spectroscopy. The four products are stable in air and to oxidation and as such could be washed with distilled water to remove the ammonium chloride by-product. The platinum complexes were then separated from any further by-products by column chromatography with a mixed eluent of 95% toluene to 5% ethyl acetate. The products obtained were often oils with some residual impurities, and as such, no IR spectroscopy or elemental analysis was performed on them. The yields of these compounds were also variable: 60% for compound (**3.1**), 48% for (**3.2**), 69% for (**3.3**) and 65% for (**3.4**). Each compound was characterised by $^{31}P\{^{1}H\}$, $^{77}Se\{^{1}H\}$ and $^{195}Pt\{^{1}H\}$ NMR spectroscopy, the results of which are given in **Table 3.2** andTable **3.3**.

Table 3.2: $^{31}P\{^{1}H\}$ NMR data for compounds (**3.1**) - (**3.4**).

	δ_P (ppm)	$^{1}J_{P\text{-}Se}$ (Hz)	$^{2}J_{P\text{-}Pt}$ (Hz)	$^{3}J_{P\text{-}P}$ (Hz)	δ_P (ppm)	$^{1}J_{P\text{-}Pt}$ (Hz)	$^{1}J_{P\text{-}P}$ (Hz)
Me_3 (**3.1**)	35.28	429	261	-	-28.76	3112	-
Me_2Ph (**3.2**)	28.76	373	237	7.04	-19.09	3130	7.04
$MePh_2$ (**3.3**)	32.22	418	275	7.04	-0.73	3208	7.04
Ph_3 (**3.4**)	30.31	418	277	7.04	18.00	3324	7.04

In the $^{31}P\{^{1}H\}$ NMR spectrum, the phenylphosphonamidodiselenoate P atom resonance for the free ^{i}PrAWR ligand has a chemical shift of δ_P = 42.2 ppm, which is downfield (compared to the Pt complex) as expected for a compound containing a P=Se bond. As stated before, however, the ligand is in fact a resonance structure, in which there are two P-Se bonds with bond order 1½ (highlighted in the $^{1}J_{P\text{-}Se}$ coupling constant of 610 Hz). The lone pair on the phosphorus is thus involved in π-bonding to the more electronegative element Se, with the negative charge residing on the Se atoms. The

phosphorus atom will therefore have lower electron density and thus a higher chemical shift. Upon complexation, there is a reduction of electron density on the Se atoms, which is reflected in the $^{1}J_{P\text{-}Se}$ coupling constants (373 – 429 Hz, compared to 610 Hz). This also results in a slight upfield shift of the phenylphosphonamidodiselenoate P atom resonance, hence lower chemical shifts are seen (28.76 – 35.28 ppm).

As a general rule, the phenylphosphonamidodiselenoate P atom resonance decreases with the increase in the number of phenyl groups in the phosphine ligands and thus a decrease in electron density on the phosphine P atoms. A possible reason for this is that the phenylphosphonamidodiselenoate P atom is less shielded with six phenyl groups pulling electron density away from the Pt centre, thus pulling electron density away from the other P atom. In this set of data, however, the data obtained for (**3.2**) is slightly anomalous and does not fit this pattern.

The peaks for (**3.1**) are uncharacteristically seen as broad singlets, as opposed to the expected triplets for the left hand peak and doublets for the right hand peak, see Figure 3.6. This is, however, a feature of the [*cis*-$(PMe_3)_2PtSe_2PPh(NHR)$]Cl complexes, but as all of the PMe_3 spectra were run on the 500 MHz spectrometer, this may have had an effect on the sharpness of the signals. It is also important to note, that the phosphine peak is usually taller than the phenylphosphonamidodiselenoate peak, although this is not the case for (**3.1**).

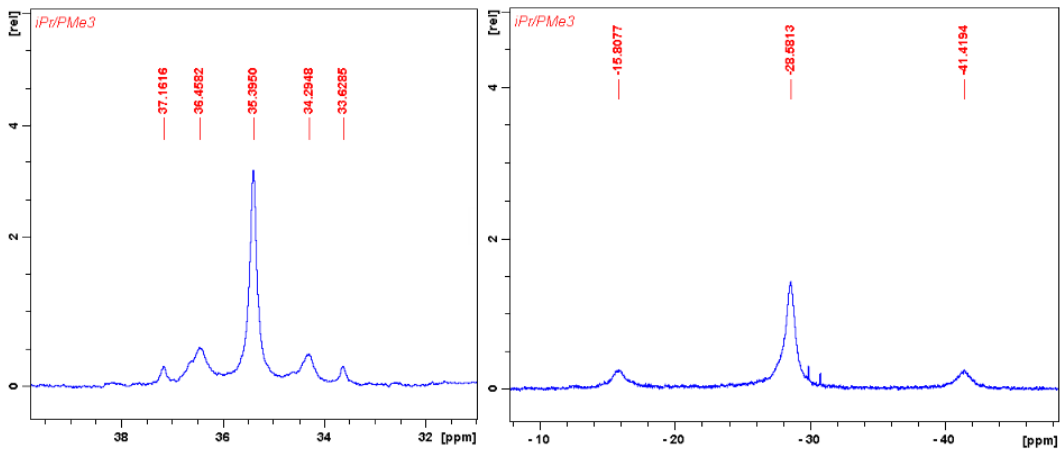

Figure 3.6: $^{31}P\{^{1}H\}$ NMR of (**3.1**)

δ_P for the phosphine P atoms follows the expected pattern: The resonance for the PMe_3 ligand exhibits the greatest upfield shift at -28.8 ppm due to the methyl groups

being most electron donating, whilst the PPh_3 species has the most positive chemical shift of all compounds in this section, at 18.0 ppm, as the rings are the least electron donating, or rather slightly electron withdrawing, as the lone pair on the P atom is taken up into the π system of the rings. The coupling constants also increase from PMe_3 to PPh_3 (3112 to 3324 Hz) indicating an increase in s-character in the P-Pt bond from PMe_3 to PPh_3.

In the $^{77}Se\{^1H\}$ and the $^{195}Pt\{^1H\}$ NMR spectra, a similar increase is observed in the value of δ_{Se} with a corresponding decrease in the value of δ_{Pt}, going from (**3.1**) to (**3.4**), with the exception of (**3.2**). The coupling constants observed in the $^{77}Se\{^1H\}$ and the $^{195}Pt\{^1H\}$ NMR spectra correspond to the data obtained from the $^{31}P\{^1H\}$ NMR spectra, see Table 3.3.

Table 3.3: $^{77}Se\{^1H\}$ and $^{195}Pt\{^1H\}$ NMR data for compounds (**3.1**) - (**3.4**).

	δ_{Se} (ppm)	$^1J_{Se\text{-}P}$ (Hz)	δ_{Pt} (ppm)	$^1J_{Pt\text{-}P}$ (Hz)	$^2J_{Pt\text{-}P}$ (Hz)
Me_3 (**3.1**)	60.6	432	-4829	3115	261
Me_2Ph (**3.2**)	152.9	372	-4849	3133	237
$MePh_2$ (**3.3**)	97.3	417	-4900	3200	267
Ph_3 (**3.4**)	122.0	418	-4933	3316	273

3.2.3 ^{n}BuAWR Compounds

Compound (**2.2**) (^{n}BuAWR) was reacted with the *cis*-$Pt(PMe_3)_2Cl_2$, *cis*-$Pt(PMe_2Ph)_2Cl_2$, *cis*-$Pt(PMePh_2)_2Cl_2$ and *cis*-$Pt(PPh_3)_2Cl_2$ in DCM at room temperature. The reaction progression was monitored by $^{31}P\{^1H\}$ NMR spectroscopy and left to stir for 16 hours. The products are stable in air and to oxidation and as such could be washed with distilled water to remove the ammonium chloride by-product. The product was separated from the other by-products by column chromatography on silica with a mixed eluent of 95% DCM to 5% ethyl acetate. The products obtained were dark orange to brown oils, with variable yields as in the previous section: 65% for compound (**3.5**), 53% for (**3.6**), 62% for (**3.7**) and 54% for (**3.8**). Each compound was characterised by $^{31}P\{^1H\}$, $^{77}Se\{^1H\}$ and $^{195}Pt\{^1H\}$ NMR spectroscopy, the results of which are given in Table 3.4 and Table **3.5**.

Table 3.4: $^{31}P\{^1H\}$ NMR data for compounds (**3.5**) - (**3.8**).

	δ_P (ppm)	$^1J_{P\text{-}Se}$ (Hz)	$^2J_{P\text{-}Pt}$ (Hz)	$^3J_{P\text{-}P}$ (Hz)	δ_P (ppm)	$^1J_{P\text{-}Pt}$ (Hz)	$^1J_{P\text{-}P}$ (Hz)
Me_3 (**3.5**)	39.86	431	261	-	-30.07	3171	-
Me_2Ph (**3.6**)	39.43	425	270	7.04	-18.07	3181	7.04
$MePh_2$ (**3.7**)	37.52	418	275	7.04	-0.74	3209	7.04
Ph_3 (**3.8**)	36.19	418	270	7.04	17.93	3324	7.04

The free ligand, ^{n}BuAWR, has a chemical shift of δ_P = 44.3 ppm in the ^{31}P NMR spectrum and as such we see an upfield shift of the phenylphosphonamidodiselenoate P atom resonance of between 5 and 8 ppm on coupling to the platinum centre. This suggests an increase in electron density on the phosphorus atom due to greater π-backbonding from the metal to selenium atoms, compared with σ-donation from the two Se atoms to the metal, as seen for ^{i}PrAWR.

As before for the ^{i}PrAWR complexes, we see the same decrease in chemical shift of the phenylphosphonamidodiselenoate P atom with the decrease in bulk in the phosphine ligands, from Me_3 to Ph_3. We know that of these species, the trimethyl species is the most electron donating of the phosphines, so it is possible that the electron donation of the phosphine results in extra shielding on the phenylphosphonamidodiselenoate P atom and therefore a higher chemical shift.

We have also previously seen that the $^{1}J_{P\text{-}Se}$, $^{2}J_{P\text{-}Pt}$ and $^{3}J_{P\text{-}P}$ values remain constant with the variation of the phosphine ligand, suggesting no measurable influence on the strength or bond order of the bond, which is also true for the ^{n}BuAWR compounds.

In the $^{77}Se\{^{1}H\}$ NMR spectra, δ_{Se} increases with an increase in the number of phenyl groups in the phosphine ligands. This may be related to the electron withdrawing nature of the phenyl groups. The values for the selenium and platinum chemical shifts are presented in **Table 3.5**.

Table 3.5: $^{77}Se\{^{1}H\}$ and $^{195}Pt\{^{1}H\}$ NMR data for compounds (**3.5**) - (**3.8**).

	δ_{Se} (ppm)	$^{1}J_{Se\text{-}P}$ (Hz)	δ_{Pt} (ppm)	$^{1}J_{Pt\text{-}P}$ (Hz)	$^{2}J_{Pt\text{-}P}$ (Hz)
Me_3 (**3.1**)	44.79	429	-4824	3165	259
Me_2Ph (**3.2**)	68.28	424	-4867	3200	273
$MePh_2$ (**3.3**)	78.10	417	-4891	3206	273
Ph_3 (**3.4**)	96.85	422	-4925	3328	261

The platinum chemical shift, becomes more negative with an increase in steric bulk of the groups of the phosphine ligands, following the observations of Pregosin[77] and Green *et al.*[78]

3.2.4 ^{s}BuAWR Compounds

Compound (**2.3**) (^{s}BuAWR) was also reacted with the four *cis*-Pt$(PR_3)_2Cl_2$ complexes in DCM at room temperature. They were left to stir for 16 hours after monitoring the reaction progression by $^{31}P\{^1H\}$ NMR spectroscopy – after four hours half the starting material had reacted, after this, the speed of the reaction appears to slow down. The products were purified by column chromatography with a mixed eluent of 93% DCM to 7% ethyl acetate. The products were obtained as dark orange to brown oils, wherein one complex, compound (**3.12**) could be crystallised and yellow chip crystals were obtained suitable for X-ray crystallographical analysis. The yields of these compounds were variable, however higher than the other groups of compounds: 61% for compound (**3.9**), 72% for (**3.10**), 54% for (**3.11**) and 75% for (**3.12**). Each compound was characterised by $^{31}P\{^1H\}$, $^{77}Se\{^1H\}$ and $^{195}Pt\{^1H\}$ NMR spectroscopy, the results of which are given in Table 3.6 and Table **3.7**. Compound (**3.12**) is discussed further in Section 3.2.4.1.

Table 3.6: $^{31}P\{^1H\}$ NMR data for compounds (**3.9**) - (**3.12**).

	δ_P (ppm)	$^1J_{P\text{-}Se}$ (Hz)	$^2J_{P\text{-}Pt}$ (Hz)	$^3J_{P\text{-}P}$ (Hz)	δ_P (ppm)	$^1J_{P\text{-}Pt}$ (Hz)	$^1J_{P\text{-}P}$ (Hz)
Me_3 (**3.9**)	35.67	429	261	-	-28.83	3126	-
Me_2Ph (**3.10**)	35.22	425	270	7.04	-17.94	3181	7.04
$MePh_2$ (**3.11**)	33.35	420	275	7.04	-0.72	3211	7.04
Ph_3 (**3.12**)	30.33	425	270	7.04	17.55 17.35	3322	7.74 6.77

As seen before in the $^{31}P\{^1H\}$ NMR spectrum, we observe a decrease in the chemical shift of the phenylphosphonamidodiselenoate ligand phosphorus atom from the free ligand to the bound species, as well as a constant decrease in chemical shift of the same peak with a decrease in steric bulk of the phosphine ligands. The $^1J_{P\text{-}Se}$ coupling constant decreases from the free to the bound ligand, however we see no significant variation of this coupling (420 – 429 Hz), or indeed the $^2J_{P\text{-}Pt}$ coupling (261 –

275 Hz), with a change in the phosphine moiety. The longest range coupling, $^{3}J_{P\text{-}P}$, is in accord with all other compounds in this series.

The chemical shifts for the phosphine moieties follow the expected pattern, with the PMe_3 moiety having the most negative shift at -28.83 ppm and the PPh_3 species being observed at ~17.45 ppm. The biggest difference observed though, is that the two phosphine moieties in compound (**3.12**) are inequivalent, hence the two chemical shifts observed in **Table 3.6**. This is the only compound of the twenty studied where this phenomenon occurs and is discussed further in Section 3.2.4.1. The $^{1}J_{P\text{-}Pt}$ coupling constants follow the expected pattern: a steady increase with the bulkiness of the phosphine.

The chemical shifts in the $^{77}Se\{^{1}H\}$ NMR spectra of the ^{s}BuAWR complexes increase with the bulk of the phosphine ligands, whilst the platinum chemical shifts decrease, suggesting an increase in shielding on selenium and a decrease on platinum, see **Table 3.7**.

Table 3.7: $^{77}Se\{^{1}H\}$ and $^{195}Pt\{^{1}H\}$ NMR data for compounds (**3.9**) - (**3.12**).

	δ_{Se} (ppm)	$^{1}J_{Se\text{-}P}$ (Hz)	δ_{Pt} (ppm)	$^{1}J_{Pt\text{-}P}$ (Hz)	$^{2}J_{Pt\text{-}P}$ (Hz)
Me_3 (**3.9**)	66.59	430	-4832	3128	259
Me_2Ph (**3.10**)	91.18	424	-4874	3183	268
$MePh_2$ (**3.11**)	98.77	420	-4900	3212	267
Ph_3 (**3.12**)	134.7 126.2	417 415	-4933	3320	281

The coupling constants seen in both sets of spectra are in accord with those observed in the corresponding $^{31}P\{^{1}H\}$ NMR spectra listed in Table 3.6, and, just as in the phosphorus NMR spectrum for (**3.12**), the selenium NMR spectrum is more complicated due to the two Se atoms being inequivalent, see Section 3.2.4.1. The values seen for $^{1}J_{Pt\text{-}P}$ are not influenced at all by the phenylphosphonamidodiselenoate ligand.

3.2.4.1 Reaction of ^{s}BuAWR and $Pt(PPh_3)_2Cl_2$

The reaction of compound (**2.3**) (^{s}BuAWR) with *cis*-$Pt(PPh_3)_2Cl_2$ in DCM (Equation 3.3) followed the above procedure yielding an orange oil. The pure product, *cis*-$[(PPh_3)_2PtSe_2PPhNHCH(CH_3)CH_2CH_3]Cl$, was recrystallised by redissolving in DCM and layering with hexane.

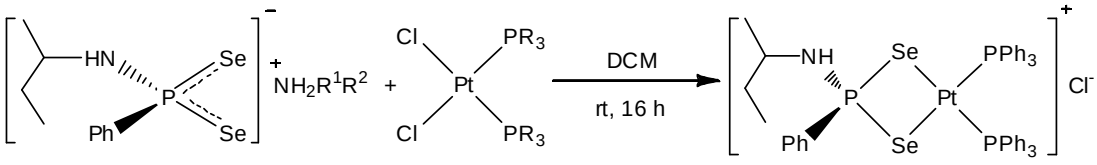

Eqn 3.3

The $^{31}P\{^{1}H\}$ NMR spectrum of the unbound ^{s}BuAWR ligand exhibits a singlet at δ_P = 41.3 ppm flanked by a set of selenium satellites, with a coupling constant of $^{1}J_{P\text{-}Se}$ = 599 Hz. The platinum complex product (**3.12**) exhibits a complex set of triplets in the $^{31}P\{^{1}H\}$ NMR spectrum, with an upfield shift at 30.3 ppm and a coupling constant of $^{1}J_{P\text{-}Se}$ = 425 Hz. This shows a change in bond order of the P-Se bonds, which was confirmed by obtaining the crystal structure for complex (**3.12**), which will be discussed later.

The $^{2}J_{P\text{-}Pt}$ and $^{3}J_{P\text{-}P}$ couplings are in accord with those seen for the other compounds in this series (270 Hz and 7.0 Hz respectively). Although the main peak for the phenylphosphonamidodiselenoate P atom is well defined, the platinum and selenium satellites are less well defined. This may be a consequence of the inequivalence of the phosphorus atoms. We observe two doublets at δ_P = 17.55 ppm and 17.35 ppm for the phosphine ligands in this complex, see Figure 3.7. We can measure the $^{3}J_{P\text{-}P}$ coupling constant of (**3.12**) much more accurately from the phosphine resonance and find that these, too, are dissimilar at 7.74 Hz and 6.77 Hz.

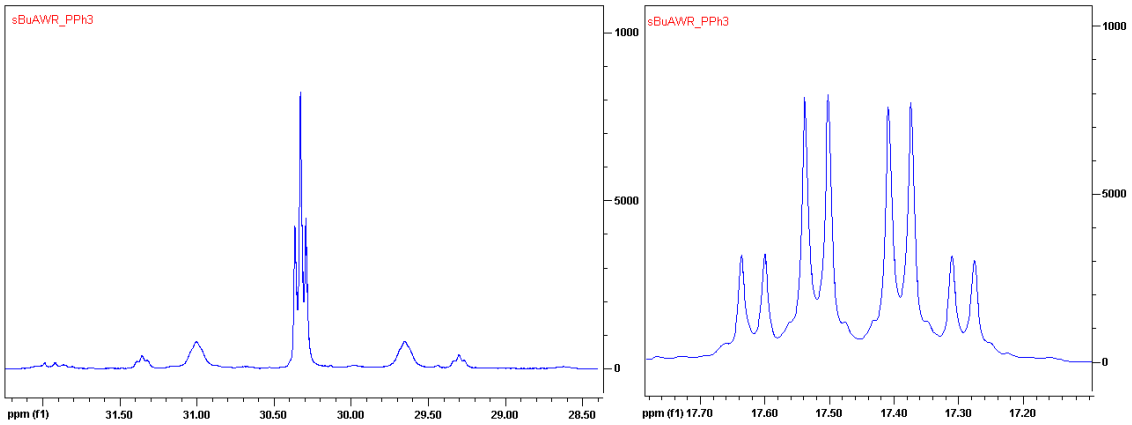

Figure 3.7: Part of the phosphorus NMR spectrum of compound (**3.12**)

The $^{77}Se\{^{1}H\}$ NMR spectrum is also much more complicated than the others shown in Figure 3.5 earlier. In **Figure 3.8 (a)** below, run at 51.5 MHz, we see what appears to be two resonances which overlap in the middle. On running the spectrum at 76.3 MHz (**Figure 3.8 (b)**), the two resonances separate apart and we see that the selenium atoms are indeed inequivalent.

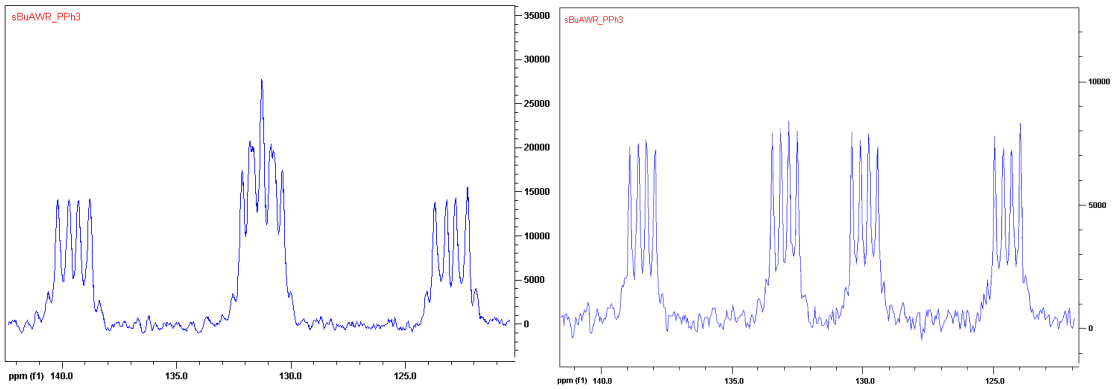

(a) **(b)**

Figure 3.8: **(a)** $^{77}Se\{^{1}H\}$ NMR spectrum of (**3.12**) run at 51.5 MHz.
(b) $^{77}Se\{^{1}H\}$ NMR spectrum of (**3.12**) run at 76.3 MHz.

From the spectrum run at higher frequency, we can read the coupling constants with much greater accuracy, since it is a first order spectrum.

The $^{195}Pt\{^{1}H\}$ NMR spectrum is unaffected by the inequivalent phosphorus atoms in (**3.12**) and the NMR spectrum remains similar to all others in this series: a triplet of doublets.

As mentioned before, crystals of compound (**3.12**), suitable for X-ray analysis were grown and measured on a Rigaku Saturn724 diffractometer with Mo-Kα radiation. The found structure is shown in Figure 3.9.

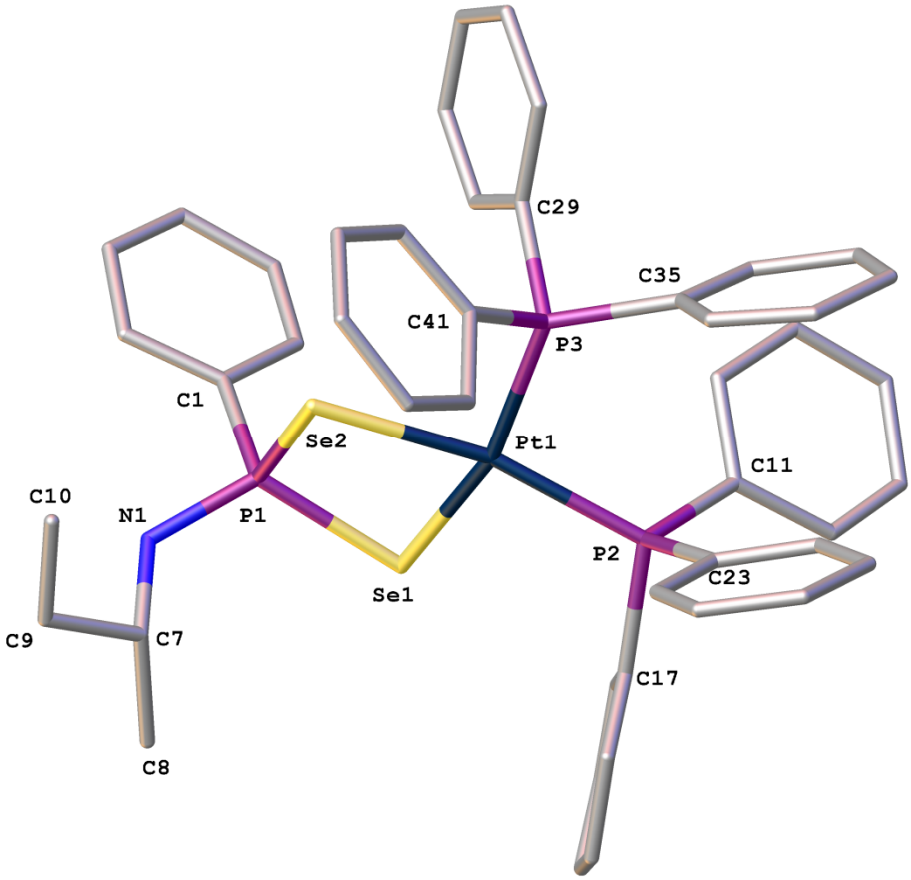

Figure 3.9: Crystal structure of complex (3.12).
H atoms and counter ion omitted for clarity.

The Pt-Se bonds in complex (**3.12**) are, at 2.4710(19) Å and 2.472(2) Å, equivalent to each other and of just above average length according to the CCDC database (average = 2.452 Å), while the Pt-P bond lengths are, at 2.262(5) Å and 2.284(4) Å, of average length compared to the mean of 2.284 Å. In the free ligand, the P-Se bond lengths are 2.152(2) Å and 2.1670(18) Å, which lie in between a bond order of one and two. The average P-Se bond length is 2.222 Å according to the CCDC database, whilst the mean P=Se bond length is 2.111 Å. In complex (**3.12**), the P1-Se1 bond length is 2.209(5) Å, whilst P1-Se2 is 2.196(5) Å in length, demonstrating that the P-Se bonds have a bond order of *circa* 1 in accord with the NMR data discussed above.

The platinum centre adopts a distorted square planar geometry wherein the angles around it are: 84.04(7)° for Se(1)-Pt(1)-Se(2), 91.78(11)° for Se(1)-Pt(1)-P(2), 85.64(12)° for Se(2)-Pt(1)-P(3) and 100.90(15)° for P(2)-Pt(1)-P(3), which are the *cis* bond angles and 163.77(13)° for Se(1)-Pt(1)-P(3) and 166.99(11)° for Se(2)-Pt(1)-P(2), the *trans* angles. This shows that the Pt geometry is distorted up to 14° away from the ideal square planar configuration. The angles around the two phosphine moieties are summarised in Table 3.8, which shows that the highest distortion of the expected tetrahedral geometry is 9.4° for P(2) and over 15° for P(3).

Table 3.8: Angles around the phosphine ligands (°).

Atoms	Angle (°)	Atoms	Angle (°)
Pt(1)-P(2)-C(11)	118.9(7)	Pt(1)-P(3)-C(29)	107.7(5)
Pt(1)-P(2)-C(17)	111.7(6)	Pt(1)-P(3)-C(35)	125.2(5)
Pt(1)-P(2)-C(23)	110.3(6)	Pt(1)-P(3)-C(41)	111.2(5)
C(11)-P(2)-C(17)	103.1(7)	C(29)-P(2)-C(35)	101.2(7)
C(11)-P(2)-C(23)	106.8(8)	C(29)-P(2)-C(41)	106.4(8)
C(17)-P(2)-C(23)	104.8(7)	C(35)-P(2)-C(41)	103.5(8)

For comparison, the angles around the phenylphosphonamidodiselenoate P atom lie in the range of 97.4(2)° to 120.0(7)°, the smallest being the Se(1)-P(1)-Se(2) angle. This 22.6° range, compared to 15.8° for P(2) and 21.7° for P(3), makes P(1) have the most distorted geometry of the three phosphorus atoms. It also shows that whilst the overall geometry of the molecule is dominated by the platinum centre, it has been forced relatively far out of its preferred geometry. The discussed bond lengths and angles are summarised in Table 3.9, whilst full crystallographic data can be found in Appendix 6.

Table 3.9: Selected crystal data for one fragment of compound (**3.12**).

Bond	Length (Å)	Atoms	Angle (°)
Pt(1)-Se(1)	2.4710(19)	Se(1)-Pt(1)-Se(2)	84.04(7)
Pt(1)-Se(2)	2.472(2)	Se(1)-Pt(1)-P(2)	91.78(11)
Pt(1)-P(2)	2.262(5)	Se(1)-Pt(1)-P(3)	163.77(13)
Pt(1)-P(3)	2.284(4)	Se(2)-Pt(1)-P(2)	166.99(11)
Se(1)-P(1)	2.209(5)	Se(2)-Pt(1)-P(3)	85.64(12)
Se(2)-P(1)	2.196(5)	P(2)-Pt(1)-P(3)	
P(1)-C(1)	1.800(19)	Pt(1)-Se(1)-P(1)	
P(1)-N(1)	1.631(16)	Pt(1)-Se(2)-P(1)	
N(7)-C(8)	1.52(3)	Se(1)-P(1)-Se(2)	
		Se(1)-P(1)-N(1)	
		Se(2)-P(1)-N(1)	
		Se(1)-P(1)-C(1)	
		Se(2)-P(1)-C(1)	

3.2.5 ^{t}BuAWR Compounds

Compound (**2.4**) (^{t}BuAWR) was reacted with platinum complexes *cis*-$Pt(PMe_3)_2Cl_2$, *cis*-$Pt(PMe_2Ph)_2Cl_2$, *cis*-$Pt(PMePh_2)_2Cl_2$ and *cis*-$Pt(PPh_3)_2Cl_2$ in DCM at room temperature. The progression of the reactions was monitored by $^{31}P\{^{1}H\}$ NMR spectroscopy and allowed to stir for 16 hours. The products were then purified by column chromatography with a mixed eluent of 95% toluene to 5% ethyl acetate. The yields of these compounds, as with the compounds before, were variable: 51% for compound (**3.13**), 52% for (**3.14**), 38% for (**3.15**) and 44% for (**3.16**), much lower than those obtained for the ^{s}BuAWR compounds. Each compound was characterised by $^{31}P\{^{1}H\}$, $^{77}Se\{^{1}H\}$ and $^{195}Pt\{^{1}H\}$ NMR spectroscopy, the results of which are given in Table 3.10 and Table **3.11**.

Table 3.10: $^{31}P\{^{1}H\}$ NMR data for compounds (**3.13**) - (**3.16**).

	δ_P (ppm)	$^{1}J_{P\text{-}Se}$ (Hz)	$^{2}J_{P\text{-}Pt}$ (Hz)	$^{3}J_{P\text{-}P}$ (Hz)	δ_P (ppm)	$^{1}J_{P\text{-}Pt}$ (Hz)	$^{1}J_{P\text{-}P}$ (Hz)
Me_3 (**3.13**)	25.37	433	265	7.04	-28.29	3148	7.04
Me_2Ph (**3.14**)	24.66	425	275	7.04	-17.75	3193	7.04
$MePh_2$ (**3.15**)	23.03	420	277	7.04	-0.70	3225	7.04
Ph_3 (**3.16**)	21.98	423	277	7.04	17.72	3342	7.04

In the $^{31}P\{^{1}H\}$ NMR, the phenylphosphonamidodiselenoate P atom resonance for free ^{t}BuAWR ligand has a chemical shift of δ_P = 29.8 ppm, much lower than all other ligands utilised herein. In the synthesised platinum complexes, the ^{t}BuA complexes, (**3.13 - 3.16**) also have the highest upfield shift of all the analogues, however the difference in chemical shift between the bound and unbound ligand is the smallest, at between 4.5 ppm and 8 ppm. The largest difference is seen in the PPh_3 complex, suggesting the phenylphosphonamidodiselenoate P atom in (**3.16**) is the least shielded of these complexes. It is proposed that this is the case due to the electron withdrawing nature of the phenyl rings in the phosphine ligands.

As stated before, the two P-Se bonds in the ligand, have a bond order of 1½ ($^1J_{P\text{-}Se}$ = 594 Hz). Upon complexation, there is a reduction of electron density on the Se atoms, wherein the two P-Se bonds become formal single bonds, which is reflected in the coupling constants (420 – 433 Hz compared to 594 Hz). As with most of the data sets, the values for $^1J_{P\text{-}Se}$, $^2J_{P\text{-}Pt}$ and $^3J_{P\text{-}P}$ do not vary by large amounts if at all between compounds. δ_P for the phosphine ligands are all as expected and the $^1J_{P\text{-}Pt}$ values are in accord with the compounds reported in the previous sections.

The chemical shifts in the $^{77}Se\{^1H\}$ NMR data are the highest recorded for all complexes that follow the pattern of increasing shift with an increasing number of phenyl groups in the phosphine ligands, most likely as the ^{t}Butyl groups strongly donate electron density into the Se atoms, causing more shielding of the nucleus, see Table 3.11.

Table 3.11: $^{77}Se\{^1H\}$ and $^{195}Pt\{^1H\}$ NMR data for compounds (**3.13**) - (**3.16**).

	δ_{Se} (ppm)	$^1J_{Se\text{-}P}$ (Hz)	δ_{Pt} (ppm)	$^1J_{Pt\text{-}P}$ (Hz)	$^2J_{Pt\text{-}P}$ (Hz)
Me_3 (**3.13**)	98.03	435	-4817	3138	264
Me_2Ph (**3.14**)	118.3	425	-4857	3194	272
$MePh_2$ (**3.15**)	129.0	420	-4884	3225	273
Ph_3 (**3.16**)	160.2	418	-4916	3337	273

The chemical shifts in the $^{195}Pt\{^1H\}$ NMR data follow the expected pattern of an increase in shift with the number of phenyl rings in the phosphine ligands. There seems to be no trend in influence observed with a variation of bulk of the phenylphosphonamidodiselenoate ligand.

3.2.6 **BenzAWR Compounds**

Compound (**2.5**) (BenzAWR) was reacted with platinum complexes *cis*-$Pt(PMe_3)_2Cl_2$, *cis*-$Pt(PMe_2Ph)_2Cl_2$, *cis*-$Pt(PMePh_2)_2Cl_2$ and *cis*-$Pt(PPh_3)_2Cl_2$ in DCM at room temperature. The reaction progression was monitored by $^{31}P\{^1H\}$ NMR spectroscopy and left to stir overnight. The product was separated from the by-products by column chromatography on silica with a mixed eluent of 95% DCM to 5% ethyl acetate. The products obtained were light to dark brown oils, for which the yields were as variable as in the previous sections: 67% for complex (**3.17**), 56% for (**3.18**), 62% for (**3.19**) and 64% for (**3.20**). Each compound was characterised by $^{31}P\{^1H\}$, $^{77}Se\{^1H\}$ and $^{195}Pt\{^1H\}$ NMR spectroscopy, the results of which are given in Table 3.12 and Table **3.13**.

Table 3.12: $^{31}P\{^1H\}$ NMR data for compounds (**3.17**) - (**3.20**).

	δ_P (ppm)	$^1J_{P\text{-}Se}$ (Hz)	$^2J_{P\text{-}Pt}$ (Hz)	$^3J_{P\text{-}P}$ (Hz)	δ_P (ppm)	$^1J_{P\text{-}Pt}$ (Hz)	$^1J_{P\text{-}P}$ (Hz)
Me_3 (**3.17**)	41.39	433	268	-	-29.36	3084	-
Me_2Ph (**3.18**)	40.87	427	270	7.04	-17.90	3179	7.04
$MePh_2$ (**3.19**)	40.81	429	264	7.04	-0.72	3229	7.04
Ph_3 (**3.20**)	37.01	418	270	7.04	18.28	3310	7.04

The chemical shifts of the phenylphosphonamidodiselenoate P atoms in the BenzAWR series have the highest of all the twenty complexes, which was also true for the free ligand. This chemical shift decreases with the increase in electron withdrawing nature of the phosphine ligands. The $^1J_{P\text{-}Se}$ coupling constant for the free ligand was the highest observed at 629 Hz, however in the bound species this is no longer the case and the values seen are in accord with all others, as are the $^2J_{P\text{-}Pt}$ and $^3J_{P\text{-}P}$ values. The phosphine resonances increase with phenyl moieties, as does the $^1J_{P\text{-}Pt}$ value.

The $^{77}Se\{^1H\}$ NMR data does not seem to follow any pattern (**Table 3.13**), with the highest chemical shift being unexpectedly seen for the Me_3 complex data and the

second highest value occurring for compound (**3.19**), the $MePh_2$ complex. The data appear to be anomalous, as the $^{195}Pt\{^1H\}$ NMR follows the expected pattern and δ_{Se} of the free BenzAWR ligand was the smallest value observed. The data for (**3.18**) and (**3.20**), in comparison, seem to fit this pattern. In spite of these anomalies, the $^1J_{Se\text{-}P}$ coupling constants are in the expected range. The $^{195}Pt\{^1H\}$ NMR shifts are as expected, as are the $^1J_{Pt\text{-}P}$ and $^2J_{Pt\text{-}P}$ thereof.

Table 3.13: $^{77}Se\{^1H\}$ and $^{195}Pt\{^1H\}$ NMR data for compounds (**3.17**) - (**3.20**).

	δ_{Se} (ppm)	$^1J_{Se\text{-}P}$ (Hz)	δ_{Pt} (ppm)	$^1J_{Pt\text{-}P}$ (Hz)	$^2J_{Pt\text{-}P}$ (Hz)
Me_3 (**3.17**)	135.6	411	-4816	3091	233
Me_2Ph (**3.18**)	67.56	427	-4856	3180	272
$MePh_2$ (**3.19**)	129.8	426	-4903	3204	261
Ph_3 (**3.20**)	98.97	417	-4914	3316	267

3.2.7 **Pt(PMe$_3$)$_2$L Compounds**

In Sections 3.2.2 – 3.2.6 trends in compounds (**3.1**) to (**3.20**) were discussed within groups determined by the phenylphosphonamidodiselenoato ligands, however, within such a study of compounds, we can determine trends by varying the fixed phosphine ligands too, which will be discussed in Sections 3.2.7 to 3.2.10.

As is to be expected, the chemical shift of the phosphine P atom stays fairly stable with the variation of the R group on the phenylphosphonamidodiselenoate phosphorus atom. It appears that, in the sequence ^{n}Bu to ^{s}Bu to ^{t}Bu, the chemical shifts become less negative (30.1, 28.8 and 28.3 ppm respectively), a trend we see for all phosphine R groups, but this is such a small decrease that a much wider range of compounds would have to be investigated to confirm this is a trend, not just coincidence. That stated, we see a large decrease in δ_P for the phenylphosphonamidodiselenoate P atom from ^{n}Bu to ^{s}Bu to ^{t}Bu: 39.9, 35.7 and 25.4 ppm, respectively. This is because there is an increase in electron donation from ^{n}Bu to ^{t}Bu.

The chemical shift for the phenylphosphonamidodiselenoate P atom in the ^{i}PrAWR and ^{s}BuAWR are seen to be similar, possibly due to the similarity in shape of the R group: branched rather than straight chain.

As a general rule the coupling constants witnessed for $^{1}J_{P\text{-}Se}$ of the phenylphosphonamidodiselenoate phosphorus atom are seen within a 25 Hz window from 410 – 435 Hz, $^{2}J_{P\text{-}Pt}$ lies within a 15 Hz window (260 – 275 Hz) and $^{3}J_{P\text{-}P}$ varies infrequently from 7.04 Hz. $^{31}P\{^{1}H\}$ NMR data for the trimethyl compounds are given in Table 3.14 and are discussed over the page.

Table 3.14: $^{31}P\{^{1}H\}$ NMR data for compounds (**3.1**), (**3.5**), (**3.9**), (**3.13**) and (**3.17**).

	δ_P (ppm)	$^{1}J_{P\text{-}Se}$ (Hz)	$^{2}J_{P\text{-}Pt}$ (Hz)	$^{3}J_{P\text{-}P}$ (Hz)	δ_P (ppm)	$^{1}J_{P\text{-}Pt}$ (Hz)	$^{1}J_{P\text{-}P}$ (Hz)
^{i}PrAWR (**3.1**)	35.28	429	261	-	-28.76	3127	-
^{n}BuAWR (**3.5**)	39.85	431	261	-	-30.07	3170	-
^{s}BuAWR (**3.9**)	35.66	429	263	-	-28.83	3125	-
^{t}BuAWR (**3.13**)	25.37	433	265	-	-28.29	3148	-
BenzAWR (**3.17**)	41.39	433	268	-	-29.36	3084	-

The $^{31}P\{^{1}H\}$ NMR spectra for the Me_3 compounds are similar to each other in that they all exhibit singlets for both the phenylphosphonamidodiselenoate P atom and the phosphine P atoms, in comparison to the triplets and doublets seen for almost all other compounds discussed in this chapter.

The chemical shift of the starting material, *cis*-$Pt(PMe_3)_2Cl_2$, is seen at δ_P = -23.26 ppm, with a $^{1}J_{P\text{-}Pt}$ coupling constant of 3484 Hz. On complexation with the phenylphosphonamidodiselenoate ligand, a downfield shift of δ_P is seen for the phosphine moiety (δ_P = -30.27 to -28.29 ppm), in conjunction with a decrease in $^{1}J_{P\text{-}Pt}$ (3084-3170 Hz), signalling a decrease in shielding around the phosphine P atoms and a decrease in the s character of the Pt-P bond. The effect on the nuclear shielding is strongest in the ^{n}BuAWR complex, whilst the benzylamine derivative experiences the largest change in bond strength.

The $^{77}Se\{^{1}H\}$ NMR spectra of the trimethylphosphine complexes appear to show a trend of increasing chemical shift from butyl (44.8 ppm) to *t*-butyl (98.0 ppm), see Table 3.15. The ^{i}Pr, ^{n}Bu, ^{s}Bu and ^{t}Bu all show a decrease in δ_{Se} compared to the free ligand, whilst the benzyl amine derivative shows a large increase in δ_{Se}.

Table 3.15: ^{77}Se and ^{195}Pt{^{1}H} NMR data for compounds (**3.1**), (**3.5**), (**3.9**), (**3.13**) and (**3.17**).

	δ_{Se} (ppm)	$^{1}J_{Se\text{-}P}$ (Hz)	δ_{Pt} (ppm)	$^{1}J_{Pt\text{-}P}$ (Hz)	$^{2}J_{Pt\text{-}P}$ (Hz)
^{i}PrAWR (**3.1**)	60.6	432	-4830	3128	261
^{n}BuAWR (**3.5**)	44.8	429	-4824	3165	259
^{s}BuAWR (**3.9**)	66.5	430	-4832	3128	259
^{t}BuAWR (**3.13**)	98.0	435	-4817	3138	264
BenzAWR (**3.17**)	135.6	411	-4816	3091	233

Compared to the dichloride starting material, *cis*-Pt(PMe$_3$)$_2$Cl$_2$, which has a chemical shift of δ_{Pt} = -4408 ppm in the ^{195}Pt{^{1}H} NMR, all of the complexes are at higher field (-4816 to -4832 ppm), indicating less shielding on the metal centre. Although the ligand species are quite different, the organic residues have little or no influence on the Pt centre, as there is no apparent trend seen in the shift data.

3.2.8 **$Pt(PMe_2Ph)_2L$ Compounds**

The $^{31}P\{^1H\}$ NMR spectra for the Me_2Ph compounds are similar to each other, exhibiting the expected triplets for the phenylphosphonamidodiselenoate ligand, flanked by platinum and selenium satellites and doublets for the phosphine peak, flanked by platinum satellites. This pattern is seen for almost all other compounds discussed in this chapter.

The chemical shift of the starting material, *cis*-$Pt(PMe_2Ph)_2Cl_2$, is seen at -14.64 ppm, with a $^1J_{P\text{-}Pt}$ coupling constant of 3550 Hz. On reacting the phenylphosphonamidodiselenoate species with $Pt(PMe_2Ph)_2Cl_2$, an upfield shift for δ_P of the phosphine groups is seen in each case (-19.1 to -17.8 ppm), with a corresponding decrease in $^1J_{P\text{-}Pt}$ (3130-3193 Hz), again signalling a decrease in shielding around the phosphine P atoms and a decrease in s character of the Pt-P bond. Compared to the trimethyl complexes, the dimethylphenylphosphine species experience less deviation from the starting material chemical shift upon complexation, however a larger change in the magnitude of the coupling constant.

The benzylamine complex has the highest chemical shift for the phenylphosphonamidodiselenoate peak, as the P atom is the most shielded, this does not appear to have any effect on the phosphine resonances though. The $^{31}P\{^1H\}$ NMR data for all the dimethylphenylphosphine complexes are exhibited in Table 3.16.

Table 3.16: $^{31}P\{^1H\}$ NMR data for compounds (**3.2**), (**3.6**), (**3.10**), (**3.14**) and (**3.18**)

	δ_P (ppm)	$^1J_{P\text{-}Se}$ (Hz)	$^2J_{P\text{-}Pt}$ (Hz)	$^3J_{P\text{-}P}$ (Hz)	δ_P (ppm)	$^1J_{P\text{-}Pt}$ (Hz)	$^1J_{P\text{-}P}$ (Hz)
^{i}PrAWR (**3.2**)	28.76	373	239	7.04	-19.09	3130	7.04
^{n}BuAWR (**3.6**)	39.43	425	270	7.04	-18.07	3181	7.04
^{s}BuAWR (**3.10**)	35.22	425	270	7.04	-17.94	3181	7.04
^{t}BuAWR (**3.14**)	24.66	425	275	7.04	-17.75	3193	7.04
BenzAWR (**3.18**)	40.87	427	270	7.04	-17.90	3179	7.04

Table 3.17: $^{77}Se\{^{1}H\}$ and $^{195}Pt\{^{1}H\}$ NMR data for compounds (**3.2**), (**3.6**), (**3.10**), (**3.14**) and (**3.18**).

	δ_{Se} (ppm)	$^{1}J_{Se\text{-}P}$ (Hz)	δ_{Pt} (ppm)	$^{1}J_{Pt\text{-}P}$ (Hz)	$^{2}J_{Pt\text{-}P}$ (Hz)
^{i}PrAWR (**3.2**)	152.9	372	-4849	3133	237
^{n}BuAWR (**3.6**)	68.3	424	-4867	3200	273
^{s}BuAWR (**3.10**)	91.2	424	-4874	3183	268
^{t}BuAWR (**3.14**)	118.4	425	-4857	3194	272
BenzAWR (**3.18**)	67.6	427	-4856	3180	272

Table 3.17 above displays the values obtained for the chemical shifts and coupling constants for compounds (**3.2**), (**3.6**), (**3.10**), (**3.14**) and (**3.18**), the dimethylphenyl phosphine complexes in the $^{77}Se\{^{1}H\}$ and $^{195}Pt\{^{1}H\}$ NMR spectra. We see a tendencial increase in δ_{Se} for the butyl compounds with increasing steric bulk, but overall there appears to be no pattern to the data. δ_{Se} for the ^{i}PrAWR species appears to be surprisingly high (152.9 ppm) and the corresponding $^{1}J_{Se\text{-}P}$ value (372 Hz) also deviates significantly from those of the remaining complexes in the series (424-427 Hz). Nevertheless, the latter does correspond to the value seen in the $^{31}P\{^{1}H\}$ NMR.

δ_{Pt} appears not to be affected by the size of the amine moiety on the ligand. The chemical shift for *cis*-$Pt(PMe_2Ph)_2Cl_2$ is -4403 ppm, and on reaction with the phenylphosphonamidodiselenoate moieties an upfield shift of up to 471 ppm is seen.

3.2.9 **Pt(PMePh$_2$)$_2$L Compounds**

The chemical shift of the starting material, *cis*-Pt(PMePh$_2$)$_2$Cl$_2$, is located at -0.30 ppm in the $^{31}P\{^1H\}$ NMR spectrum, with a $^1J_{P\text{-}Pt}$ coupling of 3618 Hz. On reaction with the phenylphosphonamidodiselenoate ligands, the average value of $\Delta\delta_P$ is just -0.42 ppm, much smaller than in all other cases seen in this chapter. The $^1J_{P\text{-}Pt}$ coupling constants all lie within 15 Hz of each other, showing that the size of the amine moiety does not have a large effect on the bond strength of the phosphine ligand.

The difference in chemical shift between (**3.7**, ^{n}Bu) and (**3.15**, ^{t}Bu) is 14.5 ppm, exactly the same as for the free ligands, suggesting there is no effect on the shielding of the P atom caused by the steric bulk of the of the *t*-butyl group.

As before, both $^1J_{P\text{-}Se}$ and $^2J_{P\text{-}Pt}$ are unaffected by the size or electronic effects of the amine moieties. All $^{31}P\{^1H\}$ NMR spectral data is presented in Table 3.18.

Table 3.18: $^{31}P\{^1H\}$ NMR data for compounds (**3.3**), (**3.7**), (**3.11**), (**3.15**) and (**3.19**).

	δ_P (ppm)	$^1J_{P\text{-}Se}$ (Hz)	$^2J_{P\text{-}Pt}$ (Hz)	$^3J_{P\text{-}P}$ (Hz)	δ_P (ppm)	$^1J_{P\text{-}Pt}$ (Hz)	$^1J_{P\text{-}P}$ (Hz)
^{i}PrAWR (**3.3**)	32.22	418	275	7.04	-0.73	3208	7.04
^{n}BuAWR (**3.7**)	37.52	418	275	7.04	-0.74	3209	7.04
^{s}BuAWR (**3.11**)	33.35	420	275	7.04	-0.72	3211	7.04
^{t}BuAWR (**3.15**)	23.03	420	277	7.04	-0.70	3223	7.04
BenzAWR (**3.19**)	40.81	429	264	7.04	-0.72	3209	7.04

The data obtained for the $^{77}Se\{^1H\}$ NMR spectra, presented in Table 3.19, shows an increase in δ_{Se} for butyl compounds (**3.7**), (**3.11**) and (**3.15**) confirming and increase in shielding on the selenium atoms with an increase in the electron donation from the amine moiety (^{n}Bu-^{t}Bu). The $^1J_{P\text{-}Se}$ coupling constants are in accord with those seen for all other compounds.

Table 3.19: $^{77}Se\{^{1}H\}$ and $^{195}Pt\{^{1}H\}$ NMR data for compounds (**3.3**), (**3.7**), (**3.11**), (**3.15**) and (**3.19**).

	δ_{Se} (ppm)	$^{1}J_{Se\text{-}P}$ (Hz)	δ_{Pt} (ppm)	$^{1}J_{Pt\text{-}P}$ (Hz)	$^{2}J_{Pt\text{-}P}$ (Hz)
^{i}PrAWR (**3.3**)	97.3	417	-4900	3200	267
^{n}BuAWR (**3.7**)	78.1	417	-4891	3206	273
^{s}BuAWR (**3.11**)	98.8	420	-4900	3212	267
^{t}BuAWR (**3.15**)	129.0	420	-4884	3225	273
BenzAWR (**3.19**)	129.8	426	-4903	3204	261

The $^{195}Pt\{^{1}H\}$ NMR spectra of compounds (**3.3**), (**3.7**), (**3.11**), (**3.15**) and (**3.19**) show resonances around -4900 ppm, with $^{1}J_{Pt\text{-}P}$ coupling constants between 3200 and 3225 Hz. The coupling constants are slightly larger than those seen for the $(PMe_2Ph)_2$ species reported in the previous section, suggesting slightly stronger bonding between the phosphine ligands and the Pt centre. The chemical shifts, on the other hand are slightly lower, meaning the platinum centre is less shielded than in the previous examples. The $^{2}J_{Pt\text{-}P}$ couplings are all in accord with those seen in previous sections.

3.2.10 **Pt(PPh$_3$)$_2$L Compounds**

The $^{31}P\{^1H\}$ NMR spectra for the *cis*-triphenylphosphine compounds are all similar to each other, exhibiting the expected triplets for the phenylphosphonamidodiselenoate ligand, with platinum and selenium satellites and doublets for the phosphine peak, surrounded by platinum satellites, apart from the ^{s}BuAWR compound, which was discussed extensively in Section 3.4.2.1. The complex starting material, *cis*-Pt(PPh$_3$)$_2$Cl$_2$, has a chemical shift of 14.9 ppm, and as such the triphenyl phosphine complexes are the only ones that have a positive chemical shift on coordination to the phenylphosphonamidodiselenoate ligand. The $^1J_{P\text{-}Pt}$ coupling constants decrease by roughly 350 Hz on coordination of the ligand. They are, however, the highest seen for all the complexes, due to the steric bulk of the phenyl groups. With the exception of the $^1J_{P\text{-}P}$ coupling for ^{s}BuAWR, for which two couplings are seen, all other coupling constants in the $^{31}P\{^1H\}$ NMR remain steady and in accord with all others seen. Of the two $^1J_{P\text{-}P}$ coupling constants seen for ^{s}BuAWR, one is a greater and one is smaller than this series of compounds (7.74 Hz and 6.77 Hz cf. 7.04 Hz). The $^{31}P\{^1H\}$ NMR data is exhibited in Table 3.20.

Table 3.20: $^{31}P\{^1H\}$ NMR data for compounds (**3.4**), (**3.8**), (**3.12**), (**3.16**) and (**3.20**).

	δ_P (ppm)	$^1J_{P\text{-}Se}$ (Hz)	$^2J_{P\text{-}Pt}$ (Hz)	$^3J_{P\text{-}P}$ (Hz)	δ_P (ppm)	$^1J_{P\text{-}Pt}$ (Hz)	$^1J_{P\text{-}P}$ (Hz)
^{i}PrAWR (**3.4**)	30.31	418	277	7.04	18.00	3324	7.04
^{n}BuAWR (**3.8**)	36.19	418	270	7.04	17.93	3324	7.04
^{s}BuAWR (**3.12**)	30.33	425	270	7.04	17.55 17.35	3322	7.74 6.77
^{t}BuAWR (**3.16**)	21.98	423	277	7.04	17.72	3342	7.04
BenzAWR (**3.20**)	37.01	418	270	7.04	18.28	3310	7.04

Just as in the $^{31}P\{^1H\}$ NMR, the ^{s}BuAWR compound exhibits the anomalous doublet pattern in the $^{77}Se\{^1H\}$ NMR spectrum, see Table 3.21. We see the expected

increase in chemical shift from (**3.8**, ^{n}Bu) to (**3.16**, ^{t}Bu), indicating the increase in electron density on the Se atoms and the $^{1}J_{Se\text{-}P}$ coupling constants correspond to those seen in the $^{31}P\{^{1}H\}$ NMR.

Table 3.21: $^{77}Se\{^{1}H\}$ and $^{195}Pt\{^{1}H\}$ NMR data for compounds (**3.4**), (**3.8**), (**3.12**), (**3.16**) and (**3.20**).

	δ_{Se} (ppm)	$^{1}J_{Se\text{-}P}$ (Hz)	δ_{Pt} (ppm)	$^{1}J_{Pt\text{-}P}$ (Hz)	$^{2}J_{Pt\text{-}P}$ (Hz)
^{i}PrAWR (**3.4**)	122.0	418	-4933	3316	273
^{n}BuAWR (**3.8**)	96.9	422	-4925	3328	261
^{s}BuAWR (**3.12**)	134.7 126.2	417 415	-4933	3320	281
^{t}BuAWR (**3.18**)	160.2	418	-4916	3337	273
BenzAWR (**3.20**)	99.0	417	-4914	3316	267

The $^{195}Pt\{^{1}H\}$ NMR spectra for compounds (**3.4**), (**3.8**), (**3.12**), (**3.16**) and (**3.20**) exhibit the lowest resonances out of all of those seen for these compounds, due to the electron withdrawing effect of the phenyl groups on the phosphine. The coupling constants are also the highest, indicating that the Pt-P bonds are strongest for the triphenyl phosphine complexes. The $^{2}J_{Pt\text{-}P}$ coupling constants are similar to all those seen within this chapter and correspond to the values seen in the $^{31}P\{^{1}H\}$ NMR spectra.

3.3 Conclusions

In this Chapter, four platinum phosphine starting materials were prepared: *cis*-$Pt(PMe_3)_2Cl_2$, *cis*-$Pt(PMe_2Ph)_2Cl_2$, *cis*-$Pt(PMePh_2)_2Cl_2$ and *cis*-$Pt(PPh_3)_2Cl_2$ and reacted with five of the ligands prepared in Chapter 2: ^{i}PrAWR (**2.1**), ^{n}BuAWR (**2.2**), ^{s}BuAWR (**2.3**), ^{t}BuAWR (**2.4**) and BenzAWR (**2.5**), synthesising twenty compounds (**3.1**) - (**3.20**). The complexes were synthesised in varying yields and obtained as yellow to brown coloured oils. Of the synthesised complexes, compound (**3.12**) could be obtained as a crystalline product, confirming the structure of all compounds produced by the similarity of the NMR spectra of the products.

δ_P of the phenylphosphonamidodiselenoate ligand is seen downfield of the phosphine peak in the $^{31}P\{^1H\}$ NMR spectra. The phenylphosphonamidodiselenoate ligands also have little to no effect on the chemical shift of the platinum complex and the $^1J_{P\text{-}Se}$ and $^2J_{P\text{-}Pt}$ coupling constants remain largely unchanged throughout the whole series. Deviations for the expected values (~ 420 Hz for $^1J_{P\text{-}Se}$ and ~265 Hz for $^2J_{P\text{-}Pt}$) are recorded as anomalous results. A trend, however, is seen in the butyl amine derivatives, in that the ^{n}BuAWR complexes have the highest chemical shifts, the ^{t}BuAWR complexes have the lowest chemical shifts and the ^{s}BuAWR complexes lie somewhere in between.

The phosphine ligands show a series of trends and have an influence on the phenylphosphonamidodiselenoate chemical shift: the larger the phosphine bulk, the lower the chemical shift of the phenylphosphonamidodiselenoate moiety. We also see a steady increase in both the phosphine chemical shift from PMe_3 to PPh_3 and the $^1J_{P\text{-}Pt}$ coupling constants.

In the $^{77}Se\{^1H\}$ NMR spectra a trend of increasing chemical shift is observed with the increasing bulk of the phosphine ligand, whilst δ_{Pt} becomes more negative. δ_{Pt} is unaffected by altering the amine moiety, however, δ_{Se} increases from ^{n}BuAWR to ^{t}BuAWR.

3.4 Experimental

Experimental conditions and information are the same as in Section 2.3. Any deviations from standard conditions are stated in the syntheses.

3.5 Preparation of Starting Materials

3.5.1 Preparation of $Pt(cod)Cl_2$[79]

Potassium tetrachloroplatinate (5.00 g, 12.0 mmol) was dissolved in distilled water (50 mL) ensuring complete dissolution. Glacial acetic acid (100 mL) was then added followed by 1,5-cyclooctadiene (5 mL, 12 mmol) under rapid stirring. The reaction mixture was allowed to stir at 90 °C for 30 mins. The mixture was left to cool to room temperature and stored at 5 °C overnight in the fridge. The formed white crystals were collected by filtration and then washed with water, ethanol and diethyl ether.

Yield: 4.08 g, 91 %.

3.5.2 Preparation of *cis*-$Pt(PMe_3)_2Cl_2$[80]

1,5-(Cyclooctadiene)platinum(II) dichloride (1.02 g, 2.71 mmol) was dissolved in dichloromethane (30 mL) under an inert atmosphere at room temperature. Trimethylphosphine (0.76 mL, 5.4 mmol) was added to the solution. The mixture was stirred at room temperature for 45 mins and then filtered. The white powdery product was precipitated *via* layering with diethyl ether and placing in the fridge overnight.

Yield: 2.941 g, 86 %.

$^{31}P\{^1H\}$ NMR: (109.4 MHz, $CDCl_3$, H_3PO_4) (ppm) δ_P = -23.3 ($^1J_{P\text{-}Pt}$ = 3484 Hz).

3.5.3 **Preparation of *cis*-Pt(PMe$_2$Ph)$_2$Cl$_2$[81]**

1,5-(Cyclooctadiene)platinum(II) dichloride (1.05 g, 2.80 mmol) was dissolved in dichloromethane (30 mL) under an inert atmosphere at room temperature. Dimethyl phenylphosphine (0.78 g, 5.6 mmol) was added to the solution. The mixture was stirred at room temperature for 45 mins and then filtered. The white powdery product was precipitated *via* layering with diethyl ether and placing in the fridge overnight.
Yield: 1.20 g, 79 %.

^{31}P{^{1}H} NMR: (109.4 MHz, $CDCl_3$, H_3PO_4) (ppm) δ_P = -14.6 ($^{1}J_{P\text{-}Pt}$ = 3550 Hz).

3.5.4 **Preparation of *cis*-Pt(PMePh$_2$)$_2$Cl$_2$[80]**

1,5-(Cyclooctadiene)platinum(II) dichloride (1.20 g, 3.21 mmol) was dissolved in dichloromethane (30 mL) under an inert atmosphere at room temperature. Dimethyl phenylphosphine (1.21 mL, 6.4 mmol) was added to the solution. The mixture was stirred at room temperature for 45 mins and then filtered. The white powdery product was precipitated *via* layering with diethyl ether and placing in the fridge overnight.
Yield: 1.77 g, 83 %.

^{31}P{^{1}H} NMR: (109.4 MHz, $CDCl_3$, H_3PO_4) (ppm) δ_P = -0.30 ($^{1}J_{P\text{-}Pt}$ = 3618 Hz).

3.5.5 **Preparation of *cis*-Pt(PPh$_3$)$_2$Cl$_2$[82]**

Potassium tetrachloroplatinate (2.35 g, 5.7 mmol) was dissolved in water (35 mL) and was slowly added to a solution of triphenylphosphine (3.00 g, 11.4 mmol) in ethanol (40 mL) under an inert atmosphere. The orange solution was refluxed until a white precipitate formed. The mixture was allowed to cool before being filtered and washed with ethanol.
Yield: 3.59 g, 80 %.

^{31}P{^{1}H} NMR: (109.4 MHz, $CDCl_3$, H_3PO_4) (ppm) δ_P = 14.9 ($^{1}J_{P\text{-}Pt}$ = 3679 Hz).

3.6 Synthesis of Platinum Complexes

For simplicity and to prevent repetition, the generic term *cis*-$Pt(PR_3)_2Cl_2$ is employed in each synthesis description. The amount used in grams and moles is entered at the beginning of the characterisation of each compound in the form (R_3 = Me_3, X g, Y mol. ^{i}PrAWR: M g, N mol).

3.6.1 Synthesis of Compounds (3.1) – (3.4) Using ^{i}PrAWR

cis-$Pt(PR_3)_2Cl_2$ was dissolved in DCM (20 mL) and stirred at room temperature. To this, ^{i}PrAWR was added. The mixture was left to stir overnight, during which a colour change from off-white to orange-light brown occurred. The resulting mixture was washed with distilled water (2 x 20 mL), dried over $MgSO_4$ and purified by column chromatography with an eluent of 95% toluene: 5% ethyl acetate. Once all the side products were washed through, the desired product was purged from the column with MeOH and the fractions evaporated to dryness under reduced pressure. The products were obtained as dark orange to brown oils.

Crystallisation was attempted *via* slow diffusion, layering with another solvent in which the product was insoluble (hexane, diethyl ether and pentane), and cooling of the Schlenk flask, all of which proved unsuccessful.

(3.1) R_3 = Me_3, 0.15 g, 0.36 mmol. ^{i}PrAWR: 0.16 g, 0.38 mmol. Yield: 0.144 g, 60%.

^{31}P{^{1}H} NMR: (162.0 MHz, $CDCl_3$, H_3PO_4) (ppm) δ_P = 35.3 ($^{1}J_{P\text{-}Se}$ = 429 Hz, $^{2}J_{P\text{-}Pt}$ = 261 Hz) and -28.8 ($^{1}J_{P\text{-}Pt}$ = 3112 Hz, $^{3}J_{P\text{-}P}$ = 7.04 Hz).

^{77}Se{^{1}H} NMR: (76.3 MHz, $CDCl_3$) (ppm) δ_{Se} = 60.6 (d, $^{1}J_{Se\text{-}P}$ = 432 Hz).

^{195}Pt{^{1}H} NMR: (107.5 MHz, $CDCl_3$) (ppm) δ_{Pt} = -4830 (dt, $^{1}J_{Pt\text{-}P}$ = 3115 Hz, $^{2}J_{Pt\text{-}P}$ = 261 Hz).

(3.2) R_3 = Me_2Ph, 0.15 g, 0.27 mmol. ^{i}PrAWR: 0.12 g, 0.28 mmol. Yield: 0.11 g, 48%.

$^{31}P\{^1H\}$ NMR: (109.4 MHz, $CDCl_3$, H_3PO_4) (ppm) δ_P = 28.8 ($^1J_{P\text{-}Se}$ = 373 Hz, $^2J_{P\text{-}Pt}$ = 237 Hz, $^3J_{P\text{-}P}$ = 7.04 Hz) and -19.1 ($^1J_{P\text{-}Pt}$ = 3130 Hz, $^3J_{P\text{-}P}$ = 7.04 Hz).

$^{77}Se\{^1H\}$ NMR: (51.5 MHz, $CDCl_3$) (ppm) δ_{Se} = 152.9 (d, $^1J_{Se\text{-}P}$ = 372 Hz).

$^{195}Pt\{^1H\}$ NMR: (58.1 MHz, $CDCl_3$) (ppm) δ_{Pt} = -4849 (dt, $^1J_{Pt\text{-}P}$ = 3133 Hz, $^2J_{Pt\text{-}P}$ = 237 Hz).

(3.3) R_3 = $MePh_2$, 0.15 g, 0.23 mmol. ^{i}PrAWR: 0.10 g, 0.24 mmol. Yield: 0.15 g, 69 %.

$^{31}P\{^1H\}$ NMR: (109.4 MHz, $CDCl_3$, H_3PO_4) (ppm) δ_P = 32.2 ($^1J_{P\text{-}Se}$ = 418 Hz, $^2J_{P\text{-}Pt}$ = 275 Hz, $^3J_{P\text{-}P}$ = 7.04 Hz) and -0.73 ($^1J_{P\text{-}Pt}$ = 3208 Hz, $^3J_{P\text{-}P}$ = 7.04 Hz).

$^{77}Se\{^1H\}$ NMR: (51.5 MHz, $CDCl_3$) (ppm) δ_{Se} = 97.3 (d, $^1J_{Se\text{-}P}$ = 417 Hz).

$^{195}Pt\{^1H\}$ NMR: (58.1 MHz, $CDCl_3$) (ppm) δ_{Pt} = -4900 (dt, $^1J_{Pt\text{-}P}$ = 3200 Hz, $^2J_{Pt\text{-}P}$ = 267 Hz).

Mass TOF MS ES$^+$: *m/z* = 919.56 (M^+).

(3.4) R_3 = Ph_3, 0.18 g, 0.23 mmol. ^{i}PrAWR: 0.10 g, 0.24 mmol. Yield: 0.16 g, 65 %.

$^{31}P\{^1H\}$ NMR: (109.4 MHz, $CDCl_3$, H_3PO_4) (ppm) δ_P = 30.3 ($^1J_{P\text{-}Se}$ = 418 Hz, $^2J_{P\text{-}Pt}$ = 277 Hz, $^3J_{P\text{-}P}$ = 7.04 Hz) and 18.0 ($^1J_{P\text{-}Pt}$ = 3324 Hz, $^3J_{P\text{-}P}$ = 7.04 Hz).

$^{77}Se\{^1H\}$ NMR: (51.5 MHz, $CDCl_3$) (ppm) δ_{Se} = 122.0 (d, $^1J_{Se\text{-}P}$ = 418 Hz).

$^{195}Pt\{^1H\}$ NMR: (58.1 MHz, $CDCl_3$) (ppm) δ_{Pt} = -4933 (dt, $^1J_{Pt\text{-}P}$ = 3316 Hz, $^2J_{Pt\text{-}P}$ = 273 Hz).

3.6.2 **Synthesis of Compounds (3.5) – (3.8) Using ^{n}BuAWR**

cis-$Pt(PR_3)_2Cl_2$ was dissolved in DCM (20 mL) and stirred at room temperature. To this, ^{n}BuAWR was added. The mixture was left to stir overnight, during which a colour change from faint yellow to light-dark brown occurred. The resulting mixture was washed with water (2 x 20 mL), dried over $MgSO_4$ and purified by column chromatography with an eluent of 95% DCM: 5% ethyl acetate. Once all the side products were eluted, the desired product was purged from the column with MeOH and the fractions evaporated to dryness under reduced pressure. The products were obtained as dark orange to brown oils.

Crystallisation was attempted *via* slow diffusion, layering with another solvent in which the product was insoluble (hexane, diethyl ether and pentane), and cooling of the Schlenk flask, all of which proved unsuccessful.

(3.5) R_3 = Me_3, 0.14 g, 0.335 mmol. ^{n}BuAWR: 0.15 g, 0.36 mmol. Yield: 0.10 g, 45%.

$^{31}P\{^{1}H\}$ NMR: (121.5 MHz, $CDCl_3$, H_3PO_4) (ppm) δ_P = 39.9 ($^{1}J_{P\text{-}Se}$ = 431 Hz, $^{2}J_{P\text{-}Pt}$ = 261 Hz) and -30.1 ($^{1}J_{P\text{-}Pt}$ = 3170 Hz).

$^{77}Se\{^{1}H\}$ NMR: (76.3 MHz, $CDCl_3$) (ppm) δ_{Se} = 44.8 (d, $^{1}J_{Se\text{-}P}$ = 429 Hz).

$^{195}Pt\{^{1}H\}$ NMR: (107.5 MHz, $CDCl_3$) (ppm) δ_{Pt} = -4824 (dt, $^{1}J_{Pt\text{-}P}$ = 3165 Hz, $^{2}J_{Pt\text{-}P}$ = 259 Hz).

(3.6) R_3 = Me_2Ph, 0.18 g, 0.33 mmol. ^{n}BuAWR: 0.15 g, 0.36 mmol. Yield: 0.15 g, 53%.

$^{31}P\{^{1}H\}$ NMR: (109.4 MHz, $CDCl_3$, H_3PO_4) (ppm) δ_P = 39.4 ($^{1}J_{P\text{-}Se}$ = 425 Hz, $^{2}J_{P\text{-}Pt}$ = 270 Hz, $^{3}J_{P\text{-}P}$ = 7.04 Hz) and -18.1 ($^{1}J_{P\text{-}Pt}$ = 3181 Hz, $^{3}J_{P\text{-}P}$ = 7.04 Hz).

$^{77}Se\{^{1}H\}$ NMR: (51.5 MHz, $CDCl_3$) (ppm) δ_{Se} = 68.3 (d, $^{1}J_{Se\text{-}P}$ = 424 Hz).

$^{195}Pt\{^{1}H\}$ NMR: (58.1 MHz, $CDCl_3$) (ppm) δ_{Pt} = -4867 (dt, $^{1}J_{Pt\text{-}P}$ = 3200 Hz, $^{2}J_{Pt\text{-}P}$ = 273 Hz).

(3.7) R_3 = $MePh_2$, 0.15 g, 0.23 mmol. ^{n}BuAWR: 0.10 g, 0.24 mmol. Yield: 0.13 g, 62%.

$^{31}P\{^{1}H\}$ NMR: (109.4 MHz, $CDCl_3$, H_3PO_4) (ppm) δ_P = 37.5 ($^{1}J_{P\text{-}Se}$ = 418 Hz, $^{2}J_{P\text{-}Pt}$ = 275 Hz, $^{3}J_{P\text{-}P}$ = 7.04 Hz) and -0.74 ($^{1}J_{P\text{-}Pt}$ = 3209 Hz, $^{3}J_{P\text{-}P}$ = 7.04 Hz).

$^{77}Se\{^{1}H\}$ NMR: (51.5 MHz, $CDCl_3$) (ppm) δ_{Se} = 78.1 (d, $^{1}J_{Se\text{-}P}$ = 417 Hz).

$^{195}Pt\{^{1}H\}$ NMR: (58.1 MHz, $CDCl_3$) (ppm) δ_{Pt} = -4891 (dt, $^{1}J_{Pt\text{-}P}$ = 3206 Hz, $^{2}J_{Pt\text{-}P}$ = 273 Hz).

Mass TOF MS ES^{+}: M = 933.63 (M^{+}).

(3.8) R_3 = Ph_3, 0.18 g, 0.23 mmol. ^{n}BuAWR: 0.10 g, 0.24 mmol. Yield: 0.13 g, 54%.

$^{31}P\{^{1}H\}$ NMR: (109.4 MHz, $CDCl_3$, H_3PO_4) (ppm) δ_P = 36.2 ($^{1}J_{P\text{-}Se}$ = 418 Hz, $^{2}J_{P\text{-}Pt}$ = 270 Hz, $^{3}J_{P\text{-}P}$ = 7.04 Hz) and 17.9 ($^{1}J_{P\text{-}Pt}$ = 3324 Hz, $^{3}J_{P\text{-}P}$ = 7.04 Hz).

$^{77}Se\{^{1}H\}$ NMR: (51.5 MHz, $CDCl_3$) (ppm) δ_{Se} = 96.9 (d, $^{1}J_{Se\text{-}P}$ = 422 Hz).

$^{195}Pt\{^{1}H\}$ NMR: (58.1 MHz, $CDCl_3$) (ppm) δ_{Pt} = -4925 (dt, $^{1}J_{Pt\text{-}P}$ = 3328 Hz, $^{2}J_{Pt\text{-}P}$ = 261 Hz).

Mass TOF MS ES^{+}: M = 1057.4 (M^{+}).

3.6.3 **Synthesis of Compounds (3.9) – (3.12) Using ^{s}BuAWR**

cis-Pt$(PR_3)_2Cl_2$ was dissolved in DCM (20 mL) and stirred at room temperature. To this, ^{s}BuAWR was added. The mixture was left to stir overnight, during which a colour change from faint yellow to light-dark brown occurred. The resulting mixture was washed with water, dried over $MgSO_4$ and purified by column chromatography with an eluent of 93% DCM: 7% ethyl acetate. Once all the side products were eluted, the desired product was purged from the column with MeOH and the fractions evaporated to dryness under reduced pressure. The products were obtained as dark orange to brown oils.

Crystallisation was attempted *via* slow diffusion, layering with another solvent in which the product was insoluble (hexane, diethyl ether and pentane), and cooling of the Schlenk flask, all of which proved unsuccessful apart from in the case of the reaction of ^{s}BuAWR with *cis*-Pt$(PPh_3)_2)Cl_2$, where crystals suitable for X-ray structural analysis were obtained.

(3.9) R_3 = Me_3, 0.14 g, 0.34 mmol. ^{s}BuAWR: 0.14 g, 0.34 mmol. Yield: 0.14 g, 61%.

$^{31}P\{^{1}H\}$ NMR: (162.0 MHz, $CDCl_3$, H_3PO_4) (ppm) δ_P = 35.7 ($^{1}J_{P\text{-}Se}$ = 429 Hz, $^{2}J_{P\text{-}Pt}$ = 263 Hz) and -28.83($^{1}J_{P\text{-}Pt}$ = 3125 Hz).

$^{77}Se\{^{1}H\}$ NMR: (76.3 MHz, $CDCl_3$) (ppm) δ_{Se} = 66.6 (d, $^{1}J_{Se\text{-}P}$ = 430 Hz).

$^{195}Pt\{^{1}H\}$ NMR: (107.5 MHz, $CDCl_3$) (ppm) δ_{Pt} = -4832 (dt, $^{1}J_{Pt\text{-}P}$ = 3128 Hz, $^{2}J_{Pt\text{-}P}$ = 259 Hz).

(3.10) R_3 = Me_2Ph, 0.16 g, 0.30 mmol. ^{s}BuAWR: 0.13 g, 0.32 mmol. Yield: 0.19 g, 72%.

$^{31}P\{^{1}H\}$ NMR: (109.4 MHz, $CDCl_3$, H_3PO_4) (ppm) δ_P = 35.2 ($^{1}J_{P\text{-}Se}$ = 425 Hz, $^{2}J_{P\text{-}Pt}$ = 270 Hz, $^{3}J_{P\text{-}P}$ = 7.04 Hz) and -17.9 ($^{1}J_{P\text{-}Pt}$ = 3181 Hz, $^{3}J_{P\text{-}P}$ = 7.04 Hz).

$^{77}Se\{^{1}H\}$ NMR: (51.5 MHz, $CDCl_3$) (ppm) δ_{Se} = 91.2 (d, $^{1}J_{Se\text{-}P}$ = 424 Hz).

^{195}Pt{^{1}H} NMR: (58.1 MHz, $CDCl_3$) (ppm) δ_{Pt} = -4874 (dt, $^{1}J_{Pt\text{-}P}$ = 3183 Hz, $^{2}J_{Pt\text{-}P}$ = 268 Hz).

(3.11) R_3 = $MePh_2$, 0.17 g, 0.26 mmol. ^{s}BuAWR: 0.11 g, 0.27 mmol. Yield: 0.13 g, 54%.

^{31}P{^{1}H} NMR: (109.4 MHz, $CDCl_3$, H_3PO_4) (ppm) δ_{P} = 33.4 ($^{1}J_{P\text{-}Se}$ = 420 Hz, $^{2}J_{P\text{-}Pt}$ = 275 Hz, $^{3}J_{P\text{-}P}$ = 7.04 Hz) and -0.72 ($^{1}J_{P\text{-}Pt}$ = 3211 Hz, $^{3}J_{P\text{-}P}$ = 7.04 Hz).

^{77}Se{^{1}H} NMR: (51.5 MHz, $CDCl_3$) (ppm) δ_{Se} = 98.8 (d, $^{1}J_{Se\text{-}P}$ = 420 Hz).

^{195}Pt{^{1}H} NMR: (58.1 MHz, $CDCl_3$) (ppm) δ_{Pt} = -4900 (dt, $^{1}J_{Pt\text{-}P}$ = 3212 Hz, $^{2}J_{Pt\text{-}P}$ = 267 Hz).

(3.12) R_3 = Ph_3, 0.20 g, 0.25 mmol. ^{s}BuAWR: 0.11 g, 0.27 mmol. Yield: 0.20 g, 75%.

^{31}P{^{1}H} NMR: (109.4 MHz, $CDCl_3$, H_3PO_4) (ppm) δ_{P} = 30.33 ($^{1}J_{P\text{-}Se}$ = 425 Hz, $^{2}J_{P\text{-}Pt}$ = 270, $^{3}J_{P\text{-}P}$ = 7.04 Hz), 17.55 ($^{1}J_{P\text{-}Pt}$ = 3322 Hz, $^{3}J_{P\text{-}P}$ = 7.74 Hz) and 17.35 ($^{1}J_{P\text{-}Pt}$ = 3322 Hz, $^{3}J_{P\text{-}P}$ = 6.77 Hz).

^{77}Se{^{1}H} NMR: (51.5 MHz, $CDCl_3$) (ppm) δ_{Se} = 134.7 (d, $^{1}J_{Se\text{-}P}$ = 417 Hz) and 126.2 (d, $^{1}J_{Se\text{-}P}$ = 415 Hz).

^{195}Pt{^{1}H} NMR: (58.1 MHz, $CDCl_3$) (ppm) δ_{Pt} = -4933 (dt, $^{1}J_{Pt\text{-}P}$ = 3320 Hz, $^{2}J_{Pt\text{-}P}$ = 281 Hz).

Mass TOF MS ES^{+}: M = 1057.63 (M^{+}).

3.6.4 **Synthesis of Compounds (3.13 – 3.16) Using ^{t}BuAWR**

cis-$Pt(PR_3)_2Cl_2$ was dissolved in DCM and stirred at room temperature. To this, ^{t}BuAWR was added. The mixture was left to stir overnight, during which a colour change from faint yellow to light-dark brown occurred. The resulting mixture was washed with water, dried over $MgSO_4$ and purified by column chromatography with an eluent of 93% DCM: 7% ethyl acetate. Once all the side products were washed through, the desired product was purged from the column with MeOH and the fractions evaporated to dryness under reduced pressure. The products were obtained as dark orange to brown oils.

Crystallisation was attempted *via* slow diffusion, layering with another solvent in which the product was insoluble (hexane, diethyl ether and pentane), and cooling of the Schlenk flask, all of which proved unsuccessful.

(3.13) R_3 = Me_3, 0.15 g, 0.35 mmol. ^{t}BuAWR: 0.15 g, 0.36 mmol. Yield: 0.12 g, 51%.

$^{31}P\{^{1}H\}$ NMR: (202.4 MHz, $CDCl_3$, H_3PO_4) (ppm) δ_P = 25.4 ($^{1}J_{P\text{-}Se}$ = 433 Hz, $^{2}J_{P\text{-}Pt}$ = 265 Hz) and -28.3 ($^{1}J_{P\text{-}Pt}$ = 3148 Hz).

$^{77}Se\{^{1}H\}$ NMR: (95.4 MHz, $CDCl_3$) (ppm) δ_{Se} = 98.0 (d, $^{1}J_{Se\text{-}P}$ = 435.0 Hz).

$^{195}Pt\{^{1}H\}$ NMR: (58.1 MHz, $CDCl_3$) (ppm) δ_{Pt} = -4817 (dt, $^{1}J_{Pt\text{-}P}$ = 3138 Hz, $^{2}J_{Pt\text{-}P}$ = 264 Hz).

(3.14) R_3 = Me_2Ph, 0.15 g, 0.27 mmol. ^{t}BuAWR: 0.12 g, 0.29 mmol. Yield: 0.12 g, 52%.

$^{31}P\{^{1}H\}$ NMR: (121.5 MHz, $CDCl_3$, H_3PO_4) (ppm) δ_P = 24.7 ($^{1}J_{P\text{-}Se}$ = 425 Hz, $^{2}J_{P\text{-}Pt}$ = 275 Hz, $^{3}J_{P\text{-}P}$ = 7.04 Hz) and -17.8 ($^{1}J_{P\text{-}Pt}$ = 3193 Hz, $^{3}J_{P\text{-}P}$ = 7.04 Hz).

$^{77}Se\{^{1}H\}$ NMR: (95.4 MHz, $CDCl_3$) (ppm) δ_{Se} = 118.4 (d, $^{1}J_{Se\text{-}P}$ = 425 Hz).

$^{195}Pt\{^{1}H\}$ NMR: (107.5 MHz, $CDCl_3$) (ppm) δ_{Pt} = -4857 (dt, $^{1}J_{Pt\text{-}P}$ = 3194 Hz, $^{2}J_{Pt\text{-}P}$ = 272 Hz).

(3.15) R_3 = $MePh_2$, 0.23 g, 0.34 mmol. ^{t}BuAWR: 0.15 g, 0.36 mmol. Yield: 0.12 g, 38%.

$^{31}P\{^1H\}$ NMR: (109.4 MHz, $CDCl_3$, H_3PO_4) (ppm) δ_P = 23.0 ($^1J_{P\text{-}Se}$ = 420 Hz, $^2J_{P\text{-}Pt}$ = 277 Hz, $^3J_{P\text{-}P}$ = 7.04 Hz) and -0.70 ($^1J_{P\text{-}Pt}$ = 3223 Hz, $^3J_{P\text{-}P}$ = 7.04 Hz).

$^{77}Se\{^1H\}$ NMR: (51.5 MHz, $CDCl_3$) (ppm) δ_{Se} = 129.0 (d, $^1J_{Se\text{-}P}$ = 420 Hz).

$^{195}Pt\{^1H\}$ NMR: (58.1 MHz, $CDCl_3$) (ppm) δ_{Pt} = -4884 (dt, $^1J_{Pt\text{-}P}$ = 3225 Hz, $^2J_{Pt\text{-}P}$ = 273 Hz).

(3.16) R_3 = Ph_3, 0.18 g, 0.23 mmol. ^{t}BuAWR: 0.10 g, 0.24 mmol. Yield: 0.11 g, 44%.

$^{31}P\{^1H\}$ NMR: (109.4 MHz, $CDCl_3$, H_3PO_4) (ppm) δ_P = 22.0 ($^1J_{P\text{-}Se}$ = 423 Hz, $^2J_{P\text{-}Pt}$ = 277 Hz, $^3J_{P\text{-}P}$ = 7.04 Hz) and 17.7 ($^1J_{P\text{-}Pt}$ = 3342 Hz, $^3J_{P\text{-}P}$ = 7.04 Hz).

$^{77}Se\{^1H\}$ NMR: (51.5 MHz, $CDCl_3$) (ppm) δ_{Se} = 160.2 (d, $^1J_{Se\text{-}P}$ = 418 Hz).

$^{195}Pt\{^1H\}$ NMR: (58.1 MHz, $CDCl_3$) (ppm) δ_{Pt} = -4916 (dt, $^1J_{Pt\text{-}P}$ = 3337 Hz, $^2J_{Pt\text{-}P}$ = 273 Hz).

3.6.5 **Synthesis of compounds (3.17 – 3.20) Using BenzAWr**

cis-$Pt(PR_3)_2Cl_2$ was dissolved in DCM and stirred at room temperature. To this, BenzAWR was added. The mixture was left to stir overnight, during which a colour change from faint yellow to light-dark brown occurred. The resulting mixture was washed with water, dried over $MgSO_4$ and purified by column chromatography with an eluent of 95% DCM : 5% ethyl acetate. Once all the side products were washed through, the desired product was purged from the column with MeOH and the fractions evaporated to dryness under reduced pressure. The products were obtained as dark yellow to brown oils.

Crystallisation was attempted *via* slow diffusion, layering with another solvent in which the product was insoluble (hexane, diethyl ether and pentane), and cooling of the Schlenk flask, all of which proved unsuccessful.

(3.17) R_3 = Me_3, 0.11 g, 0.26 mmol. BenzAWR: 0.14 g, 0.29 mmol. Yield: 0.12 g, 67%.

$^{31}P\{^1H\}$ NMR: (109.4 MHz, $CDCl_3$, H_3PO_4) (ppm) δ_P = 41.4 ($^1J_{P\text{-}Se}$ = 433 Hz, $^2J_{P\text{-}Pt}$ = 268 Hz) and -29.4 ($^1J_{P\text{-}Pt}$ = 3084 Hz).

$^{77}Se\{^1H\}$ NMR: (51.5 MHz, $CDCl_3$) (ppm) δ_{Se} = 135.6 (d, $^1J_{Se\text{-}P}$ = 411 Hz).

$^{195}Pt\{^1H\}$ NMR: (58.1 MHz, $CDCl_3$) (ppm) δ_{Pt} = -4816 (dt, $^1J_{Pt\text{-}P}$ = 3091 Hz, $^2J_{Pt\text{-}P}$ = 233 Hz).

(3.18) R_3 = Me_2Ph, 0.14 g, 0.26 mmol. BenzAWR: 0.13 g, 0.27 mmol. Yield: 0.13 g, 56%.

$^{31}P\{^1H\}$ NMR: (109.4 MHz, $CDCl_3$, H_3PO_4) (ppm) δ_P = 40.9 ($^1J_{P\text{-}Se}$ = 427 Hz, $^2J_{P\text{-}Pt}$ = 270 Hz, $^3J_{P\text{-}P}$ = 7.04 Hz) and -17.9 ($^1J_{P\text{-}Pt}$ = 3179 Hz, $^3J_{P\text{-}P}$ = 7.04 Hz).

$^{77}Se\{^1H\}$ NMR: (51.5 MHz, $CDCl_3$) (ppm) δ_{Se} = 67.6 (d, $^1J_{Se\text{-}P}$ = 427 Hz).

$^{195}Pt\{^1H\}$ NMR: (58.1 MHz, $CDCl_3$) (ppm) δ_{Pt} = -4856 (dt, $^1J_{Pt\text{-}P}$ = 3180 Hz, $^2J_{Pt\text{-}P}$ = 272 Hz).

(3.19) R_3 = $MePh_2$, 0.16 g, 0.24 mmol. BenzAWR: 0.12 g, 0.25 mmol. Yield: 0.14 g, 62%.

$^{31}P\{^1H\}$ NMR: (162.0 MHz, $CDCl_3$, H_3PO_4) (ppm) δ_P = 40.8 ($^1J_{P\text{-}Se}$ = 429 Hz, $^2J_{P\text{-}Pt}$ = 264 Hz, $^3J_{P\text{-}P}$ = 7.04 Hz) and -0.72 ($^1J_{P\text{-}Pt}$ = 3209 Hz, $^3J_{P\text{-}P}$ = 7.04 Hz).

$^{77}Se\{^1H\}$ NMR: (76.3 MHz, $CDCl_3$) (ppm) δ_{Se} = 129.8 (d, $^1J_{Se\text{-}P}$ = 426 Hz).

$^{195}Pt\{^1H\}$ NMR: (107.5 MHz, $CDCl_3$) (ppm) δ_{Pt} = -4903 (dt, $^1J_{Pt\text{-}P}$ = 3204 Hz, $^2J_{Pt\text{-}P}$ = 261 Hz).

(3.20) R_3 = Ph_3, 0.15 g, 0.20 mmol. BenzAWR: 0.10 g, 0.21 mmol. Yield: 0.14 g, 64%.

$^{31}P\{^1H\}$ NMR: (109.4 MHz, $CDCl_3$, H_3PO_4) (ppm) δ_P = 37.0 ($^1J_{P\text{-}Se}$ = 418 Hz, $^2J_{P\text{-}Pt}$ = 270 Hz, $^3J_{P\text{-}P}$ = 7.04 Hz) and 18.3 ($^1J_{P\text{-}Pt}$ = 3310 Hz, $^3J_{P\text{-}P}$ = 7.04 Hz).

$^{77}Se\{^1H\}$ NMR: (51.5 MHz, $CDCl_3$) (ppm) δ_{Se} = 99.0 (d, $^1J_{Se\text{-}P}$ = 417 Hz).

$^{195}Pt\{^1H\}$ NMR: (58.1 MHz, $CDCl_3$) (ppm) δ_{Pt} = -4914 (dt, $^1J_{Pt\text{-}P}$ = 3316 Hz, $^2J_{Pt\text{-}P}$ = 267 Hz).

4. Mesityl Phosphine Chemistry

4.1 Introduction

Of all the functional groups available for use in chemistry, phosphines are one of the most versatile groups of compounds, which find uses in organic, organometallic and inorganic chemistry. These highly valuable reagents are exploited in synthesis and homogeneous catalysis, making use of their σ-donating and π-accepting properties. Their π-acceptance stems from the reception of electron density from a metal centre *via* back donation to the available empty σ* orbitals of the P-C_3 framework, whilst σ-donation comes from electron density being pushed through to the metal centre from the lone pair on the phosphorus. Many phosphine compounds can be acquired commercially, which makes them an ideal choice for many applications, such as ligand systems for mid to late transition metal complexes, which are often used, for example, in hydroformylation processes and hydrogenation reactions. Phosphines can generally be handled using standard lab techniques, although some are quite air sensitive in the P(III) oxidation state and phosphorus containing species can be noxious or poisonous, exemplified by their use as nerve gasses and insecticides. Nonetheless, the vast range of functional groups that phosphines can accommodate allows them to be fine-tuned to enhance catalytic activity and may be tailored to an application by variation of steric and/or electronic properties.

Of the known phosphines, triarylphosphines, especially triphenylphosphine, are by far and away the most reported, used and versatile. Triphenylphosphine plays a key role in many synthetic organic reactions by way of its oxidation to $OPPh_3$ in processes utilising the Wittig,[83] Appel[85] or Mitsunobu[84] reactions. In the most famous of these, the Wittig reaction, triphenylphosphine is converted to a phosphonium salt through reaction with an alkyl halide. On reaction with strong bases, a phosphonium ylide is formed, which is subsequently used to convert the carbonyl groups of ketones and aldehydes to alkenes, as shown in Scheme 4.1.

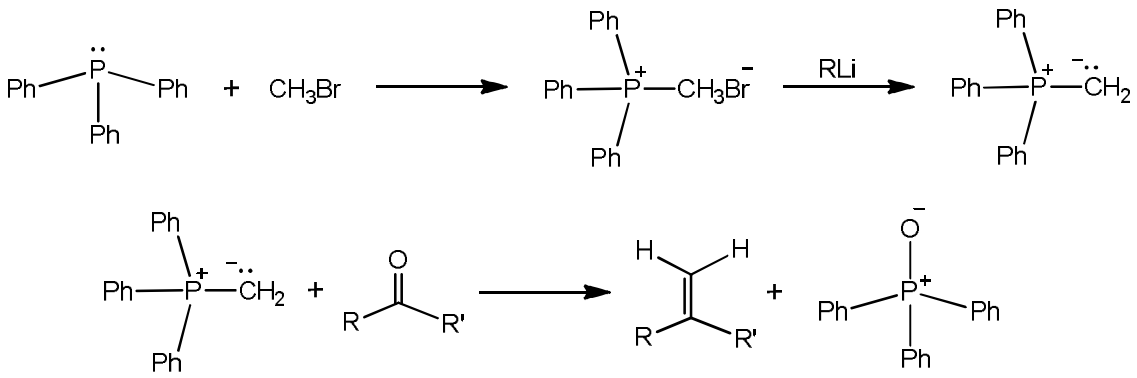

Scheme 4.1: The Wittig Reaction.

The Appel reaction[85] employs PPh_3 and either carbon tetrachloride, carbon tetrabromide or methyl iodide to convert alcohols to alkyl chlorides, bromides and iodides, as depicted in Scheme 4.2.[86] In the general case, the phosphonium salt is formed first, generating CCl_3^-, which deprotonates the alcohol. The negatively charged alkoxide is then able to attack the positively charged P atom, displacing the chloride ion, forming an intermediate, Y. At this point the reaction is driven by the formation of the very strong P=O bond of $O=PPh_3$, whereby the free chloride ion attacks the positive alpha carbon via an SN_2 reaction, forming the desired alkyl halide and $O=PPh_3$.

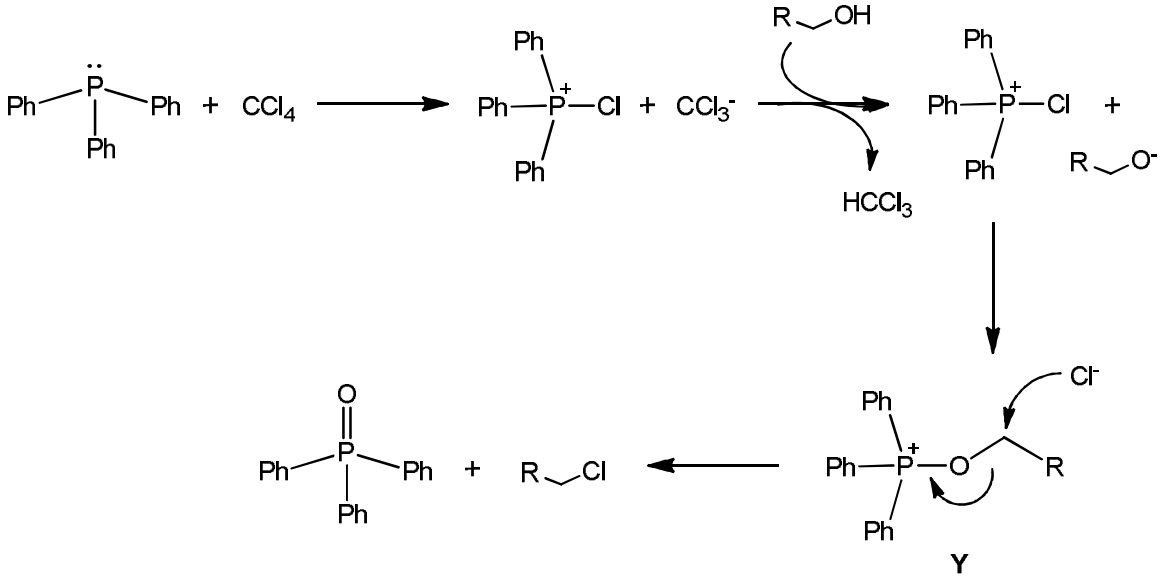

Scheme 4.2: The Appel Reaction.[86]

Triphenyl phosphine also finds use as a ligand in the well known palladium catalyst tetrakis(triphenylphosphine)palladium(0), Figure 4.1. In fact, tetrakis(triphenylphosphine)palladium(0) is an important catalytic species in many coupling reactions. In 2010, Heck, Negishi and Suzuki, were awarded the Nobel Prize for their work on palladium-catalysed cross couplings in organic syntheses, such as syntheses of natural products, most often from organo halide compounds.

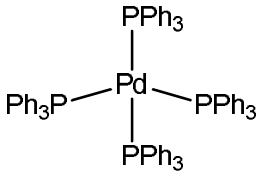

Figure 4.1: Tetrakis(triphenylphosphine)palladium(0).

The goal of the Suzuki reaction is to form a carbon-carbon bond between an organic boronic acid and an aryl halide, forming a biaryl substituent, Equation 4.1. The active species, $[Pd(PPh_3)_2]$, is formed when two of the labile PPh_3 ligands are reversibly dissociated from $[Pd(PPh_3)_4]$,[87] allowing the oxidative addition of the halide. This has a wide range of uses and is utilised in a great number of syntheses of natural products, as it is a relatively selective mechanism. In addition, the Suzuki reaction is employed in the synthesis of liquid crystal materials, which often contain biaryl systems.[88]

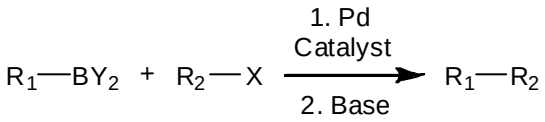

Eqn 4.1

The creation of a covalent bond between an aryl halide and an alkene substrate can also be achieved *via* the Heck reaction, using a palladium catalyst and a base, such as triethylamine, as shown in Equation 4.2.[89] The palladium catalyst in this case employs bulky ligands in its structure: triphenylphosphine, BINAP or PHOX and the products formed have a *trans*-configuration. In this case, however, the precatalyst is often palladium acetate, which is first reacted with PPh_3 *in situ* to give the same reactive species as before, bis(triphenylphosphine)palladium(0).[90]

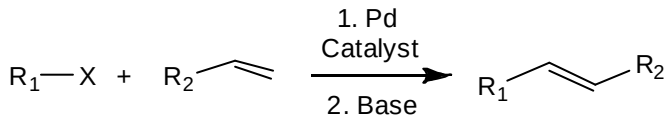

Eqn 4.2

The Negishi cross-coupling reaction is a palladium catalysed process linking an organic halide with an organozinc substrate, thus creating a C-C bond, see Equation 4.3.[91] The palladium catalyst may again incorporate triphenylphosphine or BINAP ligands, as well as dppe or chiraphos. The catalytic cycle can be divided into three main steps: oxidative addition, transmetallation and reductive elimination, represented by the overall reaction shown in Equation 4.3. The Negishi coupling can be employed in many industrial processes, including the synthesis of 2,2'-bypyridine and its derivatives.[92]

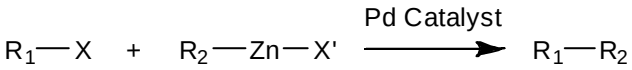

Eqn 4.3

In inorganic chemistry, by far the most famous catalyst is Wilkinson's catalyst, Figure 4.2, named after the 1973 Nobel laureate Sir Geoffrey Wilkinson. Wilkinson's catalyst is a square planar rhodium complex made up of three triphenylphosphine ligands and a chloride ion, which facilitates hydrogenation[93] and hydroboration[94] of alkenes.

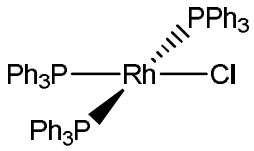

Figure 4.2: Wilkinson's Catalyst

As in some of the previously discussed examples, one of the labile PPh_3 ligands is reversibly dissociated from the catalyst to allow hydrogen gas to bind to and oxidise the rhodium centre to Rh(III). In the next step, the alkene is added, giving a 6-coordinate species, which allows for an intramolecular hydride transfer forming the alkane. This is subsequently released from the system *via* reductive elimination. The catalytic cycle for the general case is shown in Scheme 4.3.

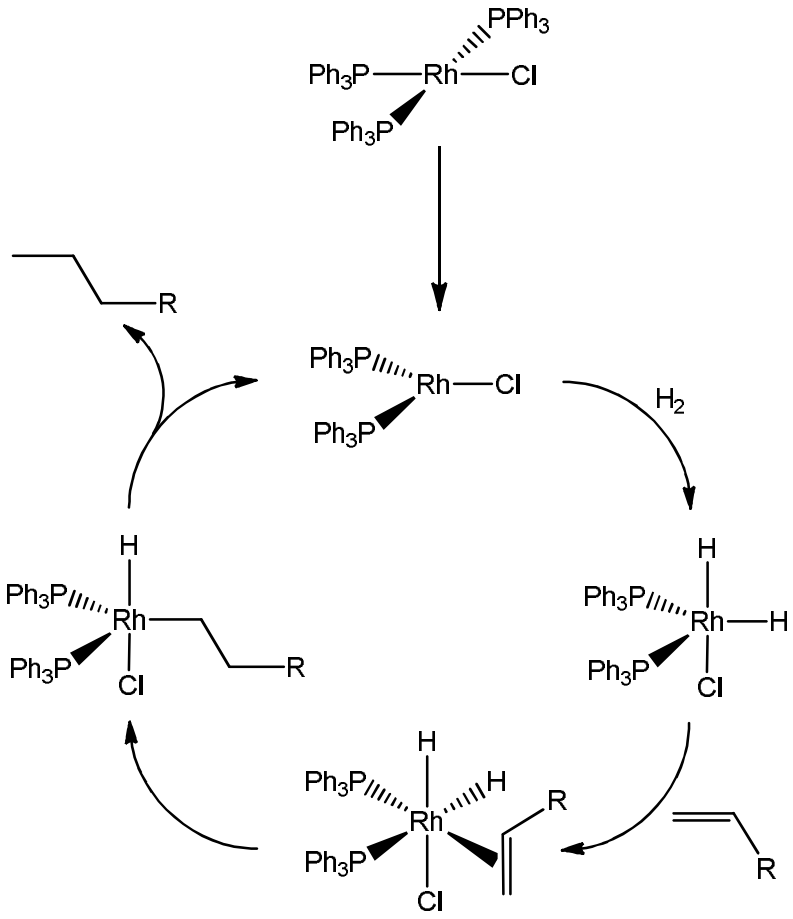

Scheme 4.3: Catalytic cycle of the hydrogenation of an alkene using Wilkinson's catalyst.

Vaska and DiLuzio first reported the synthesis of *trans*-chlorocarbonyl *bis*(triphenylphosphine)iridium(I), Vaska's complex, in 1961 in their paper "Carbonyl and Hydrido-Carbonyl Complexes of Iridium by Reaction with Alcohols. Hydrido Complexes by Reaction with Acid."[95] Vaska's complex is important in inorganic chemistry as it is used to determine the electronic and steric properties of a bound ligand or species, *via* the variation of the C=O stretching frequencies associated with the degree of π back bonding caused by the ligand in question.[96]

Triphenylphosphine is used in many of the above processes as it has fair steric bulk, is air stable and has strong donor properties. It is preferred to most other phosphines as it is widely commercially available due to its easy and inexpensive synthesis. That said, trimesityl phosphine has long been of interest to synthetic inorganic chemists also due to its reactivity, properties and relatively unique structure, although its synthesis can sometimes be problematic. As discussed above, the use of

phosphine ligands in transition metal catalysis has played a significant role in recent times, due to the relative ease of synthesis and variability of substituents, modification and optimisation. In many of the processes discussed above, the key step involves ligand dissociation to form a highly reactive catalytic intermediate. These types of reactions are more labile for bulkier ligands. This fact, combined with the prolific use of triphenylphosphine in homogeneous catalysis, suggests that bulky triarylphosphines have great potential in this area. The problem is, of course, just how bulky a phosphine can get before it cannot coordinate to a metal centre?

Very bulky triarylphosphines are most often synthesised *via* the reaction of a phosphorus halide (*e.g.* PCl_3) with an aryl Grignard reagent, or related milder organometallic reagents such as cuprates or zincates. The principle objective is how to successfully introduce the third bulky aryl group, or in this case the mesityl group, without side reactions occurring.[97] Blount *et al.*[98] followed the 1964 procedure of Schindlbauer,[99] who described both the use of Grignard reagents (yield 62%, reaction performed with the phosphine dissolved in ether with cooling) and the reaction between Ph_2PK and mesityl bromide (yield 12%, with the reaction performed at 150 °C), showing undoubtedly which of these syntheses is more successful. Yoshifuji reported an optimised, almost quantitative synthesis of $PMes_3$ in THF at -78 °C (Equation 4.4), *via* the Grignard route, whilst investigating sterically hindered *meta-* and *para-*aminophosphinobenzenes.[100]

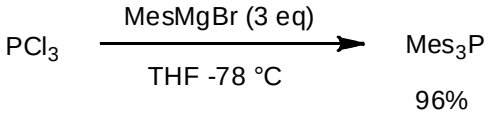

Eqn 4.4

The Grignard method, however, only works satisfactorily for aryl groups up to a certain bulk, such as the aminophosphinobenzenes. A further increase in steric bulk leads to a preference for the corresponding diaryldiphosphanes of the form $Ar_2P\text{-}PAr_2$ or diarylchlorophosphines (Ar_2PCl).[97] tris(2,4,6-Triethylphenyl)phosphine and tris(2,4,6-triisopropylphenyl)phosphine have also been successfully prepared. In order to do this, however, cuprate reagents must be utilised (Figure 4.3), the yields are low and the follow up chemistry is limited to a few redox reactions.[101] From this, it is clear to see

that such species are reaching the upper limit of steric bulk for tertiary phosphines and further reactions of these compounds are unlikely, as is their use as ligands. Trimesitylphosphine and its derivatives are thus a satisfactory middle ground for bulky, yet functional ligand systems.

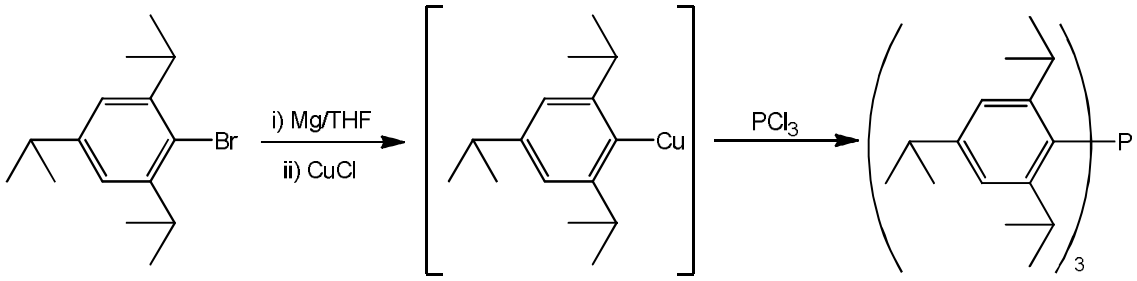

Figure 4.3: Synthesis of tris(2,4,6-triisopropylphenyl)phosphine by use of CuCl

The properties of such sterically hindered species can be recorded and compared in a number of ways, not least of all if there is crystallographic data to hand. Phosphine ligands are rarely mentioned without a reference to their Tolman's cone angle (TCA), which is used to analyse whether the steric or electronic properties of the ligand play the more dominating role in their chemistry. The TCA of a ligand is measured as the angle, θ, at the metal atom at the tip of the cone that is swept out by the H atoms on the organic rests that are attached to the central phosphorus atom, as depicted in Figure 4.4, wherein the metal-phosphorus bond length is set at 2.28 Å.

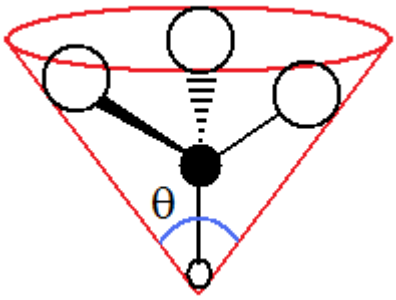

Figure 4.4: Tolman's Cone Angle

It has long been recognised that the two important factors influencing the chemical shift of a phosphorus atom in the ^{31}P NMR spectrum are the size (steric effects) and the electronegativity (electronic effects) of the three functional groups

bound to the phosphorus atom. This is also the case for the coupling constant of the P-C bonds, which will be discussed later in this chapter.

In the previous chapter only one X-ray crystal structure could be obtained for the series of platinum complexes synthesised with the phenylphosphonamidodiselenoate ligands, with the majority of reactions affording oils, which cannot be characterised to the same extent as solids. An investigation into more sterically crowded platinum-phosphine species was thus performed, which led us to research into $PMes_3$ and its derivatives, allowing a detailed look at the variation in cone angle of the ligands *versus* the ability of the species to react with a number of smaller chalcogen atoms. The steric effects and properties of mixed mesityl and phenyl phosphines could be observed in their NMR spectra, and nine previously unrecorded X-ray crystal structures were obtained. A systematic study of the molecular structures enabled an examination of the relative alignment of neighbouring aryl groups to be compared.

4.2 Discussion

From studying the trends observed in the reactions discussed in Chapter 3, it was proposed that an increase in steric bulk around the platinum centre would facilitate crystallisation of the desired products. With this in mind, the mesityl substituted phosphines $PMes_3$, $PMes_2Ph$ and $PMesPh_2$ (Equations 4.5 and 4.6) were synthesised *via* the mesityl Grignard, MesMgBr, to be used as ligands in $Pt(PR_3)_2Cl_2$ platinum complexes. It was intended that the bond angles and properties of these Pt complexes would then be studied via X-ray crystallography and the compounds reacted with the ammonium phenylphosphonamidodiselenoates described in Chapter 3.

$$MesBr \xrightarrow{Mg} MesMgBr$$

$$x\ MesMgBr \xrightarrow[Reflux]{PCl_xPh_{3-x}} PMes_3$$

Eqns 4.5 and 4.6

Reactions of $PMes_3$ with both $Pt(cod)Cl_2$ and K_2PtCl_4 were unsuccessful. The phosphine ligands proved to be too bulky to react with either platinum species; however, the results were still of interest as they highlighted the limited space around the phosphorus atom. To see exactly how much space was unoccupied in the primary coordination sphere of $PMes_3$ and having noticed that the sulfides and selenides of bulkier mesityl phosphines have not been synthesised or studied, $PMes_3$ was reacted with elemental sulfur and selenium at room, and then elevated temperature. No reaction proceeded between selenium and $PMes_3$, however colourless crystals were obtained of trimesitylphosphine sulfide (Equation 4.7), which was found to be stable in air as a solid and in solution. In the unsuccessful syntheses, the ^{31}P NMR spectrum of the reaction mixture showed no change in the chemical shift of the starting material, as depicted in Scheme 4.4.

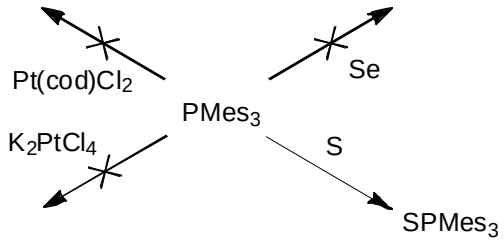

Scheme 4.4: Reactions of $PMes_3$

The oxidation reaction of $PMes_3$ with sulfur proceeded smoothly at 60 °C to give $SPMes_3$ (**4.1**). The initial $^{31}P\{^1H\}$ NMR spectrum of the reaction mixture suggested that traces of the starting material and $OPMes_3$ were present, as well as a small amount of $SPClMes_2$. These could be removed by column chromatography, using toluene as the eluent. This gave the pure product in good yield (80%) and it was characterised by $^{31}P\{^1H\}$, $^{13}C\{^1H\}$ and ^1H NMR spectroscopy, single crystal X-ray crystallography, mass spectrometry and IR spectroscopy.

$$PMes_3 + S \xrightarrow[60\ °C]{\text{Toluene}} SPMes_3 \qquad \textbf{Eqn 4.7}$$

In the $^{31}P\{^1H\}$ NMR spectrum of $SPMes_3$ a singlet is observed at δ_P = 33.2 ppm. This is in the expected region for a phosphine sulfide, at almost 70 ppm downfield from the $PMes_3$ starting material. The peak appears flanked by a small set of satellites with a coupling constant of 77.1 Hz, consistent with a coupling constant of a quaternary carbon atom bonded to a P(V) atom. Indeed in the $^{13}C\{^1H\}$ NMR spectrum, a corresponding doublet is seen at 132.9 ppm with the expected coupling constant of 77.0 Hz. It should also be noted that all peaks in the aromatic region of the $^{13}C\{^1H\}$ NMR spectrum appear as doublets with the expected variation in the magnitude of coupling constants: *p*-C < *o*-C < *m*-C << *i*-C. This trend is unsurprising as it is usual to see an increase in $^3J_{PC}$ coupling compared to $^2J_{PC}$ in an aryl species with the loss of the lone pair on a phosphorus atom, as shown in **Table 4.1**. Whilst the coupling in a P(III) species can have a negative value, the coupling in a P(V) is always positive.[102]

Table 4.1: Values of aryl $^nJ_{PC}$ coupling constants for triphenyl phosphines and derivatives.[102]

$^nJ_{PC}$ in Hz	Ph_3P	$Ph_3P{=}O$	$Mes_3P{=}O$	$Mes_3P{=}S$	$Mes_2PhP{=}Se$
$^1J_{PC}$ (*i*-C)	-12.5	104.4	99.9	77.1	73.3
$^2J_{PC}$ (*o*-C)	19.6	9.8	8.7	3.6	9.7
$^3J_{PC}$ (*m*-C)	6.8	12.1	10.8	13.5	11.0
$^4J_{PC}$ (*p*-C)	0.3	2.8	3.0	3.1	2.7

The $^{13}C\{^{1}H\}$ NMR and ^{1}H NMR spectra exhibit broadening in the peaks for the *o*-C, the *o*-Me group and the *m*-H at room temperature, when run in $CDCl_3$. This is due to the high steric bulk of the groups slowing their rotation. This makes these groups inequivalent. On heating the NMR sample to 70 °C (and changing the solvent to C_6D_6 to do so), this rotation speeds up and the broad signals sharpen up in the $^{13}C\{^{1}H\}$ NMR. A doublet can be seen for the *m*-C in the aryl region at 131.6 ppm with a coupling constant of 13.5 Hz. The remaining quaternary carbon signals cannot be seen due to the strength of the solvent signal. Upfield in the $^{13}C\{^{1}H\}$ NMR spectrum, the peak for the *o*-Me group can be clearly seen at 25.0 ppm, although it does not appear as a doublet as expected.

In the ^{1}H NMR spectrum only one signal is present in the aryl region, that of the *m*-H. At room temperature the signal is a very broad doublet, which sharpens up upon heating to a tight doublet with a coupling constant of 3.57 Hz. The peak for the *o*-Me in the room temperature spectrum exhibits two broad singlets at 2.60 and 1.92 ppm, which sharpen up to a taller, sharper singlet at 2.43 ppm as the groups become equivalent.

In the IR spectrum the ν(P=S) vibration can be seen at 643 cm^{-1} and the expected CH stretches around 2900 cm^{-1}. These are in accord with values recorded for similar species.

Crystals of $SPMes_3$ (**Figure 4.5**) were grown by dissolving the product in hexane and layering with Et_2O. The crystals are colourless prisms and were measured on a Rigaku Mercury70 diffractometer with Mo-Kα radiation, revealing a propeller-like structure in which the mesityl rings are twisted by varying degrees to accommodate the steric bulk of this functionality.

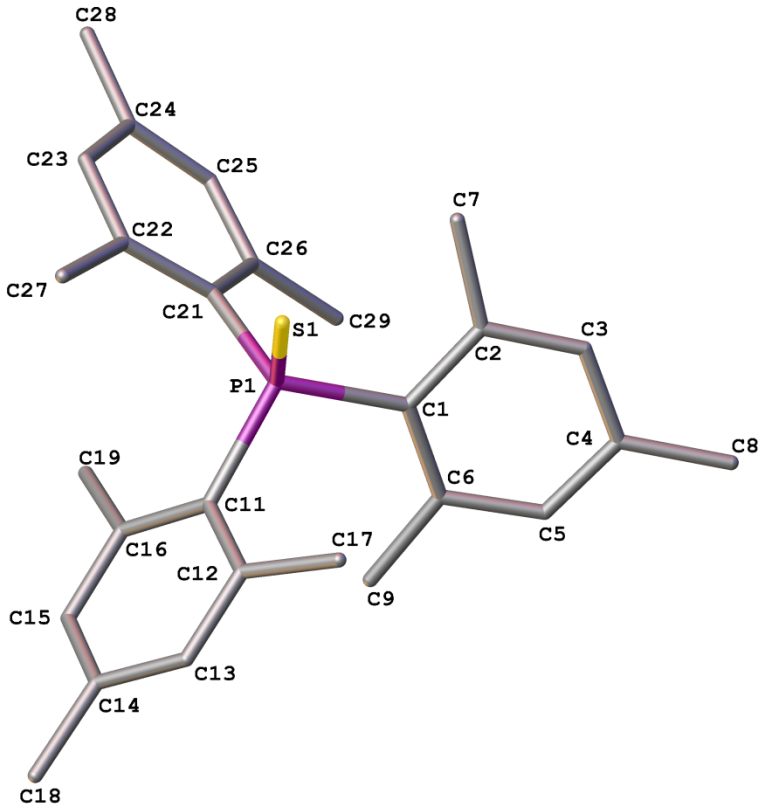

Figure 4.5: X-Ray crystal structure of $SPMes_3$. H atoms omitted for clarity.[103]

A single crystallographically independent molecule is present in the unit cell of (**4.1**). As a consequence of the P-1 symmetry element, a racemic mixture of the right-handed (Δ) orientation and the left-handed Λ orientation is present within the crystal. As such, the P atom can be regarded as a stereogenic centre as these two orientations of the molecule are non-superimposable mirror images. These molecules exhibit "propeller chirality" as demonstrated in **Figure 4.6**.[104]

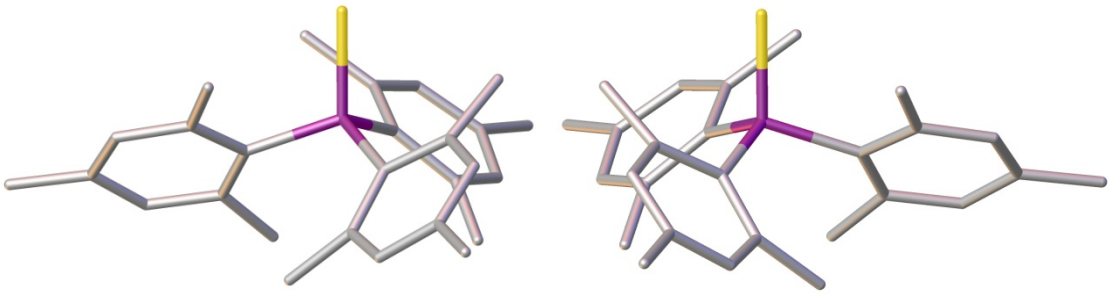

Figure 4.6: Λ-$SPMes_3$ (L) and Δ-$SPMes_3$ (R).

It was found that the P=S bond is 1.9747(13) Å in length, which is longer than average compared to other triaryl phosphine sulfides recorded in the CCDC database, the mean being 1.948 Å. The three bonds between the P atom and the *ipso* carbon atoms, C1, C11 and C21, of the mesityl rings are in the range 1.840(4) Å to 1.849(4) Å and are not significantly different from each other. Further bond lengths for (**4.1**) are given in **Table 4.2**.

Table 4.2: Selected bond lengths and angles for $SPMes_3$ (**4.1**).

Bond	Length (Å)	Atoms	Angle (°)
S1-P1	1.9747(13)	S1-P1-C1	109.50(12)
P1-C1	1.844(5)	S1-P1-C11	107.33(12)
P1-C11	1.849(4)	S1-P1-C21	109.38(12)
P1-C21	1.840(4)	C1-P1-C11	108.92(17)
C1-C2	1.421(6)	C1-P1-C21	109.23(17)
C1-C6	1.413(5)	C11-P1-C21	112.45(16)
C11-C12	1.409(5)	C2-C1-C6	118.2(4)
C11-C16	1.419(5)	C12-C11-C16	118.9(3)
C21-C22	1.421(6)	C22-C21-C26	119.3(3)
C21-C26	1.413(6)		

Equally, the angles around the phosphorus atom are also dissimilar, indicating there is a fair amount of steric strain in the molecule. This is emphasised by the magnitude of the S1-P1-C11 angle, at 107.33(12)°. Due to the lack of space around the central phosphorus atom, the "2nd" mesityl group – that of C11 – has been pushed out of the expected tetrahedral geometry. This is also true of the C11-P1-C21 angle, which, at 112.45(16)°, is the one most distorted from the expected tetrahedral angle of 109.5°. Having said that, all angles around the P centre of the $SPMes_3$ molecule are close to

109.5°, with the average being 109.47°, showing the close to perfect tetrahedral nature of the P atom.

Taking a closer look at (**4.1**), one sees that the mesityl groups are bent, with the methyl groups displaced from the mean plane of the aromatic ring. The *o*-methyl carbon atoms are displaced from the mean plane of their respective phenyl rings, at +0.17 Å and +0.18 Å for C7 and C9, +0.10 Å and +0.18 Å for C17 and C19 and -0.18 Å and -0.17 Å for C27 and C29. The *p*-methyl C atoms are displaced to a lesser extent from the mean planes at -0.09 Å (C8), -0.09 Å (C18) and +0.07 Å (C28). Within the ring system, the maximum deviations from the plane are +0.046 Å for C1, -0.033 Å for C11 and 0.044 Å for C21. Further crystallographic data for (**4.1**) can be found in Appendix 7.

One cannot mention tertiary phosphines without investigating the Tolman's cone angle of such species, especially as trimesitylphosphine is one of the bulkiest known triarylphosphines. It is worth mentioning, that the defined length of the P-M bond in the Tolman's cone angle calculation is 2.28 Å, which is significantly longer than those seen in the phosphorus mesityl sulfides presented herein. Table 4.3 lists these angles of interest, which were found by analysing the crystallographic data obtained above.

Table 4.3: Bonds and angles used to find the crystallographic Tolman's cone angle of (**4.1**).

Atoms	Angle (°)
P1- S1-H7b	87.53
P1-S1-H17b	86.42
P1-S1-H27b	88.40

The angles in Table 4.3 represent θ/2 and by taking these three angles, averaging them, then multiplying by 2, the Tolman's cone angle can be calculated for a compound, Equation 4.8. The cone angle for (**4.1**) is 174.9°, which is substantially smaller than that of $PMes_3$ at 212°.[105]

$$\theta = (2/3) \sum_{i=1}^{3} \theta_i / 2 \qquad \textbf{Eqn: 4.8}$$

Dimesitylphenyl phosphine was synthesised *via* the reaction of the mesityl Grignard reagent and dichlorophenyl phosphine at 0 °C and crystallised by standing at 5 °C.[98] Following the unsuccessful reactions of $PMes_3$, $PMes_2Ph$ was similarly treated with $Pt(cod)Cl_2$, K_2PtCl_4 and elemental selenium and sulfur. Reactions to prepare the platinum complex were again ineffective, even after varying reaction conditions from room temperature to reflux; a $^{31}P\{^1H\}$ NMR spectrum taken of the reaction mixture showed only the phosphine starting material and a small amount of oxide. The dimesitylphenylphosphine sulfide (**4.2**) and the dimesitylphenylphosphine selenide (**4.3**), however, were successfully synthesised in almost quantitative yields. The sulfide was obtained as colourless needles by extraction from the reaction mixture with hexane and layering with diethyl ether, whilst the selenide could be obtained as off-white crystals by layering the reaction mixture with hexane and will be discussed and compared later in this chapter.

In the reaction of excess elemental sulfur with dimesitylphenylphosphine, $SPMes_2Ph$ was formed by stirring the reagent in toluene at room temperature overnight. The mixture was then filtered and the solvent removed *in vacuo*, before being extracted with hexane and layered with diethyl ether. The product was characterised by single crystal X-ray diffraction crystallography, $^{31}P\{^1H\}$, $^{13}C\{^1H\}$ and ^1H NMR spectroscopy, mass spectrometry and IR spectroscopy.

The $^{31}P\{^1H\}$ NMR spectrum of $SPMes_2Ph$ is very similar to that of $SPMes_3$, exhibiting a singlet at δ_P = 37.4 ppm, flanked by small satellites with a ^{31}P-^{13}C coupling constant of 82.2 Hz, indicating coupling to a carbon atom. As was the case with $SPMes_3$, the equivalent coupling constant can be observed in the $^{13}C\{^1H\}$ NMR spectrum. It is interesting to note that only one set and not two sets of carbon satellites are observed in the phosphorus NMR spectrum. This is most likely to be because the couplings are of a similar magnitude, thus overlap occurs. The $^1J_{P\text{-}C}$ coupling constants observed in the carbon NMR spectrum differ by 4.73 Hz, with the larger value being seen for the mesityl group. This can be ascribed to the overall electron donating property of the mesityl group being larger than that of the phenyl moiety, donating more electron density into the P-C bond of the mesityl, increasing its s character and therefore making the coupling constant larger.

In the $^{13}C\{^{1}H\}$ NMR spectrum, all C atoms can be accounted for, even the quaternary carbon atoms, where every signal appears as a doublet, due to coupling to the P atom, apart from that of the methyl groups in the mesityl *para* positions, for which no ^{5}J coupling can be seen. The peaks of the mesityl *o*-, *m*-, and *p*-C atoms all appear downfield from those of the phenyl group, as they are more deshielded. By contrast, the *i*-C signal for the mesityl rings appears upfield from that of the phenyl ring, no reason for which could be found in the literature for this observation, however this is not unusual for similar species.

In the ^{1}H NMR spectrum, a complex multiplet with an integral 5H can be seen in the aryl region, confirming the presence of the Ph group, whilst a doublet at 6.81 ppm with a ^{1}H-^{31}P coupling constant of 3.87 Hz and intensity of 4 can be seen for the *m*-H's of the mesityl rings. Upfield at 2.25 and 2.15 ppm the distinctive singlets of the *p*-CH_3 and *o*-CH_3 are seen, respectively, in a 6:12 intensity ratio. It is interesting to note that the steric hindrance, which caused the broadening of the peaks in the ^{1}H NMR spectrum of (**4.1**), is not present in the spectrum, presumably as the two mesityl rings of (**4.2**) have a greater freedom of rotation.

In the IR spectrum, as well as the expected C-H stretches around 2950 cm^{-1}, the peak at 1436 cm^{-1} is assigned to the ν(P-Ph) and the νP=S signal at 662 cm^{-1} can also be observed.

In the crystal structure (**Figure 4.7**), the P=S bond is, at 1.968(2) Å, slightly shorter than that for (**4.1**), as expected. The P-C_{ipso} bonds lengths are in the range of 1.844(8) to 1.860(6) Å. It is interesting to note, that the shortest P-C_{ipso} bond is that of P1-C19, the Ph-C, as an impact of the mesityl group's steric bulk slightly lengthening the P1-C1 and P1-C10 bonds. Akin to the $SPMes_3$ structure, the rings twist outwards in a propeller-like fashion, but to a notably lesser extent. Six molecules can be seen in the unit cell of $SPMes_2Ph$, all of which adopt the Λ configuration. Whilst this is surprising, this data cannot be seen as conclusive as to whether (**4.2**) is enantiomerically pure or a racemic mixture of both optical isomers. A much larger study must be performed in order to investigate this property further.

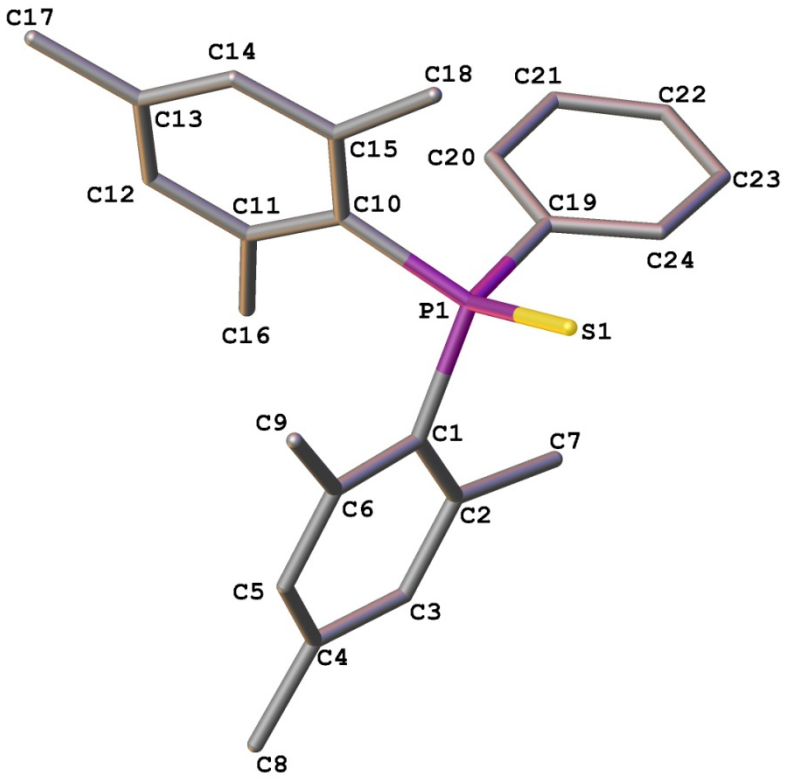

Figure 4.7: Crystal structure of $SPMes_2Ph$. H atoms omitted for clarity.

Two of the three S-P-C angles around the phosphorus atom are fairly close to tetrahedral geometry, at 107.27(16)° and 108.9(3)°. Ring two, containing C10, however, is pushed a long way out from the standard 109.5°, at 120.3(2)°. It is noteworthy that the largest deviation from the ideal tetrahedral angle relates to the 'longest' phosphorus-carbon bond, that of P1-C10. It should also be highlighted, that this distortion is much higher than any distortions seen in $SPMes_3$ or $SPMesPh_2$. This can possibly be attributed to the fact that the three mesityl groups in $SPMes_3$ have an equal demand for space, thus the angles around the central P atom are relatively similar in value, whilst in $SPMesPh_2$ the smaller phenyl groups occupy less space, so the angles are distorted to a lesser degree to accommodate the single mesityl moiety. However, in the case of $SPMes_2Ph$, the bulky mesityl groups try to orientate themselves as far away from each other as possible, leaving the phenyl group to occupy the remaining space. A selection of bond lengths and angles for (**4.2**) is listed in **Table 4.4**, whilst full data is given in Appendix 8.

Table 4.4: Selected bond lengths and angles for $SPMes_2Ph$ (**4.2**).

Bond	Length (Å)	Atoms	Angle (°)
S1-P1	1.968(2)	S1-P1-C1	107.27(16)
P1-C1	1.848(7)	S1-P1-C10	120.3(2)
P1-C10	1.860(6)	S1-P1-C19	108.9(3)
P1-C19	1.844(8)	C1-P1-C10	104.2(3)
C1-C2	1.395(8)	C1-P1-C19	115.0(3)
C1-C6	1.416(11)	C10-P1-C19	101.3(3)
C10-C11	1.417(8)	C2-C1-C6	119.6(6)
C10-C15	1.412(8)	C11-C10-C15	119.2(5)
C19-C20	1.396(8)	C20-C19-C24	117.9(8)
C19-C24	1.357(10)		

Looking at the Tolman's cone angle of $SPMes_2Ph$, we see a decrease in size compared to $SPMes_3$, as anticipated, due to the decrease in steric bulk. Unsurprisingly the smallest angle is that for the Ph ring, which, at 142.84°, is over 7° smaller than those of the mesityl groups. The actual crystallographic cone angle for (**4.2**) is 153.34° and is calculated from the angles given in **Table 4.5**.

Table 4.5: Bonds and angles used to find the Tolman's cone angle of (**4.2**).

Atoms	Angle (°)
P1- S1-H9c	74.98
P1-S1-H18a	83.61
P1-S1-H23	71.42

As stated earlier, the aim of using the bulky mesityl group was to try to synthesise a bulkier, thus less soluble platinum phosphine chloride to react with the ammonium phenylphosphonamidodiselenoate ligands to aid crystallisation of these species. Both $PMes_3$ and $PMes_2Ph$ proved to be too bulky to react with either $Pt(cod)Cl_2$, which is typically used to synthesise $Pt(PMe_3)_2Cl_2$ and the mixed phosphines $Pt(PMe_2Ph)_2Cl_2$ and $Pt(PMePh_2)_2Cl_2$, or $K_2[PtCl_4]$ which is the starting material for $Pt(PPh_3)_2Cl_2$. As such, $PMesPh_2$ was synthesised from the reaction of the mesityl Grignard with diphenylchlorophosphine at 0 °C, in much the same way as $PMes_2Ph$ was synthesised.

The reaction of $PMesPh_2$ with $K_2[PtCl_4]$ in a mixture of CH_2Cl_2 and distilled water at room temperature over night affords the *trans* isomer of $Pt(PMesPh_2)_2Cl_2$ (**4.4**) in a moderate yield (25%). The $^{31}P\{^1H\}$ NMR spectrum displays a singlet at δ_P = 10.9 ppm, surrounded by two sets of satellites: one roughly a third of the height of the main peak with a coupling constant of 2585 Hz, representing the P-Pt coupling, whilst the other set appears at the base of the main signal and has a coupling constant of 28.2 Hz, signifying the carbon-phosphorus coupling. The yield from the NMR spectrum is not high: the reaction proceeds fairly slowly and has a competing reaction to give the oxidation product.

The desired product, however, is the bulkiest known bis-phosphine platinum dichloride complex synthesised to date, where the R groups are formed of a single aromatic ring. It should be noted that the reaction of $Pt(cod)Cl_2$ with $PMesPh_2$ also yields the same thermodynamic product. This is most likely because the bulk of this ligand is too high, resulting in the cod being displaced by the first ligand moiety attaching itself to the platinum, then the intermediate rearranging itself before the second ligand moiety can attach to the centre. The alternative formation of the *cis* product first and then rearrangement is very unlikely due to the large bulk of the ligand and the expected high energy barrier of interconversion.

The $^{13}C\{^1H\}$ NMR spectrum of (**4.4**) was run on a 500 MHz spectrometer to resolve the peaks, as the usual 271 MHz spectrometer left peaks overlapping and thus unclear. Even so, all signals appear as apparent triplets with a 1:2:1 height ratio, not as the doublets seen for a *cis* complex. This arises from virtual coupling, a second order effect in compounds in which there is a strong coupling between phosphorus atoms

which are *trans* to each other.[106] The NMR active nuclei have an AXX' spin system, where A = C and X = P, wherein X couples to A ($^2J_{C\text{-}P}$), X couples to X' ($^2J_{P\text{-}P'}$), but A does not couple to X' ($^4J_{C\text{-}P'} = 0$). [107] If the $^2J_{P\text{-}P'}$ coupling were zero, a doublet would be seen, however, if the $^2J_{P\text{-}P'}$ coupling is large, a triplet is seen in the ^{13}C NMR, or indeed the ^{1}H NMR of similar complexes.[107,108,109] We do not, however, see this large coupling in the $^{31}P\{^1H\}$ NMR spectrum, as the resonances are isochronous, hence only a singlet is observed.

The exception to this observation is that of the *ipso*-carbon in the phenyl group, which is observed as two doublets which cannot be assigned to a specific ring with certainty. The signals for the *para*-carbon atoms are observed as singlets, as they are too far away from the phosphorus to see any interaction. The use of 2D NMR: COSY, HMBC and HSQC allowed the assignment of all peaks in the $^{13}C\{^1H\}$ and ^{1}H NMR spectra.

The ^{1}H NMR reveals multiplets for the phenyl protons in a 4:8:8 ratio for the *para*, *meta* and *ortho*-H but just a singlet for the *meta* hydrogen of the mesityl group, whilst the *o*-CH_3's and *p*-CH_3's are unsplit and are seen in a 12:6 ratio. ^{195}Pt NMR spectroscopy was also run on compound (**4.4**), where the peak is seen as a triplet at δ_{Pt} = -5000.0 ppm, with a ^{195}Pt-^{31}P coupling constant of 2567 Hz, corresponding to the coupling of two equivalent phosphorus atoms to the platinum centre. In comparison, *trans*-$Pt(PPh_3)Cl_2$ exhibits a ^{195}Pt-^{31}P coupling constant of 2630 Hz in the ^{31}P NMR spectrum.[110]

In the mass spectrum, a peak of only 1% intensity can be seen at *m/z* = 874.21, representing the M^+ ion. The most dominant ion peak is observed is *m/z* = 802.10, which is not the parent ion, but instead is assigned to $[Pt(PMesPh_2)_2H]^+$.

Crystals of this species were able to be grown by slow evaporation of the solvent (DCM) and were run on a Rigaku Saturn724 diffractometer with Mo-Kα radiation. The structure was found to be as per **Figure 4.8** and is observed in a P-1 (#2) space group with one crystallographically unique molecule being observed in the unit cell.

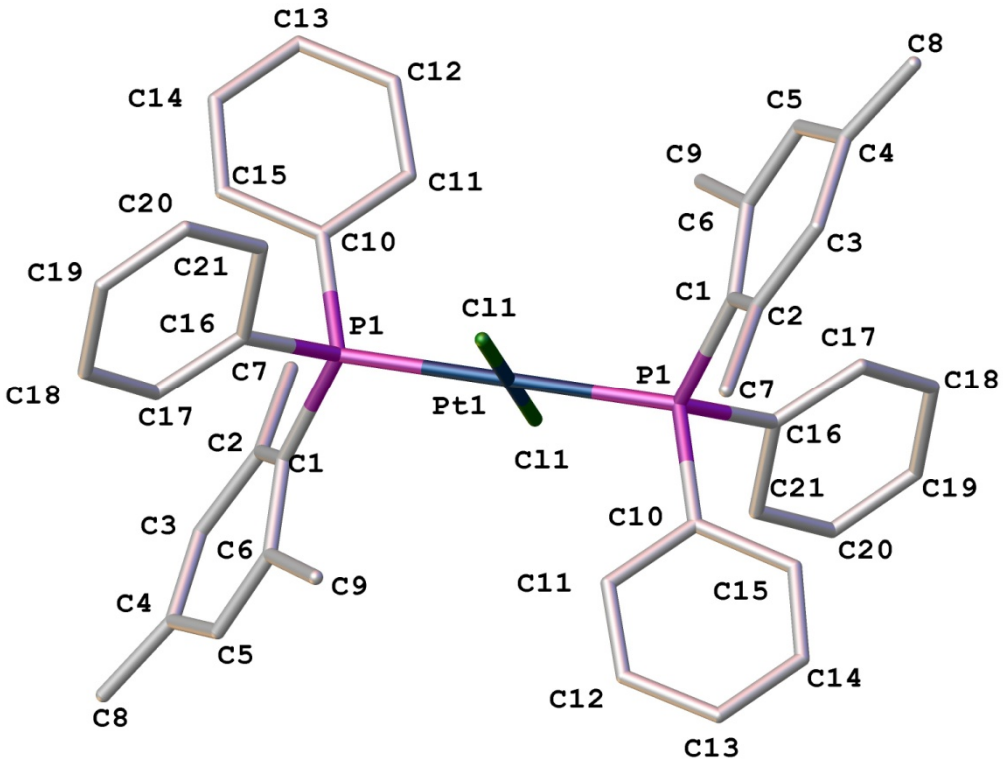

Figure 4.8: Crystal structure of *trans*-Pt(PMesPh$_2$)Cl$_2$. H atoms omitted for clarity.

The Pt-P bonds, at 2.340(4) Å, are roughly the same length as those observed for *trans*-PtCl$_2$(PPh$_3$)$_2$[111] (2.3163(11) Å) and a little longer than the mean of known compounds (2.284 Å). The Pt-Cl bonds are almost the same length as the Pt-P bonds at 2.300(6) Å, whilst the Cl1-Pt-Cl1' angle is 180.0(2)°. The P1-Pt-P1' angle is also 180.0(3)°, whilst the Cl1-Pt1-P1 and Cl1-Pt1-P1^1 angles are 94.25(18)° and 85.75(18)°, respectively. This shows that the PtP$_2$Cl$_2$ plane is indeed completely planar and the steric bulk of the ligands does not distort the plane of the centre of the molecule, but instead the distortion arises from the spatial arrangement within the plane, deviating away from the expected 90° angle associated with square planar geometry. Table 4.6 summarises the angles of interest, whilst further information can be found in Appendix 9.

Table 4.6: Selected bond lengths and angles for *trans*-Pt(PMesPh$_2$)Cl$_2$ (**4.4**).

Bond	Length (Å)	Atoms	Angle (°)
Pt1-Cl1	2.300(6)	Cl1-Pt1-Cl1’	180.0(2)
Pt1-P1	2.340(4)	Cl1-Pt1-P1	94.25(18)
P1-C1	1.86(2)	Cl1-Pt1-P1’	85.75(18)
P1-C10	1.83(3)	P1-Pt1-P1’	180.0(3)
P1-C16	1.83(3)	Pt1-P1-C1	114.1(6)
C1-C2	1.37(3)	Pt1-P1-C10	111.4(6)
C1-C6	1.40(3)	Pt1-P1-C16	119.1(6)
C10-C11	1.44(3)	C1-P1-C10	109.1(9)
C10-C15	1.44(2)	C1-P1-C16	102.2(9)
C16-C17	1.37(3)	C10-P1-C16	99.5(10)
C16-C21	1.46(3)	C2-C1-C6	118(2)
		C11-C10-C15	118.0(19)
		C17-C16-C21	121(2)

NB: As a consequence of (**4.4**) crystallising in the P-1 space group, only one crystallographically unique ligand is present in the crystal structure, resulting in the structure being symmetry grown and atoms on each side of the molecule being labelled the same.

The phenyl and mesityl rings within the species are greatly distorted from the norm, with the internal angles within the phenyl rings ranging from 117(2)° to 124.2(16)° and 115.2(18)° to 124(3)° for Rings 2 and 3 in that order. The mesityl rings in this molecule are buckled considerably, with the average deviation from the plane being 0.0555 Å, of which C1 lies the most out of plane, at 0.0961 Å. This is the largest deviation of a ring carbon atom seen in any of the species investigated in this study. The methyl group carbon atoms are also greatly distorted from the norm, as seen in Figure

4.9. C7 and C9 both lie above the mean plane of the ring, at deviations of 0.2805 Å and 0.1932 Å respectively, whereas C8 lies 0.2596 Å below the same plane. This is not unusual for highly bulky species, but is significantly larger than those mentioned before for $SPMes_3$, a structure that one would consider to be more strained due to the presence of three mesityl rings not just one.

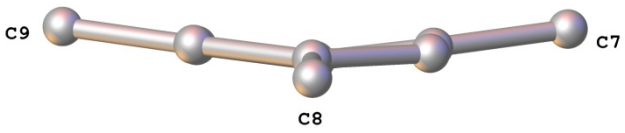

Figure 4.9: Buckling of the mesityl ring in *trans*-$Pt(PMesPh_2)_2Cl_2$.

The Tolman's cone angle of the ligands in (**4.4**) is found to be 126.92° from the angles shown in **Table 4.7**. This is, as expected, smaller for *trans*-$Pt(PMesPh_2)_2Cl_2$ than for $SePMesPh_2$, as the large size of the platinum atom pushes the ligands closer together.

Table 4.7: Bonds and angles used to find the Tolman's cone angle of (**4.4**).

Atoms	Angle (°)
P1- Pt1-H9a	70.72
P1-Pt1-H12	66.95
P1-Pt1-H20	52.72

The reaction of elemental sulfur with $PMesPh_2$ in toluene at room temperature produces $SPMesPh_2$ in a good yield (approximately 80% from the $^{31}P\{^1H\}$ NMR spectrum). The desired product (**4.5**) can be separated from the phosphine oxide byproduct and excess sulfur by removing the reaction mixture *in vacuo*, extracting the product with diethyl ether and layering the resulting solution with hexane. In this way crystals were obtained of the phosphine sulfide suitable for single crystal X-ray structural analysis. (**4.5**) was also characterised by $^{31}P\{^1H\}$, $^{13}C\{^1H\}$ and ^1H NMR spectroscopy, mass spectrometry and IR spectroscopy.

The product is observed as a singlet at δ_P = 36.8 ppm in the $^{31}P\{^1H\}$ NMR spectrum accompanied by the expected ^{13}C satellites with a ^{31}P-^{13}C coupling constant of 82.0 Hz, which is in accord with those already seen for (**4.1**) and (**4.2**). As in the $^{13}C\{^1H\}$ spectra of (**4.1**) and (**4.2**), all peaks, apart from the *p*-Me peak and the *p*-C peak, are seen as doublets due to the coupling of the phosphorus atom. As in the previous two phosphine sulfides, the peaks for the mesityl group were seen downfield from those of the phenyl groups, which is also the case for the free mesityl and phenyl moieties. The only exception to this statement is the *ipso*-carbon atoms, which are again 'swapped'. The mesityl *ipso*-C appears considerably upfield than the phenyl *ipso*-C.

In the ^1H NMR spectrum, the peaks appear in the ratio 4:6:2:3:6, where the Ar-H's of the phenyl rings cannot individually be assigned without 2D NMR analysis. The distinctive doublet for the *m*-H's of the mesityl is observed slightly upfield from the other peaks at δ_H = 6.82 ppm and the *o*- and *p*-CH_3 signals are clearly seen at 1.94 and 2.27 ppm, in that order.

The IR spectrum for $SPMesPh_2$ is almost identical to that of $SPMes_2Ph$, with the only distinctive peaks being those of the aryl CHs (3052, 2961 and 2913 cm^{-1}), the P-Ph bond (1436 cm^{-1}) and the νP=S (703 cm^{-1}).

As mentioned before, colourless platelet crystals of $SPMesPh_2$ suitable for X-ray structural analysis were grown and measured on a Rigaku Saturn724 diffractometer with Mo-Kα radiation. The resulting crystal structure (Figure 4.10) and selected bond lengths and angles (Table 4.8) are presented over the page.

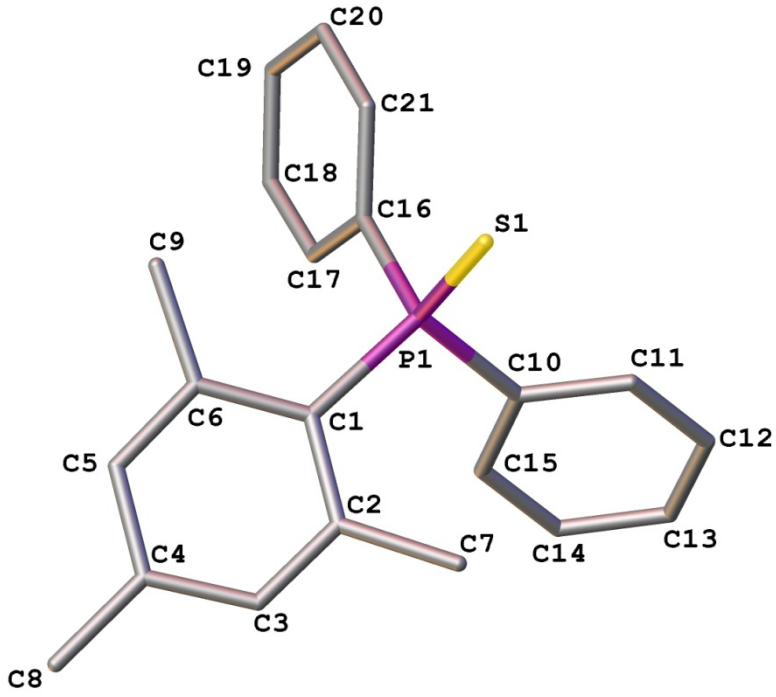

Figure 4.10: X-Ray crystal structure of $SPMesPh_2$. H atoms omitted for clarity.

At 1.9668(15) Å, the P=S bond for $SPMesPh_2$ is, as predicted, the shortest of the three P=S bonds seen for the phosphine sulfides investigated herein, however a little longer than the average value (1.948 Å) for this type of bond according to the CCDC database. The P-C bond lengths observed in (**4.5**) range from 1.822(5) to 1.828(5) Å and, as such, are around 0.02 Å smaller than the corresponding bond lengths in (**4.1**) and (**4.2**). This is again unsurprising, as this structure endures a lot less steric strain, as the phenyl rings are much smaller than the mesityl groups. The internal angles within the rings are also much more regular, lying in the range of 116.6-124.8°, compared to 114.7-126.0° for $SPMes_2Ph$ and 115.0-126.5° for $SPMes_3$. A selection of bond lengths and angles are given in Table 4.8 and full data for (**4.5**) can be seen in Appendix 10.

Table 4.8: Selected bond lengths and angles for $SPMesPh_2$ (**4.5**).

Bond	Length (Å)	Atoms	Angle (°)
S1-P1	1.9668(15)	S1-P1-C1	113.53(14)
P1-C1	1.828(5)	S1-P1-C10	114.24(15)
P1-C10	1.822(5)	S1-P1-C16	112.90(15)
P1-C16	1.823(5)	C1-P1-C10	104.56(19)
C1-C2	1.428(6)	C1-P1-C16	108.92(19)
C1-C6	1.401(6)	C10-P1-C16	101.7(2)
C10-C11	1.396(7)	C2-C1-C6	119.6(4)
C10-C15	1.390(7)	C11-C10-C15	119.7(4)
C16-C17	1.397(7)	C17-C16-C21	119.0(5)
C16-C21	1.396(7)		

As with the previous mesitylphenylphosphines in this Chapter, the crystallographic Tolman's cone angle was investigated for $SPMesPh_2$, with the angles used to calculate this number given in Table 4.9.

Table 4.9: Bonds and angles used to find the Tolman's cone angle of (**4.5**).

Atoms	Angle (°)
P1- S1-H7A	63.56
P1-S1-H11	69.82
P1-S1-H21	71.34

The crystallographic Tolman's cone angle was found to be 136.48°, significantly smaller than those obtained for (**4.1**) and (**4.2**). It is most interesting to note that the smallest angle this time is that of the mesityl group. Looking at the structure from a slightly different angle (Figure 4.11) we see that the phenyl rings sit almost parallel to the P-S vector, whilst the mesityl ring sits at almost 90° to this. The H atoms on the mesityl ring sit pointing towards the S atom, thus decreasing the cone angle of the mesityl group.

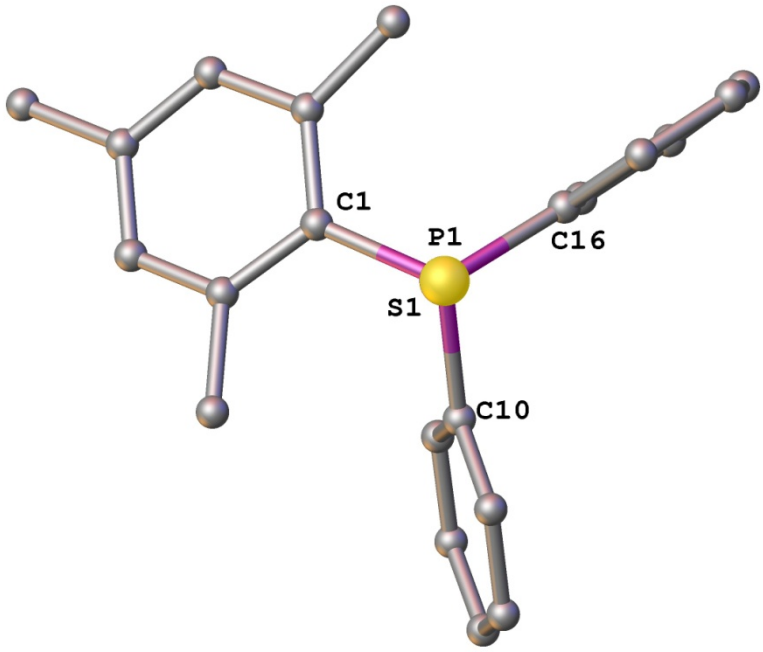

Figure 4.11: Crystal structure of $PMesPh_2$ viewed down the P=S bond.
H atoms omitted for clarity.

As mentioned before, the mesityl ring sits in a completely different position to those of the other mesityl phosphine sulfides. In fact a study of the torsion angles in this structure shows that the average plane of Ring 1 (containing C1) is at an angle of 86.4° to the plane formed by S1-P1-C1, compared to 12.80° for the angle between Ring 2 (containing C10) and the plane of S1-P1-C10 and 2.41° for the angle between Ring 3 (containing C16) and the plane of S1-P1-C16. This is compared to 46.09°, 51.99° and 46.1° for the corresponding rings in $SPMes_3$, as shown in Figure 4.12.

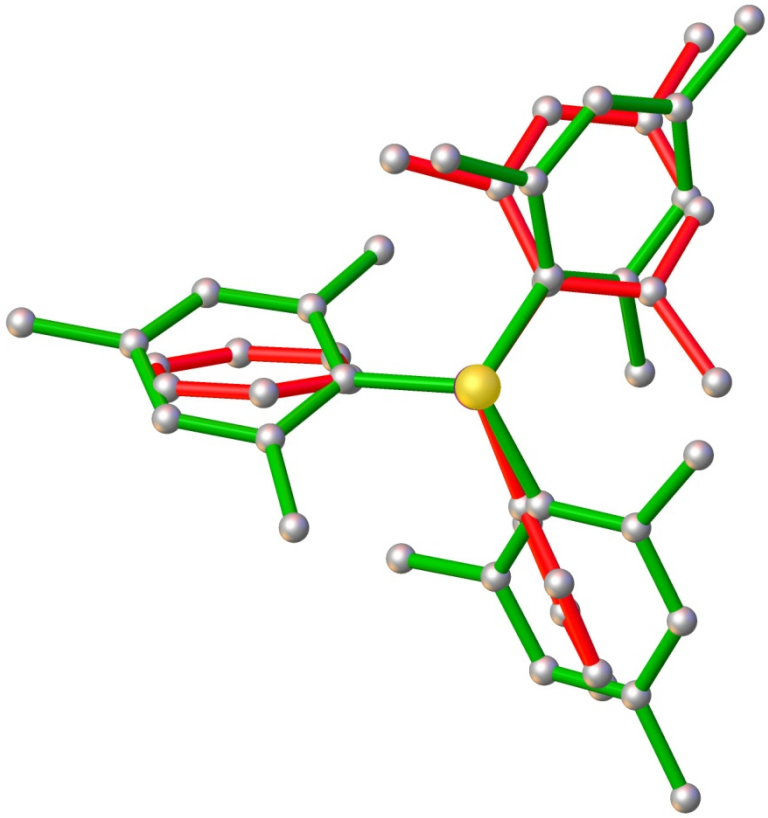

Figure 4.12: Overlay of $SPMes_3$ (green) onto $SPMesPh_2$ (red).
H atoms omitted for clarity.

4.2.1 **Mesitylphosphine Selenides**

As stated previously, the successful reactions of excess elemental selenium and $PMes_2Ph$ and $PMesPh_2$ were also carried out in refluxing toluene for 4 hours. The work up was the same for each: the reaction mixture was filtered, the solvent removed *in vacuo*, the product redissolved in toluene and layered with diethyl ether. $SePMes_2Ph$ (**4.3**) and $SePMesPh_2$ (**4.6**) were obtained as yellow and colourless platelets, respectively, which were both suitable for X-ray crystal structure analysis. Each of these compounds were also characterised by $^{31}P\{^1H\}$, $^{77}Se\{^1H\}$, $^{13}C\{^1H\}$ and ^1H NMR spectroscopy, mass spectrometry and IR spectroscopy.

The $^{31}P\{^1H\}$ NMR spectra of the two compounds exhibit the same patterns: a large singlet peak flanked by two sets of satellites: a small set of carbon satellites at the base of the main peak and a larger set of selenium satellites. There is not much of a significant upfield shift of the peak from sulfide to selenide: the resonance for $SePMes_2Ph$ appears at δ_P = 20.8 ppm and whilst that for $SePMesPh_2$ appears at δ_P = 28.4 ppm, compared to δ_P = 37.3 ppm and 36.8 ppm respectively for the corresponding sulfides. The carbon coupling constants are slightly lower for the selenides than for the sulfides at 73.5 Hz for (**4.3**) and 75.1 Hz for (**4.6**), whilst the $^1J_{P\text{-}Se}$ coupling constants observed for phosphorus-selenium double bond are 695 Hz and 725 Hz, respectively. The size and ratio of these couplings is as expected: as the s character on the P atom increases, so too does the P=Se coupling constant. The two phenyl groups are less electron donating than the two mesityl groups and as such reduce the s character on the phosphorus atom. In each of the selenium NMR spectra for these two compounds a doublet can be observed. This appears at -83.3 ppm for $SePMes_2Ph$ and -318.7 ppm for $SePMesPh_2$.

As stated in Chapter 3, selenium has a very distinctive pattern in mass spectrometry, owing to its six 'stable' isotopes. In fact the sixth of these, ^{82}Se is radioactive, and its half-life is around 10^{20} years. Even if only one selenium atom is present in a species, a tell-tale isotope pattern can be seen in the mass spectrum. Figure 4.13 depicts the comparison of the patterns in the mass spectra for sulfides (**4.2**) and (**4.3**) and selenides (**4.5**) and (**4.6**) respectively.

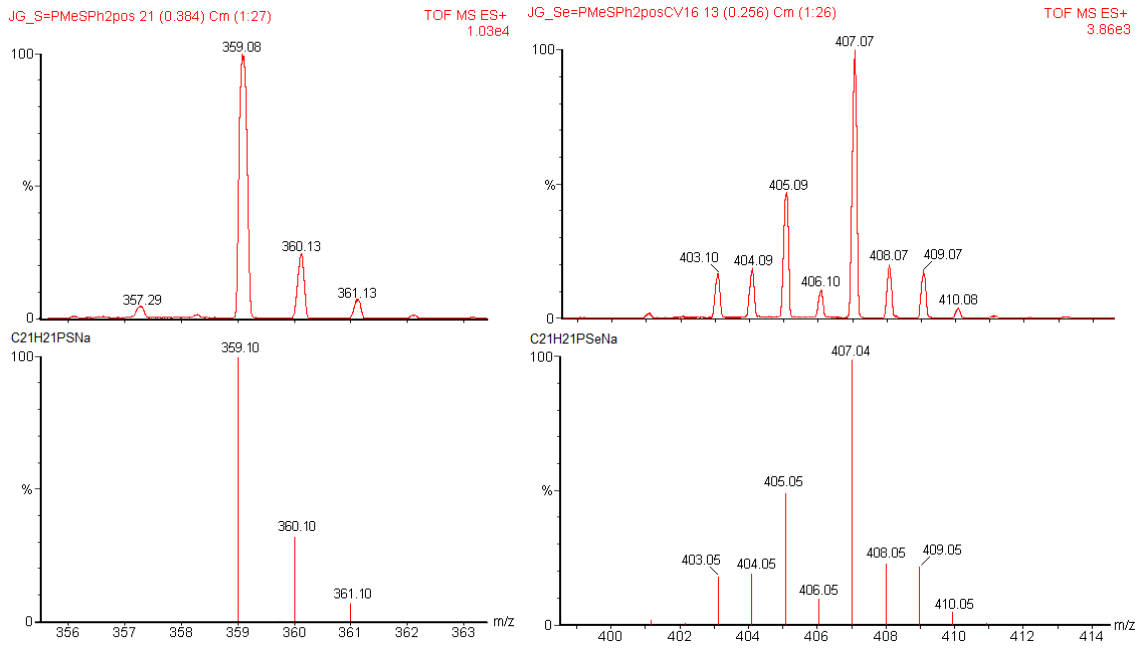

Figure 4.13: The simple mass spectrum with its simulation for $SPMesPh_2$ (L) compared to the more complicated mass spectrum and simulation for of $SePMesPh_2$ (R) both have the positive Na+ ion included.

Crystal structures of (**4.3**) and (**4.6**) were obtained by dissolving the compounds in toluene and layering the solutions with diethyl ether, crystallising as yellow and colourless platelets in that order. The P=Se bonds are, at 2.134(3) Å for (**4.3**) and 2.121(3) Å for (**4.6**), just a little above the average, which is 2.111 Å according to the CCDC database. The crystal structures are very similar to those of their sulfur analogues and exhibit similar symmetry and as such are in the same space groups. **Figure 4.14** and **Table 4.10** exhibit data for $SePMes_2Ph$ (**4.3**) and **Figure 4.15** and Table 4.11 show data for $SePMesPh_2$ (**4.6**). Full crystallographic data are given in Appendices 11 and 12.

As for the $SPMes_2Ph$ structure, the rings in $SePMes_2Ph$ twist outwards in a propeller-like fashion, but to a lesser extent than for $SPMes_3$. Six molecules can be seen in the unit cell of $SePMes_2Ph$, which are all in the Λ configuration, as in the $SPMes_2Ph$ unit cell. As before, this data cannot be seen as conclusive as to whether (**4.3**) is enantiomerically pure or a racemic mixture. A much larger study must be performed in order to investigate this property further.

In $SePMesPh_2$ there are 4 molecules in the unit cell, as for $SPMesPh_2$. These molecules are much less propeller like, as, just as in (**4.4**), the angle of the two phenyl rings to the P-Se vector are close to 0°, at 15.0° for Ring 2 and 1.39° for Ring 3, whilst the mesityl ring sits with a torsion angle of 85.4° to the same vector.

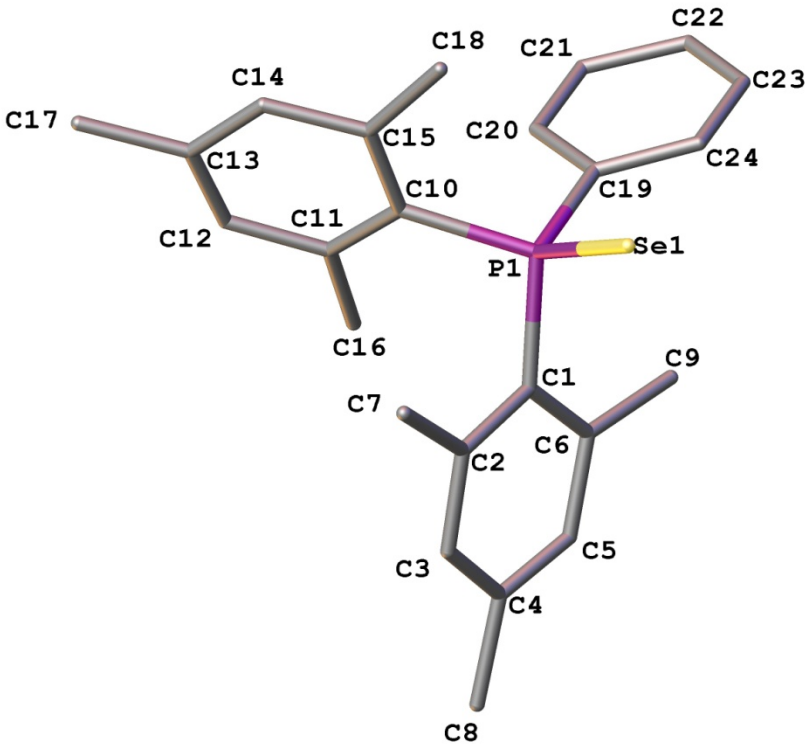

Figure 4.14: Crystal structure of $SePMes_2Ph$. H atoms omitted for clarity.

Table 4.10: Selected bond lengths and angles for $SePMes_2Ph$ (**4.3**).

Bond	Length (Å)	Atoms	Angle (°)
Se1-P1	2.134(3)	Se1-P1-C1	105.4(3)
P1-C1	1.838(7)	Se1-P1-C10	121.6(3)
P1-C10	1.859(10)	Se1-P1-C19	109.4(4)
P1-C19	1.830(7)	C1-P1-C10	103.8(4)
C1-C2	1.412(11)	C1-P1-C19	114.9(4)
C1-C6	1.412(11)	C10-P1-C19	102.2(4)
C10-C11	1.397(13)	C2-C1-C6	119.6(6)
C10-C15	1.423(11)	C11-C10-C15	119.8(9)
C19-C20	1.398(13)	C20-C19-C24	117.4(8)
C19-C24	1.402(18)		

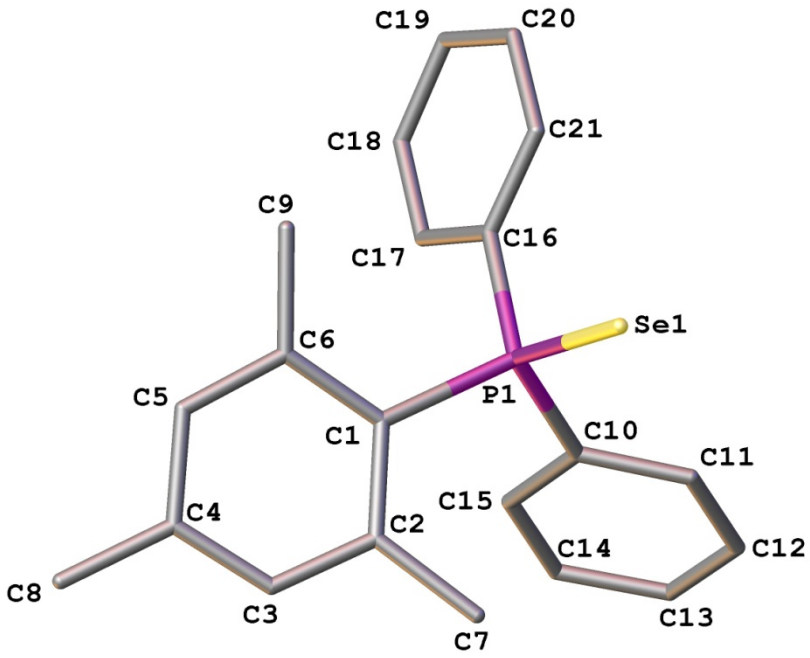

Figure 4.15: Crystal structure of $SePMesPh_2$. H atoms omitted for clarity.

Table 4.11: Selected bond lengths and angles for $SePMesPh_2$ (**4.6**).

Bond	Length (Å)	Atoms	Angle (°)
Se1-P1	2.121(3)	Se1-P1-C1	113.4(3)
P1-C1	1.823(9)	Se1-P1-C10	113.6(3)
P1-C10	1.834(9)	Se1-P1-C16	112.9(3)
P1-C16	1.841(9)	C1-P1-C10	105.2(4)
C1-C2	1.426(12)	C1-P1-C16	108.7(4)
C1-C6	1.423(12)	C10-P1-C16	102.2(4)
C10-C11	1.382(13)	C2-C1-C6	119.4(8)
C10-C15	1.406(12)	C11-C10-C15	119.6(8)
C16-C17	1.402(13)	C17-C16-C21	119.2(9)
C16-C21	1.394(13)		

On studying the Tolman's cone angles for the selenium compounds (**4.3**) and (**4.6**) we see a decrease from the sulfides to the selenides. This is very much expected as the selenium atom is much larger and therefore presses the ligands closer together. We also see a decrease from the $PMes_2Ph$ species to the $PMesPh_2$ species, which mirrors the sulfides. We have seen that the selenides and sulfides are incredibly similar in geometry, however, it is notable that the H atoms used in the cone angle calculations are the same in the $PMesPh_2$ species, but differ in the $PMes_2Ph$ species. The crystallographic Tolman's cone angle for $SePMes_2Ph$ was calculated to be 147.49°, whilst the cone angle for $SePMesPh_2$ is 132.83°. The data used for this calculation is recorded in Table 4.12.

Table 4.12: Bonds and angles used to find the Tolman's cone angle of (**4.3**) (L) and (**4.6**) (R).

Atoms	Angle (°)	Atoms	Angle (°)
P1- Se1-H7A	73.21	P1- Se1-H7A	63.72
P1-Se1-H18B	78.44	P1-Se1-H11	66.82
P1-Se1-H23	69.59	P1-Se1-H21	68.70

4.2.2 **Mesitylphosphine Oxides**

During the course of investigations into bulky arylphosphines and the sulfides and selenides thereof, it was observed that the comparable oxides were not to be found on the CCDC database, and so whilst comparisons could be made to triphenylphosphine oxide and trimesitylphosphine, the structural studies linking these two species to those synthesised within this research were not possible. On further investigation it was discovered that trimesitylphosphine oxide has been synthesised,[112] but no crystallographic data could be found for the species and there was no mention of the corresponding oxides of $PMes_2Ph$ and $PMesPh_2$. As such, the method was followed for the preparation of trimesitylphosphine oxide, whilst crystallisation was performed by simply allowing the solvent to slowly evaporate from an ethanol or acetone solution.

The reaction of $PMes_3$ with H_2O_2 in acetone at room temperature led to a full conversion to the desired oxide product. The product was recrystallised from acetone, by dissolving the crude product and then allowing it to slowly evaporate. On dissolving the crystals in $CDCl_3$, a single peak is observed in the $^{31}P\{^1H\}$ NMR at 31.8 ppm with the anticipated ^{13}C satellites. The ^{31}P-^{13}C coupling constant of the satellites is 98.6 Hz, somewhat larger than those observed for the sulfides and selenides. This is most likely the result of the oxygen being harder than sulfur and selenium, as it is a first row element, which has more s character than second and third row elements.

The $^{13}C\{^1H\}$ NMR spectrum was found to be quite similar to that of $SPMes_3$, with some moderate broadening of the peaks. This is, however, much less pronounced for the oxide than the sulfide, as the size of the oxygen atom is smaller and thus allows for freer rotation of the mesityl rings. In the crystal structure, a disordered solvent molecule is present with the molecular formular $C_3H_6O_4$, which on dissolving the obtained crystals in $CDCl_3$, could be seen in the NMR. This molecule is also soluble in C_6D_6, so could not be removed by changing solvent, nor could it be separated by chromatography. As with all the compounds described in this Chapter, the peaks for all C atoms within 4 bonds of the phosphorus centre appear as doublets.

In the ^{1}H NMR spectrum, peaks for the *m*-H, the *o*-CH_3 and the *p*-CH_3 occur in a 6:18:9 ratio, at 6.86 ppm, 2.36 ppm and 2.27 ppm. A further peak can be seen in the spectrum, which is compatible with the solvent molecule seen in the crystal structure.

The IR spectrum for (**4.7**) is typical for this class of compounds, with the νC-H around 2900 cm^{-1} and the νP-Ar peak at 1452 cm^{-1}. For the oxide, however, the expected νP=O stretch can be identified at 1140 cm^{-1}, as well as the peak for the peroxide O-H, at 3271 cm^{-1}, which is present in the crystal structure.

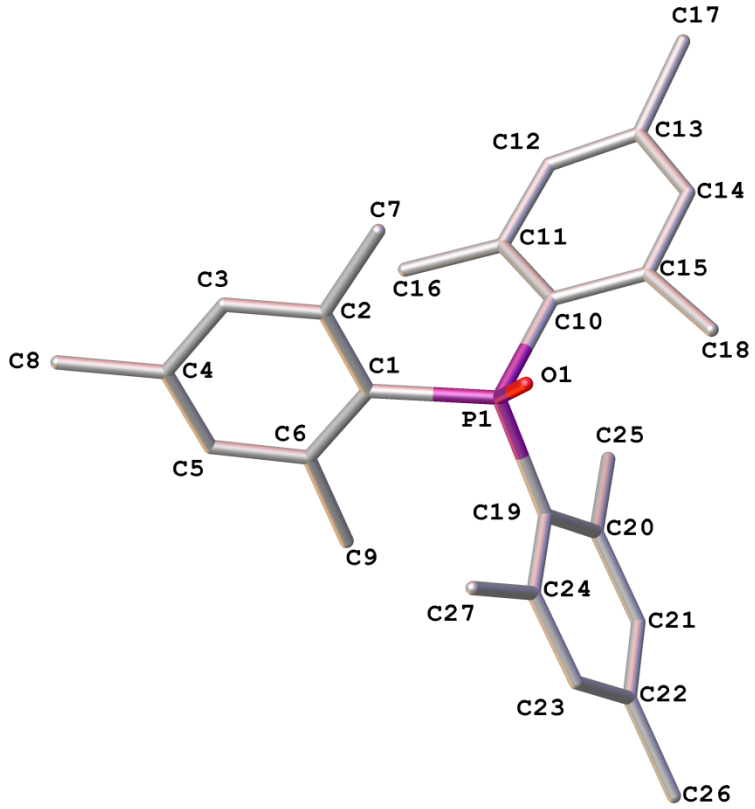

Figure 4.16: Crystal structure of $OPMes_3$.
H atoms and co-crystallised solvent molecule omitted for clarity.

The crystal structure of $OPMes_3$ was obtained on a Rigaku Saturn724 diffractometer with Mo-Kα radiation, revealing the structure shown in Figure 4.16. The phosphorus-oxygen bond length was found to be 1.506(4) Å, which is a fraction above the average, however not extraordinary. The phosphorus-carbon bond lengths lie in the range of 1.817(6) – 1.839(7) Å. The C-C bond lengths in (**4.7**) are in accordance with those seen in the other species in this chapter, in that they are non-identical within the rings or within the whole species. The angles around the phosphorus atom also confirm

that the tetrahedral geometry of $OPMes_3$ is distorted from ideal, with the O-P-C angles all being smaller than 109.5°, whilst the C-P-C angles range from 109.1(3)° – 112.1(3)°. This not only demonstrates the repulsion of the rings by the O atom is smaller than that witnessed for $SPMes_3$, but also shows that the overall geometry is less crowded, as the angle range is a lot smaller (107.8(3)° – 108.5(3)° for the oxide *versus* 107.33(12)° – 109.50(12)° for the sulfide). The relevant bond lengths and angles for (**4.7**) are given in Table 4.13, whilst further crystallographic data is given in Appendix 13.

Table 4.13: Selected bond lengths and angles for $OPMes_3$ (**4.7**).

Bond	Length (Å)	Atoms	Angle (°)
O1-P1	1.506(4)	O1-P1-C1	107.8(3)
P1-C1	1.817(6)	O1-P1-C10	108.5(3)
P1-C10	1.839(7)	O1-P1-C19	108.3(2)
P1-C19	1.839(5)	C1-P1-C10	109.1(3)
C1-C2	1.416(7)	C1-P1-C19	112.1(3)
C1-C6	1.426(8)	C10-P1-C19	110.8(3)
C10-C11	1.411(7)	C2-C1-C6	118.6(5)
C10-C15	1.405(8)	C11-C10-C15	119.5(3)
C19-C20	1.402(8)	C20-C19-C24	118.4(5)
C19-C24	1.421(9)		

The angles used for the calculation of the crystallographic Tolman's cone angle of $OPMes_3$ are recorded in the table over the page, revealing it to be 198.6°. This is, as expected, the largest seen within the species investigated. The oxygen atom is much smaller than the other chalcogens and as such (**4.7**) is less sterically demanding. With a decrease in steric hindrance, more space for freer rotation of the mesityl rings is allowed.

Table 4.14: Bonds and angles used to find the Tolman's cone angle of (**4.7**).

Atoms	Angle (°)
P1- S1-H7b	97.53
P1-S1-H18b	99.51
P1-S1-H25a	100.86

On reacting $PMes_2Ph$ with H_2O_2 in acetone at room temperature, the anticipated oxide, (**4.8**), was synthesised in almost quantitative yield. Crystals suitable for X-ray analysis were grown by removing the reaction solvent *in vacuo* and recrystallising from acetone, also allowing for characterisation by all the related multinuclear NMR spectroscopy, IR and mass spectrometry.

A single peak was observed in the $^{31}P\{^1H\}$ NMR spectrum at 35.0 ppm accompanied by its expected ^{13}C satellites with a coupling of 101 Hz. This is again, much larger than those observed for the analogous sulfide, however compatible with (**4.7**) and in accordance with other related compounds. The $^{13}C\{^1H\}$ NMR spectrum is similar to those of the corresponding selenides and sulfides, and all coupling constants lie within the range observed for the related species, as is the case for the ^1H NMR spectrum.

The mass spectrum for (**4.8**) shows a pattern not often seen in the spectra for the larger chalcogenides mentioned in this Chapter. It is characteristic of the mesitylphosphine oxides: peaks are observed for $2MNa^+$, as well as fragmentation patterns for the '2^{nd}' molecule. For $OPMes_2Ph$ and $OPMesPh_2$, no fragments with mass lower than M are seen when using ES^+, however MNa^+-Mes can be observed in the spectrum for $OPMes_3$.

Colourless prism crystals suitable for X-ray analysis were grown and data collected on a Rigaku Saturn70 diffractometer with Mo-Kα radiation. The structure is shown in Figure 4.17 and crystallises with two $OPMes_2Ph$ molecules and two solvent molecules in the unit cell. This is slightly surprising, as the analogous sulfur and selenium compounds crystallise with 6 molecules in the unit cell and are in the $P6_3$

space group, as opposed to the P-1 space group for the oxide. In comparison, both trimesitylphosphine species crystallise in the same space group as each other, P-1, and also have just two molecules in the unit cell.

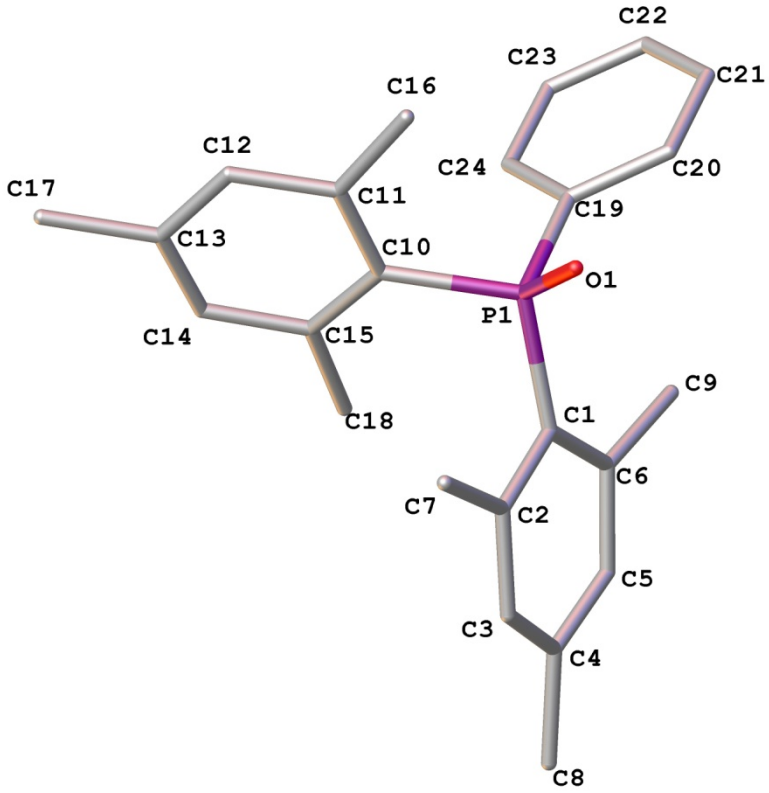

Figure 4.17: Crystal structure of $OPMes_2Ph$ (**4.8**).
H atoms and solvent molecule omitted for clarity.

$OPMes_2Ph$ (**4.8**) is a propeller-like molecule in which the P=O bond length is, at 1.1499(3) Å, of average length for a P=O bond and slightly shorter than that of $OPMes_3$. The P-C bond lengths range from 1.804(4) to 1.835(4) Å, where the shortest of which is bonded to the phenyl ring. As in $SPMes_2Ph$, the phenyl ring is pushed out of the expected 109.5° tetrahedral angle to allow for the greater steric demands of the larger mesityl rings. The mesityl rings are again not quite planar. This is, as predicted, to a lesser extent to that seen in the analogous sulfur and selenium analogues. The bond lengths and angles are presented in Table 4.15, whilst more detailed crystallographic data can be found in Appendix 14.

Table 4.15: Selected bond lengths and angles for $OPMes_2Ph$ (**4.8**).

Bond	Length (Å)	Atoms	Angle (°)
O1-P1	1.1499(3)	O1-P1-C1	109.34(15)
P1-C1	1.815(4)	O1-P1-C10	113.76(16)
P1-C10	1.835(4)	O1-P1-C19	108.48(16)
P1-C19	1.804(4)	C1-P1-C10	108.85(17)
C1-C2	1.419(6)	C1-P1-C19	114.18(17)
C1-C6	1.427(6)	C10-P1-C19	102.20(17)
C10-C11	1.416(5)	C2-C1-C6	119.3(4)
C10-C15	1.414(6)	C11-C10-C15	119.1(4)
C19-C20	1.387(5)	C20-C19-C24	118.7(4)
C19-C24	1.409(6)		

The Tolman's cone angle of (**4.8**) fits the pattern we have seen before, in being larger than that of the mesityldiphenyl species and smaller than that of the trimesityl species in this series, at 177.6°. The angles used to find this parameter are listed in Table 4.16 below.

Table 4.16: Bonds and angles used to find the Tolman's cone angle of (**4.8**).

Atoms	Angle (°)
P1- S1-H9a	86.75
P1-S1-H18a	98.24
P1-S1-H24	81.37

The reaction of $PMesPh_2$ with H_2O_2 in acetone proceeded like any synthetic inorganic chemist's dream: the phosphine was dissolved in acetone in a beaker in the fume hood, 3 mL of hydrogen peroxide was added to the solution, then it was stirred for 5 minutes at room temperature until the solution turned cloudy. In the time taken to run an NMR spectrum of the reaction mixture (roughly 12 minutes) large white crystals suitable for X-ray crystallographic structural analysis had precipitated out of the solution. The $^{31}P\{^1H\}$ NMR spectrum taken of the reaction mixture showed the phosphine had been converted to its corresponding phosphine oxide with a yield of 100%.

Similar spectra were obtained for $OPMesPh_2$ (**4.9**) as for the sulfides and selenides: in the $^{31}P\{^1H\}$ NMR, a singlet is seen at 32.4 ppm flanked by ^{13}C satellites. The ^{31}P-^{13}C coupling constant, at 103 Hz, is larger than those of the sulfides and selenides and is notably the largest for all of these species. This is because the oxides have more s character compared to those of the larger and heavier chalcogenides. We therefore see a decrease in coupling constant as we go down Group 16 and it could be postulated that if a corresponding telluride were to be synthesised, this would have an even smaller coupling constant.

The carbon NMR spectrum of $OPMesPh_2$ (**4.9**), as for all the other related derivatives, exhibits doublets for most signals due to spin-spin coupling to the central phosphorus atom, whilst the ^1H NMR displays the expected peaks in a 4:6 ratio for the phenyl rings and a 2:3:6 ratio for the *m*-Hs, the *para*-methyl group and the *ortho*-methyl groups. The IR spectrum is also typical of these compounds and is predictably very similar to that of (**4.8**), with the characteristic νC-H frequencies around 2900 cm^{-1}, the P-Ph peak at 1440 cm^{-1} and the νP=O at 1151 cm^{-1}.

The X-ray crystal structure for $OPMesPh_2$, depicted in **Figure 4.18**, was obtained on a Rigaku Saturn724 diffractometer with Mo-Kα radiation and is surprisingly different to those obtained for $SPMesPh_2$ and $SePMesPh_2$. $OPMesPh_2$ crystallises with a H_2O_2 molecule in the lattice, which has been omitted for clarity in the figure. (**4.9**) crystallises in the $P2_1/n$ space group and selected bond lengths and angles for this molecule are given in Table 4.17, whilst further crystallographic data is presented in Appendix 15.

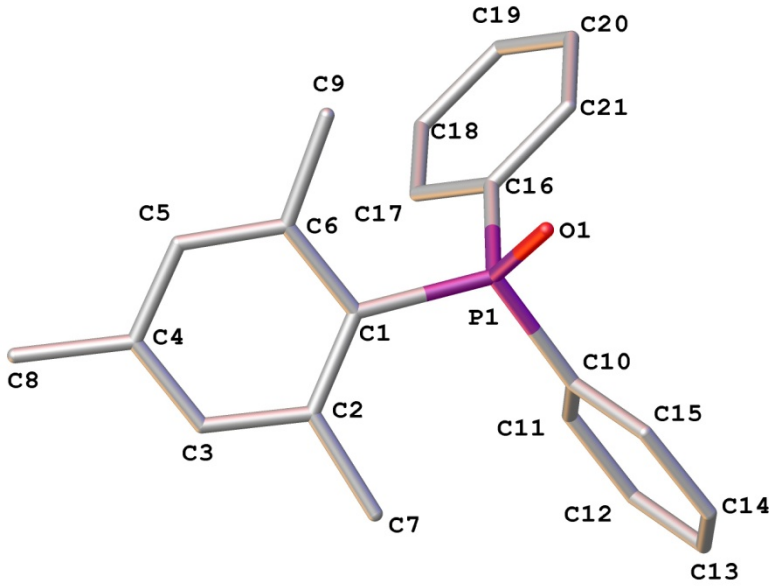

Figure 4.18: Crystal structure of $OPMesPh_2$ (**4.9**).
H atoms and co-crystallised solvent molecule omitted for clarity.

At 1.502(3) Å, the P=O bond length in $OPMesPh_2$ is slightly longer than that for $OPMes_2Ph$. There are 4 molecules in the unit cell, plus four solvent molecules, which H-bond to the O atom, slightly lengthening this bond. The rings in the system, which are the most planar and symmetrical out of all those studied.

Table 4.17: Selected bond lengths and angles for $OPMesPh_2$ (**4.9**).

Bond	Length (Å)	Atoms	Angle (°)
O1-P1	1.502(3)	O1-P1-C1	113.75(17)
P1-C1	1.819(4)	O1-P1-C10	109.84(16)
P1-C10	1.818(5)	O1-P1-C16	112.1(2)
P1-C16	1.813(5)	C1-P1-C10	113.2(2)
C1-C2	1.406(7)	C1-P1-C19	104.60(17)
C1-C6	1.438(6)	C10-P1-C19	102.68(19)
C10-C11	1.398(7)	C2-C1-C6	119.0(4)
C10-C15	1.397(6)	C11-C10-C15	119.4(5)
C16-C17	1.387(5)	C17-C16-C24	119.6(4)
C16-C21	1.397(7)		

It was shown before in **Figure 4.12** how similar the sulfide and selenide are to each other, however, overlaying the oxide onto the sulfide, we see that the rings in the oxide have a noticeably different geometry, with the torsion angles of the rings differing by up to 20°, see Figure 4.19 and Table 4.18. These observations follow the trend that elements in rows two and three of the periodic table are much more alike to each other, than those in row one. Oxygen is a hard atom, whereas sulfur and selenium are classed as soft atoms. This affects their chemistries significantly.

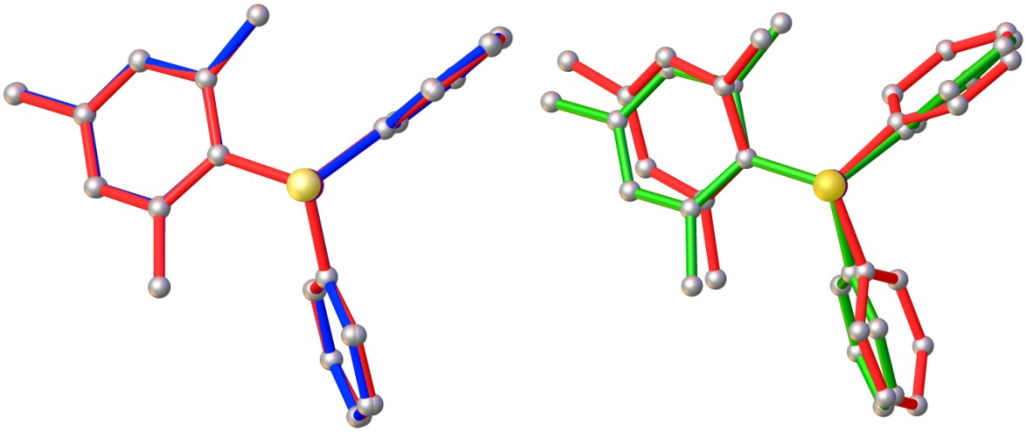

Figure 4.19: L: Overlay of $SPMesPh_2$ (red) on $SePMesPh_2$ (blue). R: Overlay of $SPMesPh_2$ (green) on $OPMesPh_2$ (red). H atoms omitted for clarity.

Table 4.18: Torsion angles observed in the structures of $EPMesPh_2$. E = O, S, Se.

	$OPMesPh_2$	$SPMesPh_2$	$SePMesPh_2$
Mes	62.3°	86.4°	85.4°
Ph (1)	23.2°	12.80°	15.0°
Ph (2)	24.6°	2.41°	1.39°

The crystallographic Tolman's cone angle for (**4.9**) is 164.5° (angles for calculation in Table 4.19) and follows the expected pattern that it has the smallest observed cone angle of the oxide species studied herein, which lies roughly in the middle between that of $SPMes_3$ and $SPMes_2Ph$.

Table 4.19: Bonds and angles used to find the Tolman's cone angle of (**4.8**).

Atoms	Angle (°)
P1- S1-H9a	86.80
P1-S1-H15	81.28
P1-S1-H21	78.70

All of the species studied fit the expected pattern showing that the larger the chalcogen, the smaller the cone angle and the bulkier the groups, the larger the cone angle, summarised in Table 4.20.

Table 4.20: Crystallographic Tolman's cone angle for mesityl phosphines studied.

	O	S	Se
Mes_3	198.6	174.9	-
Mes_2Ph	177.6	153.3	147.5
$MesPh_2$	164.5	136.5	132.8

It has also been shown that the diphenyl derivatives have the largest coupling constants out of all of these compounds studied. This is likely because, compared with the *i*C-P bond lengths to the mesityl rings, the phenyl carbon-phosphorus bond length is shorter and thus stronger, increasing the overlap of the s orbitals and thus the coupling constant. Conversely, the C-P bonds for the mesityl rings are stretched to accommodate their steric bulk, making them slightly weaker, thus diminishing the coupling constant. The ^{31}P-^{13}C coupling constants for all the triarylphosphine chalcogenides, taken from the ^{31}P NMR spectrum for each species, can be seen in Table 4.21.

Table 4.21: The coupling constants of the P-C bonds of the triarylphosphine chalcogenides (Hz).

	O	S	Se
$PMes_3$	98.6	77.2	-
$PMes_2Ph$	100.9	79.8	73.5
$PMesPh_2$	103.3	82.1	75.1

The crystal structures can be used to highlight the similarities and differences between the compounds. Whilst the sulfides and selenides have very similar geometries, the oxides follow a different patten. The P=O bond is so much shorter than the P=S and P=Se bonds, and the O atom has a much smaller radius, allowing the substituent rings more space for free rotation. In Figure 4.20 the phosphorus centres of the four $PMesPh_2$ species are overlayed to highlight these small, but significant differences. The cone angle for the platinum complex phosphorus atom is by far the smallest due to steric crowding around the P centre.

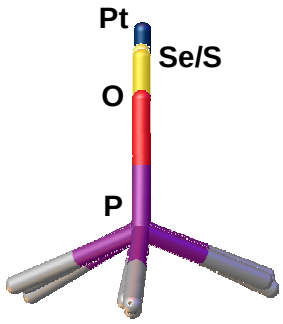

Figure 4.20: Overlay of the four $PMesPh_2$ species

The P=S, P=Se and P=O bonds are all slightly longer than the average expected bond length for each series, due to the steric bulk of the mesityl rings. The bulk also causes buckling of the rings in order for them all to be accommodated around the small phosphorus centre.

Through these experiments one can see that the upper limit of ligand bulk is being reached, and that mesityl phosphine ligands are not suitable for ligand systems for third row transition elements.

4.3 Conclusion

The aim of this research was to synthesise a platinum complex containing bulky trimesitylphosphine ligands to react with the phenylphosphonamidodiselenoate ligands synthesised in Chapter 3. This was proved to be almost impossible under the conditions investigated, with only one *trans* complex, *trans*-Pt($PMesPh_2$)Cl_2, being able to be synthesised from the reaction of $K_2[PtCl_4]$ and $PMesPh_2$ in a mixture of water and DCM. This is not to say that these phosphine ligands cannot be used with other, smaller metal centres, however this was not investigated in the presented research. The X-ray crystal structure of *trans*-Pt($PMesPh_2$)Cl_2 could be elucidated and this was confirmed and fully characterised by $^{31}P\{^1H\}$, ^{195}Pt, $^{13}C\{^1H\}$ and ^1H NMR spectroscopy, mass spectrometry and IR spectroscopy, as well as elemental analysis. The yield of this reaction was, however, not very high, due to the competing oxidation reaction.

Owing to the difficulty in synthesising the platinum complexes, the steric hindrance of the produced mesityl phosphines was investigated *via* their reaction with elemental sulfur and selenium and hydrogen peroxide. As such, trimesitylphosphine sulfide and its corresponding oxide, dimesitylphenylphosphine sulfide and its associated selenide and oxide and mesityldiphenylphosphine sulfide and its related selenide and oxide were all successfully synthesised in order to study the geometries and properties, including the Tolman's cone angle, of these species. Each of these compounds could be crystallised and characterised by X-ray crystallography, $^{31}P\{^1H\}$, $^{13}C\{^1H\}$ and ^1H NMR spectroscopy, mass spectrometry and IR spectroscopy, as well as ^{77}Se NMR spectroscopy where appropriate.

The synthesis of trimesitylphosphine was by far and away the most difficult and thus least successful synthesis of the precursors, however once formed, $PMes_3$ reacted well with sulfur and H_2O_2 to give the expected and desired products in moderate to high yields.

The trimesitylphosphine species were shown to be very sterically hindered, wherein the equivalent methyl groups in the *ortho* position are split into two broad

singlets in the ^{1}H NMR and broad doublets in the ^{13}C NMR spectra. These signals could be sharpened to the expected peaks by heating the NMR sample to 70 °C.

It could be seen that the geometries of the sulfides and selenides of $PMes_2Ph$ and $PMesPh_2$ are practically identical in the crystal structures, with the torsion angles of each ring being within 2.2° of each other, whilst across the series from Mes_3 to Mes_2Ph to $MesPh_2$ the geometry and torsion angles vary greatly. The trimesitylphosphines are the most propeller-like of the molecules, as they require the most order to accommodate the sheer size of the mesityl rings. In contrast, the diphenylmesitylphosphines have a much less symmetrical geometry, with the mesityl rings having torsion angles of close to 90° and the phenyl rings close to 0°.

It is clear from this line of investigations, that the trimesitylphosphine is ligand is too crowded to be used in reactions with platinum centres with this model. This is confirmed, as we see no mono-substituted complexes formed and no reaction with selenium is recorded Further work on this topic would involve the synthesis of tolyl or xylyl phosphines, with the view of also reacting these with $Pt(cod)Cl_2$ and $K_2[PtCl_4]$ to synthesise other bulky systems for complexation. Optimisation of the synthesis of the *trans*-Pt complex should be performed, improving the method and thus the yield. And then the follow up chemistry should be investigated.

4.4 Experimental

4.4.1 **Preparation of Trimesitylphosphine**[98]

Magnesium turnings (2.50 g, 0.10 mol) were placed in a dry three-necked flask and purged with nitrogen with stirring. Dry THF (20 mL) was added followed by dried bromomesitylene (5.01 g, 0.025 mol) with continuous stirring. Two crystals of iodine were added to the mixture to aid the reaction starting, turning the solution brown. A solution of bromomesitylene (13.90 g, 0.07 mol) in dry THF (40 mL) was then added dropwise, maintaining a gentle reflux. When the addition was almost complete, the vessel was heated to reflux and maintained at this temperature for a further hour and a quarter, and then a further 20 mL of THF was added. The clear solution was left to stand, then cooled to 0 °C. A solution of trichlorophosphine (4.08 g, 0.03 mol) in THF (20 mL) was added dropwise to the Grignard with vigorous stirring. The mixture was then warmed to room temperature and poured into a solution of ice-cold 1 M H_2SO_4 with vigorous stirring. The solution was extracted with diethyl ether (2 x 50 mL portions) and then treated with solid sodium hydrogen carbonate (~ 5 g). After filtering the resultant solution was washed with water (50 mL) and concentrated brine solution (50 mL). The solution was dried over sodium sulfate, filtered and the solvent evaporated under reduced pressure. The resulting white powder was recrystallised from ethanol.
Yield: 20% ($^{31}P\{^1H\}$ NMR)

$^{31}P\{^1H\}$ NMR: (109.4 MHz, $CDCl_3$, H_3PO_4) (ppm) δ_P = -35.88.

4.4.2 **Preparation of Dimesitylphenylphosphine**[98]

Magnesium turnings (2.51 g, 0.10 mol) were placed in a dry three-necked flask and purged with nitrogen with stirring. Dry THF (20 mL) was added followed by dried bromomesitylene (5.00 g, 0.03 mol) with continuous stirring. Two crystals of iodine were added to the mixture to aid the reaction starting, resulting in a brown solution. A solution of bromomesitylene (13.88 g, 0.07 mol) in dry THF (40 mL) was then added

dropwise, maintaining a gentle reflux. When the addition was almost complete, the colourless solution was heated to reflux and maintained at this temperature for a further hour and a quarter, and then a further 20 mL of THF was added. The reaction was left to stand, then cooled to 0 °C. A solution of dichlorophenylphosphine (8.05 g, 0.05 mol) in THF (20 mL) was added dropwise to the Grignard with vigorous stirring. The mixture was then warmed to room temperature and poured into a solution of ice-cold 1 M H_2SO_4 with vigorous stirring, turning the clear solution white. The solution was extracted with diethyl ether (2 x 50 mL portions) and then treated with solid sodium hydrogen carbonate (~ 5 g). After filtering the resultant solution was washed with water (50 mL) and concentrated brine solution (50 mL). The solution was dried over sodium sulfate, filtered and the solvent evaporated off under reduced pressure. On standing in the fridge the resulting oil yielded off-white crystals.
Yield: 9.53 g, 56%.

$^{31}P\{^{1}H\}$ NMR: (109.4 MHz, $CDCl_3$, H_3PO_4) (ppm) δ_P = -21.85.

4.4.3 **Preparation of Mesityldiphenylphosphine[98]**

Magnesium turnings (2.52 g, 0.10 mol) were placed in a dry three-necked flask and purged with nitrogen with stirring. Dry THF (20 mL) was added followed by dried bromomesitylene (5.02 g, 0.03 mol) with continuous stirring. A crystal of iodine was added to the mixture to aid the reaction starting, yielding an orange-brown solution. A solution of bromomesitylene (13.91 g, 0.07 mol) in dry THF (40 mL) was then added dropwise, maintaining a gentle reflux. When the addition was almost complete, the pale orange solution was heated to reflux and maintained at this temperature for a further hour and a quarter, and then a further 20 mL of THF was added. The reaction was left to stand, then cooled to 0 °C. A solution of chlorodiphenylphosphine (17.60 g, 0.08 mol) in THF (20 mL) was added dropwise to the Grignard with vigorous stirring. The mixture was then warmed to room temperature and poured into a solution of ice-cold 1 M H_2SO_4 with vigorous stirring. The solution was extracted with diethyl ether (2 x 50 mL portions) and then treated with solid sodium hydrogen carbonate (~ 5 g). After filtering the resultant solution was washed with water (50 mL) and concentrated brine

solution (50 mL). The solution was dried over sodium sulfate, filtered and the solvent evaporated off under reduced pressure. The resulting off-white oil could be used without further purification. On standing over time, near to colourless crystals formed. Yield: 11.76 g, 48%.

$^{31}P\{^{1}H\}$ NMR: (109.4 MHz, $CDCl_3$, H_3PO_4) (ppm) δ_P = -16.08.

4.4.4 Synthesis of Trimesitylphosphine Sulfide

Trimesitylphosphine (1.01 g, 2.60 mmol) was dissolved in toluene. Sulfur (0.20 g, 6.20 mmol) was added and the mixture was stirred for 4 hours at 60 °C. The pale yellow mixture was then filtered and the solvent evaporated off under reduced pressure. The resulting off-white powder was then redissolved in toluene and purified by column chromatography whilst being monitored by TLC. The fractions containing the product were recombined and the toluene removed once more. The resulting precipitate was then redissolved in hexane and layered with diethyl ether, yielding colourless crystals. Yield: 0.87 g, 80%.

^{1}H NMR (295 K): (270 MHz, $CDCl_3$, TMS) (ppm) δ_H = 6.83 (broad d, $^{4}J_{H\text{-}P}$ = 33 Hz, 6H, *m*-H), 2.60 (bs, *o*-CH_3), 2.25 (s, 9H, *p*-CH_3) and 1.56 (bs, *o*-CH_3).
^{1}H NMR (343 K): (270 MHz, C_6D_6, TMS) (ppm) δ_H = 6.67 (d, $^{4}J_{H\text{-}P}$ = 3.57 Hz, 6H, *m*-H), 2.43 (bs, 12H, *o*-CH_3), 2.01 (s, 9H, *p*-CH_3).

$^{13}C\{^{1}H\}$ NMR (295 K): (67.9 MHz, $CDCl_3$, TMS) (ppm) δ_C = 140.49 (d, $^{4}J_{C\text{-}P}$ = 3.11 Hz, *p*-C), 132.88 (d, $^{1}J_{C\text{-}P}$ = 77.0 Hz, C-P), 131.94 (very broad d, *o*-C), 128.73 (broad d, $^{3}J_{C\text{-}P}$ = 55 Hz, *m*-C), 25.32 (very broad d, *o*-CH_3) and 20.94 (s, *p*-CH_3).
$^{13}C\{^{1}H\}$ NMR (343 K): (67.9 MHz, C_6D_6, TMS) (ppm) δ_C = 131.62 (d, $^{3}J_{C\text{-}P}$ = 13.5 Hz, *m*-C), 24.99 (s, *o*-CH_3) and 20.30 (s, *p*-CH_3).

$^{31}P\{^{1}H\}$ NMR: (109.4 MHz, $CDCl_3$, H_3PO_4) (ppm) δ_P = 33.21 ($^{1}J_{P\text{-}C}$ = 77.1 Hz).

EA: Calculated for $C_{27}H_{33}SP.H_2O$: C: 73.94%, H: 8.04%. Found: C: 74.34%, H: 7.96%.

Mass TOF MS ES$^-$: *m/z* = 301.10 (M^- – Mes), 317.06 ($S{=}PMes_2O^-$) and 419.16 (M^-).

IR (KBr, cm^{-1}): 3020 (m), 2964 (m, C-H stretch), 2920 (s, C-H stretch), 2869 (m), 1603 (s), 1551 (m), 1442 (s), 1396 (m), 1379 (m), 1285 (m), 1261 (m), 1095 (m), 1024 (m), 853 (s), 802 (m) 726 (m), 643 (s, P=S), 631 (s), 572 (s) and 435 (s).

4.4.5 **Synthesis of Dimesitylphenylphosphine Sulfide**

Dimesitylphenylphosphine (0.75g, 2.16 mmol) was dissolved in toluene. Sulfur (0.21 g, 6.55 mmol) was added and the mixture was stirred overnight at room temperature. The pale yellow mixture was then filtered and the solvent evaporated off under reduced pressure. The off-white precipitate was then redissolved in hexane and layered with diethyl ether, yielding pale yellow crystals.
Yield: 0.78 g, 95%.

^{1}H NMR: (270 MHz, $CDCl_3$, TMS) (ppm) δ_H = 7.50-7.42 (m, 2H, Ar-H), 7.27-7.11 (m, 3H, Ar-H), 6.81 (d, $^4J_{H\text{-}P}$ = 3.87 Hz, *m*-H Mes), 2.25 (s, 6H, *p*-CH_3) and 2.15 (s, 12H, *o*-CH_3).

^{13}C{^{1}H} NMR: (67.9 MHz, $CDCl_3$, TMS) (ppm) δ_C = 140.93 (d, $^2J_{C\text{-}P}$ = 9.34 Hz, *o*-C Mes), 140.37 (d, $^4J_{C\text{-}P}$ = 2.07 Hz, *p*-C Mes), 135.61 (d, $^1J_{C\text{-}P}$ = 77.3 Hz, C-P Ph), 131.79 (d, $^3J_{C\text{-}P}$ = 12.5 Hz, *m*-C Mes), 131.58 (d, $^4J_{C\text{-}P}$ = 3.12 Hz, *p*-C Ph), 131.39 (d, $^1J_{C\text{-}P}$ = 82.0 Hz, C-P Mes), 131.21 (d, $^2J_{C\text{-}P}$ = 11.4 Hz, *o*-C Ph), 128.53 (d, $^3J_{C\text{-}P}$ = 12.5 Hz, *m*-C Ph), 24.59 (d, $^3J_{C\text{-}P}$ = 6.28 Hz, *o*-CH_3) and 20.97 (s, *p*-CH_3).

^{31}P{^{1}H} NMR: (109.4 MHz, $CDCl_3$, H_3PO_4) (ppm) δ_P = 37.35 ($^1J_{P\text{-}C}$ = 79.8 Hz).

EA: Calculated for $C_{24}H_{27}SP$: C: 76.16%, H: 7.19%. Found: C: 75.96%, H: 7.27%.

Mass TOF MS ES$^+$: *m/z* = 376.99 (M^+) and 400.89 (MNa^+).
Mass TOF MS ES$^-$: *m/z* = 274.85 ($S{=}PMesPhO^-$).

IR (KBr, cm^{-1}): 2963 (m, C-H), 2922 (s, C-H), 1601 (m), 1552 (m), 1436 (m, P-Ph), 1396 (m), 1382 (m), 1284 (w), 1261 (m), 1089 (m), 1027 (m), 849 (s), 800 (m) 746 (m), 702 (m), 662 (s, P=S), 627 (s), 568 (m) and 484 (m).

4.4.6 **Synthesis of Mesityldiphenylphosphine Sulfide**

Mesityldiphenylphosphine (1.00 g, 3.29 mmol) was dissolved in toluene. Sulfur (0.20 g, 6.21 mmol) was added and the pale yellow mixture was stirred overnight at room temperature. The mixture was then filtered and the solvent evaporated off under reduced pressure. The off-white precipitate was then redissolved in hexane and layered with diethyl ether, yielding colourless crystals.
Yield: 0.87 g, 79%.

^{1}H NMR: (270 MHz, $CDCl_3$, TMS) (ppm) δ_H = 8.02-7.93 (m, 4H, Ar-H), 7.49-7.34 (m, 6H, Ar-H), 6.82 (d, $^{4}J_{H\text{-}P}$ = 9.09 Hz, *m*-H Mes), 2.27 (s, 3H, *p*-CH_3) and 1.94 (s, 6H, *o*-CH_3).

^{13}C{^{1}H} NMR: (67.9 MHz, $CDCl_3$, TMS) (ppm) δ_C = 142.52 (d, $^{2}J_{C\text{-}P}$ = 10.4 Hz, *o*-C Mes), 141.16 (d, $^{4}J_{C\text{-}P}$ = 3.21 Hz, *p*-C Mes), 136.34 (d, $^{1}J_{C\text{-}P}$ = 82.0 Hz, C-P Ph), 131.41 (d, $^{3}J_{C\text{-}P}$ = 11.4 Hz, *m*-C Mes), 131.20 (d, $^{2}J_{C\text{-}P}$ = 10.4 Hz, *o*-C Ph), 130.87 (d, $^{4}J_{C\text{-}P}$ = 3.11 Hz, *p*-C Ph), 128.60 (d, $^{3}J_{C\text{-}P}$ = 125 Hz, *m*-C Ph), 126.97 (d, $^{1}J_{C\text{-}P}$ = 73.7 Hz, C-P Mes), 24.07 (d, $^{3}J_{C\text{-}P}$ = 5.19 Hz, *o*-CH_3) and 21.05 (s, *p*-CH_3).

^{31}P{^{1}H} NMR: (109.4 MHz, $CDCl_3$, H_3PO_4) (ppm) δ_P = 36.83 ($^{1}J_{P\text{-}C}$ = 82.2 Hz).

Mass TOF MS ES^{+}: *m/z* = 337.12 (M^{+}) and 359.08 (MNa^{+}).
Mass TOF MS ES^{-}: *m/z* = 232.92 ($S{=}PPh_2O^{-}$).

IR (KBr, cm^{-1}): 3052 (m), 2961 (m, C-H), 2912 (s, C-H), 1604 (m), 1436 (s, P-Ph), 1261 (m), 1091 (m), 1024 (s), 861 (m), 802 (m) 759 (m), 720 (m), 703 (s, P=S), 666 (s), 602 (s), 516 (m), 472 (m) and 426 (m).

4.4.7 **Synthesis of *trans*-Pt(PMesPh$_2$)$_2$Cl$_2$**

Potassium tetrachloroplatinate (0.20 g, 0.48 mmol) was dissolved in water (5 mL) at room temperature. To this, $PMesPh_2$ (0.51 g, 1.62 mmol) in dichloromethane (5 mL) was added with stirring. The orange mixture was left to stir for overnight and the resulting yellow solution was evaporated to dryness. The resulting pale yellow powder was washed with diethyl ether, toluene and hexane in that order and recrystallised from dichloromethane.
Yield: 0.10 g, 25 %.

^{1}H NMR: (500 MHz, $CDCl_3$, TMS) δ_H = 7.87-7.83 (m, 8H, *m*-H Ph), 7.40-7.37 (m, 4H, *p*-H Ph), 7.33-7.30 (m, 8H, *o*-H Ph), 6.89 (bs, 4H, *m*-H Mes), 2.33 (s, 12H, *o*-CH_3) and 2.31 (s, 6H, *p*-CH_3).

^{13}C{^{1}H} NMR: (126 MHz, $CDCl_3$, TMS) (ppm) δ_C = 142.84 (pt, *o*-C Mes)*, 139.99 (s, *p*-C Mes), 135.85 (pt, *m*-C Ph), 131.60 (dd, *i*-C-P Ph), 130.85 (pt, *m*-C Mes), 130.16 (s, *p*-C Ph), 127.68 (pt, *o*-C Ph), 123.51 (pt, *i*-C-P Mes), 25.12 (pt, *o*-CH_3) and 21.02 (s, *p*-CH_3). * No *J* couplings reported as only a pseudo triplet observed.

^{31}P{^{1}H} NMR: (109.4 MHz, $CDCl_3$, H_3PO_4) (ppm) δ_P = 10.92 ($^1J_{P\text{-}Pt}$ = 2585 Hz, $^1J_{P\text{-}C}$ = 28.2 Hz).

^{195}Pt{^{1}H} NMR: (58.1 MHz, $CDCl_3$) (ppm) δ = -5000.0 ($^1J_{Pt\text{-}P}$ = 2567 Hz).

EA: Calculated for $C_{42}H_{42}Cl_2P_2Pt$: C: 57.67%, H 4.84%. Found: C 57.82%, H 4.99%.

Mass TOF MS ES$^+$: *m/z* = 874.27 (M^+) and 802.10 ($Pt(PMesPh_2)_2^+$).

IR (KBr, cm^{-1}): 3051 (m), 2917 (w, C-H), 2854 (w, C-H), 1602 (m), 1479 (m), 1435 (s, P-Ph), 1400 (m),1377 (m), 1185 (m), 1092 (m), 1027 (m), 908 (m), 851 (m), 747 (m), 694 (s), 625 (s), 555 (s), 512 (m), 483 (m) and 469 (m).

4.4.8 **Synthesis of Dimesitylphenylphosphine Selenide**

Dimesitylphenylphosphine (0.50 g, 1.44 mmol) was dissolved in toluene. Selenium (0.51 g, 6.38 mmol) was added and the mixture was stirred for 4 hours at reflux. The mixture was then filtered and the solvent evaporated off under reduced pressure. The off-white precipitate was then redissolved in toluene and layered with diethyl ether, yielding colourless crystals.
Yield: 0.58 g, 95 %.

^{1}H NMR: (270 MHz, $CDCl_3$, TMS) (ppm) δ_H = 8.25 (m, 2H, Ar-H Ph), 7.47 (m, 3H, Ar-H Ph), 6.84 (d, $^{4}J_{H\text{-}P}$ = 4.12 Hz, 4H, *m*-CH Mes), 2.30 (s, 6H, *p*-CH_3) and 2.20 (s, 12H, *o*-CH_3).

^{13}C{^{1}H} NMR: (67.9 MHz, $CDCl_3$, TMS) (ppm) δ_C = 140.80 (d, $^{2}J_{C\text{-}P}$ = 9.65 Hz, *o*-C Mes), 140.38 (d, $^{4}J_{C\text{-}P}$ = 2.68 Hz, *p*-C Mes), 133.44 (d, $^{1}J_{C\text{-}P}$ = 67.2 Hz, C-P Ph), 131.79 (d, $^{3}J_{C\text{-}P}$ = 11.0 Hz, *m*-C Mes), 131.59 (d, $^{4}J_{C\text{-}P}$ = 2.80 Hz, *p*-C Ph), 131.15 (d, $^{2}J_{C\text{-}P}$ = 11.2 Hz, *o*-C Ph), 129.70 (d, $^{1}J_{C\text{-}P}$ = 73.3 Hz, C-P Mes), 128.43 (d, $^{3}J_{C\text{-}P}$ = 12.4 Hz, *m*-C Ph), 24.64 (d, $^{3}J_{C\text{-}P}$ = 5.72 Hz, *o*-CH_3) and 20.85 (s, *p*-CH_3).

^{31}P{^{1}H} NMR: (109.4 MHz, $CDCl_3$, H_3PO_4) (ppm) δ_P = 20.84 ($^{1}J_{P\text{-}Se}$ = 694.9 Hz, $^{1}J_{P\text{-}C}$ = 73.5 Hz).

^{77}Se{^{1}H} NMR: (51.5 MHz, $CDCl_3$) (ppm) δ_{Se} = -83.29 (d, $J_{Se\text{-}P}$ = 694 Hz).

EA: Calculated for $C_{24}H_{27}PSe$: C: 67.76%, H: 6.40%. Found: C: 67.83%, H: 6.49%.

Mass TOF MS ES^{+}: *m/z* = 449.01 (MNa^{+}).
Mass TOF MS ES^{-}: *m/z* = 322.94 ($Se{=}PMesPhO^{-}$).

IR (KBr, cm^{-1}): 2963 (m, C-H), 2925 (s, C-H), 2871 (s), 1602 (m), 1446 (s), 1435 (s, P-Ph), 1399 (m), 1085 (m), 1027 (m), 853 (m), 743 (m), 690 (s), 626 (s), 574 (s), 562 (s, P=Se), 517 (m), 489 (s) and 445 (s).

4.4.9 **Synthesis of Mesityldiphenylphosphine Selenide**

Mesityldiphenylphosphine (0.50 g, 1.64 mmol) was dissolved in toluene. Selenium (0.50 g, 6.26 mmol) was added and the mixture was stirred for 4 hours at reflux. The mixture was then filtered and the solvent evaporated off under reduced pressure. The precipitate was then redissolved in toluene and layered with diethyl ether. Yield: 0.59 g, 93 %.

^{1}H NMR: (500 MHz, $CDCl_3$, TMS) (ppm) δ_H = 8.07-7.95 (m, 4H, Ar-H Ph), 7.41-7.32 (m, 6H, Ar-H Ph), 6.83 (d, $^{4}J_{H-P}$ = 4.11 Hz, 2H, *m*-CH Mes), 2.28 (s, 3H, *p*-CH_3) and 1.92 (s, 6H, *o*-CH_3).

^{13}C{^{1}H} NMR: (126 MHz, $CDCl_3$, TMS) (ppm) δ_C = 142.25 (d, $^{2}J_{C-P}$ = 10.4 Hz, *o*-C Mes), 141.29 (d, $^{4}J_{C-P}$ = 5.22 Hz, *p*-C Mes), 134.57 (d, $^{1}J_{C-P}$ = 77.7 Hz, C-P Ph), 131.78 (d, $^{3}J_{C-P}$ = 10.4 Hz, *m*-C Mes), 131.56 (d, $^{2}J_{C-P}$ = 11.4 Hz, *o*-C Ph), 131.01 (d, $^{4}J_{C-P}$ = 3.11 Hz, *p*-C Ph), 128.65 (d, $^{3}J_{C-P}$ = 12.7 Hz, *m*-C Ph), 126.58 (d, $^{1}J_{C-P}$ = 79.9 Hz, C-P Mes), 24.04 (d, $^{3}J_{C-P}$ = 6.23 Hz, *o*-CH_3) and 21.05 (s, *p*-CH_3).

^{31}P{^{1}H} NMR: (109.4 MHz, $CDCl_3$, H_3PO_4) (ppm) δ_P = 28.16 ($^{1}J_{P-Se}$ = 725 Hz, $^{1}J_{P-C}$ = 75.1 Hz).

^{77}Se{^{1}H} NMR: (51.5 MHz, $CDCl_3$) (ppm) δ_{Se} = -318.66 (d, J_{Se-P} = 725 Hz).

EA: Calculated for $C_{24}H_{27}PSe$: C: 65.80%, H: 5.52%. Found: C: 65.63%, H: 5.70%.

Mass TOF MS ES^{+}: *m/z* = 407.07 (MNa^{+}) and 789.15 ($2M + Na^{+}$).

IR (KBr, cm^{-1}): 3053 (m), 2961 (m, C-H), 2926 (m, C-H), 1602 (m), 1479 (s), 1434 (s, P-Ph), 1403 (m), 1261 (m), 1090 (m), 1025 (m), 860 (m), 801 (m), 758 (m), 698 (s), 633 (s), 574 (s), 555 (s, P=Se), 530 (s), 507 (s), 469 (m) and 421 (m).

4.4.10 **Synthesis of Trimesitylphosphine Oxide[112]**

Trimesitylphosphine (1.00 g, 2.58 mmol) was dissolved in acetone (10 mL) and excess H_2O_2 (3 mL) was added dropwise and then stirred at room temperature until the mixture went cloudy. The solvent was removed under reduced pressure and the resulting white precipitate was recrystallised from acetone, yielding colourless crystals. Yield: 1.04 g, 100%.

^{1}H NMR: (270 MHz, $CDCl_3$, TMS) (ppm) δ_H = 6.86 (d, $^{4}J_{H\text{-}P}$ = 4.13 Hz, 6H, *m*-CH Mes), 2.36 (s, 18H, *o*-CH_3) and 2.27 (s, 9H, *p*-CH_3).

^{13}C{^{1}H} NMR: (67 MHz, $CDCl_3$, TMS) (ppm) δ_C = 141.95 (d, $^{2}J_{C\text{-}P}$ = 11.4 Hz, *o*-C), 141.77 (d, $^{4}J_{C\text{-}P}$ = 3.12 Hz, *p*-C), 130.80 (d, $^{3}J_{C\text{-}P}$ = 11.4 Hz, *m*-C), 124.42 (d, $^{1}J_{C\text{-}P}$ = 102.8 Hz, C-P), 22.57 (d, $^{3}J_{C\text{-}P}$ = 4.15 Hz, *o*-CH_3) and 20.67 (s, *p*-CH_3).

^{31}P{^{1}H} NMR: (109.4 MHz, $CDCl_3$, H_3PO_4) (ppm) δ_P = 31.82 ($^{1}J_{P\text{-}C}$ = 98.6 Hz).

EA: Calculated for $C_{27}H_{33}PO.C_3H_{10}O_5$: C: 67.90%, H: 8.17%. Found: C: 67.18%, H: 8.13%.

Mass TOF MS ES^{+}: *m/z* = 405.13 (M^+), 427.05 (MNa^+), 595.05 ($2MNa^+$ – 2Mes), 713.12 ($2MNa^+$ – Mes) and 831.25 ($2MNa^+$).
Mass TOF MS ES^{-}: *m/z* = 301.01 ($O{=}PMes_2O^-$) and 259.04 ($O{=}PMesPhO^-$).

IR (KBr, cm^{-1}): 3270 (s, O-H), 2941 (m), 2922 (m), 2889 (m), 1604 (m), 1556 (w), 1452 (s, P-Ph), 1409 (m), 1368 (m), 1258 (m), 1140 (s, P=O), 1084 (m), 1065 (w), 1038 (m), 985 (w), 869 (m), 838 (s), 646 (s), 561 (m), 517 (w), 446 (m) and 426 (m).
*O-H present from solvent molecule in crystal structure.

4.4.11 **Synthesis of Dimesitylphenylphosphine Oxide**

Dimesitylphenylphosphine (1.00 g, 2.89 mmol) was dissolved in acetone (10 mL) and excess H_2O_2 (3 mL) was added dropwise and then stirred at room temperature until the mixture went cloudy. The mixture was filtered and allowed to stand allowing the residual powder to dry in air. The powder was then dissolved in acetone and the solvent allowed to slowly evaporate off, yielding large colourless needle crystals.
Yield: 1.05 g, 100%.

^{1}H NMR: (500 MHz, $CDCl_3$, TMS) (ppm) δ_H = 8.25-8.20 (m, 1H, Ar-H Ph), 7.59-7.49 (m, 4H, Ar-H Ph), 6.88 (d, $^{4}J_{H\text{-}P}$ = 3.47 Hz, 4H, *m*-CH Mes), 2.30 (s, 6H, *p*-CH_3) and 2.12 (s, 12H, *o*-CH_3).

^{13}C{^{1}H} NMR: (126 MHz, $CDCl_3$, TMS) (ppm) δ_C = 141.94 (d, $^{2}J_{C\text{-}P}$ = 10.2 Hz, *o*-C Mes), 141.83 (d, $^{4}J_{C\text{-}P}$ = 2.31 Hz, *p*-C Mes), 135.25 (d, $^{1}J_{C\text{-}P}$ = 99.0 Hz, C-P Ph), 132.37 (d, $^{4}J_{C\text{-}P}$ = 2.12 Hz, *p*-C Ph), 131.44 (d, $^{3}J_{C\text{-}P}$ = 11.2 Hz, *m*-C Mes), 129.11 (d, $^{3}J_{C\text{-}P}$ = 11.4 Hz, *m*-C Ph), 128.83 (d, $^{2}J_{C\text{-}P}$ = 9.34 Hz, *o*-C Ph), 129.08 (d, $^{1}J_{C\text{-}P}$ = 99.2 Hz, C-P Mes), 23.47 (d, $^{3}J_{C\text{-}P}$ = 4.23 Hz, *o*-CH_3) and 21.07 (s, *p*-CH_3).

^{31}P{^{1}H} NMR: (109.4 MHz, $CDCl_3$, H_3PO_4) (ppm) δ_P = 34.99 ($^{1}J_{P\text{-}C}$ = 100.9 Hz).

EA: Calculated for $C_{24}H_{27}PO.C_3H_8O_4$: C: 68.92%, H: 7.50%. Found: C: 68.49%, H: 7.23%.

Mass TOF MS ES^{+}: *m/z* = 363.09 (M^+), 384.99 (MNa^+), 571.15($2M^+ - 2Ph$), 671.24 ($2M^+ - Ph$) and 747.00 ($2MNa^+$).
Mass TOF MS ES^{-}: *m/z* = 301.08 ($O{=}PMes_2O^-$).

IR (KBr, cm^{-1}): 3244 (s, O-H), 2972 (m, C-H), 2937 (m, C-H), 2896 (m), 1603 (m), 1553 (m), 1458 (m), 1444 (s, P-Ph), 1402 (m), 1375 (m), 1255 (w), 1203 (w), 1134 (s, P=O), 1106 (m), 1071 (w), 1029 (w), 999 (w), 865 (m), 753 (m), 695 (s), 645 (s), 570 (m), 517 (m), 499 (m) and 455 (m). *O-H present from solvent molecule in crystal structure.

4.4.12 **Synthesis of Mesityldiphenylphosphine Oxide**

Mesityldiphenylphosphine (1.01 g, 3.29 mmol) was dissolved in acetone (10 mL) and excess H_2O_2 (3 mL) was added dropwise and then stirred at room temperature until the mixture went cloudy. The solution was allowed to stand for 10 minutes in which large white crystals formed.
Yield: 1.03 g, 99 %.

^{1}H NMR: (500 MHz, $CDCl_3$, TMS) (ppm) δ_H = 7.66-7.57 (m, 4H, Ar-H Ph), 7.51-7.35 (m, 6H, Ar-H Ph), 6.85 (d, $^{4}J_{H-P}$ = 3.86 Hz, 2H, *m*-CH Mes), 2.26 (s, 3H, *p*-CH_3) and 2.07 (s, 6H, *o*-CH_3).

^{13}C{^{1}H} NMR: (126 MHz, $CDCl_3$, TMS) (ppm) δ_C = 143.56 (d, $^{2}J_{C-P}$ = 10.4 Hz, *o*-C Mes), 142.16 (d, $^{4}J_{C-P}$ = 3.11 Hz, *p*-C Mes), 134.98 (d, $^{1}J_{C-P}$ = 102.8 Hz, C-P Ph), 131.81 (d, $^{3}J_{C-P}$ = 2.08 Hz, *p*-C Ph), 131.64 (d, $^{2}J_{C-P}$ = 9.34 Hz, *o*-C Ph), 131.26 (d, $^{4}J_{C-P}$ = 11.4 Hz, *m*-C Mes), 128.82 (d, $^{3}J_{C-P}$ = 12.5 Hz, *m*-C Ph), 124.91 (d, $^{1}J_{C-P}$ = 103.8 Hz, C-P Mes), 24.10 (d, $^{3}J_{C-P}$ = 4.15 Hz, *o*-CH_3) and 21.15 (s, *p*-CH_3).

^{31}P{^{1}H} NMR: (109.4 MHz, $CDCl_3$, H_3PO_4) (ppm) δ_P = 32.41 ($^{1}J_{P-C}$ = 103.3 Hz).

EA: Calculated for $C_{21}H_{21}PO.H_2O_2$: C: 71.17%, H: 6.54%. Found: C: 71.76%, H: 6.75%.

Mass TOF MS ES^{+}: *m/z* = 321.01 (M^+), 343.02 (MNa^+), 508.09 ($2MNa^+$ – 2Ph), 662.93 ($2MNa^+$) and 983.18 ($3MNa^+$).
Mass TOF MS ES^{-}: *m/z* = 216.96 ($O{=}PPh_2O^-$) and 259.03 ($O{=}PMesPhO^-$).

IR (KBr, cm^{-1}): 3286 (s, O-H), 2985 (m, C-H), 2947 (m, C-H), 2906 (m), 1605 (m), 1440 (s, P-Ph), 1389 (m), 1151 (s, P=O), 1100 (m), 1063 (w), 1026 (w), 997 (w), 859 (m), 761 (m), 699 (s), 629 (s) 566 (m), 523 (m) and 442 (m). *O-H present from solvent molecule in crystal structure.

5. Reactions of Woollins' Reagent

5.1 Introduction

As mentioned in Section 1.3.5.1, Woollins' Reagent is a versatile selenation reagent, which not only exchanges a selenium atom for an oxygen atom, but can also form interesting heterocycles. With this is mind, it was of interest to investigate the reactions between Woollins' Reagent and suitable inorganic moieties. The simplest of these are the metal carbonyls, starting with the single centred species, such as $Cr(CO)_6$, $Mo(CO)_6$ and $W(CO)_6$. Whilst these compounds did react, the products were difficult to isolate and so the next step was to explore carbonyl complexes with labile ligands to see if this altered the reactivity of the educts or the type of products acquired. It was found that the norbornadiene ligand was not the best choice, as *WR* reacts with the leaving group, as opposed to the metal centre. The next reaction performed was with a metal carbonyl halide, which formed an interesting inorganic cage and these species appeared to be a possible starting point for a range of complexes, however attempts to synthesise related compounds all proved unsuccessful.

Metal chlorides were also reacted with Woollins' Reagent as a proposed route to new inorganic materials. The products of these syntheses, were found to be insoluble and as such characterisation was impossible.

The reaction of Woollins' Reagent and ferrocene derivatives proved slightly more fruitful and the characterisation of some novel complexes was achieved.

5.2 Discussion

5.2.1 **Metal Carbonyl Reactions**

Woollins' Reagent was reacted with the metal carbonyls of Group 6 in the Periodic Table (M = Cr (**5.1**), Mo (**5.2**), W (**5.3**)) in a toluene/THF mixture over night at 80 °C. These metal carbonyls were chosen as it was postulated that they should only react with Woollins' Reagent *via* two possible pathways. The reaction would either result in a displacement of a CO ligand, or a reaction with the CO moiety would occur. The latter of which is unlikely due to the high bond strength of the C≡O. The reaction mixtures were then filtered and evaporated to dryness, yielding a green oil for the chromium compound, a brown oil for the molybdenum compound and an orange oil for the tungsten species.

It was found that all of the $M(CO)_6$ reaction products exhibited similar $^{31}P\{^1H\}$ NMR spectra: a singlet at ~ 74 ppm surrounded by two pairs of satellites, suggesting a product containing a phosphorus atom with two inequivalent selenium atoms attached to it. The magnitude of the coupling constants of these satellites suggest that one of the selenium atoms is singly bonded, with a $^1J_{P\text{-}Se}$ value of 437 Hz whilst the other is a terminal (P=Se) selenium, where $^1J_{P\text{-}Se}$ = 836 Hz. The similarity of these NMR spectra suggested that the metal coupling has little or no effect on the chemical shift of the phosphorus atom. The ^1H and $^{13}C\{^1H\}$ NMR spectra were run, however the results were affected by the products being air sensitive to the extent that the correct information could not be elucidated and the product could not be purified further. Additionally, the crystallisation to obtain a pure product was not successful.

It was postulated that the products were oils due to residual toluene in the product and as such they were washed with small amounts of hexane to help extraction. This technique only worked on the chromium compound and as such only the infrared spectrum of the chromium complex could be run. The spectrum shows the metal-carbonyl stretch at 2000 cm^{-1}, but is much weaker than that seen for the starting material. It was found that on exposure to air, the products decompose to a dark red

colour, which has been tenuously attributed to Woollins' Reagent or red selenium, however this was not proven.

By far and away the largest peaks in the mass spectrum for the chromium complex come at *m/z* = 552.97 and 574.96 (Figure 5.1), a difference of 22 which corresponds to M^+ and MNa^+. Selenium has a very obvious pattern in the mass spectrum, as it has 6 different natural isotopes: ^{74}Se, ^{76}Se, ^{77}Se, ^{78}Se, ^{80}Se and ^{82}Se, of which ^{80}Se is the most abundant. From the pattern of the signals we can confirm that there are two selenium atoms in the product.

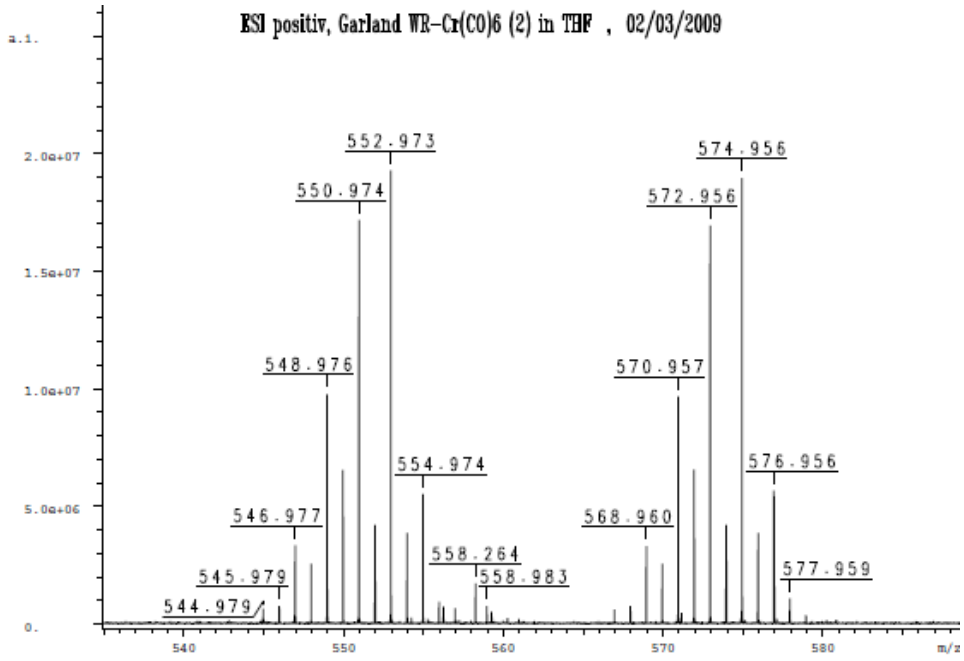

Figure 5.1: Mass spectrum of (**5.1**)

The mass peak *m/z* suggests a product containing a chromium centre bound to half a Woollins' Reagent molecule, with five of its carbonyl groups still attached and a coordinated toluene molecule. The formation of an arene product would also substantiate the difficulty in crystallising the products.

Evidence of the analogous molybdenum complex being formed was not found in the mass spectrum, as the peaks do not demonstrate the expected isotope pattern. The analogous tungsten peak is found in the mass spectrum, but in very small amounts. This could be attributed to the product decomposing within a matter of seconds, even when using dry solvents in a semi-inert atmosphere.

Exploratory reactions with further metal carbonyl complexes were attempted with more labile ligands to try to find a good starting point for these compounds. It had already been shown that Woollins' Reagent reacts with norbornadiene to form a mixture of heterocycles (Scheme 5.1).[113] It was thus of interest to look at reactions between Woollins' Reagent and metal carbonyl complexes containing norbornadiene as a ligand.

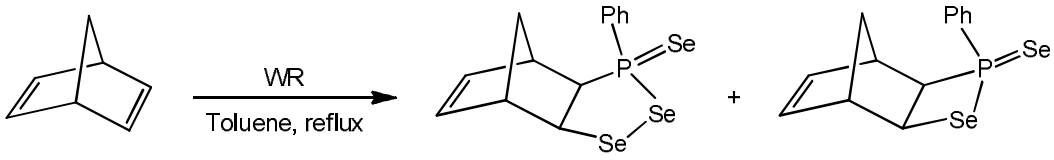

Scheme 5.1: Reaction of Woollins' Reagent with norbornadiene

The reaction of [Mo(nbd)CO_4] with *WR* was carried out in toluene under reflux. The only products visible in the $^{31}P\{^1H\}$ NMR spectrum were those seen for the products shown in Scheme 5.1 – a peak at δ_P = 29.5 ppm with two sets of selenium satellites. The other product was an insoluble solid which could not be identified by any of the normal methods: $^{31}P\{^1H\}$ NMR, IR or mass spectroscopy. This could suggest a metal carbonyl polymer, but this could not be confirmed even by powder diffraction.

The reaction of [Mo($N(CH_2CH_3)_3$)$(CO)_4$] with Woollins' Reagent at 80 °C in toluene produces a ^{31}P NMR spectrum exhibiting a singlet at δ_P = 122.2 ppm surrounded by selenium satellites with a coupling constant of $^1J_{P\text{-}Se}$ = 329 Hz and two doublets at 110.2 ppm and 88.5 ppm, each with a coupling constant of 66.1 Hz, suggesting a $J_{P\text{-}P}$ coupling. On reducing the reaction mixture, an oil was obtained which could not be crystallised from any of the attempted solvent systems or methods. Attempts to obtain the product as a solid also proved unfruitful and so an IR spectrum of the product could not be obtained to pinpoint the functional groups present in the product. The mass spectrum showed peaks contradicting the NMR data, namely no selenium was bound. The product was, however, very instable in air and so decomposition of the products is the suspected cause of this discrepancy. Since this research was carried out, we have reported the reaction of diethylamine with *WR*.[69] The chemical shift in the $^{31}P\{^1H\}$ NMR spectrum observed for this reaction is δ_P = 55.8 ppm, with a $^1J_{P\text{-}Se}$ coupling constant of 615 Hz, which does not support the idea of an interaction between *WR* and the amine ligand.

The reaction between Woollins' Reagent and $Na[MoCp(CO)_3]$ in toluene at reflux yields interesting patterns in its $^{31}P\{^1H\}$ NMR spectrum, showing a mixture of products. These products were shown to be highly air sensitive in that the reaction mixture discoloured from light yellow solution to a red-brown precipitate in five minutes after just a few seconds of exposure to air. It was suggested that there were too many side products in the reaction mixture to allow for crystallisation and so it was attempted to separate the products by inert column chromatography. This also proved unsuccessful, with the product decomposing in all attempted solvent systems. The decision was taken to move away from organic labile ligands and look to halides, as it was proposed this would narrow the possibilities for side reactions.

5.2.2 **Manganese Pentacarbonyl Bromide (5.4)**

The reaction between manganese pentacarbonyl bromide and Woollins' Reagent in toluene, at 80 °C, produced an orange solution, which gave orange-red crystals upon layering with hexane and storing at 2 °C. The compound could be characterised by $^{31}P\{^1H\}$, $^{13}C\{^1H\}$ and ^1H NMR spectroscopy, single crystal X-ray crystallography, mass spectrometry and IR spectroscopy. The X-ray diffraction of the compound (**5.4**) revealed the structure shown in Figure 5.2, with empirical formula $C_{24}H_{15}Mn_2O_6P_3Se_5$.

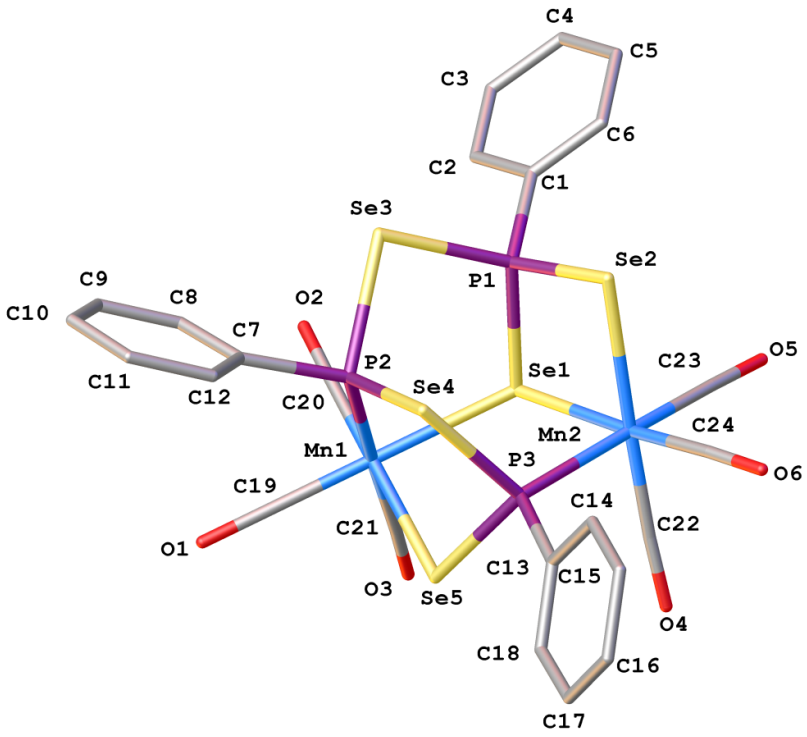

Figure 5.2: Crystal structure of $C_{24}H_{15}Mn_2O_6P_3Se_5$ with H atoms removed for clarity

The $^{31}P\{^1H\}$ NMR spectrum shows three distinct environments; two of which are seen between 175 and 178 ppm and correspond to the two phosphorus atoms (P(2) and P(3)) which are bonded to two selenium atoms and a manganese atom. The other phosphorus signal, which is shifted much further upfield at 55.9 ppm, is that of the third phosphorus atom (P(1)), which is surrounded by three selenium atoms.

All the peaks display selenium satellites, however these were too complex to readily assign coupling constants. In the $^{77}Se\{^1H\}$ NMR spectrum five discrete signals are present. The doublets of doublets at 705 and 490 ppm correspond to the selenium atoms attached to two phosphorus atoms, Se(3) and Se(4). The doublet at ~ -47 ppm is that of the selenium atom bonded to both Mn atoms, Se(1). The final two signals at 236 and 367 ppm are the selenium atoms attached to one phosphorus atom and one manganese atom, Se(2) and Se(5).

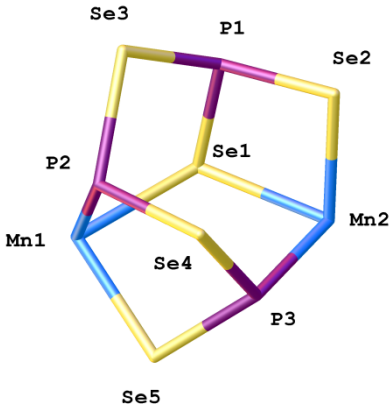

Figure 5.3: Central cage of the manganese structure with formula $Mn_2P_3Se_5$

In the crystal structure, the manganese atoms sit in slightly distorted octahedral environments, within which the angles between the carbonyls range from 90.63(12)° to 92.71(11)° for Mn (1) and 87.69(11)° to 92.65(11)° for Mn(2). **Figure 5.3** shows the central cage of the product, with all phenyl rings and carbonyls removed. The core consists of three five-membered rings, a four-membered ring and a seven-membered ring (Figure 5.4) in a cage which might be described as a doubly edge bridged cuboid.

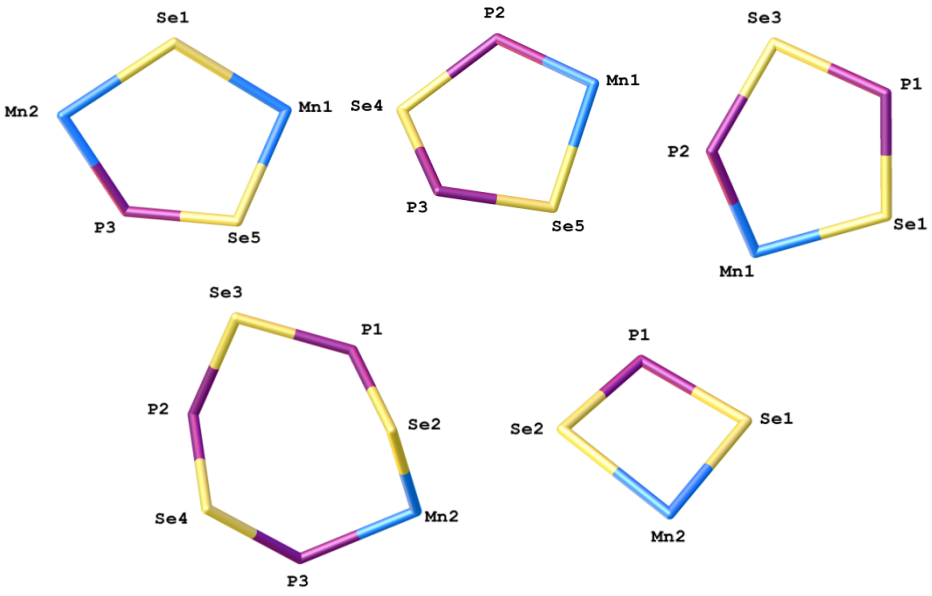

Figure 5.4: The rings within the manganese structure

Each ring is of interest because of the unique geometries of the component atoms. Each phosphorus atom sits in a pseudo-tetrahedral environment. The angles around P(1) are very different to those of P(2) and P(3), as this phosphorus atom does not bond to a manganese centre. The angles around the phosphorus atoms range from 101.75° to 115.13° for P(1), from 94.92° to 120.44° for P(2) and from 96.88° to 119.29° for P(3). The latter two show large distortions from the expected 109.5°, showing that the geometry of the complex is dominated by the manganese atoms. Of the three five-membered rings, two contain the same member atoms: two selenium atoms, two phosphorus atoms and a manganese atom. In the third ring, one of the phosphorus atoms has been replaced by a manganese atom. Each of the five-membered rings has a twist conformation, although no comparisons can be drawn between the angles within the rings.

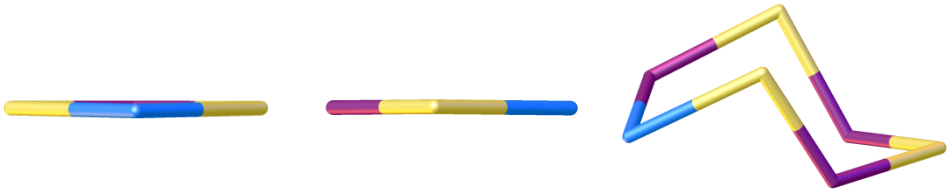

Figure 5.5: Geometries of the four and seven-membered rings within $C_{24}H_{15}Mn_2O_6P_3Se_5$

Interestingly the four-membered ring is planar, wherein the sum of the internal angles is 359.97°, with the angles between the member atoms ranging between 84.51° and 101.75°. The seven-membered ring adopts the chair form, similar to a sulfur S7 ring (Figure 5.5).

The Se-Mn bond lengths range from 2.4791(4) to 2.5415(5) Å. Se(1), which bridges the two Mn atoms has, at 2.5004(4) Å for Se(1)-Mn(1) and 2.5184(4) Å for Se(1)-Mn(1) slightly longer bonds than those of similar manganese carbonyl clusters in the literature.[114] Of the seven Se-P bonds, Se(4)-P(3) is the longest, at 2.3004(7) Å, whilst Se(2)-P(1) is the shortest at 2.1551(7) Å in length. The Se(4)-P(3) bond is thus much longer than the average P-Se bond (2.222 Å) and falls in the longest 5% of all known P-Se bonds. In structure (**5.4**) there are two Mn-P bonds: Mn(1)-P(2) and Mn(2)-P(3), which are 2.2916(8) Å and 2.3104(7) Å in length – slightly shorter than the average CCDC length (2.314 Å). Table 2.1 displays the bond lengths and angles for

compound (**5.4**), whilst further details of the crystal structure can be found in Appendix 16.

Table 5.4: Selected bond lengths and angles for $C_{24}H_{15}Mn_2O_6P_3Se_5$ (**5.4**).

Bond	Length (Å)	Atoms	Angle (°)
Se(1)-P(1)	2.2305(7)	C(1)-P(1)-Se(2)	114.36(9)
Se(1)-Mn(1)	2.5004(4)	C(1)-P(1)-Se(3)	102.61(9)
Se(1)-Mn(2)	2.5184(4)	Se(2)-P(1)-Se(3)	115.13(3)
Se(2)-P(1)	2.1551(7)	C(1)-P(1)-Se(1)	112.16(9)
Se(2)-Mn(2)	2.5415(5)	Se(2)-P(1)-Se(1)	101.75(3)
Se(3)-P(1)	2.2271(7)	Se(3)-P(1)-Se(1)	111.20(3)
Se(3)-P(2)	2.2972(7)	C(7)-P(2)-Se(4)	103.93(8)
Se(4)-P(2)	2.2441(7)	C(7)-P(2)-Mn(1)	120.44(8)
Se(4)-P(3)	2.3004(7)	Se(4)-P(2)-Mn(1)	117.74(3)
Se(5)-P(3)	2.2040(7)	C(7)-P(2)-Se(3)	94.92(8)
Se(5)-Mn(1)	2.4791(4)	Se(4)-P(2)-Se(3)	104.37(3)
Mn(1)-P(2)	2.2916(8)	Mn(1)-P(2)-Se(3)	112.12(3)
Mn(2)-P(3)	2.3104(7)	C(13)-P(3)-Se(5)	105.97(8)
		C(13)-P(3)-Se(4)	96.88(8)
		Se(5)-P(3)-Se(4)	102.10(3)
		C(13)-P(3)-Mn(2)	116.44(8)
		Se(5)-P(3)-Mn(2)	113.79(3)
		Se(4)-P(3)-Mn(2)	119.29(3)

5.2.3 **Metal Halides and Halogens**

Molecules of the form $M(E)Cl_x$, where M is a transition metal and E is a chalcogen (E = O, S, Se), have been of interest for quite a while as potential precursors for new materials and superconductors.[115] Rice *et al.*[116] demonstrated a route for the synthesis of the species containing oxygen and sulfur, but a successful and simple synthesis has never been achieved for $M(Se)Cl_x$ derivatives.

It was therefore postulated that Woollins' Reagent could provide a possible route to synthesising such species. On reacting a range of metal chlorides (M = In, Hf, Mo, W, Nb) with Woollins' Reagent in DCM at 35 °C, it was found that each of the $^{31}P\{^{1}H\}$ NMR spectra exhibited a single peak at ~ 55 ppm with selenium satellites ($^{1}J_{P\text{-}Se}$ = ~ 927 Hz) indicating the presence of the known phenylselenophosphonic dichloride, $PhP(Se)Cl_2$. This molecule is also produced as a byproduct in the synthesis of Woollins' Reagent with dichlorophenylphosphine.[50] It was postulated that the negatively charged selenium had been displaced from *WR* by two chlorides and had bonded to the transition metal centre. This hypothesis could not be proven, as the insoluble residues could not be recrystallised. Additionally, no further characterisation was possible *via* powder diffraction. Furthermore, it was found that, on leaving the Schlenk flask to stand at room temperature for *circa* 4 weeks, in just a small amount of solvent, red selenium platelets (Se_8) crystallised out of the mother liquor.

Gallium and aluminium chloride were also reacted with Woollins' Reagent in DCM at 35 °C. The products are, however, quite different, in that the chemical shift of the gallium product is shifted ~ 30 ppm downfield of the peak observed for $PhP(Se)Cl_2$ and the soluble phosphorus containing product for the aluminium reaction is located ~ 50 ppm upfield at 8.49 ppm in the $^{31}P\{^{1}H\}$ NMR spectrum. Both spectra show selenium satellites, with coupling constants of 156 Hz and 528 Hz respectively, making them much different in character to those of the above-mentioned transition metals. The previous products had a coupling constant of around 927 Hz, which is indicative of a strong P=Se double, whereas the 528 Hz coupling constant suggests a $^{1}J_{P\text{-}Se}$ coupling constant of a single bond. The 156 Hz coupling is suggestive of a ^{3}J coupling. Crystallisation of all of the products was attempted by concentrating the solution, layering, cooling and diffusion methods, all of which proved unsuccessful.

Following the reactions of the metal halides we were interested in looking at the reaction of Woollins' Reagent with the other halogens, to see if the corresponding $PhP(Se)X_2$ product could be synthesised. The $^{31}P\{^1H\}$ NMR spectrum of the reaction between bromine and Woollins' Reagent exhibits a promising signal at δ_P = -15.2 ppm, with a single set of selenium satellites visible around the main peak. The mass of the suggested compound is 347.8 g mol^{-1}, however ESI mass spectrometry of the product shows a major peak at M^+ = 341.9. A number of techniques for crystallisation were attempted, however no crystalline product was obtained.

Similarly in the reaction of iodine with Woollins' Reagent was carried out in toluene, yielding only one resonance, a broad peak, in the $^{31}P\{^1H\}$ NMR at δ_P = 70 ppm. The peak was not, however similar to that in the assumed chlorine and bromine analogues and exhibited no P-Se satellites. The reaction mixture was evaporated to dryness and analysed by ESI^+ mass spectrometry. There is a peak at m/z = 503.072 which could tentatively be assigned to $PhP(Se)Br_2$ with a sodium counter-ion and acetonitrile molecule; however this has a lower intensity (~20%). The three peaks with the highest intensity, 437.087 (100%), 577.091 (50%) and 651.112 (60%) all have isotope patterns which do not substantiate the presence of Se in the compound. This would then support the NMR data, however the product could not be crystallised, and so no X-ray data can be used to confirm the structure of this product.

5.3 Acetylferrocene and its Derivatives

5.3.1 **Acetylferrocene**

The reaction of acetylferrocene with Woollins' Reagent is more of a classic Woollins' Reagent reaction. It was not predicted that Woollins' Reagent would interact with the metal centre, but it was of interest as to whether a simple substitution reaction would occur or if a heterocycle would be synthesised. The reaction proceeded at room temperature and was crystallised by layering the reaction mixture with hexane. As most Woollins' Reagent syntheses of this type are performed in refluxing toluene, it would be of interest to change the reaction conditions and investigate the effect, if any, on the product.

In the $^{31}P\{^{1}H\}$ NMR spectrum, two peaks can be seen: one at δ_P = 97.7 ppm, a doublet, with a $^{2}J_{P\text{-}P}$ coupling constant of 20.4 Hz, surrounded by two sets of satellites with coupling constants of $^{1}J_{PA\text{-}Se1}$ = 419 Hz and $^{1}J_{PA=Se3}$ = 790 Hz, and the other at δ_P = 8.86 ppm, the corresponding doublet ($^{2}J_{P\text{-}P}$ = 20.4 Hz), with three sets of selenium satellites, $^{1}J_{Px\text{-}Se1}$ = 372 Hz, $^{1}J_{Px\text{-}Se2}$ = 412 Hz and $^{1}J_{Px=Se4}$ = 784 Hz. The largest coupling constants are caused by the P=Se double bonds having more electron density than the single P-Se bonds.

The $^{77}Se\{^{1}H\}$ NMR spectrum exhibits δ_{Se} peaks at 585.5 ppm (Se(2)), 475.9 ppm (Se(1)) and 131.0 ppm (Se(3) and Se(4)). The first two are observed to be doublets of doublets, which are split by $^{1}J_{P\text{-}Se}$ and $^{2}J_{P\text{-}Se}$ couplings. For Se(2) these are $^{1}J_{Px\text{-}Se}$ = 427 Hz and $^{2}J_{PA\text{-}Se}$ = 15.4 Hz and for Se(1) $^{1}J_{PA\text{-}Se}$ = 419 Hz and $^{1}J_{Px\text{-}Se}$ = 419 Hz. The peak much further upfield is that of Se(3) and Se(4), which have surprisingly the same chemical shift and a $^{1}J_{P=Se}$ coupling constant of 789 Hz.

In the IR spectrum, the presence of the peaks at 3050 and 2965 cm^{-1} show the aromatic C-H stretches from both the phenyl and Cp rings. The absence of the ν(C=O) at 1700 cm^{-1} shows that there is none of the original acetyl present. The product crystallises in space group P-1 and has the empirical formula $C_{22}H_{24}FeP_2Se_4.C_7H_8$ (see Figure 5.6).

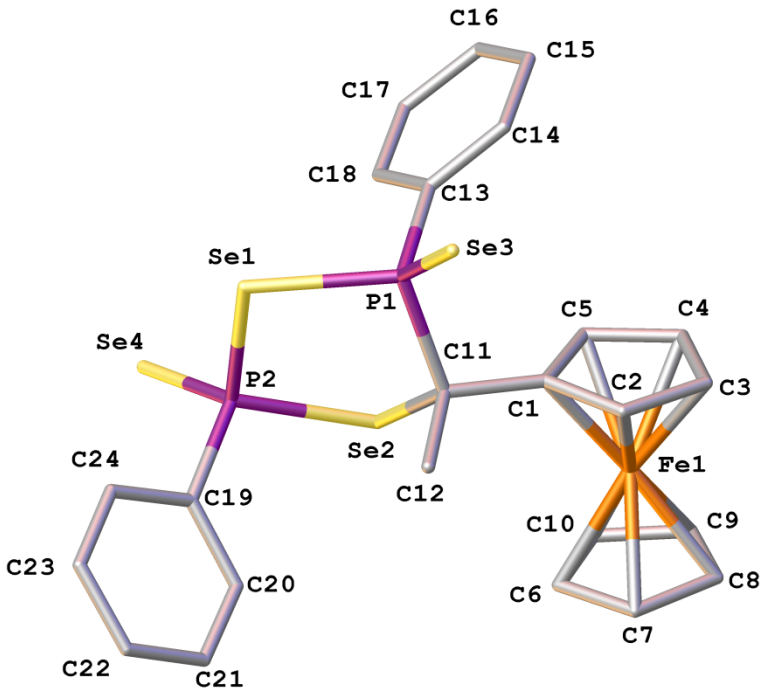

Figure 5.6: Product of the reaction of *WR* with acetylferrocene: $C_{22}H_{24}FeP_2Se_4.C_7H_8$ (**5.5**). Hydrogen atoms and solvent molecule have been omitted for clarity.

The phosphorus atoms and C(11) all sit in slightly distorted tetrahedral environments – the angles about P(1) range from 104.80(6) - 114.65(6)°, 103.57(7) - 115.15(2)° for P(2) and 106.67(13) - 112.89(15)° for C(11), demonstrating that C(11) experiences the least steric strain of the three. P(2), which experiences the largest strain, is bonded to two endocyclic selenium atoms and has one exocyclic P=Se bond. P(2)-Se(4), at 2.0996(5) Å, is longer than P(1)=Se(3) (2.0937(6) Å), although both are shorter than the average P=Se bond. At 2.2723(5) Å, P(2)-Se(1) is the longest of the P-Se bonds, which are all inequivalent. P(2)-Se(2) and P(1)-Se(1) are 2.2307(5) Å and 2.2682(5) Å, making all P-Se bonds above average (2.222 Å) in length.

The P-C bonds between the phosphorus atoms to the phenyl rings are, at 1.816(2) Å for P(1) and 1.817(2) Å for P(2), equivalent to one another. A summary of bond length and angles are found in Table 5.1, whilst further details of the crystal structure, can be found in the Appendix 17.

Table 5.1: Selected bond lengths and angles for $C_{22}H_{24}FeP_2Se_4$ (**5.5**).

Bond	Length (Å)	Atoms	Angle (°)
Se(1)-P(1)	2.2682(5)	P(1)-Se(1)-P(2)	98.305(19)
Se(1)-P(2)	2.2723(5)	C(11)-Se(2)-P(2)	99.20(5)
Se(2)-C(11)	1.9900(18)	C(13)-P(1)-C(11)	109.13(9)
Se(2)-P(2)	2.2307(5)	C(13)-P(1)-Se(3)	114.65(6)
Se(3)-P(1)	2.0937(6)	C(11)-P(1)-Se(3)	110.63(6)
Se(4)-P(2)	2.0996(5)	C(13)-P(1)-Se(1)	104.80(6)
P(1)-C(11)	1.8847(17)	C(11)-P(1)-Se(1)	104.84(6)
P(1)-C(13)	1.816(2)	Se(3)-P(1)-Se(1)	112.20(2)
P(2)-C(19)	1.817(2)	C(19)-P(2)-Se(4)	112.28(6)
		C(19)-P(2)-Se(2)	110.15(7)
		Se(4)-P(2)-Se(2)	111.02(3)
		C(19)-P(2)-Se(1)	103.57(7)
		Se(4)-P(2)-Se(1)	115.15(2)
		Se(2)-P(2)-Se(1)	104.15(2)

5.3.2 **Diacetylferrocene and Thioacetylferrocene**

The reaction of Woollins' Reagent with diacetylferrocene proceeds in a similar manner to that of acetylferrocene. It is performed at room temperature and the $^{31}P\{^{1}H\}$ NMR spectrum of the crude product shows identical peaks to (**5.5**) at 10.1 and 99.2 ppm, amongst other non-identifiable byproducts. The $^{2}J_{P\text{-}P}$ coupling constant for the doublets is similar at 19.8 Hz and selenium satellites can be observed around the main peaks. Crystallisation was attempted using a range of techniques, including layering with a selection of different solvents and diffusion of hexane, however no crystals could be obtained. The mass spectrum provided very little information about the product; none of the main peaks have the isotope pattern of a selenium containing compound. Column chromatography was attempted to separate the product from the byproducts, to aid crystallisation, however the product decomposed in the process and as such the ^{1}H and ^{13}C NMR were not run.

The reaction of thioacetylferrocene and Woollins' Reagent was also performed to see if it also reacted in the same manner. The $^{31}P\{^{1}H\}$ NMR spectrum of the crude product showed the same doublets as diacetyl- and acetylferrocene, however many other peaks were present in the spectrum and no identification of the byproducts could be made. What this does suggest is that the driving force and mode of action in these reactions is the same.

5.4 Lithiated Substrates

In the Hey-Hawkins group, much research has been carried out into carborane-containing ligands.[117, 118] In the general procedure, 1,2-*closo*-dicarbadodecaborane(12) is lithiated with *tert*-butyllithium and then reacted with a primary phosphine. This yields ligands with interesting electronic properties, owing to the carborane cluster. With this in mind, Woollins' Reagent was reacted with 1,2-dilithiodicarba-*closo*-dodecaborane(12) at 50 °C. On cooling, the orange reaction mixture was layered with hexane and stored at 2 °C. The colourless crystals that were obtained were the unexpected $C_{28}H_{42}Li_2O_4P_2Se_4$ molecule, compound (**5.6**) (Figure 5.7), wherein the Woollins' Reagent moiety acts as an isobidentate ligand.

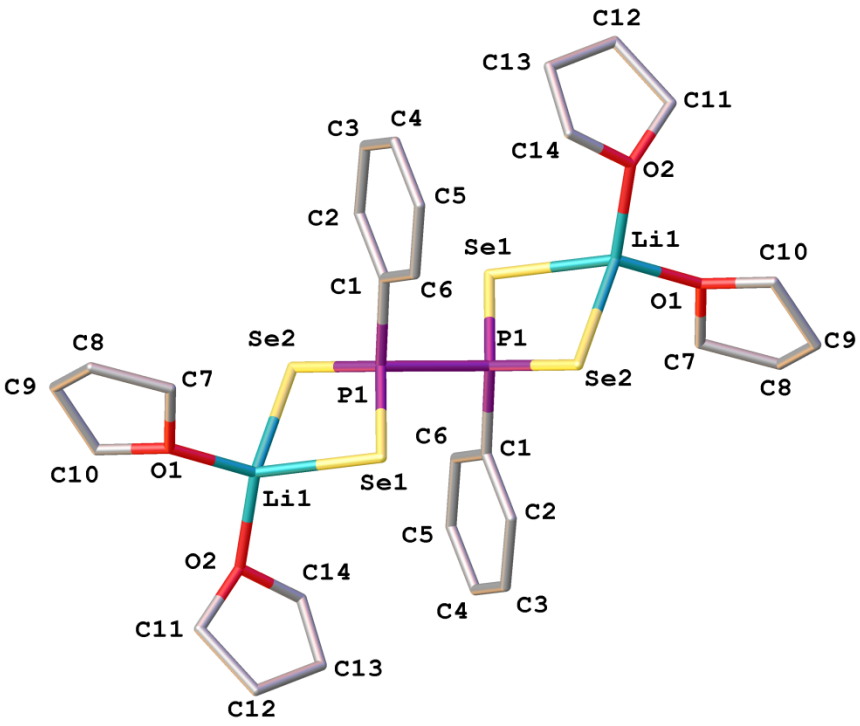

Figure 5.7: Crystal structure of $C_{28}H_{42}Li_2O_4P_2Se_4$ with hydrogen atoms omitted for clarity.

During the reaction, Woollins' Reagent appears to have dissociated into its two halves and then formed a P-P bond. The lithium centres are solvated by THF molecules. The angles around the phosphorus atoms are close to those expected in a tetrahedral environment. The P-P bond length is 2.2491(10) Å which is slightly longer than the

average (2.210 Å, CCDC), whilst Se(1)-Li(1) was found to be 2.576(5) Å and Se(1)-Li(2) 2.595(5) Å and as such are equivalent to one another.

Compared to the similar, recently reported bis(diselenophosphinate) molecule $(PhP\text{-}(Se)_2CH_2CH_2P(Se)_2Ph)Li_2(THF)_4$,[119] the P-Se bond lengths are slightly shorter at 2.1437(5) Å and 2.1453(5) Å for P(1)-Se(1) and P(1)-Se(2), respectively, compared to 2.1514 Å and 2.1508 Å. The angles within the P-Se-Li-Se ring add up to 361.25°, showing almost planarity within the ring (Figure 5.8).

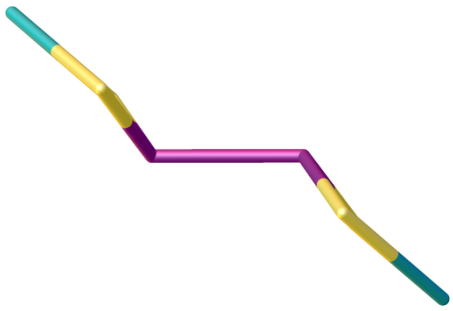

Figure 5.8: Geometry of $C_{28}H_{42}Li_2O_4P_2Se_4$.
Hydrogen atoms, phenyl and THF rings have been omitted for clarity

The reaction of 1,1'-dilithioferrocene with *WR* in toluene proceeds *via* an overnight reaction at room temperature and produces exactly the same unexpected crystal structure as the carborane cage. As both structures are aromatic, it is almost certainly the electronic properties that influence this behaviour. Both the rings of ferrocene and the cage of carborane obey Hückel's rule. The reactions between Woollins' Reagent and *n*-butyllithium or lithium metal do not yield the same product on reaction in the same manner and it is suggested that further work be performed into this topic. The bond lengths and angles of compound (**5.6**) are summarised in Table 5.2, whilst further crystallographic details can be found in Appendix 18.

Table 5.2: Selected bond lengths and angles for compound (**5.6**).

Bond	Length (Å)	Atoms	Angle (°)
Se(1)-P(1)	2.1437(5)	P(1)-Se(1)-Li(1)	77.30(10)
Se(1)-Li(1)	2.576(5)	P(1)-Se(2)-Li(1)	76.86(10)
Se(2)-P(1)	2.1453(5)	C(1)-P(1)-Se(1)	110.70(7)
Se(2)-Li(1)	2.595(5)	C(1)-P(1)-Se(2)	111.30(7)
P(1)-C(1)	1.821(2)	Se(1)-P(1)-Se(2)	115.54(2)
P(1)-P (1)'	2.2491(10)	C(1)-P(1)-P(1)'	101.77(8)
O(1)-Li(1)	1.900(5)	Se(1)-P(1)-P(1)'	108.19(3)
O(2)-Li(1)	1.903(5)	Se(2)-P(1)-P(1)'	108.36(3)
		Se(1)-Li(1)-Se(2)	116.28(10)
		O(1)-Li(1)-O(2)	107.7(2)

5.5 Conclusions

The reactions carried out in this chapter were very much speculative reactions to find a starting point for inorganic studies. The results obtained highlight the variability of Woollins' Reagent, as no two compounds characterised by X-ray crystallography show a similar bonding mode. Of the compounds synthesised, three areas showed promise to be developed further.

The manganese cluster presented a unique structure with no centre of inversion or symmetry. As such, none of the member substituents are equivalent and the NMR active phosphorus and selenium atoms exhibited interesting patterns in the spectra. The P-Se bond lengths range from 2.1551(7) Å to 2.3004(7) Å, the latter of which being the longest seen in this thesis and in the top 5% of all P-Se bond lengths reported in the CCDC. The related rhenium pentacarbonyl bromide was also reacted with *WR* under the same reaction conditions, but presented a completely different pattern in the $^{31}P\{^{1}H\}$ NMR, showing different reactivity and solubility, as the complex could not be crystallised, despite a range of techniques being employed.

The reaction of acetylferrocene with Woollins' Reagent demonstrates its ability to form heterocycles. The acquired crystal structure also exhibits five P-Se bonds, of which three are endocyclic P-Se single bonds and the other two are exocyclic P=Se double bonds. The bond lengths found are of average magnitude suggesting that although the ferrocene moiety has fair steric bulk, it has no apparent affect on the geometry of the heterocyclic ring.

The reactions of Woollins' Reagent with either 1,1'-dilithioferrocene or 1,2-dilithiodicarba-*closo*-dodecaborane(12) led to the same unexpected product, in which *WR* has dissociated into its two PSe_2Ph^- halves and reacted with one another forming a P-P bond, thus acting as an isobidentate ligand to the lithium centres. The direct and planned synthesis of this compound was not realised, despite various synthetic attempts. It is proposed that this would be of synthetic value for a range of follow up reactions.

5.6 Experimental

Experimental conditions and information are the same as in Section 2.3. Any deviations from standard conditions are stated in the syntheses.

5.7 Preparation of Starting Materials

5.7.1 **Preparation of Manganese Pentacarbonyl Bromide**[120]

$Mn_2(CO)_{10}$ (1.00 g, 2.6 mmol) was dissolved in cyclohexane (25 mL). Bromine (0.41 g, 2.6 mmol) was added and left to stir overnight at 40 °C. The resulting mixture was filtered, dried *in vacuo* and washed with water (3 x 25 mL). The product was then dried again.
Yield: 0.44 g, 63%.

5.7.2 **Preparation of Acetylferrocene**

Ferrocene (10.01 g, 54 mmol) was dissolved in dichloromethane (80 mL). Acetylchloride (4.22 g, 54 mmol) was added dropwise to aluminium chloride (7.16 g, 54 mmol) in DCM (50 mL) and allowed to stir for 1 h. The yellow suspension was transferred to a dropping funnel and slowly added dropwise to ferrocene with constant stirring, turning the solution deep purple. The mixture was allowed to stir for ~24 h, then ice (~90 g) was added. The phases were separated and the organic layer was dried over $MgSO_4$, before being filtered and the solvent evaporated to dryness. The resulting orange powder was recrystallised in petroleum ether (60/80).
Yield (9.85 g, 80 %).

^{1}H NMR: (270 MHz, $CDCl_3$, TMS) (ppm) δ_H = 2.29 (s, 3H, CH_3), 4.12 (s 5H, Cp ring), 4.45 (s, 2H) and 4.78 (s, 2H).

5.7.3 **Preparation of Diacetylferrocene**

Anhydrous aluminium chloride (3.80 g, 57 mmol) was stirred in dry DCM (30 mL). Acetyl chloride (8.94 g, 0.11 mol) was added to it dropwise. Ferrocene (5.00 g, 27 mmol) was dissolved in dry DCM (90 mL) was added dropwise over 20 min forming a purple solution. The reaction mixture was stirred for 24 h at room temperature and then the reaction mixture was poured onto ice (~75 g). The phases were then separated and the organic phase washed until neutral and dried over anhydrous magnesium sulfate. The DCM solution was filtered and the solvent evaporated under reduced pressure. The crude product was recrystallised from methanol, yielding orange-red crystals.
Yield (5.23 g, 72 %).

^{1}H NMR: (270 MHz, $CDCl_3$, TMS) (ppm) δ_H = 2.32 (s, 6H, CH_3), 4.48 (s, 4H) and 4.73 (s, 4H).

5.7.4 **Preparation of Thioacetylferrocene** [121]

Acetylferrocene (0.30 g, 1.3 mmol) was dissolved in dichloromethane (5 mL) and diethyl ether (65 mL). $NaHCO_3$ (0.66 g, 7.9 mmol) and P_4S_{10} (2.92 g, 6.6 mmol) were added and the mixture refluxed at 40 °C for 3 hours. The mixture was allowed to cool to room temperature, filtered and purified by column chromatography (alumina), resulting in a purple solution. The solution was evaporated to dryness.
Yield: 0.10 g, 31%

5.8 Synthetic Procedures

5.8.1 **Metal Carbonyls, $M(CO)_6$ (M = Cr, Mo, W)**

M = Cr (5.1)

Chromium hexacarbonyl (0.10 g, 0.47 mmol) was dissolved in THF and added to a solution of Woollins' Reagent (0.25 g, 0.47 mmol) in toluene. The mixture was heated and stirred at 80 °C overnight, yielding a green solution. The solution was allowed to cool to room temperature and filtered. The product was evaporated to dryness and an oil was obtained. No crystals could be grown.
Yield: 0.19 g, 75.6%.

$^{31}P\{^1H\}$ NMR: (161.98 MHz, no solvent) (ppm) δ_P = 74.4 ($^1J_{P\text{-}Se}$ = 840 Hz, $^1J_{P\text{-}Se}$ = 435 Hz).

$^{77}Se\{^1H\}$ NMR: (76.32 MHz, no solvent) (ppm) δ_{Se} = -21.5 (d, $^1J_{P\text{-}Se}$ = 840 Hz) and 395.7 (d, $^1J_{P\text{-}Se}$ = 435 Hz).

Mass TOF MS ES$^+$: *m/z* = 552.97 (M^+) and 574.96 (MNa^+).

IR (nujol) (cm^{-1}): 3432 (m, C-H), 1979 (m, C≡O), 1630 (m), 1437 (m, P-Ph), 1263 (m), 1145 (m), 1084 (m), 1025 (m), 981 (m), 811 (m), 743 (m), 688 (m), 666 (s), 533.9 (s, P=Se), 502.5 (s) and 445.5 (m).

M = Mo (5.2)

Molybdenum hexacarbonyl (0.12 g, 0.47 mmol) was dissolved in THF and added to a solution of Woollins' Reagent (0.25 g, 0.47 mmol) in toluene. The mixture was heated and stirred at 80 °C overnight, yielding a brown solution. The solution was allowed to cool to room temperature and filtered. The product was evaporated to dryness and an oil was obtained which could not be crystallised.
Yield 0.20 g.

$^{31}P\{^1H\}$ NMR: (161.98 MHz, no solvent) (ppm) δ_P = 74.9 ($^1J_{P\text{-}Se}$ = 835 Hz, $^1J_{P\text{-}Se}$ = 437 Hz).

M = W (5.3)

Tungsten hexacarbonyl (0.16 g, 0.47 mmol) was dissolved in THF and added to a solution of Woollins' Reagent (0.25 g, 0.47 mmol) in toluene. The mixture was heated and stirred at 80 °C overnight, yielding an orange solution. The solution was allowed to cool to room temperature and filtered. The product was evaporated to dryness and an oil was obtained. No crystals could be grown.
Yield 0.23 g.

^{31}P{^{1}H} NMR: (161.98 MHz, no solvent) (ppm) δ_P = 74.2 ($^{1}J_{P\text{-}Se}$ = 839 Hz, $^{1}J_{P\text{-}Se}$ = 437 Hz).

^{77}Se{^{1}H} NMR: (76.31 MHz, no solvent) (ppm) δ_{Se} = -22.8 (d, $J_{P\text{-}Se}$ = 841 Hz) and 394.5 (d, $^{1}J_{P\text{-}Se}$ = 436 Hz).

5.8.2 **Synthesis of Compound (5.4)**

Woollins' Reagent (1.45 g, 2.7 mmol) and $Mn(CO)_5Br$ (0.74 g, 2.7 mmol) were added together in toluene and stirred at 60 °C overnight. The resulting orange-red solution was allowed to cool to room temperature and filtered. The solution was then condensed, layered with hexane and stored in the refrigerator at 2 °C. Orange-red crystals formed in needle-like structures.
Yield: 0.40 g, 33 %.

^{1}H NMR: (400.1 MHz, $CDCl_3$) (ppm) δ_H = 8.31 (s, Ar-H, 2H), 8.17 (m, Ar-H, 2H) 7.99 (s, Ar-H, 2H), 7.68 (s, Ar-H, 3H), 7.59 (s, Ar-H, 2H) and 7.54 (s, Ar-H, 4H).
Note: All peaks quite broad.

^{13}C{^{1}H} NMR: δ_C (100.6 MHz, $CDCl_3$) (ppm) δ_C = 221.98 (s, C≡O), 218.91 (s, C≡O), 218.14 (s, C≡O), 134.98 (d, $^{4}J_{C\text{-}P}$ = 3.01 Hz, Ar-*p*C), 132.39 (s, Ar-C), 131.45 (d, $^{2}J_{C\text{-}P}$ = 9.50 Hz, Ar-*o*C), 131.00 (s, Ar-C), 130.67 (d, $^{2}J_{C\text{-}P}$ = 9.09 Hz, Ar-*o*C), 130.56 (d, $^{3}J_{C\text{-}P}$ = 12.2 Hz, Ar-*m*C), 129.53 (d, $^{3}J_{C\text{-}P}$ = 12.2 Hz, Ar-*m*C), 128.63 (d, $^{3}J_{C\text{-}P}$ = 81.5 Hz, Ar-*i*C) and 128.54 (d, $^{2}J_{C\text{-}P}$ = 8.14 Hz, Ar-*o*C).

$^{31}P\{^{1}H\}$ NMR: (162.0 MHz, $CDCl_3$) (ppm) δ_P = 175.3 ($^2J_{P-P}$ = 37.5 Hz), 178.2 ($^2J_{P-P}$ = 37.5 Hz) and 55.9 (dd, $^2J_{P-P}$ = 58.0 Hz, $^3J_{P-P}$ = 10.7 Hz). Selenium satellites visible but too small to be assigned.

$^{77}Se\{^{1}H\}$ NMR: (76.3 MHz, $CDCl_3$) (ppm) δ_{Se} = 705.4 (dd, J_{Se-P} = 205 Hz, J_{Se-P} = 416 Hz), 489.5 (dd, J_{Se-P} = 233 Hz, J = 357 Hz), 366.5 (d, J_{Se-P} = 384 Hz), 236.4 (d, J_{Se-P} = 345 Hz) and -46.8 (d, J_{Se-P} = 574 Hz).

EA: Calculated for $C_{24}H_{15}Mn_2O_6P_3Se_5$: C: 28.76%, H: 1.50%. Found: C: 29.38%, H: 1.70%.

Mass TOF MS ES$^+$: *m/z* = 998.49 (M^+).

IR υ max (KBr disc)/cm^{-1}: 3054 (w), 2963 (w, C-H), 2016 (s, C≡O), 1957 (s, C≡O), 1927 (s, C≡O), 1580 (w), 1477 (w), 1434 (m, P-Ph stretch), 1305 (w), 1261 (w), 1186 (w), 1160 (w), 1084 (m), 1025 (w), 998 (w), 805 (w), 742 (m), 687 (m), 654 (m), 618 (m), 535 (w), 507 (s, P-Se), 494 (s, P-Se), 449 (w) and 424 (w).

5.8.3 M_xCl_y – General Procedure

The metal chloride was dissolved in dichloromethane (15 mL). Woollins' Reagent was then added and the mixture allowed to stir overnight. The resulting mixture was then filtered and ^{31}P NMRs were taken of the filtrate and precipitate.

$MoCl_5$

Molybdenum pentachloride (0.12 g, 0.47 mmol) was dissolved in dichloromethane (15 mL). Woollins' Reagent (0.25 g, 0.47 mmol) was then added and the mixture allowed to stir at 35 °C overnight. The resulting brown mixture was then filtered. No crystals could be grown of the product.

$^{31}P\{^{1}H\}$ NMR: (162.0 MHz, $CDCl_3$) (ppm) δ_P = 58.6 (J_{P-Se} = 933 Hz).

IR υ max (KBr disc)/cm^{-1}: 3421 (m, br), 3057 (m, C-H), 1594 (w), 1478 (w), 1438 (m, P-Ph), 1333 (w), 1309 (w), 1263 (m), 1144 (s), 1090 (s), 1024 (s), 996 (s), 921 (m), 815 (m), 748 (m), 721 (m), 688 (m), 616 (w), 519 (s, νP-Se) and 470 (m).

WCl_6

Tungsten hexachloride (0.24 g, 0.47 mmol) was dissolved in dichloromethane (15 mL). Woollins' Reagent (0.25 g, 0.47 mmol) was then added and the mixture allowed to stir at 35 °C overnight. The resulting dark brown mixture was then filtered. No crystals could be grown of the product.

$^{31}P\{^1H\}$ NMR: (162.0 MHz, $CDCl_3$) (ppm) δ_P = 58.6 ($J_{P\text{-}Se}$ = 922 Hz).

$HfCl_4$

Hafnium tetrachloride (0.18 g, 0.56 mmol) was dissolved in dichloromethane (15 mL). Woollins' Reagent (0.30 g, 0.56 mmol) was then added and the mixture allowed to stir overnight. The resulting orange mixture was then filtered. No crystals could be grown of the product.

$^{31}P\{^1H\}$ NMR: (162.0 MHz, $CDCl_3$) (ppm) δ_P = 60.0 ($^1J_{P\text{-}Se}$ = 638 Hz).

IR υ max (KBr disc)/cm^{-1}: 3405 (m, br), 3053 (s, Ar-CH), 1625 (w), 1594 (w), 1578 (w), 1476 (w), 1434 (m, P-Ph), 1303 (w), 1258 (m), 1146 (s), 1079 (s), 1024 (s), 997 (s), 940 (m), 815 (w), 744 (m), 735 (m), 719 (w), 692 (m), 679 (m), 615 (w), 508 (s, P-Se) 487 (s) and 430(s).

$InCl_3$

Indium trichloride (0.11 g, 0.50 mmol) was dissolved in dichloromethane (15 mL). Woollins' Reagent (0.27 g, 0.50 mmol) was then added and the mixture allowed to stir at 40 °C overnight. The resulting yellow mixture was then filtered. No crystals could be grown of the product.

$^{31}P\{^1H\}$ NMR: (162.0 MHz, $CDCl_3$) (ppm) δ_P = 58.7.

$GaCl_3$

Gallium trichloride (0.20 g, 1.14 mmol) was dissolved in dichloromethane (15 mL). Woollins' Reagent (0.30 g, 0.56 mmol) was then added and the mixture allowed to stir overnight at room temperature. The resulting brown mixture was then filtered, evaporated to dryness and an IR taken of the product. No crystals could be grown of the product.

$^{31}P\{^1H\}$ NMR: (161.98 MHz, $CDCl_3$) (ppm) δ_P = 87.1 ($^1J_{P\text{-}Se}$ = 156 Hz).

IR υ max (KBr disc)/cm^{-1}: 3060 (s, Ar-CH), 2151 (w), 1998 (w), 1968 (w), 1893(w), 1796 (w), 1665 (w), 1574 (m), 1472 (w), 1435 (m, P-Ph), 1386 (w), 1333 (w), 1305 (w), 1263 (w), 1183 (m), 1163 (w), 1094 (w), 1077 (s), 995 (m), 925 (w), 809 (m, br), 738 (s), 709 (s), 675 (s), 613 (w), 518 (s, P-Se), 489 (s, P-Se) and 446 (m).

$NbCl_5$

Niobium pentachloride (0.1 g, 0.37 mmol) was dissolved in dichloromethane (15 mL). Woollins' Reagent (0.25 g, 0.37 mmol) in toluene (10 mL) was then added and the mixture allowed to stir at room temperature overnight. The mixture changed from yellow to dark red and was then filtered. No crystals could be grown of the product.

$^{31}P\{^1H\}$ NMR: (162.0 MHz, $CDCl_3$) (ppm) δ_P = 55.8 ($^1J_{P\text{-}Se}$ = 944 Hz).

$ZnCl_2$

Zinc dichloride (0.10 g, 0.73 mmol) was dissolved in dichloromethane (15 mL). Woollins' Reagent (0.39 g, 0.73 mmol) was then added and the mixture allowed to stir at room temperature overnight. The resulting orange mixture was then filtered. No crystals could be grown of the product.

$^{31}P\{^1H\}$ NMR: (162.0 MHz, $CDCl_3$) (ppm) δ_P = 55.8 ($^1J_{P\text{-}Se}$ = 946 Hz).

$AlCl_3$

Aluminium trichloride (0.10 g, 0.75 mmol) was dissolved in dichloromethane (15 mL). Woollins' Reagent (0.40 g, 0.75 mmol) was then added and the mixture allowed to stir overnight at 50 °C. The resulting yellow mixture was then filtered. No crystals could be grown of the product.

$^{31}P\{^1H\}$ NMR: (162.0 MHz, $CDCl_3$) (ppm) δ_P = 8.49 ($^1J_{P\text{-}Se}$ = 529 Hz).

5.8.4 Reactions with Halogens

Bromine

Woollins' Reagent (0.25 g, 0.47 mmol) was added to a solution of bromine (0.15 g, 0.93 mmol) dissolved in cyclohexane (15 mL). The mixture was left to stir overnight, then filtered and an NMR taken of the crude reaction mixture.

$^{31}P\{^1H\}$ NMR: (162.0 MHz, no solvent) (ppm) δ_P = -15.2 ($^1J_{P\text{-}Se}$ = 885 Hz).

Iodine

Woollins' Reagent (0.25 g, 0.47 mmol) was added to a solution of iodine (0.24 g, 0.93 mmol) dissolved in toluene (20 mL). The mixture was left to stir overnight, then filtered and an NMR was taken of the crude reaction mixture.

$^{31}P\{^1H\}$ NMR: (162.0 MHz, no solvent) (ppm) δ_P = 74.4 and 70.4.

5.8.5 Complex (5.5)

Woollins' Reagent (0.20 g, 0.37 mmol) and acetylferrocene (0.09 g, 0.37 mmol) were added together and covered in toluene (20 mL). The mixture was stirred overnight, filtered and layered with hexane. The resulting crystals were filtered off, washed with cold toluene and recrystallised from toluene/hexane.
Yield: 0.09g, 30 %.

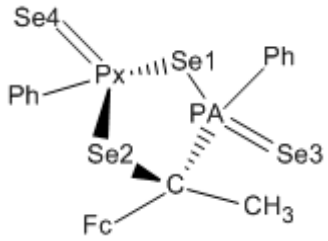

^{1}H NMR: (400.1 MHz, C_6D_6) (ppm) δ_H = 6.93-7.13 (br m, 10H, Ph-H), 4.04 (s, 1H, $Cp_{(subst)}$-H), 3.89 (s, 1H, $Cp_{(subst)}$-H), 3.78 (s, 5H, $Cp_{(unsubst)}$), 3.58 (s, 1H, $Cp_{(subst)}$-H), 3.43 (s, 1H, $Cp_{(subst)}$-H) and 2.49 (d, $^{2}J_{P\text{-}H}$ = 20.0 Hz, 3H, CH_3).

^{31}P{^{1}H} NMR: (162.0 MHz, C_6D_6) (ppm) δ_P = 97.7 (d, $^{2}J_{P\text{-}P}$ = 20.4 Hz, $J_{PA\text{-}Se1}$ = 419 Hz, $J_{PA=Se3}$ = 790 Hz) and 8.86 (d, $^{2}J_{P\text{-}P}$ = 20.4 Hz, $^{1}J_{Px\text{-}Se1}$ = 372 Hz, $^{1}J_{Px\text{-}Se2}$ = 412 Hz, $^{1}J_{Px=Se4}$ = 784 Hz).

^{77}Se{^{1}H} NMR: (76.3 MHz, C_6D_6) (ppm) δ_{Se} = 585.5 (dd, Se2, $^{1}J_{Px\text{-}Se}$ = 427 Hz, $^{2}J_{PA\text{-}Se}$ = 15.4 Hz), 475.9 (dd, Se1, $^{1}J_{PA\text{-}Se}$ = 419 Hz, $^{1}J_{Px\text{-}Se}$ = 419 Hz) and 131.0 (d, $^{1}J_{P=Se}$ = 789 Hz).

IR υ max (KBr disc)/cm^{-1}: 3050 (m, Ar-CH), 2965 (m, Ar-CH), 1581 (w), 1494 (w) 1477, 1434 (m,P-Ph), 1392 (w), 1366 (w), 1306 (w), 1261 (w), 1185 (w), 1086 (m), 1019 (m), 999 (m), 900 (w), 824 (m), 746 (m), 688 (m), 620 (w), 530 (s, P=Se), 485 (s) and 411(m).

5.8.6 **Diacetylferrocene**

Woollins' Reagent (0.40 g, 0.67 mmol) and diacetylferrocene (0.10 g, 0.34 mmol) were added together and covered in toluene (20 mL). The mixture was stirred overnight, filtered and layered with hexane. Despite numerous attempts, no crystals could be grown of the product. ^{31}P{^{1}H} NMR of the reaction mixture shows corresponding peaks to those shown in the product of the reaction of acetylferrocene and Woollins' Reagent. Yield: 0.15 g.

$^{31}P\{^{1}H\}$ NMR: (162.0 MHz, No solvent) (ppm) δ_P = 99.2 (d, $^{2}J_{P\text{-}P}$ = 19.7 Hz, $^{1}J_{P\text{-}Se}$ = 816 Hz) and 10.09 (d, $^{2}J_{P\text{-}P}$ = 19.7 Hz, $^{1}J_{P\text{-}Se}$ = 411 Hz).

5.8.7 **Thioacetylferrocene**

Woollins' Reagent (0.11 g, 0.02 mmol) and thioacetylferrocene (0.05 g, 0.02 mmol) were added together and covered in dichloromethane (10 mL). The mixture was stirred overnight. $^{31}P\{^{1}H\}$ NMR was taken of the mixture showing the main product to be the same as that of the reaction with acetylferrocene.

$^{31}P\{^{1}H\}$ NMR: (162.0 MHz, No solvent) (ppm) δ_P = 9.42 (d, $^{2}J_{P\text{-}P}$ = 19.8 Hz, $^{1}J_{P\text{-}Se}$ = 395 Hz) and 97.00 (d, $^{2}J_{P\text{-}P}$ = 19.9 Hz, $^{1}J_{P\text{-}Se}$ = 420 Hz).

5.8.8 **Lithiated Carborane**

1,2-*closo*-dicarbadodecaborane(12) (0.12 g, 0.83 mmol) was dissolved in toluene (20 mL) and cooled to 0 °C. *n*-Butyllithium in *n*-hexane (1.1 mL, 1.66 mmol) was slowly added with constant stirring and maintained at 0 °C for 30 mins. The reaction mixture was allowed to warm slowly to room temperature (~ 2 h) and 1,2-dilithiodicarba-*closo*-dodecaborane(12) formed as a white precipitate. Tetrahydrafuran (10 mL) was given to the solution, dissolving the precipitate and Woollins' Reagent (0.45 g, 0.84 mmol) was added. The mixture was heated to 50 °C and allowed to stir overnight, forming a clear yellow solution. This solution was the covered with hexane and put in the fridge to crystallise. This formed an orange oil and colourless crystals. NMR and further data proved inconclusive, as separation of the crystals and oil was not achieved. The experiment was repeated three times to prove the product was as found in the crystal structure.

5.8.9 **Lithiated Ferrocene**

n-BuLi (0.71 mL, 1.07 mmol) was given to TMEDA (0.1 mL, mmol) at 0 °C and left to stir for 30 mins. The mixture was then added to ferrocene (0.1 g, 0.54 mmol) in toluene (15 mL) at 0 °C and then left to stir overnight. Woollins' Reagent (0.29 g, 0.54 mmol) in tetrahydrofuran (5 mL) was added and left to stir for a further 24 h period. The red-brown reaction mixture was then filtered, condensed to 10 mL, layered with hexane and stored at 2 °C. Colourless crystals formed. X-ray crystal analysis proved the crystals to be the same as those yielded above, however NMR data between the two substances proved inconclusive.

6. Zusammenfassung

Während der letzten Jahrzehnte sind Sulfonierungs- und Selenierungsreaktionen zu wichtigen Verfahren geworden. Insbesondere Dithiadiphosphetandisulfide und ihre Selenanaloga sind für solche Anwendungen bekannt.[122] Seit 1956 ist 2,4-bis(*p*-methoxyphenyl)-1,3-dithiadi-phosphetan-2,4-disulfid, Lawesson's Reagenz, bekannt,[30] jedoch wurde erst in den 1970ern, als tiefer gehende Forschungen zu dieser Verbindung und deren Anwendungen betrieben. Lawesson und seine Mitarbeiter stellten fest, dass diese Verbindung vielfältige Anwendungsmöglichkeiten hatte.[123] Selenierungsreaktionen sind im Vergleich dazu nicht so gut erforscht, weshalb weniger Beispiele in der Literatur zu finden sind.[124] Seit den späten 1980ern forschen Arbeitskreise mit 2,4-Bis(phenyl)-1,3,2,4-diselenadiphosphetan-2,4-diselenid, Woollins' Reagenz, (*WR*), einem Selenanalogon zum Lawesson's Reagenz. Je nach Ausgangsverbindung kann das *WR* als Selenierungsreagenz verwendet werden oder zur Erzeugung von Heterocyclen dienen.[125] Außerdem ist die Bildung anorganischer Käfige möglich.[126]

Die ursprungliche Synthese von Woollins' Reagenz erfolgt durch die Reaktion des $(PPh)_5$-Pentamers mit elementaren Selen in Toluol.[40] Es wurde jedoch herausgefunden, dass diese Methode nicht optimal ist, da unerwünschte Nebenreaktionen stattfinden können (siehe Abbildung 6.1), welches ein großes Problem für die Herstellung des Woollins' Reagenz in großen Mengen ist. Die unten gezeigte Reaktion funktioniert nur bei geringen Mengen von <1,0 g. Ab einer Ausgangsmenge von ca. 10 g $(PPh)_5$ wird daher eine modifizierte Reaktionsmethode genutzt, bei der weniger Nebenreaktionen stattfinden und eine höhere Ausbeute erzielt werden kann.

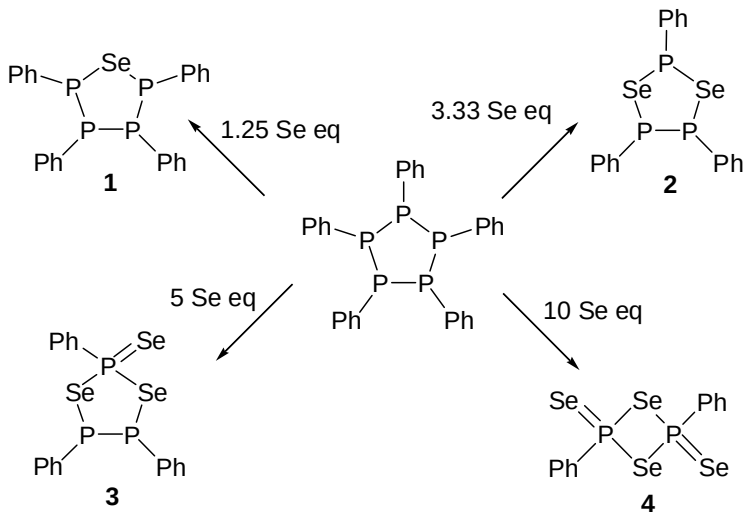

Abbildung 6.1: Die Reaktionen des $(PPh)_5$-Pentamers mit verschiedenen Äquivalenten Selen

Im Jahre 2005 wurde eine neue Synthesemöglichkeit des Woollins' Reagenz entwickelt,[50] die zwar aufwändiger ist, jedoch zu weniger Nebenprodukten führt und es erlaubt, die Verbindung in Mengen von bis zu 150 g herzustellen. Diese neue Synthese wird durch die Reaktion von Natriumselenid mit Dichlorphenylphosphan in siedendem Toluol durchgeführt. Das Produkt kann aus der Reaktionslösung abfiltriert werden und als ein tief rotes Pulver erhalten werden. Reaktionen mit Woollins' Reagenz wurden über die letzten sieben Jahren weiter entwickelt und werden meist in siedendem Toluol durchgeführt, da das *WR* nur schwer löslich ist.

Woollins' Reagenz reagiert mit Carbonylverbindungen, in denen das Sauerstoffatom durch einen Selenatom ersetzt und dadurch ein Selenocarbonyl hergestellt wird. In

Abbildung **6.2** sind ausgewählte Produkte abgebildet, die mit Hilfe von *WR* hergestellt wurden.[46]

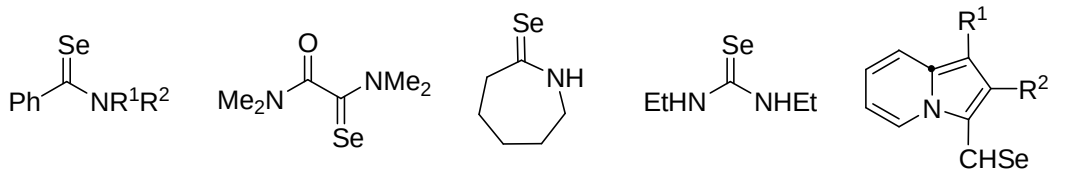

R^1 = Me, R^2 = Me
R^1 = H, R^2 = Me
R^1 = H, R^2 = ^{t}Bu
R^1 = R^2 = H

R^1 = H, R^2 = Me
R^1 = H, R^2 = ^{t}Bu
R^1 = Me, R^2 = ^{t}Bu

Abbildung 6.2: Selenierungsprodukte die durch Reaktionen

mit dem Woollins' Reagenz hergestellt wurden.

Die Reaktion von *WR* mit Natriumalkoxiden in MeOH oder EtOH führt zur Bildung von Diselenophosphonaten,[66] siehe Abbildung 6.3. Die hergestellten Liganden können danach mit Metallensalzen, wie z.B. $NiCl_2$ oder Cadmiumacetat umgesetzt werden und bilden dabei neuartige Metallkomplexe.

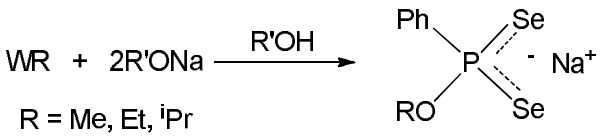

Abbildung 6.3: Die Umsetzung von *WR* mit einem Natriumalkoxid in dem entsprechenden Alkohol

6.1 Reaktionen des Woollins' Reagenz mit Aminen

Die Umsetzung des Woollins' Reagenz mit Aminen ohne Lösungsmittel und bei Raumtemperatur führt zu Ammoniumphenylphosphonamidodiselenoaten, wie in Abbildung **6.4** gezeigt.

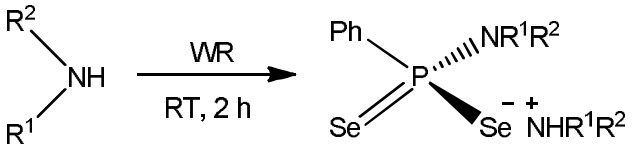

Abbildung 6.4: Bildung von Phenylphosphonamidodiselenoaten durch die direkte Reaktion des *WR* mit einem Amin

Hierbei wird das Woollins' Reagenz unter Rühren zum Amin gegeben und für 10-30 Minuten gerührt. Das Ende der Reaktion kann einfach beobachtet werden, da die Lösung sich von einer roten Suspension zu einer grün/grauen Lösung umwandelt. Anschließend wird die Lösung filtriert und das Lösungsmittel entfernt. Das so erhaltene gelbe Pulver kann durch Lösen in Dichlormethan und anschließendes Überschichten mit Hexan kristallisiert werden. Auf diese Art und Weise konnten die Produkte Diisopropylamin-*N*-isopropyl-*P*-phenylphosphonamidodiselenoat (^{i}PrAWR), (**2.1**), Butan-1-amin-*N*-butyl-*P*-phenylphosphonamidodiselenoat (^{n}BuAWR), (**2.2**), und 2-Aminobutan-*N*-*sec*-butyl-*P*-phenylphosphonamidodiselenoat (^{s}BuAWR), (**2.3**), als Kristalle erhalten werden, welche mittels Röntgenkristallstrukturanalyse charakterisiert werden konnten (siehe Abbildung 6.5).

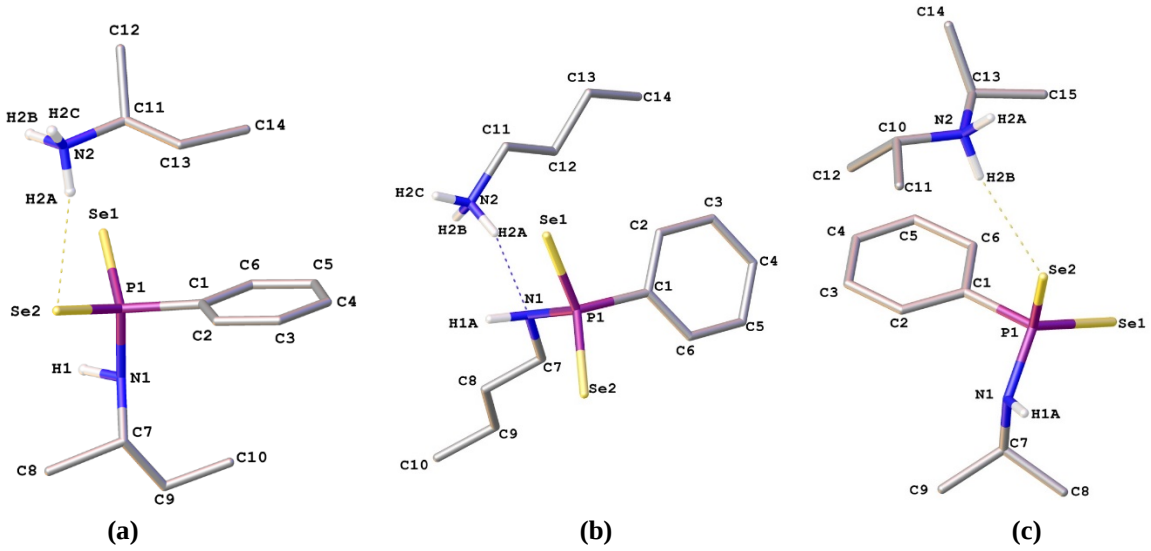

Abbildung 6.5: Kristallstrukturen von (a) (**2.1**), (b) (**2.2**) und (c) (**2.3**).
C-H Wasserstoffatome sind zur besseren Übersicht weggelassen.

Verbindungen (**2.1**), (**2.2**) und (**2.3**)wurden durch $^{31}P\{^{1}H\}$-, $^{77}Se\{^{1}H\}$-, $^{13}C\{^{1}H\}$- und ^{1}H-NMR Spektroskopie, Einkristallröntgenstrukturanalyse, Massenspektrometrie und IR-Spektroskopie charakterisiert. Die Signale in den Phosphor-NMR Spektren sind für Verbindung (**2.1**) bei 42,2 ppm, für Verbindung (**2.2**) bei 44,3 ppm und für Verbindung (**2.3**) bei 41,3 ppm zu beobachten und werden von sowohl $^{77}Se\{^{1}H\}$- als auch ^{13}C-Satelliten flankiert. Die $^{1}J_{P\text{-}Se}$ Kopplungskonstanten liegen bei 610 Hz, 599 Hz und 599 Hz für Verbindung (**2.1**), (**2.2**) und (**2.3**) und zeigen eine Bindungordnung von ca. 1½ an (für eine Einfachbindung erwartet man eine $^{1}J_{P\text{-}Se}$-Kopplungskonstante von 200-600 Hz, wohingegen man für eine Doppelbindung eine $^{1}J_{P\text{-}Se}$-Kopplungskonstante von 800-1200 Hz erwartet).[127] Die größten Kopplungkonstanten können für die Isopropylverbindung beobachtet werden, was darauf hindeutet, dass die beteiligten Orbitale in der P-C bzw. P-Se Bindung mehr s-Charakter haben.

In den $^{77}Se\{^{1}H\}$-NMR Spektren von ^{i}PrAWR und ^{n}BuAWR werden Dubletts gefunden, die durch die Kopplung zu dem Phosphoratom entstehen. Dies ist jedoch im $^{77}Se\{^{1}H\}$-NMR Spektrum der ^{s}BuAWR Verbindung nicht der Fall. Dieses zeigt zwei Dubletts, die eine ähnliche chemische Verschiebung haben. Die zwei Dubletts werden bei 73,3 ppm und 69,2 ppm beobachtet, mit jeweils einer Kopplungskonstante von 598 Hz und 601 Hz. Dieses Muster entsteht durch eine H-Brückenbindung, die

zwischen dem Selenatom und den Wasserstoffatom des Stickstoffs entsteht (siehe Abbildung 6.6).

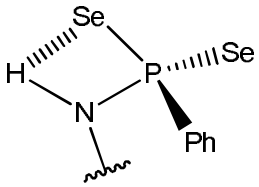

Abbildung 6.6: Schwache intermolekulare H-Brückenbindung in ^{s}BuAWR

Die $^{13}C\{^{1}H\}$-NMR Spektren der drei Verbindungen bestätigen die oben gezeigten Strukturen. Die Signale des gebundenes Amins sind auf Grund der $J_{C\text{-}P}$-Kopplung als Dubletts zu sehen, während die Signale für das Gegenion als Singuletts erscheinen. Im ESI-Massenspektrum sieht man M^+ bei *m/z* = 325,85 (**2.1**), 339,79 (**2.2**) und 339,78 (**2.3**), was jeweils mit den berechneten Massen des Kations übereinstimmt. Die IR-Spektren weisen die charakteristischen Banden der P-Se-Bindung im Bereich von ~400-500 cm^{-1}, der P-Ph-Bindung bei 1430 cm^{-1}, sowie der N-H- und C-H-Bindung zwischen 2800 cm^{-1} und 3200 cm^{-1} auf. Eine Zusammenfassung der spektroskopischen Daten von Verbindungen (**2.1**), (**2.2**) und (**2.3**) ist in Tabelle 6.1 zu sehen.

Tabelle 6.1: Ausgewählte Bindungslängen (Å) und -winkel (°), sowie chemische Verschiebungen (ppm) und Kopplungkonstanten (Hz) derVerbindungen (**2.1**), (**2.2**) und (**2.3**).

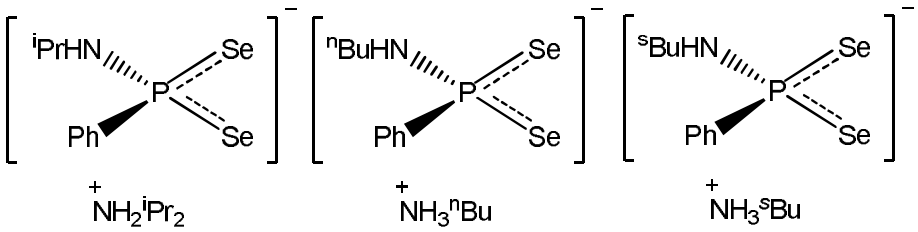

	^{i}PrAWR	**^{n}BuAWR**	**^{s}BuAWR**
P1-Se1	2,156(2)	2,139(1)	2,152(2)
P1-Se2	2,161(2)	2,1613(9)	2,167(2)
P1-N1	1,669(5)	1,695(2)	1,683(6)
P1-C1	1,825(7)	1,824(3)	1,821(7)
N1-C7	1,470(8)	1,486(4)	1,504(9)
N2-H2···Se2	2,52(3)	-	2,52(2)
N2-H2A···N1	-	2,05(2)	-
N1-P1-C1	102,7(3)	101,9(1)	103,1(3)
N1-P1-Se1	115,1(2)	106,41(9)	105,6(2)
C1-P1-Se1	104,7(2)	110,9(1)	110,8(2)
N1-P1-Se2	105,8(2)	111,73(9)	113,5(2)
C1-P1-Se2	109,0(2)	110,0(1)	107,1(2)
Se1-P1-Se2	118,33(8)	115,06(3)	116,00(8)
Spektroskopische Daten			
δ_P (ppm)	42,2	44,3	41,3
$^1J_{P\text{-}Se}$ (Hz)	610	599	599
$^1J_{P\text{-}C}$ (Hz)	79,8	75,1	77,2
δ_{Se} (ppm)	69,4	63,0	73,3, 69,2
$^1J_{Se\text{-}P}$ (Hz)	610	601	598, 601
$\nu_{P\text{-}Se}$ (cm^{-1})	541	557	549

Die Molekülstrukturen im Festkörper von (**2.1**), (**2.2**) und (**2.3**) zeigen P-Se Bindungslängen von 2,156(2) und 2,161(2) Å für (**2.1**), 2,139(1) und 2,1613(9) Å für (**2.2**), und 2,152(2) und 2,167(2) Å für (**2.3**). Dies bestätigt, dass die Bindungsordnung der Bindungen bei 1½ liegen, da die durchschnittliche Länge einer P-Se Bindung bei 2,222 Å und bei 2,111 Å für eine P=Se Bindung liegt, laut der CCDC Datenbank. Die Geometrie der zentralen Phosphoratome ist in den drei Verbindungen ähnlich. Einen Unterschied gibt es jedoch in der Natur der Wasserstoffbrückenbindungen. In der ^{n}BuAWR-Struktur wird eine Wasserstoffbrücke zu dem Gegenion zwischen N1 und H2 gebildet wird, wogegen beiden anderen beiden Verbindungen diese zwischen Se1 und H2 geformt wird. Die N1···H2A Wasserstoffbrückenbindung ist dabei 0,47 Å kürzer als die zu Se1 in (**2.1**) und (**2.2**).

Vier weitere Reaktionen zwischen Aminen und Woollins' Reagenz wurden mit *t*-Butylamin (**2.4**), Benzylamin (**2.5**), *s*-Pentylamin (**2.6**) und Propargylamin (**2.7**) als Ausgangstoffen durchgeführt. Die ^{31}P{^{1}H}-NMR Spektren für alle Produkte sehen ähneln denen der oben diskutierten Verbindungen. Hingegen zeigen die ^{77}Se{^{1}H}-NMR Spektren für (**2.4**), (**2.5**) und (**2.7**) ein Dublett und für (**2.6**) und (**2.3**) zwei Dubletts. Die ^{1}H und ^{13}C{^{1}H}-NMR Spektren zeigen die charakteristischen Signale der Aminreste und Phenylringe. Von allen Verbindungen hat die *t*-Butylaminverbindung die niedrigste chemische Verschiebung durch die höhere Elektrondichte am Phosphoratom, was auf den starken +I-Effekt der Methylgruppen der *t*-Butylgruppe zurückzuführen ist.

Von den sieben hergestellten Liganden wurden die ersten fünf, ^{i}PrAWR, ^{n}BuAWR, ^{s}BuAWR, ^{t}BuAWR und BenzAWR ausgewählt, um die Folgechemie zu erforschen. Wir konzentrierten uns dabei auf die Synthese von Übergangsmetallkomplexen, wobei die ersten Reaktionen mit ^{i}PrAWR durchgeführt wurden und ein paar ungewöhnliche Verbindungen hervorbrachten.

6.1.1 **Reaktionen von ^{i}PrAWR**

Die Reaktion von 2 Äquivalenten ^{i}PrAWR (**2.1**) mit Nickel(I)-acetat in Dichlormethan führt bei Raumtemperatur zu der Bildung von dem in Abbildung 6.7 dargestellten Nickelkomplex (**2.8**). Der Komplex wurde in guten Ausbeuten hergestellt (77%) und konnte durch Überschichtung der Reaktionslösung mit Hexan kristallisiert werden. Das erhaltene Produkt ist ähnlich zu dem in der literaturbekannten NiL_2 (L = $[Ph(OMe)PSe_2]^-$) Komplex von Gray *et al.*[66]

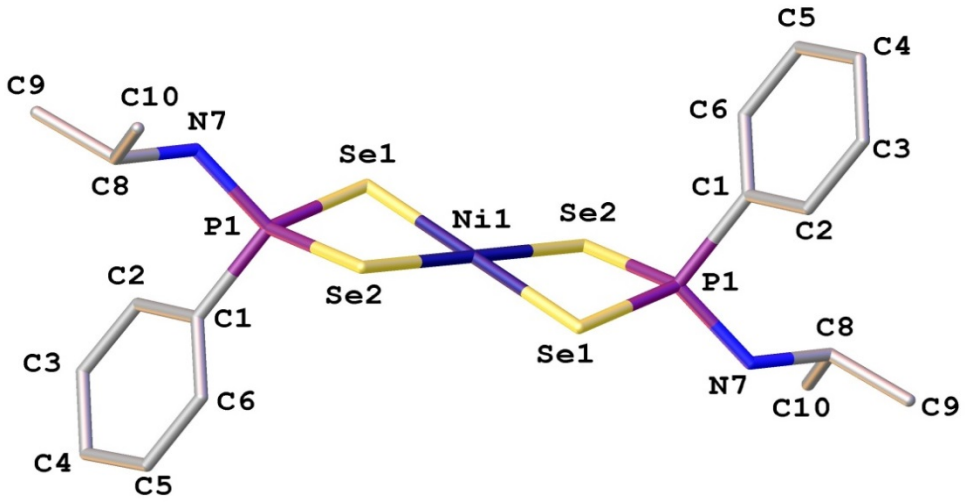

Abbildung 6.7: Molekülstruktur von Nickelkomplex (**2.8**).
Wasserstoffatome sind zur besseren Übersicht nicht dargestellt.

Im $^{31}P\{^{1}H\}$-NMR Spektrum von Verbindung (**2.8**) sieht man ein Singulett flankiert von Selen- und Kohlenstoffsatelliten mit Kopplungkonstanten von 490 Hz und 73 Hz. Durch die Komplexierung des Liganden ^{i}PrAWR und der Bildung der Ni-Se Bindungen verlängern sich die P-Se Bindungen. Die Bindungsordnung der P-Se Bindungen wird dabei auf ca. eins reduziert. Das Signal des Nickelkomplexes im $^{31}P\{^{1}H\}$-NMR Spektrum kann bei einer chemischen Verschiebung von 21,8 ppm beobachtet werden und zeigt somit eine elektronische Abschirmung des Phosphoratoms im Vergleich zum freien Liganden.

Im $^{77}Se\{^{1}H\}$-NMR Spektrum hat das Selenatom eine chemische Verschiebung von -17,0 ppm und eine $^{1}J_{Se\text{-}P}$ Kopplungskonstante von 496 Hz. Dies ist eine große Tieffeldverschiebung im Vergleich zum freien Liganden. Die ^{1}H und $^{13}C\{^{1}H\}$-NMR

Spektren, sowie das IR-Spektrum zeigen fast die gleichen Muster wie die des freien Liganden.

Die P-Se Bindungslängen liegen bei 2,162(5) Å und 2,191(4) Å. Diese Inäquivalenz zeigt, dass eine der Bindungen eher eine Dativbindung zu dem Metallzentrum ist und die andere eher den Charakter einer kovalente Einfachbindung hat. Dies wird durch die Änderung in den Kopplungkonstanten in den $^{31}P\{^{1}H\}$- und $^{77}Se\{^{1}H\}$-NMR Spektren bestätigt. Die Ni-Se Bindungen haben Bindungslängen von 2,345(2) Å and 2,362(2) Å und sind damit länger als die einer durchschnittlichen Ni-Se Bindungslänge. Das Ni-Zentrum ist quadratisch-planar von den Selenatomen umgeben und weist Winkel im Bereich von 89,41(6)° bis 90,59(6)° auf. Das Phosphoratom befindet sich in einer tetraedrischen Umgebung mit Winkeln von 99,9(2)° bis 118,9(6)°, was beweist, dass die Geometrie von (**2.8**) von dem Nickelatom kontrolliert wird. Die Phenylringe haben eine *trans*-Konfiguration, wobei einer der Ringe oberhalb der Se1-Se2-Ni-Ebene und der andere unterhalb sitzt. Dies ist zu erwarten, da die drei in Literatur bekannten ähnlichen Selenverbindungen[66,128] auch eine *trans*-Orientierung haben, ebenso wie fast alle Gruppe-10-phosphonodithionatkomplexe.

Die Umsetzung von ^{i}PrAWR (**2.1**) mit Kupfer(I)-acetat in Dichlormethan, bei erhöherter Temperatur führt zu der Bildung von zwei verschiedenen Produkten, die im $^{31}P\{^{1}H\}$-NMR Spektrum der Reaktionslösung beobachtet werden konnten. Eine Spezies weist ein breites Signal bei 39,3 ppm, die andere ein Singulett bei 10,0 ppm auf. Leider konnten nur vier Kristalle einer Reinverbindung erhalten werden, wodurch keine komplette Charakterisierung möglich war. Jedoch konnte eine Röntgenstrukturanalyse angefertigt werden, siehe Abbildung 6.8.

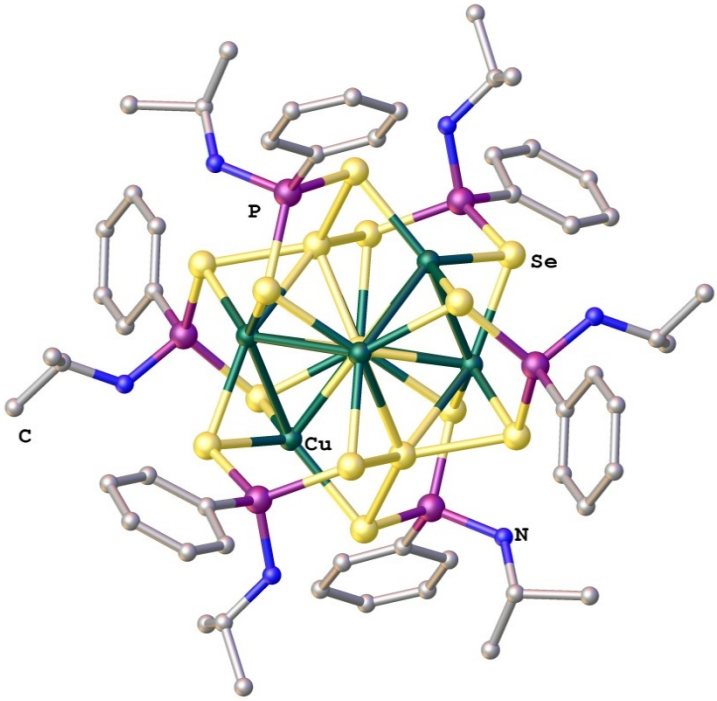

Abbildung 6.8: Molekülstruktur von Kupferkomplex (**2.9**).
Wasserstoffatome sind zur besseren Übersicht nicht abgebildet.

Die Molekülstruktur von (**2.9**) besteht aus sechs Ligandenmolekülen, sechs Kupferatomen und drei „freien“ Selenatomen. Der gebildete Cluster ist vergleichbar mit dem $\{Cu_8(\mu_8\text{-}Se)[Se_2P(OPr^{i})_2]_6\}$-Cluster von Liu *et al.*[68] Das Zentrum des Clusters bildet ein achtfach-koordiniertes Selenatom (Se(7)) (Abbildung 6.9 **(a)**) mit pseudokubischer Geometrie. Es ist sowohl an sechs Kupferatomen (Cu(1), Cu(2) und Cu(3)), als auch an die zwei anderen „freien“ Selenatomen (Se(8)) unter Ausbildung einer Se_3 Kette, gebunden. Diese zwei Selenatome sind auch die zentralen Atome zweier Selentetraeder, die insgesamt ein Se_4-Se-Se_4 Rückgrat formen (siehe Abbildung 6.9 **(b)**).

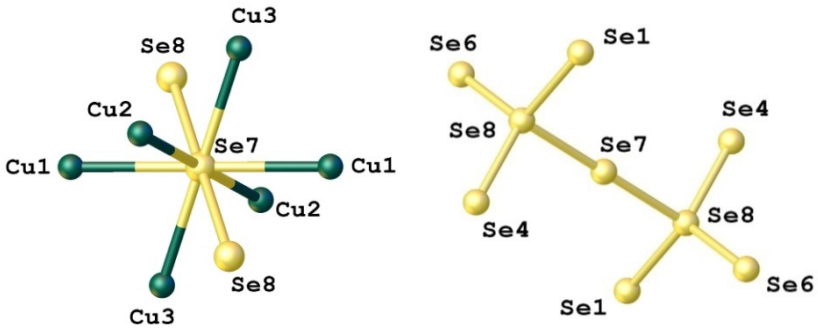

(a) **(b)**

Abbildung 6.9: **(a)** 8-bindiges zentrales Selenatom und **(b)** die zentrale Se-Kette

Eines der Selenatome des Liganden verbrückt zwei Kupferatome, während das andere eine Bindung zu einem Kupferatom und zu einem der endständigen Selenatome ausbildet. Die Kupferatome sind nicht äquivalent. Cu(1) ist ein sechsbindiges Atom, das eine trigonal prismatische Geometrie aufweist, zu vier Selenatomen und zwei Kupferatomen gebunden ist, und dessen Bindungswinkel zwischen 53.42(10)° und 141.39(13)° liegen. Die anderen beiden Kupferatome sind siebenbindig, da sie zu zwei Kupferatomen und fünf Selenatomen gebunden sind. Es gibt im Molekül (**2.9**) drei verschiedene Sorten Cu-Se Bindungen: Cu-Se_L, Cu-Se_T und Cu-Se_C, die in Abschnitt 2.2.2 ausführlich beschrieben wurden und daher hier nicht nochmals näher erläutert werden. Die Bindungen zwischen einem Kupferatom und einen Ligandenselenatom sind am kürzesten und die zwischen einen Kupferatom und dem zentralen Selenatom sind am längsten. Die P-Se Bindungen haben eine Bindungsordnung von ca. eins, und sind somit länger als die im freien Liganden. Die Se-Se Bindungen in (**2.9**) sind alle länger als der Durchschnittswert für solch eine Bindung (CCDC Datenbank).

6.2 Platinkomplex Chemie

Es wurden eine Vielzahl von Reaktionen mit den Ammoniumphenylphosphonamidodiselenoatliganden (**2.1**) – (**2.5**) und *cis*-$Pt(PR_3)_2Cl_2$ durchgeführt, bei der 20 Komplexe gebildet wurden (siehe Abbildung 6.10). Die Platinverbindung wurde dazu erst in Dichlormethan gelöst und anschließend der Ligand zugegeben. Die Reaktionen wurden über Nacht gerührt, filtriert, mit Wasser gewaschen und durch Säulenchromatographie gereinigt.

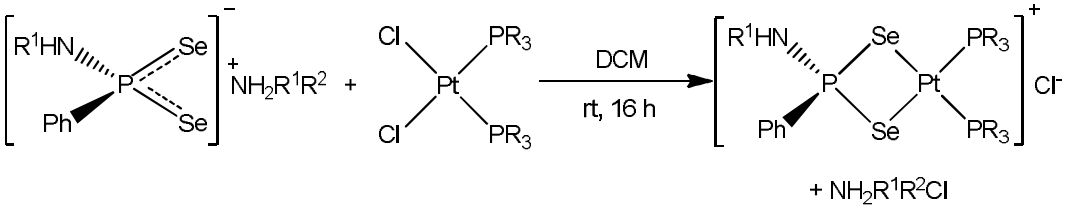

Abbildung 6.10: Die Umsetzung von dem Ammoniumphenylphosphonamidodiselenoatenligand mit Platinverbindungen der Form *cis*-$Pt(PR_3)_2Cl_2$

Bei jeder Reaktion wurde ein monosubstituiertes Monomer des Platinkomplexes als einziges Produkt erhalten. Dieses Studie wurde durchgeführt, um die Trends in den $^{31}P\{^1H\}$-, $^{77}Se\{^1H\}$- und $^{195}Pt\{^1H\}$-NMR Spektren zu untersuchen. In den meisten Fällen kann das Signal für das Phenylphosphonamidodiselenoat als ein Triplett mit einer $^3J_{P\text{-}P}$ Kopplungkonstante von ~7 Hz beobachtet werden. Dieses ist sowohl von ^{195}Pt-Satelliten als auch von ^{77}Se-Satelliten flankiert. Das Signal für das Phosphan kann hingegen als ein Dublett ($^3J_{P\text{-}P}$ = ~7 Hz) beobachtet werden, das eine große Kopplung von über 3000 Hz zum Platinatom aufweist. Im $^{77}Se\{^1H\}$-NMR Spektrum ist meist ein komplexes Dublett von Multipletts zu sehen, was schwierig zu interpretieren ist, während die $^{195}Pt\{^1H\}$-NMR Spektren ein Triplett von Dubletts zeigen, die durch die zwei verschiedenen Sorten von Phosphoratomen verursacht werden.

In Tabelle 6.2 sind die beiden chemischen Verschiebungen der drei Phosphoratome und deren Kopplungskonstanten zusammengefasst. Für die Reaktion zwischen ^{s}BuAWR und *cis*-$Pt(PPh_3)_2Cl_2$ ist nur eine chemische Verschiebung aufgeführt, da die Phosphoratome in dem hierbei gebildeten Komplex die gleiche chemische Verschiebung aufweisen. Die *cis*-[$Pt(PR_3)_2(^t$BuAWR)]Cl Komplexe haben,

bezogen auf das Phenylphosphonamidodiselenoat-Phosphoratom, die niedrigste chemische Verschiebung. Dies ist auf die höchste Elektronendichte am Phosphoratom wegen des starken +I-Effekts der Methylgruppen der *t*-Butylgruppe zurückzuführen. Die *cis*-[$Pt(PR_3)_2$(BenzAWR)]Cl Komplexe haben im Vergleich dazu die größte chemische Verschiebung, weil der Phenylring Elektrondichte vom Phosphoratom abzieht. Man sieht jedoch keinen großen Unterschied in den $^1J_{P\text{-}Se}$ und $^2J_{P\text{-}Pt}$ Kopplungen zwischen allen Verbindungen, was zeigt, dass das Amin keinen großen Einfluss auf den Bindungsmodus hat.

Tabelle 6.2: $^{31}P\{^1H\}$-NMR Daten für Komplexe (**3.1**) – (**3.20**). Die Werte für δ_P sind in ppm angegeben, die $^1J_{P\text{-}Se}$, $^2J_{P\text{-}Pt}$ und $^1J_{P\text{-}Pt}$ Kopplungskonstanten, in Klammern, in Hz.

	^{i}PrAWR	^{n}BuAWR	^{s}BuAWR	^{t}BuAWR	BenzAWR
cis-$Pt(PMe_3)_2Cl_2$	35,3 (429, 261) -28,8 (3112)	39,9 (431, 261) -30,1 (3171)	35,7 (429, 261) -28,8 (3126)	25,4 (433, 265) -28,29 (3148)	41,4 (433, 268) -29,4 (3084)
cis-$Pt(PMe_2Ph)_2Cl_2$	28,8 (373, 237) -19,1 (3130)	39,4 (425, 270) -18,1 (3181)	35,2 (425, 270) -17,9 (3181)	24,7 (425,275) -17,8 (3193)	40,9 (427, 270) -17,9 (3179)
cis-$Pt(PMePh_2)_2Cl_2$	32,2 (418, 275) -0,73 (3208)	37,5 (418, 275) -0,74 (3209)	33,4 (420, 275) -0,72 (3211)	23,03 (420, 277) -0,70 (3225)	40,8 (429, 264) -0,72 (3229)
cis-$Pt(PPh_3)_2Cl_2$	30,3 (418, 277) 18,0 (3324)	36,19 (418, 270) 17,9 (3324)	30,3 (425, 270) 17,6, 17,4 (3322)	22,0 (423, 277) 17,7 (3342)	37,0 (418, 270) 18,3 (3310)

Mit der Vergrößerung des Phosphans beobachtet man eine kleine geringfügige Erniedrigung der chemischen Verschiebungen des Phenylphosphonamidodiselenoat-Phosphoratoms, was laut Pregosin zu erwarten ist.[77] Sowohl die chemische Verschiebung, als auch die Kopplungskonstanten werden von PMe_3 zu PPh_3 größer. Dies geschieht, da die Methylgruppen mehr Elektrondichte als die Phenylringe

übertragen, was einen Einfluss auf die Abschirmung der Phosphoratome hat. Die Erhöhung der $^{1}J_{P\text{-}Pt}$ Kopplungskonstanten bedeutet eine Erhöhung des s-Charakters der Bindung.

Tabelle 6.3 zeigt die chemischen Verschiebungen und Kopplungskonstanten der Komplexe (**3.1**) – (**3.20**) für die $^{77}Se\{^{1}H\}$-NMR Spektroskopie. Interessant ist, dass sich die $^{1}J_{Se\text{-}P}$ Kopplungen kaum ändern, unabhängig davon welches Amin oder Phosphan in dem Komplex zu finden ist. Man beobachtet auch, dass sich die chemischen Verschiebungen mit steigender Zahl der Phenylringe am Phosphoratom erhöhen. Im Vergleich zu den $^{1}J_{P\text{-}Pt}$ Kopplungskonstanten werden die $^{1}J_{Se\text{-}P}$ Kopplungen nicht von den Phosphansubstituenten beeinflusst. Man sieht eine Verschiebung der ^{77}Se-Signale von ^{n}BuAWR bis ^{t}BuAWR zu tiefem Feld, was einer Erhöhung der Elektrondichte an den Selenatomen entspricht. Dies ist auf die elektronenschiebende Wirkung des Liganden zurückzuführen.

Tabelle 6.3: $^{77}Se\{^{1}H\}$-NMR Daten für Komplexe (**3.1**) – (**3.20**). Die Werte für δ_{Se} werden in ppm angegeben, die $^{1}J_{Se\text{-}P}$ Kopplungskonstanten, in Klammern, in Hz.

	^{i}PrAWR	^{n}BuAWR	^{s}BuAWR	^{t}BuAWR	BenzAWR
cis-$Pt(PMe_3)_2Cl_2$	60,5 (432)	44,8 (429)	66,6 (430)	98,0 (435)	135,6 (411)
cis-$Pt(PMe_2Ph)_2Cl_2$	152,9 (372)	68,3 (424)	91,2 (424)	118,3 (425)	67,6 (427)
cis-$Pt(PMePh_2)_2Cl_2$	97,3 (417)	78,1 (417)	98,8 (420)	129,0 (420)	129,8 (426)
cis-$Pt(PPh_3)_2Cl_2$	122,0 (418)	96,9 (422)	134,7, 126,2 (417), (415)	160,2 (418)	99,0 (417)

Tabelle 6.4 zeigt die chemischen Verschiebungen und Kopplungskonstanten der Komplexe (**3.1**) – (**3.20**) für die $^{195}Pt\{^{1}H\}$-NMR Spektroskopie. Die höchste chemische Verschiebung ist in der Trimethylphosphan-Verbindung zu beobachten, während die Triphenylphosphan-Verbindung am anderen Ende der Liste steht und somit am stärksten entschirmt ist. Man sieht jedoch keinen Trend zwischen den Aminsubstituenten und δ_{Pt}. Die $^{1}J_{Pt\text{-}P}$ Kopplungskonstanten steigen mit der Anzahl der Phenylringe und dadurch der sterischen Abschirmung am Phosphan, während die $^{2}J_{Pt\text{-}P}$

Kopplungskonstanten fast gleich bleiben. Eine schwache Tendenz kann für die $^{2}J_{Pt\text{-}P}$-Werte beobachtet werden, da diese ebenfalls steigen. Jedoch müssten mehr Beispiele gesammelt werden, um dies zu beweisen.

Tabelle 6.4: $^{195}Pt\{^{1}H\}$-NMR Daten für Komplexe (**3.1**) – (**3.20**). Die Werte für δ_{Pt} sind in ppm angegeben, die $^{1}J_{Pt\text{-}P}$ und die $^{2}J_{Pt\text{-}P}$ Kopplungskonstanten, in Klammern, in Hz.

	^{i}PrAWR	^{n}BuAWR	^{s}BuAWR	^{t}BuAWR	BenzAWR
cis-$Pt(PMe_3)_2Cl_2$	-4829 (3115, 261)	-4824 (3165, 259)	-4832 (3128, 259)	-4817 (3138, 264)	-4816 (3091, 233)
cis-$Pt(PMe_2Ph)_2Cl_2$	-4849 (3133, 237)	-4867 (3200, 273)	-4874 (3183, 268)	-4857 (3194, 272)	-4856 (3180, 272)
cis-$Pt(PMePh_2)_2Cl_2$	-4900 (3200, 267)	-4891 (3206, 273)	-4900 (3212, 267)	-4884 (3225, 273)	-4903 (3204, 261)
cis-$Pt(PPh_3)_2Cl_2$	-4933 (3316, 273)	-4925 (3328, 261)	-4933 (3320, 281)	-4916 (3337, 273)	-4914 (3316, 267)

Von allen Platinverbindungen, die hier aufgeführt wurden, konnte nur eine, *cis*-[$Pt(PPh_3)_2$(^{s}BuAWR)]Cl, (**3.12**), in kristalliner Form erhalten werden. Für die Verbindung konnten P-Se-Bindungslängen von 2.209(5) Å und 2.196(5) Å bestimmt werden. Die Pt-Se-Bindungslängen sind äquivalent und liegen bei 2.471(2) Å und 2.472(2) Å und sind damit etwas länger als die durchschnittliche Länge. Die Bindungswinkel um das Platinzentrum haben eine Werte zwischen 84.04(7)° und 100.90(15)° für die *cis*-Winkel, und 163.77(13)° für Se(1)-Pt(1)-P(3) und 166.99(11)° für Se(2)-Pt(1)-P(2) für die *trans*-Winkel. Dies zeigt, dass es eine große Verzerrung der quadratisch-planaren Form der Geometrie um das zentrale Platinatom gibt.

Zusammenfassend konnte gezeigt werden, dass bei der Komplexierung des Phenylphosphonamidodiselenoat-Liganden eine Erniedrigung der chemischen Verschiebung des Phosphoratoms, jedoch eine Erhöhung der chemischen Verschiebung des Selenatoms beobachtet werden kann. Die Bindungsordnung wird geringer, da die $^{1}J_{P\text{-}Se}$ Kopplung kleiner wird, was zeigt, dass es eine Änderung im Bindungsmodus gegeben hat.

6.3 Mesitylphosphan Chemie

Von allen Verbindungen der anorganische Chemie gehören Phosphane zu den am nutzvollsten und vielseitigsten, funktionellen Gruppen, da sie sowohl in Synthesen, als auch in Katalysatoren verwendet werden können. Speziell ihre σ-Donor- und π-Akzeptor-Eigenschaften machen sie so einizgartig. Viele Phosphane sind kommerziell erhältlich und ihre Anwendungen als Liganden in der Übergangsmetallkatalyse, z.B. der Hydrierung oder Hydroformulierung, zählt zu den wichtigsten industriellen Prozessen.

Sterisch gehinderte Phosphane, wie zum Beispiel Triphenylphosphan, spielen große Rollen in organischen Chemie, so z.B. in Wittig[83]-, Appel[85]- und Mitsonobu[84]-Reaktionen. In allen Fällen wird das Phosphan zu einem Phosphanoxid oxidiert, während eine Umwandlung der funktionellen Gruppe der organischen Spezies stattfindet. In den Palladium-katalysierten Cross-Coupling Reaktionen wie Heck[89]-, Negishi[91]- und Suzuki[87]-Reaktionen wird eine neue C-C Bindung generiert weswegen sie zu den wichtigsten Reaktionen bei organischen Totalsynthesen zählen. Dabei wird Triphenylphosphan als labiler Ligand verwendet, weil es eine einfach zu handhabende, günstige und sterisch anspruchsvolle Verbindung ist, welche starke Donatoreigenschaften hat. Aus ähnlichen Gründen ist auch Trimesitylphosphan seit langem für synthetische Chemiker interessant. Wie in Kapitel 3 beschrieben, konnte nur eine Verbindung kristallin erhalten werden, was vermutlich an der schlechten Löslichkeit der Verbindungen lag. Deswegen wurde vorgeschlagen, den Phosphanligand am Platinkomplex zu vergrößern, um die Löslichkeit des Platinkomplexes zu ändern und dadurch die Verbindungen möglicherweise kristallisiert zu erhalten.

In diesem Sinne wurde Trimesityl-, Dimesitylphenyl- und Mesityldiphenylphosphan hergestellt und jeweils mit $Pt(cod)Cl_2$ und $K_2[PtCl_4]$ umgesetzt. Die Reaktion von Trimesityl- und Dimesitylphenylphosphan mit $Pt(cod)Cl_2$ und $K_2[PtCl_4]$ waren nicht erfolgreich, da kein Umsatz erfolgte. Die Reaktion von Mesityldiphenylphosphan mit sowohl $Pt(cod)Cl_2$ als auch $K_2[PtCl_4]$ waren erfolgreich und es wurde wie erwartet *trans*-$Pt(PMesPh_2)_2Cl_2$ (**4.4**) synthetisiert, das auch kristallisiert werden konnte(Abbildung 6.11). Da $K_2[PtCl_4]$ ein Salz ist und nur schlecht

in organischen Lösungsmitteln löslich ist, wurde diese Reaktion in Wasser durchgeführt. Dies führte zur Oxidation des Phosphans und daher zu geringen Ausbeuten.

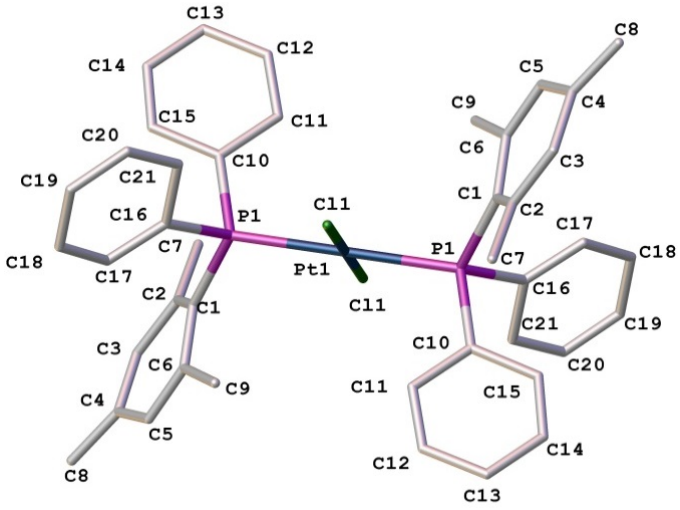

Abbildung 6.11: Molekülstruktur von *trans*-Pt(PMesPh$_2$)Cl$_2$ (**4.4**).
Wasserstoffatome sind zur besseren Übersicht nicht abgebildet.

Die Pt-P Bindungslängen (2,340(4) Å) in *trans*-Pt(PMesPh$_2$)$_2$Cl$_2$ sind etwas länger als die für *trans*-Pt(PPh$_3$)$_2$Cl$_2$ (2,3163(11) Å) und andere analoge Phosphankomplexe.[111] Die Geometrie um das Platinatom zeigt ein planares Zentrum (P1-Pt-P1' 180,0(3)°, Cl1-Pt-Cl1' 180,0(2)°) mit einem Cl1-Pt1-P1 Winkel von 94,3(2)° und einem Cl1-Pt1-P1^1 Winkel von 85,8(2)°. Dies zeigt, dass der sterische Anspruch des Phosphans nur innerhalb des Molekülebene einen Einfluss hat. Die Geometrie des Pt-Zentrums hat eine Wirkung auf die Geometrie des Phosphoratoms. Die Bindungswinkel um die Phosphoratomen sind im Bereich von 99,5(10)° und 114,1(6)° zu beobachten, ein etwas größerer Bereich, als den für den freien Phosphan beobachtet wurde.

Mit der dargestellten Platinverbindung wurde die Geometrie der anderen Mesitylphosphane untersucht und die analogon Sulfid- und Selenidverbindungen hergestellt. Durch die Untersuchungen wurde festgestellt, dass obwohl die Synthese von Trimesitylphosphanoxid existiert, die Kristallstruktur jedoch nicht literaturbekannt ist. Für Dimesitylphenyl- und Mesityldiphenylphosphanoxid wurde keine Synthese

gefunden. Demzufolge wurden $P(S)Mes_3$ (**4.1**), $P(S)Mes_2Ph$ (**4.2**), $P(S)MesPh_2$ (**4.5**), $P(Se)Mes_2Ph$ (**4.3**), $P(Se)MesPh_2$ (**4.6**), $P(O)Mes_3$ (**4.7**), $P(O)Mes_2Ph$ (**4.8**) und $P(O)MesPh_2$ (**4.9**) synthetisiert. Alle Verbindungen konnten kristallin erhalten und vollständig analysiert werden. So konnten die P=E Bindungslängen (E = O, S, Se) und der kristallografische Tolmanwinkel bestimmt werden. Tabelle 6.5, Tabelle **6.6** und Tabelle **6.7** zeigen die wichtigsten Daten der Sulfide, Selenide und Oxide. Die Mesitylphosphane wurden in Toluol gelöst und elementarer Schwefel oder Selen wurde dazugegeben. Nach 16 Stunden rühren wurde die Lösung filtriert, eingeengt, in Hexan gelöst und mit Diethylether überschichtet, um die hergestellte Verbindung zu kristallisieren.

Tabelle 6.5: Ausgewählte Bindungslängen (Å) und -winkel (°), sowie chemische Verschiebungen (ppm) und Kopplungkonstanten (Hz) von Verbindungen (**4.1**), (**4.2**) und (**4.5**).

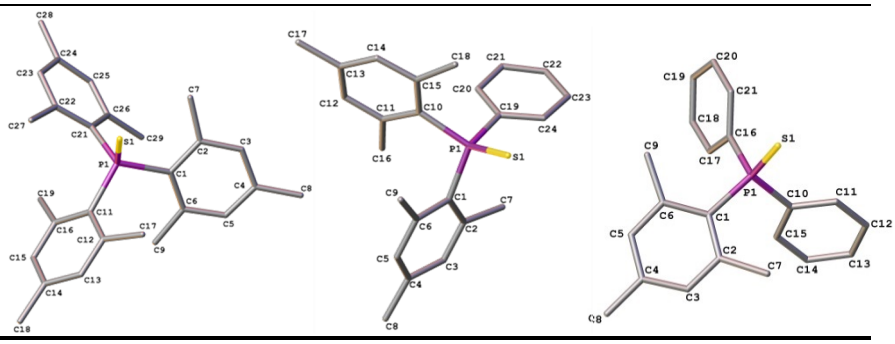

	$SMes_3$ (4.1)	**$SMes_2Ph$ (4.2)**	**$SMesPh_2$ (4.5)**
S1-P1	1,975(1)	1,968(2)	1,967(2)
P1-C_{R1}*	1,844(5)	1,848(7)	1,828(5)
P1-C_{R2}*	1,849(4)	1,860(6)	1,822(5)
P1-C_{R3}*	1,840(4)	1,844(8)	1,823(5)
S1-P1-C_{R1}	109,5(1)	107,3(2)	113,5(1)
S1-P1-C_{R2}	107,3(1)	120,3(2)	114,2(2)
S1-P1-C_{R3}	109,4(1)	108,9(3)	112,9(2)
C_{R1}-P1-C_{R2}	108,9(2)	104,2(3)	104,6(2)
C_{R1}-P1-C_{R3}	109,2(2)	115,0(3)	108,9(2)
C_{R2}-P1-C_{R3}	112,5(2)	101,3(3)	101,7(2)
Spektroskopische Daten			
δ_P (ppm)	33,2	37,4	36,8
$^1J_{P\text{-}C}$ (Hz)	77,2	79,8	82,1
$\nu_{P\text{-}S}$ (cm^{-1})	643	662	703
Tolmanwinkel	174,9°	153,3°	136,5°

*C_{R1}, C_{R2}, C_{R3} = *ispo*-Kohlenstoffatom der Ringe 1, 2, 3. Für P(S)Mes_3, C_{R1} = C1, C_{R2} = C11 und C_{R3} = C21, für P(S)Mes_2Ph C_{R1} = C1, C_{R2} = C10 und C_{R3} = C19 und für P(S)$MesPh_2$ C_{R1} = C1, C_{R2} = C10 und C_{R3} = C16.

Die P-S Bindungen werden mit der Vergrößerung des sterischen Anspruchs der Substituenten am Phosphoratom länger, was auch eine Vergrößerung des Tolmanwinkels verursacht. Die P-C Bindungslängen in allen Verbindungen sind gleich lang, jedoch ist die Geometrie durch die sterischen Ansprüche der Mesitylanteile zwischen den Verbindungen unterschiedlich. In $P(S)Mes_3$ ist die Geometrie am nächsten an der erwarteten tetraederischen Geometrie, da die Mesitylgruppen einen ähnlichen sterischen Anspruch haben. In (**4.2**) wird der Phenylring aus dem erwarteten Winkel geschoben, um sich den sterischen Ansprüchen der zwei Mesitylringe anzupassen. In (**4.5**) sind die Bindungswinkeln wieder kleiner, da die Phenylringe auch kleiner sind. Man sieht auch, dass mit der Verkleinerung des sterischen Anspruchs eine Erhöhung der $^1J_{P\text{-}C}$ Kopplungskonstante erfolgt, was auf einen erhöhten s-Charakter am Phosphoratom und eine stärkere P-C Bindung hinweist.

In Tabelle 6.6 sind die Bindungslängen und -winkel sowie die spektroskopischen Daten der Selenmesitylphosphane angegeben. Darin sieht man wie auch in den Schwefelanaloga, dass je sterisch anspruchsvoller die Verbindung ist, desto länger ist die P-Se Bindungslänge und desto kleiner die $^1J_{P\text{-}Se}$ Kopplungskonstante. Die Bildungswinkel um das Phosphorzentrum für (**4.3**) sind durch den sterischen Anspruch der Mesitylringe wiederum größer als die für die Mesityldiphenyl-Verbindungen. Trimesitylphosphanselenid konnte trotz mehrerer Versuche und Änderungen der Reaktionsbedingungen nicht dargestellt werden, was vermutlich auf sterische Gründe zurückzuführen ist. Im $^{31}P\{^1H\}$-NMR Spektrum konnte nur den Ausgangsstoff beobachtet und somit keine Umsetzung festgestellt werden.

Die P=Se Bindungslängen sind etwas länger als die durchschnittliche P=Se Bindung, was vermutlich durch den sterischen Anspruch der Mesitylringe begründet ist. Die P-C Bindungslängen, sowie die Bindungswinkel sind sehr ähnlich zu denen der Sulfidesehr ähnlich. Die beobachteten kristallographischen Tolmanwinkel für die Selenide sind, wie erwartet, etwas kleiner als die für die Sulfide. Die Gründe sind die etwas längeren P=Se Bindungen und eine etwas größere Abstoßung der Ringe.

Tabelle 6.6: Ausgewählte Bindungslängen (Å) und -winkel (°), sowie chemische Verschiebungen (ppm) und Kopplungkonstanten (Hz) von Verbindungen (**4.3**) und (**4.6**).

	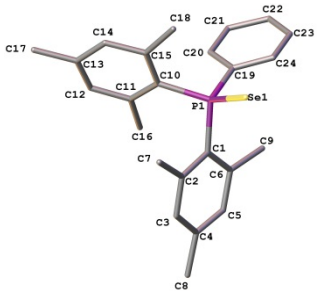	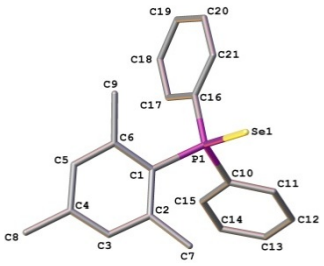
	$SeMes_2Ph$ (4.3)	**$SeMesPh_2$ (4.6)**
Se1-P1	2,134(3)	2,121(3)
P1-C_{R1}*	1,838(7)	1,823(9)
P1-C_{R2}*	1,86(1)	1,834(9)
P1-C_{R3}*	1,830(7)	1,841(9)
Se1-P1-C_{R1}	105,4(3)	113,4(3)
Se1-P1-C_{R2}	121,6(3)	113,6(3)
Se1-P1-C_{R3}	109,4(4)	112,9(3)
C_{R1}-P1-C_{R2}	103,8(4)	105,2(4)
C_{R1}-P1-C_{R3}	114,9(4)	108,7(4)
C_{R2}-P1-C_{R3}	102,2(4)	102,2(4)
Spektroskopische Daten		
δ_P (ppm)	20,8	28,4
$^1J_{P\text{-}Se}$ (Hz)	695	725
$^1J_{P\text{-}C}$ (Hz)	73,5	75,1
δ_{Se} (ppm)	-83,3	-318,7
$^1J_{Se\text{-}P}$ (Hz)	694	725
$\nu_{P\text{-}Se}$ (cm^{-1})	562	555
Tolmanwinkel	149,5°	132,8°

*C_{R1}, C_{R2}, C_{R3} = *ispo*-Kohlenstoffatom der Ringe 1, 2, 3. Für P(Se)Mes_2Ph C_{R1} = C1, C_{R2} = C10 und C_{R3} = C19 und für P(Se)$MesPh_2$ C_{R1} = C1, C_{R2} = C10 und C_{R3} = C16.

Die Oxide waren die Verbindungen, die am einfachsten zu kristallisieren waren. Die Phosphane wurden mit H_2O_2 in Aceton bei Raumtemperatur umgesetzt und eine halbe Stunde gerührt. Nach Filtrierung wurden die Verbindungen durch Einengen der Mutterlaugekristallisiert. In Tabelle 6.7 sind die Bindungslängen und -winkel sowie die spektroskopischen Daten der Mesitylphosphanoxide angegeben.

Tabelle 6.7: Ausgewählte Bindungslängen (Å) und -winkel (°), sowie chemische Verschiebungen (ppm) und Kopplungkonstanten (Hz) von Verbindungen (**4.7**), (**4.8**) und (**4.9**).

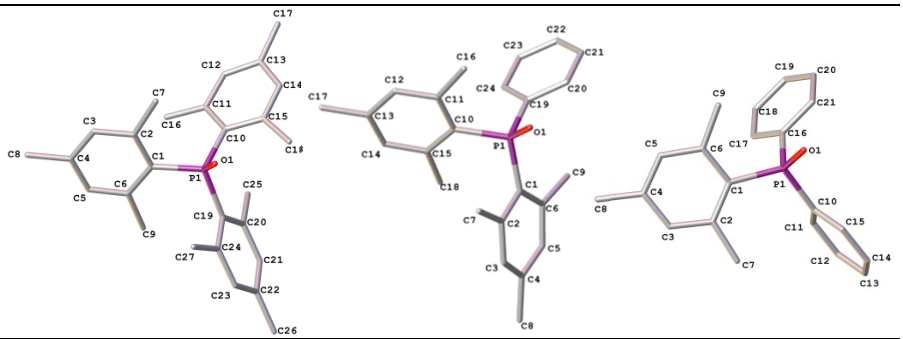

	P(O)Mes$_3$ (4.7)	**P(O)Mes$_2$Ph (4.8)**	**P(O)MesPh$_2$ (4.9)**
O1-P1	1,506(4)	1,1499(3)	1,502(3)
P1-C_{R1}*	1,817(6)	1,815(4)	1,819(4)
P1-C_{R2}*	1,839(7)	1,835(4)	1,818(5)
P1-C_{R3}*	1,839(5)	1,804(4)	1,813(5)
O1-P1-C_{R1}	107,8(3)	109,3(2)	113,8(2)
O1-P1-C_{R2}	108,5(3)	113,8(2)	109,8(2)
O1-P1-C_{R3}	108,3(2)	108,5(2)	112,1(2)
C_{R1}-P1-C_{R2}	109,1(3)	108,9(2)	113,2(2)
C_{R1}-P1-C_{R3}	112,1(3)	114,2(2)	104,6(2)
C_{R2}-P1-C_{R3}	110,8(3)	102,2(2)	102,7(2)
Spektroskopische Daten			
δ_P (ppm)	31,8	35,0	32,4
$^1J_{P-C}$ (Hz)	98,6	101	103
ν_{P-O} (cm^{-1})	1140	1134	1151
Tolmanwinkel	198,6°	177,6°	164,5

*C_{R1}, C_{R2}, C_{R3} = *ispo*-Kohlenstoffatom der Ringe 1, 2, 3. Für P(O)Mes$_3$, C_{R1} = C1, C_{R2} = C10 und C_{R3} = C19,für P(O)Mes$_2$Ph C_{R1} = C1, C_{R2} = C10 und C_{R3} = C19 und für P(O)MesPh$_2$ C_{R1} = C1, C_{R2} = C10 und C_{R3} = C16.

6.4 Weitere Reaktionen des Woollins' Reagenz

Wie einleitend erwähnt, führen die Reaktionen zwischen Carbonylen und *WR* oft zu Selenierungsprodukten und interessanten Heterocyclen. Bis jetzt wurden die meisten Reaktionen mit organischen Verbindungen durchgeführt. Daher wurde beschlossen, ähnliche anorganische Verbindungen zu untersuchen.

Die Umsetzung des *WR* mit $M(CO)_6$ (M = Cr (**5.1**), Mo (**5.2**), W (**5.3**)) führte zu drei Verbindungen, die in den $^{31}P\{^1H\}$-NMR Spektren ähnliche chemische Verschiebungen von etwa 74 ppm haben und zwei Paar Selensatelliten besitzten. Leider konnte keine der drei Verbindungen kristallin erhalten werden und eine genaue Struktur der Verbindung kann somit postuliert werden. Im Spektrum für die $Cr(CO)_6$ Verbindung lagen die $^1J_{P\text{-}Se}$ Kopplungskonstanten bei 437 Hz und 836 Hz, was zwei Selenatome in unterschiedlichen chemischen Umgebungen und Bindungsmotiven impliziert: eine P-Se und eine P=Se Bindung. Das Massenspektrum bestätigt diese Interpretation, da das Isotopenmuster mit dem einer Verbindung mit zwei Selenatomen und einem Chromatom in Einklang steht. Der *m/z* Wert von Verbindung (**5.1**) beträgt 552,97, was den Schluss nahe legt, dass die Hälfte eines Woollins' Reagenz an das Metallcarbonyl gebunden ist, wodurch ein Kohlenmonoxidmolekül abgespalten und ein Toluolmolekül koordiniert wurde. Für die Wolframverbindung wurden ähnliche $^{31}P\{^1H\}$-NMR, Massen- und IR-Spektren erhalten und es kann somit vermutet werden, dass eine ähnliche Verbindung erhalten wurde. Für die Molybdänverbindung wurden abweichende Daten erhalten. Daher kann nicht eindeutig gesagt werden, ob die postulierte Struktur für alle Verbindungen mit Gruppe VI Metallen zutrifft.

Die Umsetzung von $Mn(CO)_5Br$ mit Woollins' Reagenz in Toluol bei 60 °C führte zu einem unerwarteten Produkt (Verbindung (**5.4**)), das in Abbildung 6.12 zu finden ist.

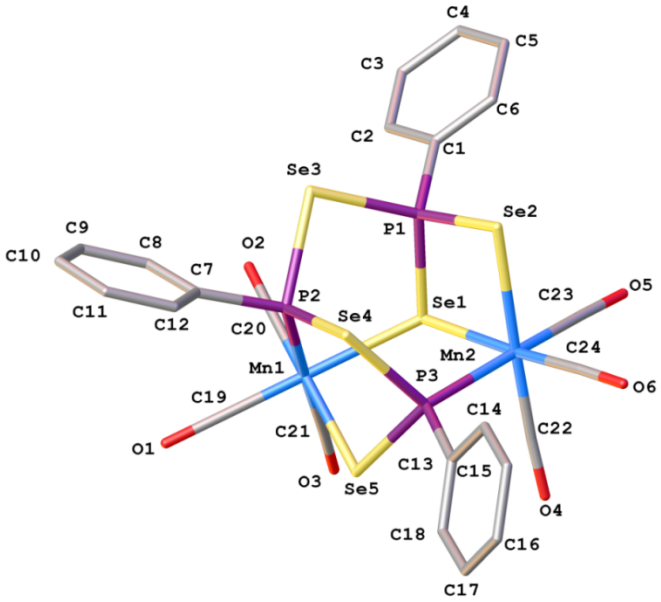

Abbildung 6.12: Molekülstruktur von Verbindung (**5.4**).
Wasserstoffatome sind zur besseren Übersicht nicht abgebildet.

Der Käfig besteht aus drei Phosphoratomen, fünf Selenatomen und zwei Manganzentren. Das Molekül hat kein Symmetriezentrum und dadurch hat keines von den enthaltenen Atomen die gleiche chemische Verschiebung, weder im $^{31}P\{^{1}H\}$-NMR noch im $^{77}Se\{^{1}H\}$-NMR Spektrum. Im $^{31}P\{^{1}H\}$-NMR Spektrum können zwei Signale bei ~176 ppm beobachtet werden, die P(2) und P(3) zugeordnet werden können. Beide Atome weisen eine ähnliche chemische Umgebung auf, da sie zu zwei Selenatomen, einem Manganatom und einem Phenylring gebunden sind. Bei ~55 ppm erscheint ein drittes Signal, welches P(1) zugeordnet werden kann, das an drei Selenatome gebunden ist. Alle drei Signale haben ^{77}Se Satelliten, die sich jedoch überlagern: somit konnten keine Kopplungskonstanten bestimmt werden. Das $^{77}Se\{^{1}H\}$-NMR Spektrum zeigt fünf Signale. Zwei Dubletts von Dubletts bei 705 and 489 ppm können den Selenatomen Se(3) und Se(4) zugeordnet werden, wobei deren Muster durch die Kopplung zu zwei Phosphoratomen hervorgerufen wird. Ein Dublett bei ca. -47 ppm entstammt Se(1), welches durch die Kopplung zu nur einem Phosphoratom und zwei Mn-Atomen hervorgerufen wird, zwei Signale bei 236 und 366 ppm gehören die zu Se(2) und Se(5).
In der Kristallstruktur haben die Manganatome eine oktaedrische Geometrie, während die Phosphoratome eine verzerrt tetraedrische Geometrie besitzen, indem die Bindungswinkeln für P(1) bei 101.75° - 115.13°, bei 94.92° - 120.44° für P(2) und bei 96.88° - 119.29° für P(3) liegen. Die Se-P-Bindungenslängen betragen zwischen

2.1551(7) Å für Se(2)-P(1) und 2.3004(7) Å für Se(4)-P(3). Die letztere gehört zu den längsten Se-P-Bindungen, die in der CCDC Datenbank zu finden sind.

Die Umsetzung des Woollins' Reagenzes mit verschiedenen Metallchloriden führte zu $PPhSe_2Cl$ und einem amorphen Feststoff, der auf Grund seiner Unlöslichkeit nicht charakterisiert werden konnte. Möglich ist, dass sich ein Metallselenid gebildet hat, welches jedoch nicht nachgewiesen werden konnte.

Die Reaktion zwischen *WR* und Acetylferrocen bei Raumtemperatur führte zu der Bildung der in Abbildung 6.13 gezeigten Struktur, (**5.5**). Man sieht, dass der P_2Se_2-Ring geöffnet und ein Sauerstoffatom durch Se ersetzt wurde. Die Verbindung kann im $^{31}P\{^1H\}$-NMR bei δ_P = 97,7 und 8,86 ppm beobachtet werden. Im $^{77}Se\{^1H\}$-NMR können drei Signale beobachtet werden. Die zwei endozyklischen Selenatome bei δ_{Se} = 586 und 476 ppm unterscheiden sich drastisch auf grund ihrer chemischen Inäquivalenz. Die beiden exozyklischen Selenatome hingegen unterscheiden sich in ihrer chemischen Verschiebung kaum (δ_{Se} = 131 ppm).

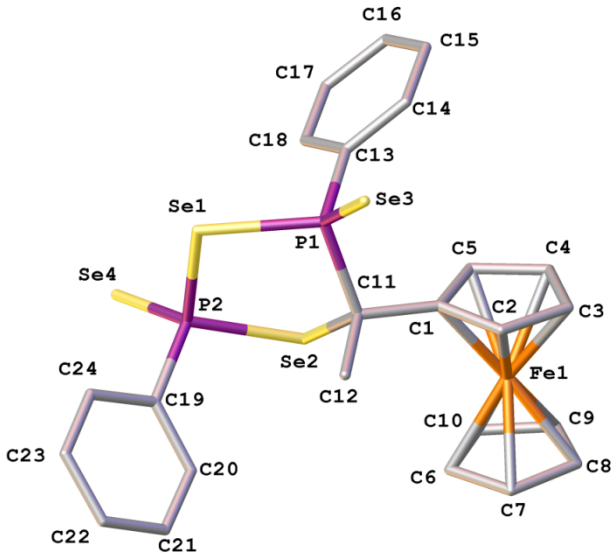

Abbildung 6.13: Molekülstruktur von Verbindung (**5.5**).Wasserstoffatome und fehlgeordnete Toluolmolekül sind zur besseren Übersicht nicht abgebildet.

Im Festkörper haben die endozyklischen P-Se Bindungen eine Länge von 2.2307(5) Å bis 2.2723(5) Å, im Vergleich zu 2.0996(5) Å und 2.0937(6) Å für die exozyklischen P=Se Bindungen.

Die Reaktion zwischen *WR* und Thioacetylferrocen führt zu dem gleichen Produkt (**5.5**). Dies zeigt, dass die Reaktion über einen gleichen Mechanismus stattfindet und wird nicht durch das größere Chalcogenatom beeinflusst wird. Hingegen führt die Umsetzung von Diacetylferrocen und *WR* zu einer nur einfach substituierten Verbindung. Das Produkt wird hierbei nicht vom molaren Verhältnis der Edukte beeinflusst, da auch mit einem Überschuss von Woollins' Reagenz keine Disubstitution beobachtet wurde. Auch eine thermische Aktivierung führte zu keiner Zweifachsubstitution. Dies beweist, dass Ferrocen nicht groß genug ist um Platz für zwei solch sterisch anspruchsvolle Substituenten zu bieten.

Ein Forschungsgebiet des Hey-Hawkins Arbeitskreises befasst sich mit der Synthese von Carbaboran-haltigen Liganden. Zugrunde liegt eine Zweistufen-Reaktion, in der 1,2-*closo*-dicarbadodecaboran(12) erst lithiiert und anschließend mit einem primären Phosphan umgesetzt wird. Die erhaltenen Verbindungen besitzten aufgrund des Carbaboranclusters herausragende elektronische Eigenschaften. Im Hinblick darauf wurde das Woollins' Reagenz mit 1,2-dilithiodicarba-*closo*-dodecaboran(12) bei einer Temperatur von 50 °C umgesetzt. Die erhaltene Molekülarstruktur ist in Abbildung 6.14 zu sehen.

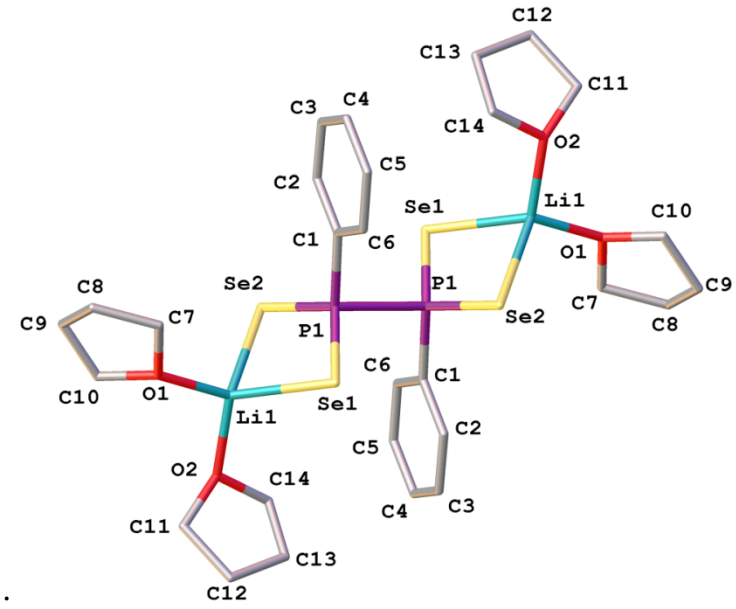

Abbildung 6.14: Molekülstruktur von Verbindung (**5.6**).
Wasserstoffatome sind zur besseren Übersicht nicht abgebildet.

In dieser Struktur ist das Woollins'-Reagenz-anteil als isobidentater Ligand involviert. Um diese Struktur zu verwirklichen, muss das Woollins' Reagenz während der Reaktion in zwei Hälften dissoziieren und eine P-P-Bindung neu ausbilden. Die Lithiumzentren sind durch THF-Moleküle solvatisiert. Die Bindungslänge der neuen P-P-Bindung beträgt 2,2491(10) Å und ist gegenüber der durchschnittlicher P-P-Bindungslängen leicht verlängert (2.210 Å, CCDC). Die beide Phosphoratome sowie das Lithiumatom besitzen eine nahezu tetraedrische Umgebung.

Zusammenfassend konnte Woollins' Reagenz mit diversen Aminen zu einer Reihe von vielseitigen Phenylphosphonamidodiselenoato-Liganden umgesetzt werden. Diese Liganden wurden zur Komplexbildung mit einer Auswahl von Metallkomplexen genutzt. Einige der Produkte konnten kristallin erhalten und strukturell charakterisiert werden.

Des Weiteren wurde eine Reihe von neuen sterisch anspruchsvollen Phosphanoxiden, -sulfiden und -seleniden wurde synthetisiert und ihre Eigenschaften und Reaktivität untersucht. Während $P(O)Mes_3$ und $P(S)Mes_3$ problemlos erhalten werden konnten, konnte Trimesitylphosphanselenid konnte nicht dargestellt werden, was vermutlich auf sterische Gründe zurückzuführen ist.

7. References

[1] *The Chemistry of Organic Selenium and Tellurium Compounds, Vol. 2*, W.-W. Du Mont, R. Hensel, S. Kubiniok and L. Lange, Wiley New York, 1987, 591

[2] R. Davies in *Handbook of Chalcogen Chemistry*, F.A. Devillanova (ed.), RSC Publishing, 2007, Chapter 5

[3] *The Chemistry of Inorganic Homo- and Heterocycles Vol 2*, I. Haiduc and D.B. Sowerby, Academic Press, 1987, Chapter 23

[4] Scifinder Scholar search

[5] US Pat. Appl. Pub. 2008 US2008153950A1

[6] www.noria.com/learning_center/category_article.asp?articleid=496

[7] *Chemistry of the Elements*, N. N. Greenwood and A. Earnshaw, Butterworth Heinemann, Oxford, 1997, p. 509

[8] *Chemistry of the Elements*, N. N. Greenwood and A. Earnshaw, Butterworth Heinemann, Oxford, 1997, p. 503

[9] D. Heinz, *Z. Anorg. Allg. Chem.*, 1966, **347**, 167

[10] D. Heinz, *Pure Appl. Chem.*, 1975, **44**, 141

[11] *Inorganic Chemistry*, D. F. Shriver and P. W. Atkins, Oxford University Press, 1999

[12] *Inorganic Chemistry*, C.E. Housecroft, A.G. Sharpe, Prentice Hall, 2001

[13] R. Blachnik, H.-P. Baldus, P. Lönnecke and B. W. Tattershall, *Angew. Chem.*, 1991, **103**, 621

[14] R. Blachnik, P. Lönnecke, K. Boldt and B. Engelen, *Acta Crystallogr., Sect. C: Cryst. Struct. Commun.*, 1994, **50**, 659

[15] R. Blachnik, P. Lönnecke and J. Nuß, *Z. Anorg. Allg. Chem.*, 1994, **620**, 160

[16] D. Lathrop and H. Eckert, *J. Phys. Chem.*, 1989, **93**, 7895

[17] G. J. Penney and G. M. Sheldrick, *J. Chem. Soc. A: Inorganic, Physical, Theoretical*, 1971, **2**, 245

[18] C. D. Mickey and R. A. Zingaro, *Inorg. Chem.*, 1973, **12**, 2115

[19] Y. Monteil and H. Vincent, *J. Inorg. Nucl. Chem.*, 1975, **37**, 2053

[20] H. Behrens and G. Haschka, *Chem. Ber.*, 1961, **94**, 1191

[21] M. V. Kudchadker, R. A. Zingaro and K. J. Irgolic, *Can. J. Chem.*, 1968, **46**, 1415

[22] R. G. Melton and R. A. Zingaro, *Can. J. Chem.*, 1968, **46**, 1425

[23] K. Chondroudis and M. G. Kanatzidis, *J. Solid State Chem.*, 1998, **138**, 321

[24] W. Tejchman, K. Zborowski, W. Lasocha and L. M. Proniewicz, *Heterocycles*, 2008, **75**, 1931

[25] I. A. Sokolov, I. V. Murin, Y. K. Startsev, M. Y. Zubkova and A. A. Pronkin, *Glass Phys. Chem.*, 2010, **36**, 21

[26] M. Baudler, H. Suchomel, G. Furstenberg and U. Schings, *Angew. Chem., Int. Ed. Engl.*, 1981, **20**, 1044

[27] W.-W. Du Mont, T. Severengiz and B. Meyer, *Angew. Chem., Int. Ed. Engl.*, 1983, **22**, 983

[28] B. M. Goldstein, S. D. Kennedy and W. J. Hennen, *J. Am. Chem. Soc.*, 1990, **112**, 8265

[29] a) H. S. Angel, E. W. Fuller and H. G. Berger, US Patent 2381377 August 7, 1943
b) R. L. May, US Patent 2356073, August 15, 1944

[30] P. Fay and H. P. Lankelma, *J. Am. Chem. Soc.*, 1952, **74**, 4933

[31] H. Z. Lecher, R. A. Greenwood, K. C. Whitehouse and T. H. Chao, *J. Am. Chem. Soc.*, 1956, **78**, 5018

[32] R. A. Cherkasov, G. A. Kutyrev and A. N. Pudikov, *Tetrahedron*, 1985, **41**, 2567

[33] M. Jesberger, T. P. Davis, L. Barner, *Synthesis*, 2003, **13**, 1929

[34] M. P. Cava and M. I. Levinson, *Tetrahedron*, 1985, **41**, 22, 5061

[35] P. Grisenti, A. Magni, A. Manzocchi and P. Ferraboschi, *Steroids*, 1997, **62**, 504

[36] Y. Hitotsuyanagi, J. Suzuki, Y. Matsumoto, K. Takeya and H. Itokawa, *J. Chem. Soc., Perkins Trans.*, 1994, **1**, 1887

[37] B. S. Pederson, S. Scheibye, N. H. Nilsson and S.-O.Lawesson, *Bull. Soc. Chim. Belg.*, 1978, **87**, 223

[38] S. Scheibye, R. Shabana, S.-O.Lawesson and C. Roemming, *Tetrahedron*, 1982, **38** (7), 933

[39] S. Scheibye, B. S. Pederson and S.-O.Lawesson, *Bull. Soc. Chim. Belg*, 1978, **87**, 229

[40] P. Kilian, A. M. Z. Slawin and J. D. Woollins, *J. Chem. Soc., Chem. Commun.*, 2003, 2288

[41] K. M. Ok and P. S. Halasyamani, *Chem. Mater.*, 2002, **14**, 2360

[42] M. St. J. Foreman and J. D. Woollins, *J. Chem. Soc., Dalton Trans.*, 2000, 1533

[43] J. T. Shore, W. T. Pennington, M. C. Noble and A. W. Cordes, *Phosphorus Sulfur*, 1988, **39**, 153

[44] P. T. Wood and J. D. Woollins, *J. Chem. Soc., Chem. Commun.*, 1988, 1190

[45] P. Bhattacharyya, A. M. Z. Slawin and J. D. Woollins, *J. Chem. Soc., Dalton Trans.*, 2001, **3**, 300

[46] P. Bhattacharyya and J. D. Woollins, *Tetrahedron Lett.*, 2001, **42**, 5949

[47] G. Hua, Y. Li, A. M. Z. Slawin and J. D. Woollins, *Org. Lett.*, 2006, **8**, 5251

[48] K. Geisler, A. Jacobs, A. Künzler, M. Mathes, I. Girrleit, B. Zimmermann, E. Bulka, W.-D. Pfeiffer and P. Langer, *Synlett*, 2002, **12**, 1983

[49] P. Bhattacharyya, A. M. Z. Slawin and J. D. Woollins, *Chem. Eur. J.*, 2002, **8**, 2705

[50] I. P. Gray, P. Bhattacharyya, A. M. Z. Slawin and J. D. Woollins, *Chem. Eur. J.*, 2005, **11**, 6221

[51] G. Hua, Y. Li, A. M. Z. Slawin and J. D. Woollins, *Chem. Commun.*, 2007, 1465

[52] G. Hua, Y. Li, A. M. Z. Slawin and J. D. Woollins, *Dalton Trans.*, 2007, **48**, 3677

[53] I. P. Parkin, M. J. Pilkington, A. M. Z. Slawin, D. J. Williams and J. D. Woollins, *Polyhedron*, 1990, **7**, 987

[54] I. Baxter, A. F. Hill, J. M. Malget, A. J. P. White and D. J. Williams, *Chem. Commun.*, 1997, 2049

[55] W. Shi, M. Shafaei-Fallah and A. Rothenberger, *Dalton Trans.*, 2007, **38**, 4255

[56] W. Shi, M. Shafaei-Fallah, L. Zhang, C. E. Anson, E. Matern and A. Rothenberger, *Chem. Eur. J.*, 2007, **13**, 598

[57] D. Fenske and H. Krautscheid, *Angew. Chem., Int. Ed. Engl.*, 1990, **29**, 1452

[58] C. W. Liu, I.-J. Shang, J.-C. Wang and T.-C. Keng, *Chem. Commun.*, 1999, 995

[59] W. Kuchen and B. Knop, *Angew. Chem., Int. Ed. Engl.*, 1964, **3** (7), 507

[60] W. Kuchen and B. Knop, *Angew. Chem., Int. Ed. Engl.*, 1965, **4** (3), 244

[61] W. Kuchen and H. Hertel, *Angew. Chem., Int. Ed. Engl.*, 1969, **8** (2), 89

[62] G. E. Coates and R. N. Mulcherjee, *J. Chem. Soc.*, 1964, 1295

[63] R. P. Davies and M. G. Martinelli, *Inorg. Chem.*, 2002, **41**, 348

[64] R. P. Davies, C. V. Francis, A. P. S. Jurd, M. G. Martinelli, A. J. P. White and D. J. Williams, *Inorg. Chem.*, 2004, **43** (16), 4802

[65] I. P. Gray, A. M. Z. Slawin and J. D. Woollins, *Dalton Trans.*, 2005, **12**, 2188

[66] I. P. Gray, A. M. Z. Slawin and J. D. Woollins, *Dalton Trans.*, 2004, **16**, 2477

[67] C. W. Liu, H.-C. Chen, J.-C. Wang and T.-C. Keng, *Chem. Commun.*, 1998, **17**, 1831

[68] C. W. Liu, I.-J. Shang, J.-C. Wang and T.-C. Keng, *Chem. Commun.*, 1998, **11**, 995

[69] G. Hua, R. A. M. Randall, A. M. Z. Slawin and J. D. Woollins, *Z. Anorg. Allg. Chem.*, 2011, **637**, 1800

[70] a) G. Hua and J. D. Woollins, *Polyhedron*, 2012, **42** (1), 190

b) G. Hua, Y. Li, A. M. Z. Slawin and J. D. Woollins, *Tetrahedron*, 2008, **64**, 5442

[71] V. D. Leemput, T. W. Hummelink, J. H. Noordik and P. T. Beurskens, *Cryst. Struct. Commun.*, 1975, **4**, 167; I. P. Gray, H. L. Milton, A. M. Z. Slawin and J. D. Woollins, *Dalton Trans.*, 2003, 3450

[72] A. W. Hofmann, *Ann. Chem. Liebigs*, 1857, **103**, 357

[73] B. W. Malerbi, *Platinum Metals Rev.*, 1965, **9** (2), 47

[74] T. B. Rauchfuss, *Platinum Metals Rev.*, 1980, **24** (3), 95

[75] B. M. Still, P. G. A. Kumar, J. R. Aldrich-Wright and W. S. Price, *Chem. Soc. Rev.*, 2007, **36**, 665

[76] P. G. Waddell, A. M. Z. Slawin and J. D. Woollins, *Dalton Trans.*, 2010, **39**, 8620

[77] P. S. Pregosin, *Coord. Chem. Rev.*, 1982, **44**, 247

[78] L. M. Green, Y.-A. Park and D. W. Meek, *Inorg. Chem.*, 1988, **27**, 1658

[79] D. Drew, J. R. Doyle, *Inorg. Synth.*, 1972, **13**, 47

[80] P. L. Goggin, R. J. Goodfellow, S. R. Haddock, B. F. Taylor and F. R. H. Marshall, *J. Chem. Soc., Dalton Trans.*, 1976, 459

[81] J. Bailar, H. Itatani, *Inorg. Chem.*, 1965, **4**, 1618

[82] F. J. Ramos-Lima, A. G. Quiroga, J. M. Pérez, M. Font-Bardía, X. Solans, C. Navarro-Ranninger, *Eur. J. Inorg. Chem.*, 2003, **2003**, 1591

[83] G. Wittig and U. Schöllkopf, *Chem. Ber.*, 1954, **87** (9), 1318

[84] O. Mitsunobu, Y. Yamada, *Bull. Chem. Soc. Jpn.*, 1967, **40** (10), 2380

[85] R. Appel, *Angew. Chem., Int. Ed. Engl.*, 1975, **14** (12), 801

[86] J. G. Calzada and J. Hooz, *Org. Synth.*, 1974, **54**, 63

[87] N. Miyaura, K. Yamada and A. Suzuki, *Tetrahedron Lett.*, 1979, **20** (36), 3437

[88] N. Miyaura, T. Yanagi, A. Suzuki, *Synth. Commun.*, 1981, **11**, 513

[89] H. A. Dieck and R. F. Heck, *J. Am. Chem. Soc.*, 1974, **96** (4), 1133

[90] F. Ozawa, A. Kubo and T. Hayashi, *Chemistry Lett.*, 1992, **11**, 2177

[91] A. O. King, N. Okukado and E.-I. Negishi, *J. Chem. Soc., Chem. Commun.*, 1977, **19**, 683

[92] A. P. Smith, S. A. Savage, J. C. Love and C. L. Fraser, *Organic Syntheses*, 2002, **78**, 51

[93] J. A. Osborn, F. H. Jardine, J. F. Young and G. Wilkinson, *J. Chem. Soc. A*, 1966, 1711

[94] D. A. Evans, G. C. Fu and A. H. Hoveyda, *J. Am. Chem. Soc.*, 1988, **110** (20), 6917

[95] L. Vaska and J. W. DiLuzio, *J. Am. Chem. Soc.*, 1961, **83** (12), 2784

[96] L. Vaska and J. W. DiLuzio, *J. Am. Chem. Soc.*, 1962, **84** (4), 679

[97] S. Sasaki and M. Yoshifuji, *Curr. Org. Chem.*, 2007, **11**, 17

[98] J. F. Blount, D. Camp, R. D. Hart, P. C. Healy, B. W. Skelton and A. H. White, *Aust. J. Chem.*, 1994, **47** (8), 1631

[99] H. Schindlbauer, *Monatsh. Chem.*, 1965, **96**, 2051

[100] S. Sasaki, F. Murakami and M. Yoshifuji, *Tetrahedron Lett.*, 1997, **38** (40), 7095

[101] S. Sasaki, K. Sutoh, F. Murakami and M. Yoshifuji, *J. Am. Chem. Soc.*, 2002, **124** (50), 14830

[102] *Phosphorus-31 NMR Spectroscopy*, O. Kühl, Springer, 2008

[103] All structures are drawn with Olex 2: O. V. Dolomanov, L. J. Bourhis, R. J. Gildea, J. A. K. Howard, H. Puschmann, OLEX2: A complete structure solution, refinement and analysis program, *J. Appl. Cryst.*, 2009, **42**, 339

[104] K. Mislow, *Acc. Chem. Res.*, 1976, **9**, 26

[105] C. A. Tolman, *Chem. Rev.*, 1977, **77**, 313

[106] J. G. Verkade, *Coordin. Chem. Rev.*, 1972, **2**, 1

[107] J. M. Jenkins and B. L. Shaw, *J. Chem. Soc. (A)*, 1966, 770

[108] J. G. Verkade, R. E. McCarley, D. G. Hendricker and R. W. King, *Inorg. Chem.*, 1965, **4**, 228

[109] D. A. Redfield, J. H. Nelson and L. W. Cary, *Inorg. Nucl. Chem. Lett.*, 1974, **10**, 721

[110] L. Rigamonti, C. Manassero, M. Rusconi, M. Manassero and A. Pasini, *J. Chem. Soc. Dalton Trans.*, 2009, **7**, 1206

[111] M. H. Johansson and S. Otto, *Acta. Cryst.*, 2000, **C56**, e12

[112] E. C. Alyea and J. Malito, *Phosphorus, Sulfur, Silicon Relat. Elem.*, 1969, **46**, 175

[113] P. Bhattacharyya, A. M. Z. Slawin, J. D. Woollins, *J. Chem. Soc. Dalton Trans.*, 2001, 300

[114] M. Shieh and M.-H. Hsu, *J. Clust. Sci.*, 2004, **15**, 91

[115] T. V. Russo, R. L. Martin, P. J. Hay, A. K. Rappe, J. Chem. Phys., 1995, **102** (23), 9315

[116] D. Britnell, G. W. A. Fowles and D. A. Rice, *J. Chem. Soc., Dalton Trans.*, 1974, **0**, 2191

[117] A. Kreienbrink, M. B. Sárosi, E. G. Rys, P. Lönnecke and E. Hey-Hawkins, *Angew. Chem. Int. Ed.*, 2011, **50**, 4701

[118] S. E. Lyubimov, V. A. Davankov, P. V. Petrovskii, E. Hey-Hawkins, A. A. Tyutyunov, E. G. Rys and V. N. Kalinin, *J. Org. Chem.*, 2008, **693**, 3689

[119] R. P. Davies, M. G. Martinelli, L. Patel and A. J. P. White, *Inorg. Chem.*, 2010, **49**, 4626

[120] E. W. Abel and G. Wilkinson, *J. Chem. Soc.*, 1959, 1501

[121] J. C. Barnes, W. Bell, C. Glidewell and R. A. Howie, *J. Organomet. Chem.*, 1990, **385** (3), 369

[122] M. P. Cava and M. I. Levinson, *Tetrahedron*, 1993, **49**, 5061

[123] I. Thomsen, K. Clausen, S. Scheibye and S.-O. Lawesson, *Org. Synth.*, 1990, **7**, 372

[124] M. St. J. Foreman and J. D. Woollins, *J. Chem. Soc, Dalton Trans.*, 2000, 1533

[125] G. Hua, A. L. Fuller, Y. Li, A. M. Z. Slawin and J. D. Woollins, *New J. Chem.*, 2010, **34** (8), 1565

[126] G. Hua and J. D. Woollins, *Angew. Chem. Int. Ed.*, 2009, **48**, 1368

[127] H. Duddeck, *Prog. Nucl. Mag. Res. Sp.*, 1995, **27**, l

[128] V. D. Leeput, T. W. Hummelink, J. H. Noordik and P. T. Beurskens, *Cryst. Struct. Commun.*, 1975, **4**, 167

Appendix

Appendix 1

Compound (**2.1**) – ^{i}PrAWR

Identification code	jgdw22	
Empirical formula	C15 H29 N2 P Se2	
Formula weight	426.29	
Temperature	93(2) K	
Crystal system	Monoclinic	
Space group	P 21/c	
Unit cell dimensions	a = 10.957(4) Å	α= 90°
	b = 11.846(4) Å	β= 107.991(9)°
	c = 15.570(5) Å	γ = 90°
Volume	1922.2(11) Å^3	
Z	4	
Density (calculated)	1.473 Mg/m^3	
F(000)	864	
μ(MoKα)	4.002 cm^{-1}	
Crystal size	0.30 x 0.30 x 0.03 mm	
Reflections collected	11741	
Independent reflections (no. variables)	3492 (192)	
Rint	0.0421	
Goodness-of-fit on F^2	1.088	
R indices (all data)	R1 = 0.0720, wR2 = 0.1841	
Largest diff. peak and hole	2.022 and -1.769 e.Å^{-3}	

Appendix 2

Compound (**2.2**) – ^{n}BuAWR

Identification code	jgdw23	
Empirical formula	C14 H27 N2 P Se2	
Formula weight	412.27	
Temperature	93(2) K	
Crystal system	Monoclinic	
Space group	I 2/a	
Unit cell dimensions	a = 21.737(11) Å	α= 90°
	b = 7.6822(19) Å	β= 99.048(6)°
	c = 22.049(6) Å	γ = 90°
Volume	3636(2) Å^3	
Z	8	
Density (calculated)	1.506 Mg/m^3	
F(000)	1664	
μ(MoKα)	4.147 cm^{-1}	
Crystal size	0.10 x 0.10 x 0.10 mm	
Reflections collected	10969	
Independent reflections (no. variables)	3298 (188)	
Rint	0.0509	
Goodness-of-fit on F^2	1.048	
R indices (all data)	R1 = 0.0400, wR2 = 0.0760	
Largest diff. peak and hole	0.509 and -0.601 e.Å^{-3}	

Appendix 3

Compound (**2.3**) – ^{s}BuAWR

Identification code	jgdw27	
Empirical formula	$C_{14}H_{27}N_2PSe_2$	
Formula weight	412.27	
Temperature	93(2) K	
Crystal system	Triclinic	
Space group	P-1	
Unit cell dimensions	a = 7.740(3) Å	α = 84.00(2)°
	b = 10.214(4) Å	β= 83.06(2)°
	c = 11.867(5) Å	γ = 82.97(2)°
Volume	920.5(6) $Å^3$	
Z	2	
Density (calculated)	1.487 Mg/m^3	
F(000)	416	
μ(MoKα)	4.095 cm^{-1}	
Crystal size	0.18 x 0.03 x 0.03 mm	
Reflections collected	5913	
Independent reflections (no. variables)	3229 (192)	
Rint	0.0492	
Goodness-of-fit on F^2	1.058	
R indices (all data)	R1 = 0.0809, wR2 = 0.1736	
Largest diff. peak and hole	1.881 and -0.829 e.$Å^{-3}$	
Flack parameter		

Appendix 4

Compound (**2.8**) – Ni Complex

Identification code	4	
Empirical formula	$C_{18}H_{26}N_2NiP_2Se_4$	
Formula weight	706.90	
Temperature	93(2) K	
Crystal system	Triclinic	
Space group	P-1	
Unit cell dimensions	a = 8.323(5) Å	α = 94.25(2)°
	b = 11.049(7) Å	β= 91.00(2)°
	c = 13.297(8) Å	γ = 91.54(2)°
Volume	920.5(6) $Å^3$	
Z	2	
Density (calculated)	1.926 Mg/m^3	
F(000)	684.00	
μ(MoKα)	6.9080 cm^{-1}	
Crystal size	0.120 x 0.100 x 0.100 mm	
Reflections collected	7687	
Independent reflections (no. variables)	4246 (247)	
Rint	0.0587	
Goodness-of-fit on F^2	1.086	
R indices (all data)	R1 = 0.1055, wR2 = 0.2630	
Largest diff. peak and hole	2.56 and -2.64 e.$Å^{-3}$	

Appendix 5

Compound (**2.9**) – Cu Complex

Identification code	14	
Empirical formula	$C_{54}H_{78}Cu_6N_6P_6Se_{15}$	
Formula weight	2562.77	
Temperature	93(2) K	
Crystal system	Triclinic	
Space group	P-1	
Unit cell dimensions	a = 8.072(2) Å	α = 85.04(2)°
	b = 9.053(3) Å	β = 117.8(2)°
	c = 16.788(5) Å	γ = 98.49(5)°
Volume	1180.2(5) $Å^3$	
Z	1	
Density (calculated)	2.193 Mg/m^3	
F(000)	1218.00	
μ(MoKα)	8.8144 cm^{-1}	
Crystal size	0.030 x 0.030 x 0.030 mm	
Reflections collected	12222	
Independent reflections (no. variables)	6809 (394)	
Rint	0.0704	
Goodness-of-fit on F^2	1.103	
R indices (all data)	R1 = 0.1055, wR2 = 0.2630	
Largest diff. peak and hole	3.12 and -1.86 e.$Å^{-3}$	

Appendix 6

Compound (**3.12**) – *cis*-[Pt(PPh_3)$_2$(^{s}BuAWR)Cl]

Identification code	Jacqui2-2	
Empirical formula	$C_{46}H_{44}NP_3PtSe_2$	
Formula weight	1056.79	
Temperature	93(2) K	
Crystal system	Triclinic	
Space group	P-1	
Unit cell dimensions	a = 11.165(3) Å	α = 103.41(4)°
	b = 14.403(5) Å	β= 93.69(4)°
	c = 14.976(5) Å	γ = 109.19(2)°
Volume	2186.5(12) Å^3	
Z	2	
Density (calculated)	1.605 Mg/m^3	
F(000)	1036.00	
μ(MoKα)	50.026 cm^{-1}	
Crystal size	0.120 x 0.090 x 0.020 mm	
Reflections collected	19066	
Independent reflections (no. variables)	9553 (478)	
Rint	0.0753	
Goodness-of-fit on F^2	1.238	
R indices (all data)	R1 = 0.1311, wR2 = 0.3612	
Largest diff. peak and hole	14.49 and -3.73 e.Å^{-3}	

Appendix 7

Compound (**4.1**) – $SPMes_3$

Identification code	JGDW35	
Empirical formula	$C_{27}H_{33}PS$	
Formula weight	420.59	
Temperature	93(2) K	
Crystal system	Triclinic	
Space group	P-1	
Unit cell dimensions	a = 8.072(2) Å	α = 85.04(2)°
	b = 9.053(3) Å	β= 76.36(2)°
	c = 16.788(5) Å	γ = 82.60(2)°
Volume	1180.2(5) $Å^3$	
Z	2	
Density (calculated)	1.183 Mg/m^3	
F(000)	452.00	
μ(MoKα)	2.156 cm^{-1}	
Crystal size	0.120 x 0.050 x 0.030 mm	
Reflections collected	7473	
Independent reflections (no. variables)	4145 (262)	
Rint	0.0376	
Goodness-of-fit on F^2	0.909	
R indices (all data)	R1 = 0.0873, wR2 = 0.2248	
Largest diff. peak and hole	0.55 and -0.58 e.$Å^{-3}$	

Appendix 8

Compound (**4.2**) – $SPMes_2Ph$

Identification code	jacks23spacegroup
Empirical formula	$C_{24}H_{27}PS$
Formula weight	378.51
Temperature	125(2) K
Crystal system	Hexagonal
Space group	$P6_3$
Unit cell dimensions	a = 20.578(7) Å
	c = 8.421(3) Å
Volume	3088(2) $Å^3$
Z	6
Density (calculated)	1.221 Mg/m^3
F(000)	1212.00
μ(MoKα)	2.398 cm^{-1}
Crystal size	0.120 x 0.090 x 0.020 mm
Reflections collected	23527
Independent reflections (no. variables)	3612 (235)
Rint	0.1099
Goodness-of-fit on F^2	1.136
R indices (all data)	R1 = 0.0910, wR2 = 0.2238
Largest diff. peak and hole	0.66 and -0.79 e.$Å^{-3}$

Appendix 9

Compound (**4.4**) – *trans*-$Pt(PMesPh_2)_2Cl_2$

Identification code	Jacksb-2	
Empirical formula	$C_{42}H_{42}Cl_2P_2Pt$	
Formula weight	874.74	
Temperature	125(2) K	
Crystal system	Triclinic	
Space group	P-1	
Unit cell dimensions	a = 9.075(11) Å	α = 108.03(2)°
	b = 10.759(12) Å	β= 102.450(11)°
	c = 10.974(13) Å	γ = 107.66(2)°
Volume	912(2) $Å^3$	
Z	1	
Density (calculated)	1.592 Mg/m^3	
F(000)	436.00	
μ(MoKα)	40.924 cm^{-1}	
Crystal size	0.120 x 0.030 x 0.020 mm	
Reflections collected	7060	
Independent reflections (no. variables)	3584 (214)	
Rint	0.0908	
Goodness-of-fit on F^2	1.258	
R indices (all data)	R1 = 0.1289, wR2 = 0.3419	
Largest diff. peak and hole	2.85 and -5.69 $e.Å^{-3}$	

Appendix 10

Compound (**4.5**) – $SPMesPh_2$

Identification code	Jacks38-1
Empirical formula	$C_{21}H_{21}PS$
Formula weight	336.43
Temperature	125(2) K
Crystal system	Orthorhombic
Space group	$P2_1P2_1P2_1$
Unit cell dimensions	a = 8.7846(13) Å
	b = 12.118(2) Å
	c = 16.810(3) Å
Volume	1789.5(5) $Å^3$
Z	4
Density (calculated)	1.249 Mg/m^3
F(000)	712.00
μ(MoKα)	2.673 cm^{-1}
Crystal size	0.150 x 0.090 x 0.030 mm
Reflections collected	14782
Independent reflections (no. variables)	3614 (208)
Rint	0.0792
Goodness-of-fit on F^2	1.199
R indices (all data)	R1 = 0.0746, wR2 = 0.1822
Largest diff. peak and hole	0.45 and -0.56 e.$Å^{-3}$

Appendix 11

Compound (**4.3**) – $SePMes_2Ph$

Identification code	Jacks34-1
Empirical formula	$C_{24}H_{27}PSe$
Formula weight	425.41
Temperature	125(2) K
Crystal system	Hexagonal
Space group	$P6_3$
Unit cell dimensions	a = 20.638(4) Å
	c = 8.451(2) Å
Volume	3117.3(10) $Å^3$
Z	6
Density (calculated)	1.360 Mg/m^3
F(000)	1320.00
μ(MoKα)	18.890 cm^{-1}
Crystal size	0.210 x 0.090 x 0.030 mm
Reflections collected	25850
Independent reflections (no. variables)	4227 (235)
Rint	0.1076
Goodness-of-fit on F^2	1.263
R indices (all data)	R1 = 0.0861, wR2 = 0.1908
Largest diff. peak and hole	0.95 and -0.91 $e.Å^{-3}$

Appendix 12

Compound (**4.6**) –$SePMesPh_2$

Identification code	Jacks35-2
Empirical formula	$C_{21}H_{21}PSe$
Formula weight	383.33
Temperature	125(2) K
Crystal system	Orthorhombic
Space group	$P2_12_12_1$
Unit cell dimensions	a = 8.798(2) Å
	b = 12.316(3) Å
	c = 16.968(4) Å
Volume	1838.5(8) $Å^3$
Z	4
Density (calculated)	1.385 Mg/m^3
F(000)	784.00
μ(MoKα)	21.269 cm^{-1}
Crystal size	0.120 x 0.090 x 0.030 mm
Reflections collected	15263
Independent reflections (no. variables)	3697 (208)
Rint	0.0878
Goodness-of-fit on F^2	1.102
R indices (all data)	R1 = 0.0930, wR2 = 0.2048
Largest diff. peak and hole	0.64 and -0.80 e.$Å^{-3}$

Appendix 13

Compound (**4.7**) – $OPMes_3$

Identification code	jacks4-6	
Empirical formula	$C_{30}H_{39}O_5P$	
Formula weight	510.61	
Temperature	125(2) K	
Crystal system	Triclinic	
Space group	P-1	
Unit cell dimensions	a = 8.160(3) Å	α = 75.56(3)°
	b = 10.229(3) Å	β = 77.47(3)°
	c = 18.214(4) Å	γ = 79.99(3)°
Volume	912(2) $Å^3$	
Z	2	
Density (calculated)	1.189 Mg/m^3	
F(000)	552.00	
μ(MoKα)	1.320 cm^{-1}	
Crystal size	0.150 x 0.120 x 0.020 mm	
Reflections collected	11024	
Independent reflections (no. variables)	4989 (325)	
Rint	0.0904	
Goodness-of-fit on F^2	1.056	
R indices (all data)	R1 = 0.1529, wR2 = 0.3233	
Largest diff. peak and hole	0.61 and -0.62 e.$Å^{-3}$	

Appendix 14

Compound (**4.8**) – $OPMes_2Ph$

Identification code	jacks4-1	
Empirical formula	$C_{26.25}H_{31.5}O_4P$	
Formula weight	422.01	
Temperature	125(2) K	
Crystal system	Triclinic	
Space group	P-1	
Unit cell dimensions	a = 8.975(4) Å	α = 91.908(7)°
	b = 10.422(4) Å	β= 96.849(7)°
	c = 14.223(5) Å	γ = 103.616(10)°
Volume	1281.1(8) $Å^3$	
Z	2	
Density (calculated)	1.146 Mg/m^3	
F(000)	422.00	
μ(MoKα)	1.344 cm^{-1}	
Crystal size	0.150 x 0.120 x 0.020 mm	
Reflections collected	9837	
Independent reflections (no. variables)	4470 (298)	
Rint	0.0538	
Goodness-of-fit on F^2	1.214	
R indices (all data)	R1 = 0.1258, wR2 = 0.3498	
Largest diff. peak and hole	1.19 and -0.68e.$Å^{-3}$	

Appendix 15

Compound (**4.9**) – $OPMesPh_2$

Identification code	jacks1-2
Empirical formula	$C_{21}H_{21}O_3P$
Formula weight	352.37
Temperature	125(2) K
Crystal system	Monoclinic
Space group	$P2_1/n$
Unit cell dimensions	a = 9.912(4) Å
	b = 18.611(7) Å β= 114.323(9)°
	c = 10.813(5) Å
Volume	1817.7(13) $Å^3$
Z	4
Density (calculated)	1.288 Mg/m^3
F(000)	744.00
μ(MoKα)	1.676 cm^{-1}
Crystal size	0.120 x 0.090 x 0.030 mm
Reflections collected	13770
Independent reflections (no. variables)	3192 (226)
Rint	0.1012
Goodness-of-fit on F^2	1.080
R indices (all data)	R1 = 0.1119, wR2 = 0.2366
Largest diff. peak and hole	0.56 and -0.79 $e.Å^{-3}$

Appendix 16

Compound (**5.4**) – Mn Cluster

Identification code	x0765fin	
Empirical formula	$C_{24}H_{15}Mn_2O_6P_3Se_5$	
Formula weight	996.95	
Temperature	130(2) K	
Crystal system	Monoclinic	
Space group	$P2_1/c$	
Unit cell dimensions	a = 15.1306(3) Å	α = 90º
	b = 17.3820(3) Å	β= 105.072(2)°
	c = 12.2897(2) Å	γ = 90º
Volume	3121.00(10) $Å^3$	
Z	4	
Density (calculated)	2.122 Mg/m^3	
F(000)	1888	
μ(MoKα)	6.831 cm^{-1}	
Crystal size	0.120 x 0.090 x 0.030 mm	
Reflections collected	36885	
Independent reflections (no. variables)	9504 (361)	
Rint	0.0519	
Goodness-of-fit on F^2	0.708	
R indices (all data)	R1 = 0.0628, wR2 = 0.0368	
Largest diff. peak and hole	0.583 and -0.450 e.$Å^{-3}$	

Appendix 17

Compound (**5.6**) – Acetyl ferrocene complex

Identification code	x0773fin	
Empirical formula	$C_{31}H_{30}FeP_2Se_4$	
Formula weight	836.18	
Temperature	130(2) K	
Crystal system	Triclinic	
Space group	P-1	
Unit cell dimensions	a = 979.59(4) Å	α = 105.583(3)°
	b = 1029.16(3) Å	β= 99.588(3)°
	c = 1617.69(5) Å	γ = 99.020(3)°
Volume	1712.31(6) $Å^3$	
Z	2	
Density (calculated)	1.835 Mg/m^3	
F(000)	816	
μ(MoKα)	5.434 cm^{-1}	
Crystal size	0.35 x 0.10 x 0.05 mm	
Reflections collected	16454	
Independent reflections (no. variables)	9068 (386)	
Rint	0.0219	
Goodness-of-fit on F^2	0.853	
R indices (all data)	R1 = 0.0407, wR2 = 0.0460	
Largest diff. peak and hole	0.725 and -0.517 e.$Å^{-3}$	

Appendix 18

Compound (**5.5**) – Li Complex

Identification code	x0768fin	
Empirical formula	$C_{28}H_{42}Li_2O_4P_2Se_4$	
Formula weight	834.28	
Temperature	130(2) K	
Crystal system	Monoclinic	
Space group	$P2_1/n$	
Unit cell dimensions	a = 10.8443(2) Å	α = 90º
	b = 11.6425(2) Å	β= 92.227(2)°
	c = 13.5726(3) Å	γ = 90º
Volume	1712.31(6) $Å^3$	
Z	2	
Density (calculated)	1.618 Mg/m^3	
F(000)	828	
μ(MoKα)	4.408 cm^{-1}	
Crystal size	0.40 x 0.40 x 0.40 mm	
Reflections collected	41491	
Independent reflections (no. variables)	5231 (181)	
Rint	0.0270	
Goodness-of-fit on F^2	0.708	
R indices (all data)	R1 = 0.0428, wR2 = 0.0870	
Largest diff. peak and hole	1.112 and -0.738 $e.Å^{-3}$	

Ich bin jetzt fertig mit fertigwerden.